QCD Corrections to the Rare Decays $B \to X_s \ell^+ \ell^-$ and $B \to X_d \ell^+ \ell^-$ in the Standard Model

Inauguraldissertation
der Philosophisch-naturwissenschaftlichen Fakultät
der Universität Bern

vorgelegt von

Manuel Philipp Walker

von Biel/BE

Leiter der Arbeit: PD Dr. Ch. Greub
Institut für theoretische Physik
Universität Bern

QCD Corrections to the Rare Decays $B \to X_s \ell^+\ell^-$ and $B \to X_d \ell^+\ell^-$ in the Standard Model

Inauguraldissertation
der Philosophisch-naturwissenschaftlichen Fakultät
der Universität Bern

vorgelegt von

Manuel Philipp Walker

von Biel/BE

Leiter der Arbeit: PD Dr. Ch. Greub
Institut für theoretische Physik
Universität Bern

Von der Philosophisch-naturwissenschaftlichen Fakultät angenommen.

Der Dekan:

Bern, den 20. Juni 2002

Prof. Dr. P. Bochsler

Why we concentrate on semileptonic decays in this thesis:

"If you drink the non-leptonic tonic, your physics career will be ruined and you will end up face down in the gutter."

M. Wise in advice to theorists

Abstract

In this PhD thesis we present the calculation of the $\mathcal{O}(\alpha_s)$ QCD corrections to the semileptonic inclusive rare decays $B \to X_s\,\ell^+\ell^-$ and $B \to X_d\,\ell^+\ell^-$ ($\ell = e, \mu$) in the Standard Model. Rare decays are of great interest for mainly two reasons. First, they provide sensitive checks on the Standard Model and allow to retrieve valuable information on the Cabibbo-Kobayashi-Maskawa matrix elements V_{ts} and V_{td}, which cannot be measured directly. Secondly, there is the chance that particles present in extensions of the Standard Model contribute considerably to physical observables measured in rare B decays. Of special interest in this context are additional sources of CP violation. Inclusive decays are exceptionally suited for a theoretical analysis as they are well approximated by the underlying partonic transitions. The main achievement of this work is the calculation of the virtual $\mathcal{O}(\alpha_s)$ corrections to the quark transition $b \to s\,\ell^+\ell^-$ and the corresponding gluon bremsstrahlung contributions. The result of our calculation drastically reduces the renormalization scale dependence. The calculation of the QCD corrections to $b \to d\,\ell^+\ell^-$ is not yet fully accomplished, but we expect to finalize it within a few weeks. Our work on $b \to s\,\ell^+\ell^-$ has already been applied by several authors, mainly in studies on exclusive rare decays like $B \to K e^+e^-$, $B \to K^* e^+e^-$ and on extensions of the Standard Model.

Contents

Introduction

First evidence for the existence of the bottom quark (b quark) was found at Fermilab in 1977 [1]. During the last twenty-five years, many experiments have been conducted to study B physics, the physics and phenomenology of B mesons. Many experiments are still running, others are planned and expected to supply new data within the next few years. Besides the experimental work, also the theoretical framework appropriate for studies on B decays has been developed. A very comprehensive review, mainly on the experimental aspects of B physics at BaBar, is given in "The BaBar Physics Book" [2]. A very thorough introduction to the theoretical side can be found eg in [3].

It stands out of question that the Standard Model has proved to be extraordinarily successful so far. However, most likely it won't be the end of the story. There are many open questions concerning the Standard Model itself, as eg the origin of the mass hierarchy, as well as observations not explained by the Standard Model[1]. The most serious reason not to trust absolutely in the Standard Model is maybe the fact that it does not provide enough sources of CP violation to explain the baryogenesis[2]. The only source of CP violation within the Standard Model is the complex phase of the Cabibbo-Kobayashi-Maskawa (CKM) matrix[3]. Possible extensions of the Standard Model are eg Supersymmetry (SUSY) or Grand Unified Theories (GUT), to mention only the most popular ones. Evidently, the energy scales required to produce the corresponding particles directly are out of reach of today's accelerators. (This may change, once LHC [5] becomes operational.) But even without having next-generation accelerators at hand, our search for "New Physics" is not doomed to fail. Our hope is in observing small deviations from the Standard Model that reveal themselves in processes feasible by today's experiments. Rare, loop-induced decays might have some of the Standard Model particles in the loop replaced by Supersymmetric particles, for instance. These additional contributions could have a substantial effect on decay rates and other observables. An example for a "New Physics" contribution is shown in Fig. 1. On the other hand, precise measurement of physical quantities combined with their reliable prediction allows to put stringent constraints on certain extensions of the Standard Model. See eg Ref. [6]. Experiments running at B factories also allow to extract more precise information on the elements of the CKM matrix. The aim is to measure

[1] The Standard Model does, for example, not account for neutrino masses, which today stand more or less out of question.

[2] There are many cosmological models where the baryon number asymmetry $\left[n_B/n_\gamma = (5.5 \pm 0.5) \times 10^{-10}\right]$ (see eg Ref. [4]) is generated at the weak phase transition. They all require additional sources of CP violation.

[3] This is not quite true; non-perturbative QCD effects induce an additional, CP violating term to the Standard Model Lagrangian: $\mathcal{L}_\theta = \frac{\theta_{\rm QCD}}{32\,\pi^2}\epsilon_{\mu\nu\rho\sigma}F^{\mu\nu a}F^{\rho\sigma a}$. The experimental bounds on the electric dipole moment of the neutron imply $\theta_{\rm QCD} \leq 10^{-10}$, which is unnaturally small. This puzzle, ie the smallness of $\theta_{\rm QCD}$, is called the strong CP problem.

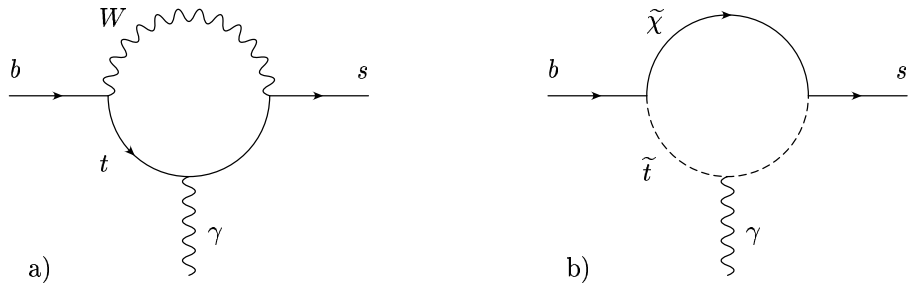

Figure 1: a) A Standard Model penguin diagram for the transition $b \to s\gamma$. b) Feynman diagram for the same process $b \to s\gamma$, where the W boson and the t quark have been replaced by a t squark and a chargino, respectively.

enough quantities to impose redundant constraints on Standard Model parameters. These constraints will either allow to fully determine the CKM parameters or they will force one to go beyond the Standard Model – equipped with some hints which direction to follow, however. Of particular interest are possible inconsistencies among different parameters describing the unitary triangle ($V_{ud}V_{ub}^* + V_{cd}V_{cb}^* + V_{td}V_{tb}^* = 0$). CP violation has first been observed in K decays [7]. A multitude of CP violating effects are expected in B decays, and almost any extension of the Standard Model generates additional CP violation.

In the past ten years, great progress has been made in B physics, not only on the theoretical side but also on the experimental one. The most important experiments are

- **CLEO** (@CESR; Ithaca, NY) [8]
  $e^+e^- \to \Upsilon(4S) \to B\bar{B}$
  The detectors CLEO II, CLEO II.V and CLEO III have collected about 17.1×10^6 $B\bar{B}$ data samples at the $\Upsilon(4S)$ resonance. The resonance $\Upsilon(4S)$ (10.58 GeV) is the first $b\bar{b}$ bound state heavy enough to decay into a pair of B mesons. Recently, about 9.6×10^6 $B\bar{B}$ events have been analyzed in the search for lepton-flavor-violating processes as, for example, $B \to K^- e^\pm \mu^\mp$ or $B^+ \to K^- e^+ e^+$ with a resulting upper limit for the corresponding branching fractions of about a few 10^{-6} [9].

- **BELLE** (@KEK-B; Tsukuba, Japan) [10]
  $e^+e^- \to \Upsilon(4S) \to B\bar{B}$
  BELLE is running since February 2000. The integrated luminosity up to now is about 70 fb^{-1}, which corresponds to 73×10^6 $B\bar{B}$ events. Recent BELLE results are eg the observation of mixing-induced CP violation in the neutral B meson system and the corresponding measurement of the CP violation parameter $\sin(2\beta)$ [11], or the measurement of the exclusive semileptonic decay modes $B \to K\, e^+e^-$ and $B \to K\, \mu^+\mu^-$ [12]. Anybody interested in BELLE results should bare in mind the different notation used at BELLE to name the angles of the unitarity triangle, ie $\alpha \equiv \phi_2$, $\beta \equiv \phi_1$ and $\gamma \equiv \phi_3$.

- **BaBar** (@PEP-II, SLAC; Stanford, CA) [13]
  $e^+e^- \to \Upsilon(4S) \to B\bar{B}$
  BaBar[4] had its first event on May 26, 1998. The integrated luminosity has a current value of about 81 fb^{-1} corresponding to 84.5×10^6 $B\bar{B}$ pairs. Both BELLE and BaBar work at asymmetric e^+e^- colliders with beams tuned on the $\Upsilon(4S)$ resonance. $\Upsilon(4S) \to B\bar{B}$ results in B mesons almost at rest in the center of mass frame. The asymmetric mode allows to produce B mesons with significant momenta in the laboratory frame. This enables to infer the B mesons' decay times from their decay length. However, the required vertex resolution is of $\mathcal{O}(100\mu\text{m})$, which is a demanding task for experimentalists. A recent BaBar result is an improved measurement of the CP violating asymmetry amplitude, which is proportional to $\sin(2\beta)$ [14].

- **HERA-B** (@HERA p, DESY; Hamburg, Germany) [15]
  $pA \to b\bar{b}X$
  HERA-B is a fixed target experiment at the 920 GeV HERA proton beam at DESY. For the measurement of the $b\bar{b}$ production in proton-nucleus interactions HERA-B uses inclusive $B \to J/\Psi + X$ decays. The number of reconstructed $B \to J/\Psi + X$ candidates in the year 2000 sample is small [$\mathcal{O}(10)$], reflecting the low efficiency of the not-fully commissioned detector and trigger. Up to now, HERA-B has not fulfilled the expectations. The poor efficiency does not allow to compete in CP violation measurements. However, HERA-B is the first experiment running in a LHC like environment and many useful experiences for future B factories have been made.

- **LHCb** (@LHC, CERN; Geneva, Switzerland) [16]
  $pp \to b\bar{b}X$
  LHC is supposed to become operational in 2006. It is expected to produce about $5 \times 10^{11} - 5 \times 10^{12}$ $B\bar{B}$ samples per year at $\sqrt{s} = 14$ TeV. This has to be compared to the $\mathcal{O}(10^7)$ events per year at the present $\Upsilon(4S)$ B factories. The new machine will provide very good statistics for B_d and B_s processes, the latter not accessible through the $\Upsilon(4S)$ machines [17].

- **BTeV** (@Tevatron, Fermilab (FNAL); Batavia, IL) [18]
  $p\bar{p} \to b\bar{b}X$
  BTeV is, as LHCb, a second generation B factory. About 2×10^{11} $B\bar{B}$ events per year are expected. This experiment too, will allow for high precision measurements of CP violation parameters in decays of B^0, $B^\pm$, B_s,... mesons and the search for "New Physics" in rare and FCNC (flavor changing neutral current) decays. BTeV is expected to become operational before LHCb. It is worth mentioning that both LHCb and BTeV pose many requirements not only to the detectors themselves but also to the data acquisition systems. B physics related experiments currently running at Tevatron are **CDF** [19] and **DØ** [20].

[4] BaBar is not only famous for producing many valuable experimental results: its collected data are stored in the world's largest database, which currently exceeds 500 TBytes of size!

For completeness, we mention that already at LEP studies on B physics have been done (ALEPH, DELPHI, L3, OPAL) ($e^+e^- \to Z^0 \to b\bar{b}$). $B\bar{B}$ mixing was measured for the first time with the ARGUS detector @DORIS ($e^+e^- \to \Upsilon(4S) \to B\bar{B}$) [21].

Recent experimental results related to the present work are the first measurements of the exclusive semileptonic rare B decays $B \to K\,\mu^+\mu^-$ and $B \to K\,e^+e^-$, reported by the BELLE collaboration [12]. The result is based on a 29.1 fb^{-1} sample accumulated at the $\Upsilon(4S)$ resonance. The branching fraction is obtained to be $\mathcal{B}(B \to K\,\ell^+\ell^-) = \left(0.75^{+0.25}_{-0.21} \pm 0.09\right) \times 10^{-6}$. In Ref. [6], where also our calculation on $b \to s\,\ell^+\ell^-$ entered, the theoretical predictions for these branching fractions have been improved and compared with experimental data. The results are found to be consistent with the Standard Model and some Supersymmetric extensions. As what concerns the inclusive semileptonic decays $B \to X_s\,e^+e^-$ and $B \to X_s\,\mu^+\mu^-$, only upper bounds for the inclusive branching ration are available today. These values too, may be found in [12]:

$$\mathcal{B}(B \to X_s\,e^+e^-) \leq 10.1 \times 10^{-6} \text{ at } 90\% \text{ C.L. } ,$$
$$\mathcal{B}(B \to X_s\,\mu^+\mu^-) \leq 19.1 \times 10^{-6} \text{ at } 90\% \text{ C.L. } .$$

Let us now turn to the theoretical side. Albeit CP violation will not be discussed further in this thesis, it is worthwhile looking briefly at the three types of CP violation in meson decays. This is, as should have become clear by now, because the main reason for doing B physics is to put the Standard Model to the test and to look for "New Physics", which most likely will be accompanied by CP violating effects. The *flavor* and CP eigenstates $B^0 = \bar{b}d$ and $\bar{B}^0 = b\bar{d}$, for example, obey

$$\text{CP } |B^0\rangle = \omega_B|B^0\rangle, \quad \text{CP } |\bar{B}^0\rangle = \omega_B^*|\bar{B}^0\rangle, \quad |\omega_B| = 1.$$

The light and heavy *mass* eigenstates are given by

$$|B_L\rangle = p|B^0\rangle + q|\bar{B}^0\rangle, \quad |B_H\rangle = p|B^0\rangle - q|\bar{B}^0\rangle \quad \text{with} \quad |q|^2 + |p|^2 = 1.$$

The time evolution of the flavor eigenstates is described by the Schrödinger-like equation

$$i\frac{d}{dt}\begin{pmatrix} B^0 \\ \bar{B}^0 \end{pmatrix} = \left(M - \frac{i}{2}\Gamma\right)\begin{pmatrix} B^0 \\ \bar{B}^0 \end{pmatrix},$$

where M and Γ are Hermitian matrices. Fig. 2 shows the lowest order Feynman diagrams that induce $B^0 - \bar{B}^0$ mixing.

The three types of CP violation are

1. **CP violation in mixing**
   Mixing arises because mass eigenstates need not to be CP eigenstates. For the neutral B system, this effect can be observed through asymmetries in semileptonic decays:

$$a_{\text{sl}} = \frac{\Gamma\left(\bar{B}^0_{\text{phys}}(t) \to \ell^+\nu X\right) - \Gamma\left(B^0_{\text{phys}}(t) \to \ell^-\bar{\nu}\bar{X}\right)}{\Gamma\left(\bar{B}^0_{\text{phys}}(t) \to \ell^+\nu X\right) + \Gamma\left(B^0_{\text{phys}}(t) \to \ell^-\bar{\nu}\bar{X}\right)}\,.$$

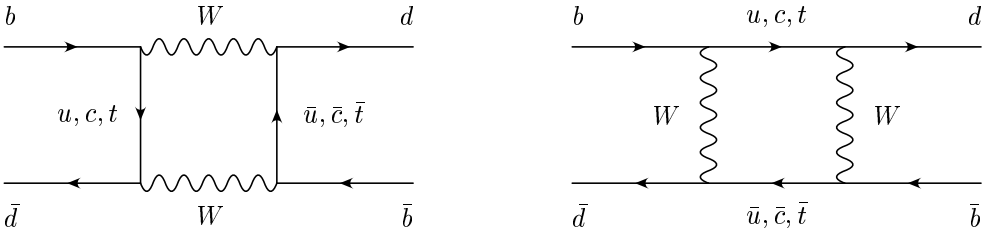

Figure 2: Leading order Feynman diagrams accounting for $B^0 - \bar{B}^0$ mixing in the Standard Model.

CP violation in mixing has been observed in the neutral K system [$\mathrm{Re}(\epsilon) \neq 0$].

2. **CP violation in decays**
   CP asymmetries in decays are often referred to as direct CP violation. Any CP asymmetry in charged B decays,

$$a_f = \frac{\Gamma(B^+ \to f^+) - \Gamma(B^- \to f^-)}{\Gamma(B^+ \to f^+) + \Gamma(B^- \to f^-)},$$

   are purely an effect of CP violation in decay. Direct CP violation has been observed in the neutral K system [$\mathrm{Re}(\epsilon') \neq 0$)].

3. **CP violation in the interference between decays with and without mixing**
   This effect is the result of interference between a direct decay amplitude and a first-mix-then-decay path to the final state. For the neutral B system, the effect can be observed by comparing decays into final CP eigenstates of a time-evolving neutral B state that begins at time zero as B^0 to those of the state that begins as $\bar{B}^0$:

$$a_{f_{\mathrm{CP}}} = \frac{\Gamma\big(\bar{B}^0_{\mathrm{phys}}(t) \to f_{\mathrm{CP}}\big) - \Gamma\big(B^0_{\mathrm{phys}}(t) \to f_{\mathrm{CP}}\big)}{\Gamma\big(\bar{B}^0_{\mathrm{phys}}(t) \to f_{\mathrm{CP}}\big) + \Gamma\big(B^0_{\mathrm{phys}}(t) \to f_{\mathrm{CP}}\big)}.$$

   Note that this asymmetry is time dependent. CP violation in the interference between decays with and without mixing has been observed again in the neutral K system [$\mathrm{Im}(\epsilon') \neq 0$)] but also in the neutral B system ($a_{\Psi K_S} \neq 0$). Very recently, the BELLE collaboration has reported finding CP violating asymmetries in $B^0 \to \pi^+\pi^-$ decays [22].

We have followed [2, 23] in this discussion.

Bottom quarks are bound by QCD into color neutral baryons. In order to probe the Standard Model and to look for "New Physics" effects, we have to disentangle them from non-perturbative QCD effects. For the non-perturbative analysis of QCD, the strong coupling constant α_s cannot serve as expansion parameter. One approach to non-perturbative QCD are effective theories. They have shown to be very powerful methods. For processes

involving light quarks, ie u, d and s, Chiral Perturbation Theory (χPT) is a very successful approach. It exploits the fact that $m_{u,d,s}$ are small compared to $\Lambda_{\rm QCD}$, the scale of non-perturbative QCD. χPT is, however, not appropriate for the description of B and C physics. Instead, we may use Heavy Quark Effective Theory (HQET) [24]. HQET is an expansion in $\Lambda_{\rm QCD}/m_{c,b}$ where the lowest order term is given by the corresponding quark level transition, which can be treated within ordinary perturbation theory. Both theories are derived from formal limits of QCD, ie $m_{u,d,s} \to 0$ and $m_{c,b} \to \infty$, respectively, in which new and useful symmetries arise. Other methods, based directly on QCD, are lattice QCD and QCD sum rules. Even with the approaches mentioned above, there remains a great variety of problems which to address requires yet other, less predictive, ways. However, for inclusive weak decays (where the problems discussed in this thesis belong to), some exclusive semileptonic decays and some static properties, effective field theories lead to theoretical predictions that are well controlled.

This thesis focuses only on the rare decays $b \to s\,\ell^+\ell^-$ and $b \to d\,\ell^+\ell^-$ in the Standard Model. The basic achievement is the calculation of the $\mathcal{O}(\alpha_s)$ QCD corrections to the inclusive semileptonic rare decay $b \to s\,\ell^+\ell^-$. The new contributions reduce the renormalization scale dependence drastically by a factor of two. We have also completed the calculation of the corresponding gluon bremsstrahlung corrections. The calculation of the $\mathcal{O}(\alpha_s)$ QCD corrections to $b \to d\,\ell^+\ell^-$, which was not part of the basic concept to this thesis, is not yet fully accomplished. It will be interesting to complete this calculation, especially because the process $b \to d\,\ell^+\ell^-$ is much more sensitive to CP violation than the transition $b \to s\,\ell^+\ell^-$, where it is strongly Cabibbo-suppressed. In our calculation we have therefore neglected the combination $|V_{us}V_{ub}^*|$. This is a save approximation, but at the same time predicts vanishing CP violation in the corresponding process.

The thesis is organized as follows:

- **PART I**
  In part I we give an introduction to the theoretical framework used to study inclusive weak B meson decays.

- **PART II**
  "Two-Loop Virtual Corrections to $B \to X_s\,\ell^+\ell^-$ in the Standard Model",
  published in *Phys. Lett.* **B 507** (2001) 162, (hep-ph/0103087).

  This is a short letter in which we just present the results for the virtual corrections to $b \to s\,\ell^+\ell^-$. The main result is that our calculation reduces the dependence on the renormalization scale by a factor of two.

- **PART III**
  "Calculation of Two-Loop Virtual Corrections to $b \to s\,\ell^+\ell^-$ in the Standard Model",
  published in *Phys. Rev.* **D 65** (2002) 074004, (hep-ph/0109140).

  Here we present in detail the calculation of the virtual corrections to $b \to s\,\ell^+\ell^-$. In particular, we discuss the application of multiple Mellin-Barnes representations to

solve certain Feynman parameter integrals. We do also explain how to include those bremsstrahlung corrections that are necessary to cancel the infrared and collinear singularities present in the virtual corrections.

- **PART IV**
  "Results of the $\mathcal{O}(\alpha_s)$ Two-Loop Virtual Corrections to $B \to X_s\,\ell^+\ell^-$ in the Standard Model",
  Talk given at HEP01 in Budapest, Hungary, July 2001; published in "Budapest 2001, High energy physics" hep2001/091, (hep-ph/0110388).

  For completeness, I have also included our contribution to the proceedings of the "International Europhysics Conference on High-Energy Physics (HEP01), Budapest, Hungary, 12-18 Jul 2001" where in a short talk our results on $B \to X_s\,\ell^+\ell^-$ were presented.

- **PART V**
  "Complete Gluon Bremsstrahlung Corrections to the Process $b \to s\,\ell^+\ell^-$",
  accepted for publication in *Phys. Rev.* **D**, (hep-ph/0204341).

  In the preceding three papers we have only included those bremsstrahlung corrections that are necessary to cancel the infrared and collinear singularities present in the virtual corrections. In this paper we revise the results obtained before and give all bremsstrahlung corrections to $b \to s\,\ell^+\ell^-$. The additional contributions change the result only marginally. We further comment on the issue of the definition of m_c, ie the pole mass and the $\overline{\rm MS}$ mass definition.

- **PART VI**
  "Calculation of Two-Loop Virtual Corrections to $b \to d\,\ell^+\ell^-$ in the Standard Model".

  The calculation of the process $b \to d\,\ell^+\ell^-$ is in some parts almost identical to that of $b \to s\,\ell^+\ell^-$. However, since the CKM structure no longer factorizes in good approximation, we do also have to calculate diagrams where the massive c quark is replaced by a massless u quark. This substantially complicates the calculation of some diagrams in the sense that the techniques used in the previous work fail. We present another approach, which unfortunately does not yet solve all problems. At the present time there remains still one integral which resists our attempt to solve it. In Part VI, we therefore give but what might serve as a draft of a next paper, which we hope to finalize within a few weeks.

Our work on $b \to s\,\ell^+\ell^-$ has already been applied by several authors, mainly in studies on exclusive rare decays, as eg $B \to Ke^+e^-$, $B \to K^*e^+e^-$ [6, 25], and on extensions of the Standard Model [26]–[30].

References

[1] S. W. Herb *et al.*, *Phys. Rev. Lett.* **39** (1977) 252.

[2] The BaBar Physics Book, SLAC-R-504.
http://www.slac.stanford.edu/BFROOT/www/doc/PhysBook/physBook.html

[3] A. J. Buras, hep-ph/9806471.

[4] A. G. Cohen, D. B. Kaplan and A. E. Nelson,
Ann. Rev. Nucl. Part. Sci. **43** (1993) 27, hep-ph/9302210;
S. Burles, K. M. Nollett and M. S. Turner,
Astrophys. J. **552** (2001) L1, astro-ph/0010171.

[5] http://lhc-new-homepage.web.cern.ch/lhc-new-homepage/.

[6] A. Ali, C. Greub, G. Hiller and E. Lunghi, hep-ph/0112300,
to appear in *Phys. Rev.* **D**.

[7] J. H. Christenson, J. W. Cronin, V. L. Fitch and R. Turlay,
Phys. Rev. Lett. **13** (1964) 138.

[8] http://www.lns.cornell.edu/public/CLEO/.

[9] K. W. Edwards *et al.* [CLEO Collaboration], CLNS 02/1781, CLEO 02-4,
submitted to *Phys. Rev. D Rapid Communications*, hep-ex/0204017.

[10] http://belle.kek.jp/.

[11] K. Abe *et al.* [BELLE Collaboration], KEK Preprint 2001-172,
BELLE Preprint 2002-6, hep-ex/0202027.

[12] K. Abe *et al.* [BELLE Collaboration], BELLE-CONF-0110, hep-ex/0107072.
K. Abe *et al.* [BELLE Collaboration], *Phys. Rev. Lett.* **88** (2002) 031802,
KEK Preprint 2001-118, BELLE Preprint 2001-13, DPNU-01-30, hep-ex/0109026.

[13] http://www-public.slac.stanford.edu/babar/.

[14] B. Aubert *et al.* [BaBar Collaboration], BaBar-CONF-02/01, SLAC-PUB-9153,
hep-ex/0203007.

[15] http://www-hera-b.desy.de/.

[16] http://lhcb.web.cern.ch/.

[17] P. Ball *et al.*, CERN-TH/2000-101, hep-ph/0003238.

[18] http://www-btev.fnal.gov/.

[19] http://www-cdf.fnal.gov/.

[20] http://www-d0.fnal.gov/.

[21] H. Albrecht *et. al* [ARGUS Collaboration], *Phys. Lett.* **B 192** (1987) 245, DESY-87-029.

[22] K. Abe *et al.* [BELLE Collaboration], KEK Preprint 2002-6, Belle Preprint 2002-8, submitted to *Phys. Rev. Lett.*, hep-ex/0204002.

[23] Y. Nir, Lectures given at the **"55$^{\rm th}$ Scottish Universities Summer School of Physics"** on **"Heavy Flavour Physics"**, WIS/18/01-Aug-DPP, hep-ph/0109090.

[24] M. Neubert, *Adv. Ser. Direct. High Energy Phys.* **15** (1998) 239, hep-ph/9702375.

[25] M. Beneke, T. Feldmann and D. Seidel, *Nucl. Phys.* **B 612** (2001) 25, hep-ph/0106067.

[26] D. A. Demir, K. A. Olive and M. B. Voloshin, hep-ph/0204119.

[27] T. M. Aliev, A. Ozpineci and M. Savici, hep-ph/0203045.

[28] G. K. Yeghiyan, *Mod. Phys. Lett.* **A 16** (2001) 2151.

[29] C.-S. Huang, W. Liao, Q. Yan and S. Zhu, hep-ph/0110147.

[30] Z. Xiong and J. M. Yang, hep-ph/0105260.

PART I

Preliminaries

1 The Standard Model

We do not want to give a thorough overview of the Standard Model in this place. There are many text books that discuss the Standard Model in detail. We restrict ourselves to give the symmetries and the matter content of the model and the Lagrangian. Furthermore, we will briefly discuss the Yukawa couplings. The latter give, together with the spontaneous symmetry breaking in the Higgs sector, rise to the fermion masses and the Cabibbo-Kobayashi-Maskawa (CKM) matrix. The CKM matrix induces quark mixing, which is crucial for transitions as for example $b \to s\,\ell^+\ell^-$: in a scenario with unity CKM matrix, it were simply absent. We will not, however, investigate the questions of quantization and gauge fixing in this place.

We follow Nir [1] and define a model of elementary particles and their interactions by

1. the symmetries of the Lagrangian;
2. the representations of fermions and scalars;
3. the pattern of spontaneous symmetry breaking.

1.1 Symmetries and Particles

The Standard Model is defined as follows:

1. The gauge symmetry group G_{SM} of the Standard Model is
$$G_{\text{SM}} = SU(3)_C \otimes SU(2)_L \otimes U(1)_Y.$$
2. The particle content and transformation properties of the matter and gauge fields of the Standard Model we list in Tab. 1.1.
3. The only scalar field in the Standard Model, ϕ, picks up a non-vanishing vacuum expectation value
$$\langle \phi \rangle = \frac{1}{\sqrt{2}} \begin{pmatrix} 0 \\ v \end{pmatrix},$$
and the symmetry group of the Standard Model is spontaneously broken:
$$G_{\text{SM}} \longrightarrow SU(3)_C \otimes U(1)_Q.$$

Field		$SU(3)_C \otimes SU(2)_L \otimes U(1)_Y$	Q
Quarks	$Q'^{\alpha}_{Li} = \left\{ \begin{pmatrix} u'^{\alpha} \\ d'^{\alpha} \end{pmatrix}_L, \begin{pmatrix} c'^{\alpha} \\ s'^{\alpha} \end{pmatrix}_L, \begin{pmatrix} t'^{\alpha} \\ b'^{\alpha} \end{pmatrix}_L \right\}$	$\left(\mathbf{3}, \mathbf{2}, +\frac{1}{6}\right)$	$\begin{pmatrix} +\frac{2}{3} \\ -\frac{1}{3} \end{pmatrix}$
	$U'^{\alpha}_{Ri} = \{u'^{\alpha}_R, c'^{\alpha}_R, t'^{\alpha}_R\}$	$\left(\mathbf{3}, \mathbf{2}, +\frac{2}{3}\right)$	$+\frac{2}{3}$
	$D'^{\alpha}_{Ri} = \{d'^{\alpha}_R, s'^{\alpha}_R, b'^{\alpha}_R\}$	$\left(\mathbf{3}, \mathbf{2}, -\frac{1}{3}\right)$	$-\frac{1}{3}$
Leptons	$L'_{Li} = \left\{ \begin{pmatrix} \nu'_e \\ e' \end{pmatrix}_L, \begin{pmatrix} \nu'_\mu \\ \mu' \end{pmatrix}_L, \begin{pmatrix} \nu'_\tau \\ \tau' \end{pmatrix}_L \right\}$	$\left(\mathbf{1}, \mathbf{2}, -\frac{1}{2}\right)$	$\begin{pmatrix} 0 \\ -1 \end{pmatrix}$
	$E'_{Ri} = \{e'_R, \mu'_R, \tau'_R\}$	$(\mathbf{1}, \mathbf{1}, -1)$	-1
Higgs	$\phi = \begin{pmatrix} \phi^+ \\ \phi^0 \end{pmatrix}$	$\left(\mathbf{1}, \mathbf{2}, +\frac{1}{2}\right)$	$\begin{pmatrix} +1 \\ 0 \end{pmatrix}$
	$\widetilde{\phi} = \begin{pmatrix} \phi^{0*} \\ -\phi^- \end{pmatrix}$	$\left(\mathbf{1}, \mathbf{2}, -\frac{1}{2}\right)$	$\begin{pmatrix} 0 \\ -1 \end{pmatrix}$
Gauge Bosons	G_μ	$(\mathbf{8}, \mathbf{1}, 0)$	
	W_μ	$(\mathbf{1}, \mathbf{3}, 0)$	
	B_μ	$(\mathbf{1}, \mathbf{1}, 0)$	

Table 1.1: Particle content and transformation properties of the matter and gauge fields in the Standard Model. The notation $(\boldsymbol{C}, \boldsymbol{L}, Y)$ means that the corresponding fields [$SU(2)$ singlets or doublets] transform according to a C and L dimensional representation of $SU(3)_C$ and $SU(2)_L$, respectively, and have hypercharge Y. α is the color index and Q denotes the electrical charge of the particles. $\widetilde{\phi} = -\tau_2 \phi^*$ does not represent an additional degree of freedom of the Standard Model. We merely list it here in order to have its transformation properties ready at hand.

1.2 Lagrangian

The Standard Model Lagrangian is the most general renormalizable Lagrangian that is consistent with the gauge symmetry G_{SM}. The complete Standard Model Lagrangian (we give it only in parts here) can be found eg in [2]. We divide the Lagrangian into three parts:

$$\mathcal{L}_{\mathrm{SM}} = \mathcal{L}_{\mathrm{kinetic}} + \mathcal{L}_{\mathrm{Higgs}} + \mathcal{L}_{\mathrm{Yukawa}}.$$

In order to locally preserve gauge invariance, ie the symmetries of the Lagrangian, the ordinary derivatives have to be replaced by the covariant ones:

$$\partial^\mu \longrightarrow D'^\mu = \partial^\mu + i g_s G^{a\mu} L^a + i g W^{b\mu} T^b + i g' B^\mu Y.$$

$G^{a\mu}$, $W^{b\mu}$ and B^μ are the eight gluon fields, the three weak interaction and the hypercharge fields, respectively. L^a denotes the $SU(3)_C$ and T^b the $SU(2)_L$ generators, whereas Y are the $U(1)_Y$ charges. The interaction between gauge and matter fields is described by the covariant derivatives. We include the corresponding terms in $\mathcal{L}_{\mathrm{kinetic}}$. In order to clarify the notation, we give the definitions of generic left- and right-handed fermion fields as we use them in the following:

$$X_L = \frac{1-\gamma_5}{2}\, X, \qquad X_R = \frac{1+\gamma_5}{2}\, X,$$

$$\overline{X}_L = \overline{X}\, \frac{1+\gamma_5}{2}, \qquad \overline{X}_R = \overline{X}\, \frac{1-\gamma_5}{2}.$$

We have the following contributions to the kinetic part of $\mathcal{L}_{\mathrm{SM}}$:

$$\mathcal{L}_{\mathrm{kinetic}}(Q'_{Li}) = i\, \overline{Q}'_{Li}\, \gamma_\mu \left(\partial^\mu + \frac{i}{2}\, g_s G^{a\mu} \lambda^a + \frac{i}{2}\, g W^{b\mu} \tau^b + \frac{i}{6} g' B^\mu \right) Q'_{Li},$$

$$\mathcal{L}_{\mathrm{kinetic}}(U'_{Ri}) = i\, \overline{U}'_{Ri}\, \gamma_\mu \left(\partial^\mu + \frac{i}{2}\, g_s G^{a\mu} \lambda^a + \frac{2\, i}{3}\, g' B^\mu \right) U'_{Ri},$$

$$\mathcal{L}_{\mathrm{kinetic}}(D'_{Ri}) = i\, \overline{D}'_{Ri}\, \gamma_\mu \left(\partial^\mu + \frac{i}{2} g_s\, G^{a\mu} \lambda^a - \frac{i}{3}\, g' B^\mu \right) D'_{Ri},$$

$$\mathcal{L}_{\mathrm{kinetic}}(L'_{Li}) = i\, \overline{L}'_{Li}\, \gamma_\mu \left(\partial^\mu + \frac{i}{2}\, g W^{b\mu} \tau^b - \frac{i}{2} g'\, B^\mu \right) L'_{Li},$$

$$\mathcal{L}_{\mathrm{kinetic}}(E'_{Ri}) = i\, \overline{E}'_{Ri}\, \gamma_\mu \left(\partial^\mu - i g' B^\mu \right) E'_{Ri},$$

$$\mathcal{L}_{\text{kinetic}}(\phi) = \left[\left(\partial_\mu + \frac{i}{2} g W^{b\mu}\tau^b + \frac{i}{2} g' B_\mu\right)\phi^\dagger\right] \cdot \left[\left(\partial^\mu - \frac{i}{2} g W^{b\mu}\tau^b - \frac{i}{2} g' B^\mu\right)\phi\right],$$

$$\mathcal{L}_{\text{kinetic}}(G) = -\frac{1}{4} G^a_{\mu\nu} G^{a\mu\nu},$$

$$\mathcal{L}_{\text{kinetic}}(W) = -\frac{1}{4} W^a_{\mu\nu} W^{a\mu\nu},$$

$$\mathcal{L}_{\text{kinetic}}(B) = -\frac{1}{4} B^a_{\mu\nu} B^{a\mu\nu},$$

The matrices λ^a and τ^b are the Gell-Mann and Pauli matrices, respectively. The field strength tensors are given by

$$G^a_{\mu\nu} = \partial_\mu G^a_\nu - \partial_\nu G^a_\mu - g_s f^{abc} G^b_\mu G^c_\nu,$$

$$W^a_{\mu\nu} = \partial_\mu W^a_\nu - \partial_\nu W^a_\mu - g\, \epsilon^{abc} W^b_\mu W^c_\nu,$$

$$B^a_{\mu\nu} = \partial_\mu B^a_\nu - \partial_\nu B^a_\mu.$$

where f^{abc} and ϵ^{abc} denote the $SU(3)$ and $SU(2)$ structure constants, respectively.

The scalar self-interactions of the Higgs field are described by the Higgs potential. We have

$$\mathcal{L}_{\text{Higgs}} = \mu^2 \phi^\dagger\phi - \lambda\left(\phi^\dagger\phi\right)^2.$$

Note that both $\mathcal{L}_{\text{kinetic}}$ and $\mathcal{L}_{\text{Higgs}}$ are CP conserving. In extensions of the scalar sector, as eg multi Higgs-doublet models, $\mathcal{L}_{\text{Higgs}}$ may give rise to CP violation.

Finally, we turn to the Yukawa couplings. We split the corresponding term $\mathcal{L}_{\text{Yukawa}}$ into a quark and lepton contribution. They are given by

$$\mathcal{L}^{\text{leptons}}_{\text{Yukawa}} = -Y^e_{ij}\, \overline{L}'_{Li}\, \phi^\dagger\, E'_{Rj} + \text{h.c.} \qquad \text{and},$$

$$\mathcal{L}^{\text{quarks}}_{\text{Yukawa}} = -Y^d_{ij}\, \overline{Q}'_{Li}\, \phi\, D'_{Rj} - Y^u_{ij}\, \overline{Q}'_{Li}\, \widetilde{\phi}\, U'_{Rj} + \text{h.c.}.$$

We stress that we have been working in the basis of flavor eigenstates up to now.

1.3 Symmetry Breaking and the Generation of Masses

We write the Higgs field in the form

$$\phi = \begin{pmatrix} \phi^+ \\ \phi^0 \end{pmatrix} = \langle\phi\rangle + \phi_d = \frac{1}{\sqrt{2}} \begin{pmatrix} 0 \\ v \end{pmatrix} + \begin{pmatrix} \phi_d^+ \\ \phi_d^0 \end{pmatrix},$$

where the vacuum expectation value v corresponds to the classical minimum of the Higgs potential:

$$v = \sqrt{\frac{\mu^2}{\lambda}}\,.$$

The direction of $\langle\phi\rangle$ has been chosen such that the photon remains massless and the electromagnetic interaction an unbroken symmetry. The Yukawa interactions give rise to mass terms. For the gauge bosons it reads

$$\mathcal{L}_M^G = g^2 \frac{v^2}{2} W_\mu^+ W^{\mu-} + \frac{v^2}{4} \left(g^2 + g'^2\right) Z_\mu Z^\mu,$$

where

$$W_\mu^\pm = \frac{1}{\sqrt{2}} \left(W_\mu^1 \mp i\, W_\mu^2\right) \quad \text{and} \quad Z_\mu = \frac{g\, W_\mu^3 - g' B_\mu}{\sqrt{g^2 + g'^2}} \equiv \cos\theta_W\, W_\mu^3 - \sin\theta_W\, B_\mu.$$

θ_W denotes the Weinberg angle. The field orthogonal to Z_μ obtains no mass and couples only to the electron (equally strongly to left- and right-handed components) and not to the neutrino. It is identified with the electromagnetic field A_μ:

$$A_\mu = \frac{g\, W_\mu^3 + g' B_\mu}{\sqrt{g^2 + g'^2}} \equiv \cos\theta_W\, W_\mu^3 + \sin\theta_W\, B_\mu.$$

The masses of the physical gauge bosons are given by

$$m_W^2 = \frac{g^2\, v^2}{2} \quad \text{and} \quad m_Z^2 = \frac{m_W^2}{\cos^2\theta_W}\,.$$

The vacuum expectation value of the Higgs field gives rise to mass terms for the charged leptons, whereas the neutrinos stay massless[1]. We have

$$\mathcal{L}_M^\ell = -(M'_\ell)_{ij}\, \overline{E}'_{Li}\, E'_{Ri} + \text{h.c.}\,,$$

where

$$M'_\ell = \frac{v}{\sqrt{2}}\, Y^e \quad \text{and} \quad L'_{Li} = \begin{pmatrix} \nu'_{Li} \\ E'_{Li} \end{pmatrix}.$$

[1] There is evidence from several observations and experiments that neutrinos actually are equipped with a tiny mass. We do in this thesis, however, not discuss extensions of the Standard Model that might explain those masses.

We may transformation the lepton fields according to $L_L = V_L L'_L$, $E_R = V_R E'_R$ with unitary matrices V_L and V_R, which can be chosen to diagonalize the mass matrix M'_e:

$$M'_\ell = V_R \, M_\ell \, V_L^\dagger, \quad \text{with} \quad M_\ell = \text{diag}(m_e, m_\mu, m_\tau).$$

This automatically diagonalizes the interaction terms, too. Splitting the Yukawa couplings of the leptons into mass and interaction terms, we get

$$\mathcal{L}_{\text{Yukawa}}^{\text{lepton masses}} = -M_{ij} \, \overline{L}_{Li} \, E_{Rj} + \text{h.c.}\,,$$

$$\mathcal{L}_{\text{Yukawa}}^{\text{lepton interaction}} = -\frac{1}{\sqrt{2}} \, M_{ij} \, \overline{L}_{Li} \, \phi_d^\dagger \, E_{Rj} + \text{h.c.}\,.$$

Similarly, in the quark sector we find

$$\mathcal{L}_{\text{Yukawa}}^{\text{quark masses}} = \mathcal{L}_M^q = -\overline{U}_L \, M'_U \, U_R - \overline{D}_L \, M'_D \, D_R + \text{h.c.}\,,$$

where

$$M'_u = \frac{v}{\sqrt{2}} \, Y^u, \quad M'_d = \frac{v}{\sqrt{2}} \, Y^d \quad \text{and} \quad Q_{Li} = \begin{pmatrix} U_{Li} \\ D_{Li} \end{pmatrix}.$$

Again we may transform the fields in order to diagonalize the mass matrices:

$$\begin{aligned} U_{R,L} &= V_{R,L}^U \, U'_{R,L}, & M_U &= V_R^U \, M'_U \, \left(V_L^U\right)^\dagger = \text{diag}(m_u, m_c, m_t), \\ D_{R,L} &= V_{R,L}^D \, D'_{R,L}, & M_D &= V_R^D \, M'_D \, \left(V_L^D\right)^\dagger = \text{diag}(m_d, m_s, m_b). \end{aligned}$$

In the new basis, the interaction between the $W^\pm$ bosons and fermions is of the form

$$\mathcal{L}_{CC} = -\frac{1}{2} \frac{e}{\sin\theta_W} \, W_\mu^+ \, J^{-\mu} - \frac{1}{2} \frac{e}{\sin\theta_W} \, W_\mu^- \, J^{+\mu},$$

where

$$\begin{aligned} J_\mu^- &= \overline{U}'_L \gamma_\mu D'_L + \bar{\nu}_{\ell L} \gamma_\mu \ell_L = \overline{U}_L \gamma_\mu V_{\text{CKM}} D_L + \bar{\nu}_{\ell L} \gamma_\mu \ell_L \\ &= (\bar{u}_L, \bar{c}_L, \bar{t}_L) \, \gamma_\mu V_{\text{CKM}} \begin{pmatrix} d_L \\ s_L \\ b_L \end{pmatrix} + (\bar{\nu}_{eL}, \bar{\nu}_{\mu L}, \bar{\nu}_{\tau L}) \, \gamma_\mu \begin{pmatrix} e_L \\ \mu_L \\ \tau_L \end{pmatrix}, \end{aligned}$$

where the Cabibbo-Kobayashi-Maskawa matrix $V_{\text{CKM}} = V_L^U (V_L^D)^\dagger$. There is one important difference between the lepton and the quark sector. In the lepton case we have the freedom to transform the neutrinos ν_L in the same manner as the left-handed charged leptons. This is because we do not have to diagonalize a mass matrix for the neutrinos. For the quarks, however, the transformation matrices for up and down type quarks are fixed independently, when diagonalizing M'_U and M'_D.

The quark-Higgs interaction term in the mass basis, finally, is given by

$$\mathcal{L}_{\text{Yukawa}}^{\text{quark-Higgs}} = -\frac{2}{v}\Big\{\overline{U}_R\, M_U\, U_L\, \phi_d^{0*} - \overline{U}_R\, M_U\, V_{\text{CKM}}\, D_L\, \phi_d^{+} + \overline{D}_R\, M_D\, V_{\text{CKM}}^{\dagger}\, U_L\, \phi_d^{-} + \overline{D}_R\, M_D\, D_L\, \phi_d^{0} + \text{h.c.}\Big\}\,.$$

1.4 The CKM Matrix

We will now give two parametrizations of the CKM matrix and then shortly discuss some issues of the knowledge we have on its parameters.

The entries of the CKM matrix are conveniently called

$$V_{\text{CKM}} = \begin{pmatrix} V_{ud} & V_{us} & V_{ub} \\ V_{cd} & V_{cs} & V_{cb} \\ V_{td} & V_{ts} & V_{tb} \end{pmatrix}.$$

There are actually three real and one imaginary physical parameter: three angles and one complex phase. The standard parameterization [3], used by the particle data group, is given by

$$V_{\text{CKM}} = \begin{pmatrix} c_{12}\, c_{13} & s_{12}\, c_{13} & s_{13}\, \mathrm{e}^{-i\,\delta} \\ -s_{12}\, c_{23} - c_{12}\, s_{23}\, s_{13}\, \mathrm{e}^{i\,\delta} & c_{12}\, c_{23} - s_{12}\, s_{23}\, s_{13}\, \mathrm{e}^{i\,\delta} & s_{23}\, s_{13} \\ s_{12}\, s_{23} - c_{12}\, c_{23}\, s_{13}\, \mathrm{e}^{i\,\delta} & -s_{23}\, s_{12} - s_{12}\, c_{23}\, s_{13}\, \mathrm{e}^{i\,\delta} & c_{23}\, c_{13} \end{pmatrix},$$

where $c_{ij} \equiv \cos\theta_{ij}$ and $s_{ij} \equiv \sin\theta_{ij}$.

A very useful parameterization is the Wolfenstein parameterization [4] with the four parameters λ, A, ρ and η. It makes use of the fact that $s_{13} = \mathcal{O}(10^{-3})$ and $s_{23} = \mathcal{O}(10^{-2})$, and thus $c_{13} = c_{23} = 1$ to very good accuracy.

$$V_{\text{CKM}} = \begin{pmatrix} 1 - \frac{\lambda^2}{2} & \lambda & A\,\lambda^3(\rho - i\eta) \\ -\lambda & 1 - \frac{\lambda^2}{2} & A\,\lambda^2 \\ A\,\lambda^3(1 - \rho - i\eta) & -A\,\lambda^2 & 1 \end{pmatrix} + \mathcal{O}(\lambda^4).$$

$\lambda = |V_{us}| \approx 0.22$ plays the role of an expansion parameter. The Wolfenstein parameterization makes it easy to keep track of the magnitude of the elements of V_{CKM}.

The unitarity of the CKM matrix implies certain relations among the matrix elements, as for example

$$\begin{aligned} V_{ud}V_{us}^* + V_{cd}V_{cs}^* + V_{td}V_{ts}^* &= 0, \\ V_{us}V_{ub}^* + V_{cs}V_{cb}^* + V_{ts}V_{tb}^* &= 0, \\ V_{ud}V_{ub}^* + V_{cd}V_{cb}^* + V_{td}V_{tb}^* &= 0. \end{aligned} \tag{1}$$

Geometrically, these relations may be interpreted as triangles, called unitarity triangles.

The three angles of the unitarity triangle defined by the second equation in (1) are defined as

$$\alpha \equiv \arg\left[-\frac{V_{td}V_{tb}^*}{V_{ud}V_{ub}^*}\right], \qquad \beta \equiv \arg\left[-\frac{V_{cd}V_{cb}^*}{V_{td}V_{tb}^*}\right], \qquad \gamma \equiv \arg\left[-\frac{V_{ud}V_{ub}^*}{V_{cd}V_{cb}^*}\right].$$

They are physical quantities and can be measured independently in B decays.

We conclude this abstract of the Standard Model and give the numerical values for some of the parameters and show a plot (see Fig. 1.1) illustrating the present Standard Model constraints on the CKM matrix.

$$\begin{aligned} \lambda &= 0.2221 \pm 0.0021, & A &= 0.827 \pm 0.058, & & \\ \rho &= 0.23 \pm 0.11, & \eta &= 0.37 \pm 0.08, & & \\ \sin(2\beta) &= 0.77 \pm 0.08, & \sin(2\alpha) &= -0.21 \pm 0.56, & 0.43 \lesssim \sin^2\gamma &\leq 0.91\,. \end{aligned}$$

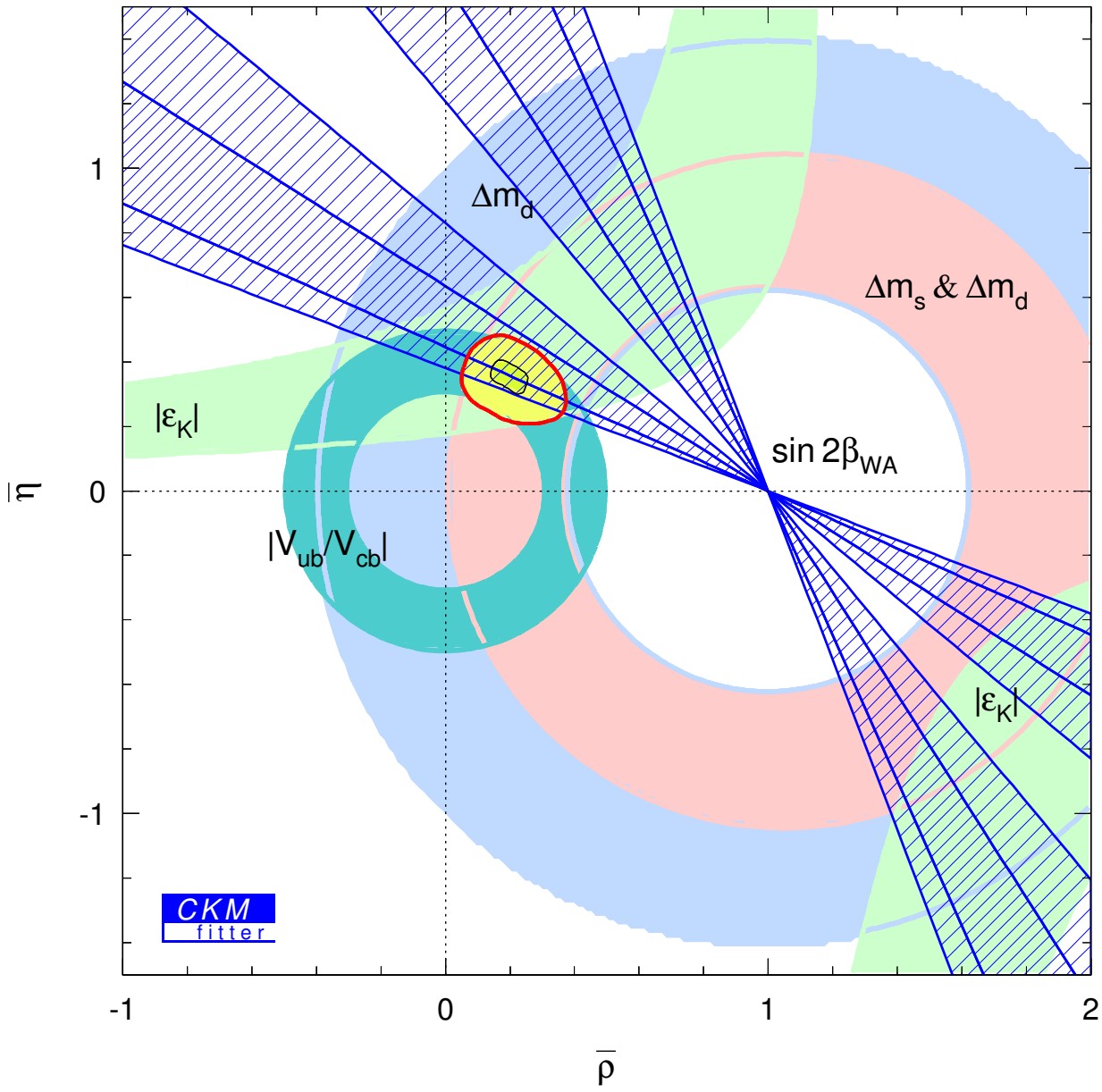

Figure 1.1: Present Standard Model constraints and the result from the global CKM fit visualized in the $\rho-\eta$ plane. This and further plots may be obtained from the "CKMfitter" home page [5].

2 Effective Hamiltonian

The strong interaction, binding quarks into hadrons, is characterized by the typical energy scale of hadrons [$\mathcal{O}(1\text{ GeV})$]. As we will discuss in Section 3, this allows to describe B decays by the corresponding b quark transitions, which involve the scale m_b [$\mathcal{O}(4.8\text{ GeV})$]. The decay of a b quark, on the other hand, is mediated through W and Z exchange, which involves the much higher scale $m_{W,Z}$. The fact that we have two energy scales of very different magnitude, ie $m_b \ll m_{W,Z}$, allows us to look for an expansion in the small parameter given by the ratio of these two scales.

The following example shows the basic idea of the effective theory describing weak interactions of quarks. In the Standard Model, the tree level amplitude for the transition $b\,c \to s\,c$ is given by

$$A = -\frac{4\,G_F}{\sqrt{2}}\,V_{cs}^* V_{cb}\,\frac{m_W^2}{k^2 - m_W^2}\,(\bar{s}_L\gamma_\mu c_L)(\bar{c}_L\gamma^\mu b_L).$$

The momentum transfer through the W propagator is much smaller than m_W. Therefore, we may expand the W propagator in terms of k^2/m_W^2:

$$A = \frac{4\,G_F}{\sqrt{2}}\,V_{cs}^* V_{cb}(\bar{s}_L\gamma_\mu c_L)(\bar{c}_L\gamma^\mu b_L) + \mathcal{O}\left(\frac{k^2}{m_W^2}\right).$$

The same result is obtained from the effective Hamiltonian

$$\mathcal{H}_{\text{eff}} = \frac{4\,G_F}{\sqrt{2}}\,V_{cs}^* V_{cb}(\bar{s}_L\gamma_\mu c_L)(\bar{c}_L\gamma^\mu b_L) + \text{higher dimensional operators.}$$

Neglecting terms of $\mathcal{O}(k^2/m_W^2)$, ie discarding higher dimensional operators, is an excellent approximation.

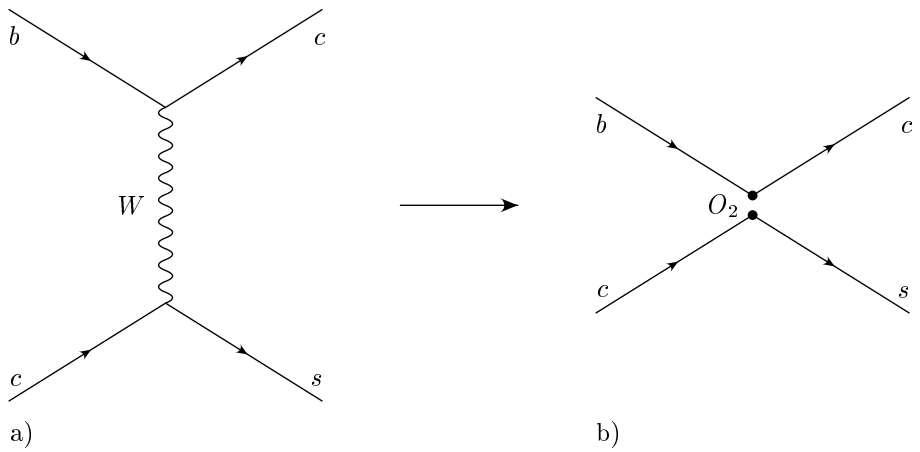

Figure 2.1: $b\,c \to s\,c$ at tree level in the full a) and effective theory b).

The general idea of the effective Hamiltonian technique is to integrate out *all* heavy degrees of freedom of a given theory. Formally, this is achieved in the framework of Operator Product Expansion (OPE). For an excellent introduction to effective Hamiltonians we refer to [6]. After integrating out the heavy fields, the higher dimensional operators, ie operators with dimension greater than six, are dropped. Notice that OPE is not an approximation by itself. We approximate by retaining the operators of dimension six only.

In this thesis we need the effective Hamiltonian that describes the process $b \to s\,\ell^+\ell^-$. It is of the form

$$\mathcal{H}_{\text{eff}} = \frac{4\,G_F}{\sqrt{2}} \left[\sum_{i=1}^{2} C_i(\lambda_c\, O_i^c + \lambda_u O_i^u) - \lambda_t \sum_{i=3}^{10} C_i\, O_i \right],$$

where $\lambda_q = V_{qs}^* V_{qb}$. O_i are dimension six operators and C_i are the corresponding Wilson coefficients. As long as we are not interested in CP asymmetries, we may further simplify $\mathcal{H}_{\text{eff}}$ by exploiting $|\lambda_u| \ll |\lambda_c| \approx |\lambda_t|$. Neglecting λ_u, we have, by the unitarity of the CKM matrix, $\lambda_c = -\lambda_t$ and thus

$$\mathcal{H}_{\text{eff}} = -\frac{4\,G_F}{\sqrt{2}}\,\lambda_t \sum_{i=1}^{10} C_i\, O_i\,.$$

Note that the last simplification is no longer valid for the process $b \to d\,\ell^+\ell^-$. The operators O_i are advantageously chosen as in [7]:

$$\begin{aligned}
O_1 &= (\bar{s}_L\gamma_\mu T^a c_L)(\bar{c}_L\gamma^\mu T^a b_L), & O_2 &= (\bar{s}_L\gamma_\mu c_L)(\bar{c}_L\gamma^\mu b_L),\\
O_3 &= (\bar{s}_L\gamma_\mu b_L)\textstyle\sum_q(\bar{q}\gamma^\mu q), & O_4 &= (\bar{s}_L\gamma_\mu T^a b_L)\textstyle\sum_q(\bar{q}\gamma^\mu T^a q),\\
O_5 &= (\bar{s}_L\gamma_\mu\gamma_\nu\gamma_\rho b_L)\textstyle\sum_q(\bar{q}\gamma^\mu\gamma^\nu\gamma^\rho q), & O_6 &= (\bar{s}_L\gamma_\mu\gamma_\nu\gamma_\rho T^a b_L)\textstyle\sum_q(\bar{q}\gamma^\mu\gamma^\nu\gamma^\rho T^a q),\\
O_7 &= \tfrac{e}{g_s^2} m_b(\bar{s}_L\sigma^{\mu\nu} b_R)F_{\mu\nu}, & O_8 &= \tfrac{1}{g_s} m_b(\bar{s}_L\sigma^{\mu\nu} T^a b_R)G^a_{\mu\nu},\\
O_9 &= \tfrac{e^2}{g_s^2}(\bar{s}_L\gamma_\mu b_L)\textstyle\sum_\ell(\bar{\ell}\gamma^\mu\ell), & O_{10} &= \tfrac{e^2}{g_s^2}(\bar{s}_L\gamma_\mu b_L)\textstyle\sum_\ell(\bar{\ell}\gamma^\mu\gamma_5\ell).
\end{aligned}$$

This basis has the advantage that no traces involving γ_5 have to be evaluated in calculations of physical processes. The operators O_i involve only light degrees of freedom, whereas the short distance effects are described through the Wilson coefficients C_i. The asymptotic freedom of QCD allows to reliably calculate the Wilson coefficients at high scales in fixed order perturbation theory. In the context of the Standard Model the heavy degrees of freedom are the t quark and the W and Z^0 boson. Extensions of the Standard Model involve additional heavy particles. At least in many popular extensions, these particles only affect the Wilson coefficients; the operators remain unchanged.

The Wilson coefficients are determined by matching the full theory to the effective theory. It turns out that the Wilson coefficients depend on $\alpha_s(\mu)\ln(m_W/\mu)$. If we choose $\mu = \mu_W \approx m_W$, these logarithms are small and the matching may be done in fixed order perturbation theory. However, the matrix elements of the operators O_i involve typically scales that are much lower; in the case of B decays of $\mathcal{O}(m_b)$. Consequently, the matrix elements depend on $\alpha_s(\mu)\ln(m_b/\mu)$. If we set $\mu = \mu_b \approx m_b$ in order to make these logarithms

small, we spoil the fixed order perturbation theory for the Wilson coefficients because $\alpha_s(\mu_b)\ln(m_W/\mu_b)$ is of $\mathcal{O}(1)$ now. The renormalization group (RG) technique allows us to sum these large logarithms. The renormalization group improved perturbation theory is organized as follows:
The leading logarithmic (LL) or leading order (LO) approximation collects all terms of the form

$$\left[\alpha_s(\mu)\,\ln\!\left(\frac{m_W}{\mu}\right)\right]^n.$$

The next-to-leading logarithmic (NLL) contribution consequently involves the resummation of the terms

$$\alpha_s(\mu)\left[\alpha_s(\mu)\,\ln\!\left(\frac{m_W}{\mu}\right)\right]^n.$$

For the construction of the effective Hamiltonian the fact that hadrons are bound states of quarks is irrelevant. However, once we want to calculate a physical process involving hadrons, we have to deal with non-perturbative matrix elements. As mentioned in the introduction, there exist different methods to achieve this task, each depending on the energy scale and class of process. The natural tool in the case of inclusive B decays is the heavy quark effective theory (HQET). To leading order in this expansion the hadronic matrix elements are given by the corresponding quark level transitions. The leading term of HQET can therefore be determined by ordinary perturbation theory.

3 Heavy Quark Effective Theory

The QCD Lagrangian describing a quark Q of mass m_Q and its interaction with gluons is given by

$$\mathcal{L} = \bar{\psi}_Q \, iD_\mu \gamma^\mu \psi_Q - m_Q \bar{\psi}_Q \psi_Q \,, \quad \text{where} \quad D_\mu = \partial_\mu - ig_s T^a A^a_\mu .$$

In the heavy quark limit ($m_Q \to \infty$), the velocity v_μ of the quark is conserved and its four-momentum may be decomposed into an on-shell part, $m_Q v_\mu$, and an off-shell part k_μ:

$$p_\mu = m_Q v_\mu + k_\mu, \quad \text{with} \quad v^2 = 1.$$

The components of the residual momentum k are much smaller than m_Q and are changed by interactions of the heavy quark with light degrees of freedom by $\Delta k \sim \Lambda_{\text{QCD}}$. The large- and small-component fields

$$h_v(x) \equiv \mathrm{e}^{imv\cdot x} \, \frac{1+\not{v}}{2} \, \psi_Q(x)$$

and

$$H_v(x) \equiv \mathrm{e}^{imv\cdot x} \, \frac{1-\not{v}}{2} \, \psi_Q(x)$$

satisfy $\not{v}\, h_v = h_v$ and $\not{v}\, H_v = -H_v$, respectively. Expressed in terms of the new fields, the quark field $\psi_Q(x)$ reads

$$\psi_Q(x) = \mathrm{e}^{-imv\cdot x}\big(h_v(x) + H_v(x)\big).$$

We may split the covariant derivative D into "longitudinal" and "transverse" parts:

$$D^\mu_\perp = D^\mu - v^\mu v\cdot D, \quad \text{with} \quad v\cdot D_\perp = 0, \quad \big\{\not{D}_\perp, \not{v}\big\} = 0.$$

Using relations as $\bar{h}_v H_v = 0$ and $\bar{h}_v \not{D}_\perp h_v = 0$, the Lagrangian $\mathcal{L}$ takes the form

$$\mathcal{L} = \bar{h}_v i(v\cdot D) h_v - \bar{H}_v (i\, v\cdot D + 2\, m_Q) H_v + \bar{h}_v i\not{D}_\perp H_v + \bar{H}_v i\not{D}_\perp h_v.$$

From this equation, taking the derivative with respect $\bar{H}_v$, we find the equation of motion

$$H_v = \frac{1}{2\, m_Q + i\, v\cdot D} \, i\, \not{D}_\perp h_v.$$

This allows us, on a classical level, to eliminate the heavy degree of freedom H_v from the Lagrangian:

$$\begin{aligned}\mathcal{L}_{\text{eff}} &= \bar{h}_v i(v\cdot D) h_v + \bar{h}_v i\not{D}_\perp \frac{1}{2\, m_Q + i\, v\cdot D} \, i\not{D}_\perp h_v \\ &= \bar{h}_v i(v\cdot D) h_v + \frac{1}{2\, m_Q} \sum_{n=0}^{\infty} \bar{h}_v i\not{D}_\perp \left(-\frac{i\, v\cdot D}{2\, m_Q}\right)^n i\not{D}_\perp h_v. \quad (2)\end{aligned}$$

It is possible to integrate out the heavy field H_v on the level of the generating functional for QCD Green functions. This approach yields the same effective Lagrangian $\mathcal{L}_{\text{eff}}$ (2).

$\mathcal{L}_{\text{eff}}$ can be written as

$$\mathcal{L}_{\text{eff}} = \bar{h}_v \, i(v \cdot D) h_v + \frac{1}{2\, m_Q} \bar{h}_v (iD_\perp)^2 h_v + \frac{g_s}{4\, m_Q} \bar{h}_v \, \sigma_{\mu\nu} \, G^{\mu\nu} h_v + \mathcal{O}(1/m_Q^2).$$

In the limit $m_Q \to \infty$, only the term

$$\mathcal{L}_\infty = \bar{h}_v \, i(v \cdot D) h_v.$$

survives. There appear neither Dirac matrices nor quark masses in this equation. For $m_Q \to \infty$, the interactions of heavy quarks and gluons become independent of the spin of the quark. Furthermore, when extending the theory to more than one heavy quark moving at the same velocity, the Lagrangian $\mathcal{L}_\infty$ is symmetric under rotations in the flavor space. This is the heavy-quark spin-flavor symmetry [8]. We refrain from some subtleties concerning the definition of the heavy quark mass m_Q and refer to [9] and references therein. The spin-flavor symmetry leads to many interesting relations between the properties, especially the spectroscopy, of hadrons containing a heavy quark. We go into further detail concerning this issue neither.

4 Inclusive Semileptonic Decays

We make some comments on inclusive decays, without going into detail. We mainly draw from [9]. Inclusive decay rates determine the probability of the decay of a particle into the sum of all possible final states with a given set of quantum numbers. Inclusive decays of hadrons containing a heavy quark can be analyzed using the heavy quark expansion. Furthermore, there is the hypothesis of quark-hadron duality. The assumption is that physical quantities are calculable after a "smearing" or "averaging" procedure has been applied. In the case of semileptonic decays the averaging is provided by integrating over the leptonic phase space. It provides a smearing of the invariant hadronic mass of the final state (so-called global duality). For non-leptonic decays, on the other hand, the hadronic mass is fixed, and the smearing effect comes only from the summation over many hadronic states (so-called local duality). Clearly, local duality is a stronger assumption than global duality. The quark-hadron duality, though it is a natural assumption, cannot be derived from first principles.

We make use of the optical theorem and write the decay width of a hadron H_b containing a b quark as

$$\Gamma(H_b \to X) = \mathrm{Im}\left[\frac{1}{2\,m_{H_b}}\langle H_b|\mathcal{T}|H_b\rangle\right].$$

The transition operator $\mathcal{T}$ is given by

$$\mathcal{T} = i\int d^4x\, T\big\{\mathcal{H}_{\rm eff}(x), \mathcal{H}_{\rm eff}(0)\big\}.$$

T denotes the time-ordering operator and $\mathcal{H}_{\rm eff}$ is the weak effective Lagrangian, obtained from the Standard Model by integrating out the heavy degrees of freedom (t, W and Z). Inserting a complete set of states, we recover the standard expression for the decay rate:

$$\Gamma(H_b \to X) = \frac{1}{2\,m_{H_b}}\sum_X (2\,\pi)^4\,\delta^4(p_H - p_X)\,\big|\langle X|\mathcal{H}_{\rm eff}|H_b\rangle\big|^2.$$

It is possible to construct an operator product expansion for the transition operator $\mathcal{T}$. The result is

$$\mathcal{T} = \Gamma_b\,\bar b b + \frac{Z_G}{m_b^2}\,\bar b\,\sigma_{\mu\nu} b\,G^{\mu\nu} + \sum\frac{z_i}{m_b^3}\big(\bar b\Gamma_i q\big)\big(\bar q\Gamma_i b\big) + \mathcal{O}\left(m_b^{-4}\right).$$

We apply the results of the last section and express $\langle H_b|\bar b b|H_b\rangle$ as

$$\langle H_b|\bar b b|H_b\rangle = 1 + \frac{1}{2\,m_b^2}\,\langle H_b|\bar h (iD)^2 h|H_b\rangle + \frac{1}{4\,m_b^2}\,\langle H_b|\bar h\sigma_{\mu\nu}G^{\mu\nu}h|H_b\rangle + \mathcal{O}\left(m_b^{-3}\right).$$

A few concluding remarks are appropriate:

- In the limit $m_b \to \infty$, the inclusive decay rate of a B meson is given by the decay rate of the underlying quark transition: $\Gamma_{H_b} = \Gamma_b$ $(m_b \to \infty)$.

- There are no corrections of $\mathcal{O}(1/m_b)$.
- The leading corrections, which are of $\mathcal{O}(1/m_b^2)$, are due to interactions of the b quark with the gluon field and to the fact that the b quark is not at rest.
- Spectator effects, accounting for non-perturbative contributions, contribute only at $\mathcal{O}(1/m_b^3)$.

This justifies the ansatz to approximate the inclusive B meson decays by the underlying quark level transition. The decay of a b quark may be analyzed in the framework of weak effective Hamiltonians. QCD corrections are calculated in ordinary perturbation theory because typical gluons carry momenta set by the scale $m_b \gg \Lambda_{\text{QCD}}$, ie we are in the region where asymptotic freedom applies.

In this work we calculate the $\mathcal{O}(\alpha_s)$ correction to the processes $b \to s\,\ell^+\ell^-$ and $b \to d\,\ell^+\ell^-$. The corrections to $B \to X_s\,\ell^+\ell^-$ due to the heavy quark matrix elements are discussed in Ref. [10].

5 Matching Calculation for O_1 and O_2 and Operator Mixing

In this chapter we look at an example for the matching procedure. This serves as an illustration of operator mixing and, later on, the renormalization group evolution of Wilson Coefficients.

Since the Wilson coefficients depend on the masses of the heavy particles only, we may set all light quark masses equal to zero. Retaining these masses finite would lead to terms proportional to m_q^2/m_W^2, ie give rise to higher dimensional operators. In the present case we thus set $m_q = 0$, where $q = u, d, c, s, b$. Note that in a matching calculation for O_7, for example, m_b as to be kept finite. The external momenta we choose to be all equal p with $p^2 < 0$. We do not put $p = 0$. This is to avoid infrared and collinear singularities.

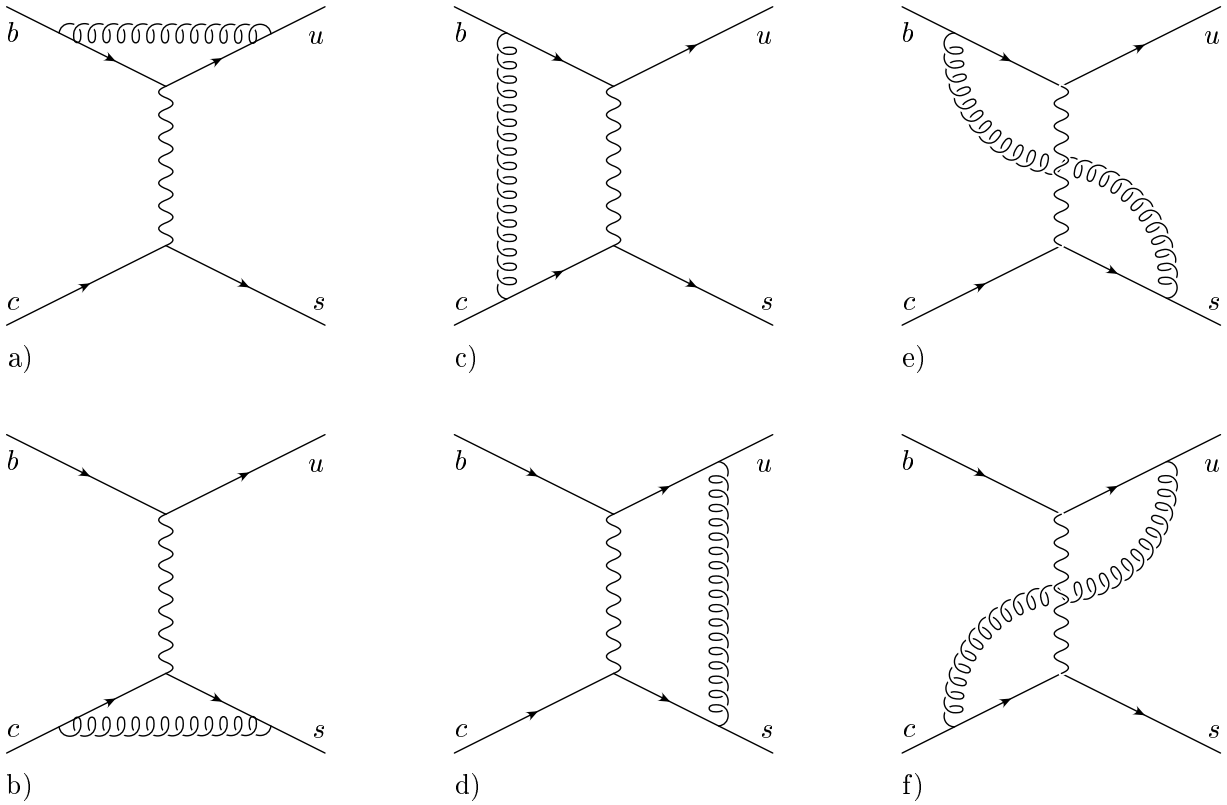

Figure 5.1: Feynman diagrams of $\mathcal{O}(\alpha_s)$ for the process $b\,c \to s\,u$ in the Standard Model.

5.1 Calculation of the Amplitude in the Full Theory

The relevant Feynman diagrams for the process $b\,c \to s\,u$ in the Standard Model are shown in Fig. 5.1. The diagrams where the W boson is replaced by an unphysical Higgs particle yield no contribution since all light quark masses are put to zero in the present calculation. The evaluation of the diagrams is straight forward. The contributions from diagrams 5.1c)-f) are ultraviolet finite and may be evaluated in $d = 4$ dimensions where the following relations hold:

$$\gamma_\alpha\gamma_\beta\gamma_\mu L \otimes \gamma^\alpha\gamma^\beta\gamma^\mu L = 16\,\gamma_\mu L \otimes \gamma^\mu L \quad \text{and} \quad \gamma_\alpha\gamma_\beta\gamma_\mu L \otimes \gamma^\mu\gamma^\beta\gamma^\alpha L = 4\,\gamma_\mu L \otimes \gamma^\mu L. \tag{3}$$

The sum of diagrams 5.1a)-f) and the counterterm associated with quark field renormalization is given by

$$A_{\text{full}}^{\text{ren}} = \frac{4\,G_F}{\sqrt{2}} V_{bc} V_{cd}^* \left[S_2 - 6\frac{\alpha_s}{4\,\pi}\,S_1\,\ln\!\left(-\frac{m_W^2}{p^2}\right) + 2\,C_F\frac{\alpha_s}{4\,\pi}\,S_2\,\ln\!\left(-\frac{\mu^2}{p^2}\right)\right], \tag{4}$$

where S_1 and S_2 denote the tree level matrix elements of the operators O_1 and O_2, respectively. Since we are working in the leading logarithmic (LL) approximation, we have discarded constant terms of $\mathcal{O}(\alpha_s)$.

5.2 Calculation of the Amplitude in the Effective Theory

To get the amplitude in the effective theory we have to calculate diagrams 5.2a)-f). The result reads

$$\langle O_1\rangle^{(0)} = 2\,C_F\,\frac{\alpha_s}{4\,\pi}\frac{1}{\epsilon} + \frac{N_c^2+5}{N_c}\frac{\alpha_s}{4\,\pi}\,S_1\left[\frac{1}{\epsilon} + \ln\!\left(-\frac{\mu^2}{p^2}\right)\right] + \frac{3(N_c^2-1)}{2\,N_c^2}\frac{\alpha_s}{4\,\pi}\,S_2\left[\frac{1}{\epsilon} + \ln\!\left(-\frac{\mu^2}{p^2}\right)\right],$$

$$\langle O_2\rangle^{(0)} = 2\,C_F\,\frac{\alpha_s}{4\,\pi}\,S_2\left[\frac{1}{\epsilon} + \ln\!\left(-\frac{\mu^2}{p^2}\right)\right] - 6\,\frac{\alpha_s}{4\,\pi}\,S_1\left[\frac{1}{\epsilon} + \ln\!\left(-\frac{\mu^2}{p^2}\right)\right].$$

Adding the tree level and quark field renormalization contributions yields

$$\langle O_1\rangle^{\text{qfr}} = S_1 + \frac{N_c^2+5}{N_c}\frac{\alpha_s}{4\,\pi}\,S_1\left[\frac{1}{\epsilon} + \ln\!\left(-\frac{\mu^2}{p^2}\right)\right] + \frac{3(N_c^2-1)}{2\,N_c^2}\frac{\alpha_s}{4\,\pi}\,S_2\left[\frac{1}{\epsilon} + \ln\!\left(-\frac{\mu^2}{p^2}\right)\right],$$

$$\langle O_2\rangle^{\text{qfr}} = S_2 + 2\,C_F\,\frac{\alpha_s}{4\,\pi}\,S_2\,\ln\!\left(-\frac{\mu^2}{p^2}\right) - 6\,\frac{\alpha_s}{4\,\pi}\,S_1\left[\frac{1}{\epsilon} + \ln\!\left(-\frac{\mu^2}{p^2}\right)\right]. \tag{5}$$

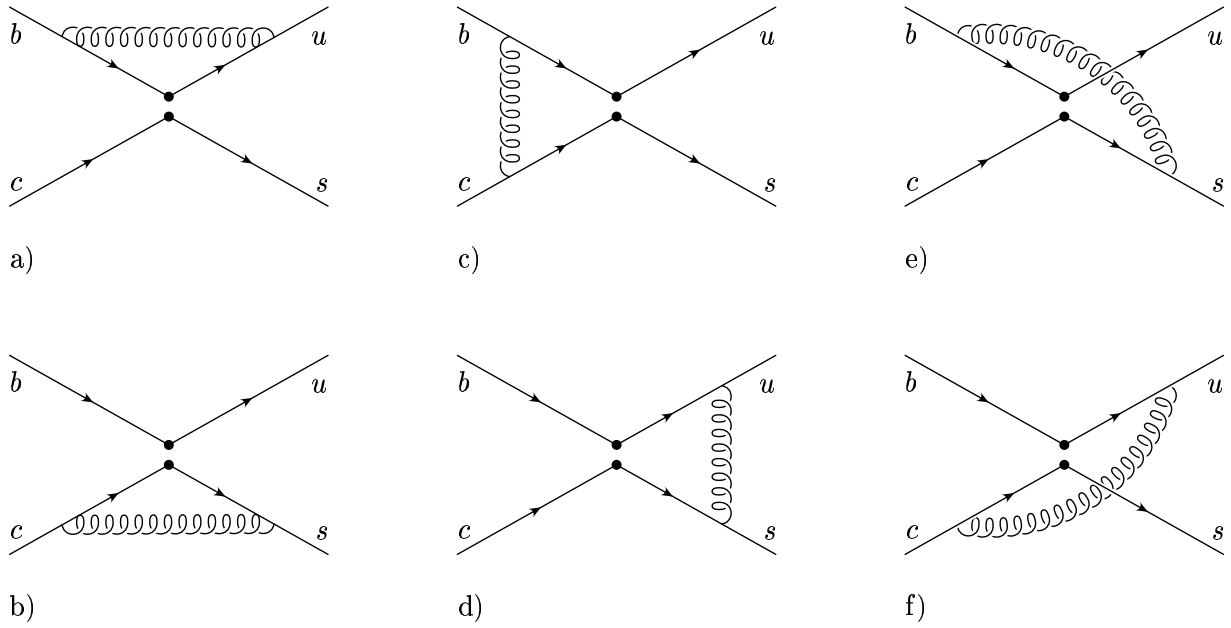

Figure 5.2: Feynman diagrams of $\mathcal{O}(\alpha_s)$ for the process $b\,c \to s\,u$ in the effective theory.

Again we have discarded constant terms of $\mathcal{O}(\alpha_s)$. The calculation of the relevant integrals had to be done in $4-2\,\epsilon$ dimensions. This causes the problem that Eqs. (3), valid for $d=4$, pick up a correction proportional to ϵ. This correction depends on the choice of the evanescent operators and is related to the issue of γ_5 in d dimensions . However, being of next-to-leading order these additional contributions do not affect the present calculation. The labels 'qfr' stand to indicate that the bare fields are expressed through the renormalized ones already, ie that we have included the counter terms associated with quark field renormalization:

$$q_{\text{bare}} = \sqrt{Z_2}\, q_{\text{ren}}, \quad \text{where} \quad Z_2 = 1 - C_F\, \frac{\alpha_s}{4\,\pi}\, \frac{1}{\epsilon}\,.$$

5.3 Operator Mixing

The divergences that have not been cancelled by the quark field renormalization have to be removed by operator renormalization. We introduce new operators O_j^{ren} according to

$$O_i = Z_{ij}\, O_j^{\text{ren}}$$

and require their matrix elements to be finite. The matrix Z can easily be read off from Eq. (5). The result is

$$Z = \mathbf{1} + \frac{\alpha_s}{4\,\pi}\,\frac{1}{\epsilon}\begin{pmatrix} \frac{6}{N_c} & -\frac{3(N_c^2-1)}{2\,N_c^2} \\ -6 & 0 \end{pmatrix} + \mathcal{O}(\alpha_s^2) = \mathbf{1} + \frac{\alpha_s}{4\,\pi}\,\frac{1}{\epsilon}\begin{pmatrix} 2 & -\frac{4}{3} \\ -6 & 0 \end{pmatrix} + \mathcal{O}(\alpha_s^2). \qquad (6)$$

Z being a matrix, the operators O_1 and O_2 mix under renormalization. This fact goes by the name of *operator mixing*. The renormalized matrix elements of O_1 and O_2 now read

$$\langle O_1\rangle^{\rm ren} = S_1 + \frac{N_c^2+5}{N_c}\frac{\alpha_s}{4\,\pi}\,S_1\,\ln\!\left(-\frac{\mu^2}{p^2}\right) - \frac{3(N_c^2-1)}{2\,N_c^2}\frac{\alpha_s}{4\,\pi}\,S_2\,\ln\!\left(-\frac{\mu^2}{p^2}\right), \quad \text{and}$$

$$\langle O_2\rangle^{\rm ren} = S_2 - 6\,\frac{\alpha_s}{4\,\pi}\,S_1\ln\!\left(-\frac{\mu^2}{p^2}\right) + \frac{N_c^2-1}{N_c}\frac{\alpha_s}{4\,\pi}\,S_2\,\ln\left(-\frac{\mu^2}{p^2}\right).$$

5.4 Wilson Coefficients

The Wilson coefficients C_1 and C_2 are determined by the requirement

$$A_{\rm full}^{\rm ren} = A_{\rm eff}^{\rm ren} = \frac{4\,G_F}{\sqrt{2}}V_{bc}V_{cd}^*\left[C_1\langle O_1\rangle^{\rm ren} + C_2\langle O_2\rangle^{\rm ren}\right],$$

and we immediately find

$$C_1(\mu) = 6\,\frac{\alpha_s}{4\,\pi}\,\ln\left(\frac{m_W^2}{\mu^2}\right) + \mathcal{O}(\alpha_s^2), \quad C_2(\mu) = 1 + \mathcal{O}(\alpha_s^2). \tag{7}$$

A different approach is to consider not only fields, masses and coupling constants in $\mathcal{H}_{\rm eff}$ but also the Wilson coefficients as bare quantities, ie we consider them as additional coupling constants. The bare Wilson coefficients in terms of the renormalized ones read

$$C_i^{\rm bare} = Z_{ij}^c\,C_j.$$

The effective Hamiltonian is then given by

$$\mathcal{H}_{\rm eff} = \frac{4\,G_F}{\sqrt{2}}V_{bc}V_{cd}^*\,C_j\,Z_{ij}^c\,\mathcal{Z}_{ik}^{m,q,g}\,O_k,$$

where O_i are composed of renormalized quantities only, and the diagonal matrix $\mathcal{Z}^{m,q,g}$ collects all factors associated with the renormalization of fields, masses and coupling constants. In the present case we have $\mathcal{Z}^{m,q,g} = Z_2^2\,\mathbf{1}$. The connection between the matrices Z and Z^c is obtained from

$$A_{\rm eff} = \frac{4\,G_F}{\sqrt{2}}V_{bc}V_{cd}^*\,C_j\left(Z^{-1}\right)_{ji}\mathcal{Z}_{ik}^{m,q,g}\langle O_k\rangle^0 = \frac{4\,G_F}{\sqrt{2}}V_{bc}V_{cd}^*\,C_j\,Z_{ij}^c\,\mathcal{Z}_{ik}^{m,q,g}\langle O_k\rangle^0.$$

We conclude

$$Z^{-1} = Z^{c^T}.$$

This alternative way of looking at renormalization is more suitable for the renormalization group treatment of the operator mixing. In the last step we have already generalized to an arbitrary number of operators that may possibly depend on masses and coupling constants.

6 Renormalization Group Equation

6.1 Renormalization of QCD

QCD is renormalized by expressing the bare quantities of the QCD Lagrangian through their renormalized counterparts:

$$g_s^{(0)} = \mu^\epsilon \, Z_g \, g_s, \qquad m^{(0)} = Z_m^{1/2} \, m, \tag{8}$$

$$G_\mu^{A(0)} = Z_3^{1/2} \, G_\mu^A, \qquad q^{(0)} = Z_2^{1/2} \, q. \tag{9}$$

The bare quantities are indicated by the superscript (0). In the $\overline{\text{MS}}$ scheme the renormalization constants to $\mathcal{O}(\alpha_s)$ read

$$Z_g = 1 - \frac{1}{\epsilon} \frac{\alpha_s}{4\,\pi} \left(\frac{11}{6} \, N_c - \frac{1}{3} \, N_f \right), \qquad Z_m = 1 - 3 \, C_F \frac{1}{\epsilon} \frac{\alpha_s}{4\,\pi},$$

$$Z_3 = 1 - \frac{1}{\epsilon} \frac{\alpha_s}{4\,\pi} \left(\frac{2}{3} \, N_c - \frac{5}{3} \, N_f \right), \qquad Z_2 = 1 - C_F \frac{1}{\epsilon} \frac{\alpha_s}{4\,\pi}.$$

They may be cast in the general form

$$Z_i = 1 + \sum_{k=1}^{\infty} \frac{Z_{i,k}(g_s)}{\epsilon^k}.$$

Physical quantities must be independent of the renormalization scale μ. This implies equations like

$$\mu \frac{d}{d\mu} g_s^{(0)} = 0.$$

The above requirement leads to the renormalization group equation

$$\mu \frac{d}{d\mu} g_s = -\epsilon g_s + \beta(g_s), \quad \text{with} \quad \beta(g_s) = -\frac{g_s}{Z_g} \left(\mu \frac{d}{d\mu} Z_g \right) = g_s^2 \frac{\partial Z_{g,1}}{\partial g_s}.$$

The last step shows that only the $1/\epsilon$ term is needed to get the β function $\beta(g_s)$. We define the constants β_i through

$$\beta(g_s) =: -\frac{g_s^3}{16\,\pi^2} \sum_{i=0}^{\infty} \beta_i \left(\frac{g_s^2}{16\,\pi^2} \right)^i.$$

The constants β_0 and β_1 are given by

$$\beta_0 = \frac{11\,N_c - 2\,N_f}{3} \quad \text{and} \quad \beta_1 = \frac{34}{3} \, N_c^2 - \frac{10}{3} \, N_c \, N_f - 2 \, C_F \, N_f.$$

Retaining the leading term of the β function, we have the following first order differential equation for α_s:

$$\mu\frac{d}{d\mu}\alpha_s(\mu) = -2\,\beta_0\frac{\alpha_s^2(\mu)}{4\,\pi}\,,$$

with the solution

$$\alpha_s(\mu) = \frac{\alpha_s(\mu_0)}{1+\beta_0\frac{\alpha_s(\mu_0)}{4\,\pi}\ln\left(\frac{\mu^2}{\mu_0^2}\right)}\,. \tag{10}$$

$\alpha_s(\mu_0 = m_Z)$ can be extracted from LEP precision measurements. In the $\overline{\rm MS}$ scheme one finds $\alpha_s(m_Z) = 0.118\pm0.003$, which we may take as initial condition for the renormalization group equation. In the range $m_b \le \mu \le m_t$ we have $N_f = 5$. Together with $N_c = 3$ this yields $\beta_0 = \frac{23}{3}$.

Similarly, we find

$$\mu\frac{d}{d\mu}m^{(0)} = 0 \quad \Rightarrow \quad \mu\frac{d}{d\mu}m(\mu) = -\gamma_m m(\mu),$$

with the anomalous dimension of the mass operator

$$\gamma_m(g_s) = \frac{1}{Z_m}\mu\frac{d}{d\mu}Z_m = -g_s\frac{\partial Z_m}{\partial g_s}\,.$$

We may decompose γ_m as

$$\gamma_m(g_s) = \gamma_m^{(0)}\frac{g_s^2(\mu)}{16\,\pi^2} + \gamma_m^{(1)}\frac{g_s^4(\mu)}{(16\,\pi^2)^2} + \mathcal{O}\left(g_s^6(\mu)\right),$$

where the leading term of γ_m is determined by

$$\gamma_m^{(0)} = 6\,C_F.$$

To the lowest order in the β and γ_m functions, the solution to the differential equation for $m(\mu)$ is

$$m(\mu) = m(\mu_0)\left[\frac{\alpha_s(\mu)}{\alpha_s(\mu_0)}\right]^{\frac{\gamma_m^{(0)}}{2\,\beta_0}}\,.$$

6.2 RGE for the Wilson Coefficients

As mentioned before, the relation between bare and renormalized Wilson coefficients is given by

$$\vec{C}^{(0)} = (Z^{-1})^T\vec{C}.$$

The starting point for finding the renormalization group equations for the Wilson coefficients C_i is

$$\mu\frac{d}{d\mu}\vec{C}^{(0)} = \left(\mu\frac{d}{d\mu}{Z^{-1}}^T\right)\vec{C} + {Z^{-1}}^T\left(\mu\frac{d}{d\mu}\vec{C}\right) = 0.$$

This gives rise to the equation

$$\mu \frac{d}{d\mu} \vec{C} = \gamma^T \vec{C},$$

where the anomalous dimension matrix $\gamma = \gamma(g_s(\mu))$ is defined as

$$\gamma := Z^{-1} \mu \frac{d}{d\mu} Z. \tag{11}$$

We may write the solution to this equation in terms of an evolution matrix $U(\mu, \mu_W)$

$$\vec{C}(\mu) = U(\mu, \mu_W) \vec{C}(\mu_W),$$

which solves the same differential equation as $\vec{C}$:

$$\mu \frac{d}{d\mu} U(\mu, \mu_W) = \gamma^T U(\mu, \mu_W).$$

The general solution to this equation is given by

$$U(\mu, \mu_W) = 1 + \int_{g(\mu_W)}^{g(\mu)} dg_1 \, \frac{\gamma^T(g_1)}{\beta(g_1)} + \int_{g(\mu_W)}^{g(\mu)} dg_1 \int_{g(\mu_W)}^{g_1} dg_2 \, \frac{\gamma^T(g_1)}{\beta(g_1)} \frac{\gamma^T(g_2)}{\beta(g_2)} + \dots . \tag{12}$$

For $g(\mu) > g(\mu_W)$, the g-ordering operator T_g is defined through

$$T_g \, f(g_1) \dots f(g_n) = \sum_{\text{perm}} \Theta(g_{i_1} - g_{i_2}) \dots \Theta(g_{i_{n-1}} - g_{i_n}) \, f(g_{i_1}) \dots f(g_{i_n}).$$

The sum runs over all permutations $\{i_1, ..., i_n\}$ of $\{1, ..., n\}$. T_g provides ordering of the functions $f(g_i)$ such that the arguments g_i increase from left to right. g-ordering is necessary because, in general, the matrices $\gamma(g_1)$ and $\gamma(g_2)$ do not commute. The operator T_g allows us to write Eq. (12) in a more compact way:

$$U(\mu, \mu_W) = T_g \, \exp\left[\int_{g(\mu_W)}^{g(\mu)} dg' \, \frac{\gamma^T(g')}{\beta(g')} \right]. \tag{13}$$

Expanding the anomalous dimension matrix in the usual perturbative way,

$$\gamma(\alpha_s) = \gamma^{(0)} \frac{\alpha_s}{4\,\pi} + \gamma^{(1)} \left(\frac{\alpha_s}{4\,\pi} \right)^2 + \mathcal{O}(\alpha_s^3),$$

we readily find the LL approximation for $U(\mu, \mu_W)$:

$$U^{(0)}(\mu, \mu_W) = V \left(\eta^{\frac{\tilde{\gamma}^{(0)}}{2\,\beta_0}} \right)_D V^{-1},$$

where

$$\gamma_D^{(0)} = V^{-1}\gamma^{(0)T}V \quad \text{and} \quad \eta = \frac{\alpha_s(\mu_W)}{\alpha_s(\mu)}\,.$$

The vector $\vec{\gamma}^{(0)}$ contains the diagonal elements of the diagonal matrix $\gamma_D^{(0)}$.

Next, we consider the derivation of the NLL correction to the evolution matrix $U(\mu,\mu_W)$. We make the ansatz

$$U(\mu,\mu_W) = \left[1 + \frac{\alpha_s(\mu)}{4\,\pi}\,J\right] U^{(0)}(\mu,\mu_W) \left[1 - \frac{\alpha_s(\mu_W)}{4\,\pi}\,J\right].$$

Differentiating this equation and Eq. (13) with respect to $g(\mu)$ and expanding up to $\mathcal{O}(g_s^2)$ yields

$$2\,J + \left[\frac{\gamma^{(0)T}}{\beta_0}, J\right] = -\frac{\gamma^{(1)T}}{\beta_0} + \gamma^{(0)T}\frac{\beta_1}{\beta_0^2}\,. \tag{14}$$

In the basis where $\gamma^{(0)}$ is diagonal and with the definitions

$$J_D := V^{-1}J\,V \quad \text{and} \quad G := V^{-1}\gamma^{(1)T}V,$$

the solution to Eq. (14) is obtained easily. We get

$$(J_D)_{ij} = \frac{\beta_1}{2\,\beta_0^2}\,\delta_{ij}\Gamma_i - \frac{\left(\gamma_D^{(1)}\right)_{ij}}{2\,\beta_0 + \Gamma_i - \Gamma_j}\,,$$

where Γ_i are the eigenvalues of $\gamma^{(0)T}$, ie $\vec{\gamma}^{(0)} = (\Gamma_1, ..., \Gamma_n)$. The leading and next-to-leading logarithmic approximations to the Wilson coefficients

$$\vec{C} = \vec{C}^{(0)} + \frac{\alpha_s}{4\,\pi}\,\vec{C}^{(1)} + \mathcal{O}(\alpha_s^2)$$

are then given by

$$\vec{C}^{(0)}(\mu) = U^{(0)}\vec{C}^{(0)}(\mu_W),$$

$$\vec{C}^{(1)}(\mu) = \eta\,U^{(0)}\vec{C}^{(1)}(\mu_W) + \left[J\,U^{(0)} - \eta\,U^{(0)}\,J\right]\vec{C}^{(0)}(\mu_W).$$

We decompose the renormalization matrix Z according to

$$Z = \mathbf{1} + \frac{1}{\epsilon}\frac{\alpha_s}{4\,\pi}Z^{(1)} + \mathcal{O}\left(\alpha_s^2\right).$$

To leading order, the connection between the renormalization matrix Z and the anomalous dimension matrix γ is given by the equation

$$\gamma_{ij}^{(0)} = -2\,Z_{ij}^{(1)}. \tag{15}$$

The leading order contribution to the anomalous dimension matrix reads [7]

$$\gamma^{(0)} = \begin{pmatrix} -4 & \frac{8}{3} & 0 & -\frac{2}{9} & 0 & 0 & 0 & 0 & -\frac{32}{27} & 0 \\ 12 & 0 & 0 & \frac{4}{3} & 0 & 0 & 0 & 0 & -\frac{8}{9} & 0 \\ 0 & 0 & 0 & -\frac{52}{3} & 0 & 2 & 0 & 0 & -\frac{16}{9} & 0 \\ 0 & 0 & -\frac{40}{9} & -\frac{100}{9} & \frac{4}{9} & \frac{5}{6} & 0 & 0 & \frac{32}{27} & 0 \\ 0 & 0 & 0 & -\frac{256}{3} & 0 & 20 & 0 & 0 & -\frac{112}{9} & 0 \\ 0 & 0 & -\frac{256}{9} & \frac{56}{9} & \frac{40}{9} & -\frac{2}{3} & 0 & 0 & \frac{512}{27} & 0 \\ 0 & 0 & 0 & 0 & 0 & 0 & \frac{32}{3} - 2\,\beta_0 & 0 & 0 & 0 \\ 0 & 0 & 0 & 0 & 0 & 0 & -\frac{32}{9} & \frac{28}{3} - 2\,\beta_0 & 0 & 0 \\ 0 & 0 & 0 & 0 & 0 & 0 & 0 & 0 & -2\,\beta_0 & 0 \\ 0 & 0 & 0 & 0 & 0 & 0 & 0 & 0 & 0 & -2\,\beta_0 \end{pmatrix}.$$

The upper left 2×2 block of $\gamma^{(0)}$ is readily obtained from Eq. (6) using relation (15). To conclude, we explicitly solve the renormalization group equation for C_1 and C_2 to leading order. This is rather simple, because the operators O_i, $i > 2$ do not mix into O_1 and O_2. To leading order, the problem is thus only two dimensional. The aforementioned block we denote by $\widetilde{\gamma}^{(0)}$. After diagonalization of $\widetilde{\gamma}^{(0)}$ we find

$$\widetilde{U}^{(0)}(\mu, m_W) = \begin{pmatrix} -3 & \frac{3}{2} \\ 1 & 1 \end{pmatrix} \begin{pmatrix} \eta^{-\frac{8}{2\,\beta_0}} & 0 \\ 0 & \eta^{\frac{4}{2\,\beta_0}} \end{pmatrix} \begin{pmatrix} -\frac{2}{9} & \frac{1}{3} \\ \frac{2}{9} & \frac{2}{3} \end{pmatrix}.$$

The Wilson coefficients $C_1(\mu)$ and $C_2(\mu)$ are then given by

$$C_1^{(0)}(\mu) = \eta^{\frac{6}{23}} - \eta^{-\frac{12}{23}},$$

$$C_2^{(0)}(\mu) = \frac{2}{3}\,\eta^{\frac{6}{23}} + \frac{1}{3}\,\eta^{-\frac{12}{23}}.$$

Inserting expression (10) into $\eta = \alpha_s(m_W)/\alpha_s(\mu)$ and expanding up to $\mathcal{O}\big(\alpha_s(m_W)\big)$ we recover the solutions (7).

6.3 Renormalization of Composite Operators

In the previous chapter we considered the mixing of the operators O_1 and O_2. In general, the operator mixing is somewhat subtler, ie we have to take into account the different

canonical dimensions of the operators. We follow Ref. [11]. In d space-time dimensions the fields and coupling constants bare dimension

$$[q] = [q^{(0)}] = \frac{d-1}{2}\,, \qquad [G^A_\mu] = [G^{A(0)}_\mu] = \frac{d-2}{2}\,,$$
$$[g_s^{(0)}] = \frac{4-d}{2}\,, \qquad [g_s] = 0.$$

The dimensions of the operators O_i are

$$[O_{1,\ldots,6}] = [O^{(0)}_{1,\ldots,6}] = 2\,d-2, \qquad [O_7^{(0)}] = \frac{5\,d}{2} - 4, \qquad [O_{9,10}] = 2\,d-2,$$
$$[O_{7,8}] = \frac{3\,d}{2}, \qquad [O_8^{(0)}] = 2\,d-2, \qquad [O^{(0)}_{9,10}] = 3\,d-6.$$

We define the dimensionless renormalization matrix

$$Z := \mathbf{1} + \frac{1}{\epsilon}\frac{\alpha_s}{4\,\pi}\,Z^{(1)} + \mathcal{O}(\alpha_s)$$

through

$$O_j(\mu) = \sum_i \mu^{2\epsilon D_j}\left(Z^{-1}\right)_{ji}\,\mu^{-2\epsilon D_i^{(0)}}\,O_i^{(0)}.$$

The constants D_i, $D_i^{(0)}$ are defined by

$$2\,\epsilon\,D_i = [O_i] - (2\,d-2), \quad 2\,\epsilon\,D_i^{(0)} = [O_i^{(0)}] - (2\,d-2).$$

Consequently, we have to replace Eq. (11) by

$$\gamma = \widetilde{Z}^{-1}\mu\frac{d}{d\mu}\widetilde{Z},$$

where

$$\widetilde{Z} = \mathrm{diag}\left(\mu^{2\,\epsilon\vec{D}^{(0)}}\right)\,Z\,\mathrm{diag}\left(\mu^{-2\,\epsilon\vec{D}}\right).$$

The connection between the anomalous dimension matrix γ and the renormalization matrix Z reads, to $\mathcal{O}(\alpha_s)$,

$$\gamma_{ij} = -2\,\frac{\alpha_s}{4\,\pi}\,Z^{(1)}_{ij}\left(1 + D_j^{(0)} - D_i^{(0)}\right).$$

7 LL, NLL and NNLL Contributions to the transition $b \to s\,\ell^+\ell^-$

We want to conclude Part I of this thesis with some comments on the operators O_9 and O_{10}, and say a few clarifying words about the organization of our calculation of the virtual corrections to $b \to s\,\ell^+\ell^-$. The latter is necessary because otherwise the leading logarithmic (LL), next-to-leading logarithmic (NLL),... counting, as used in our papers, might cause confusion in some points.

In the Standard Model, the process $b \to s\,\ell^+\ell^-$ takes place only on the one-loop level. The relevant $\mathcal{O}(\alpha_s^0)$ diagrams are shown in Fig. 7.1.

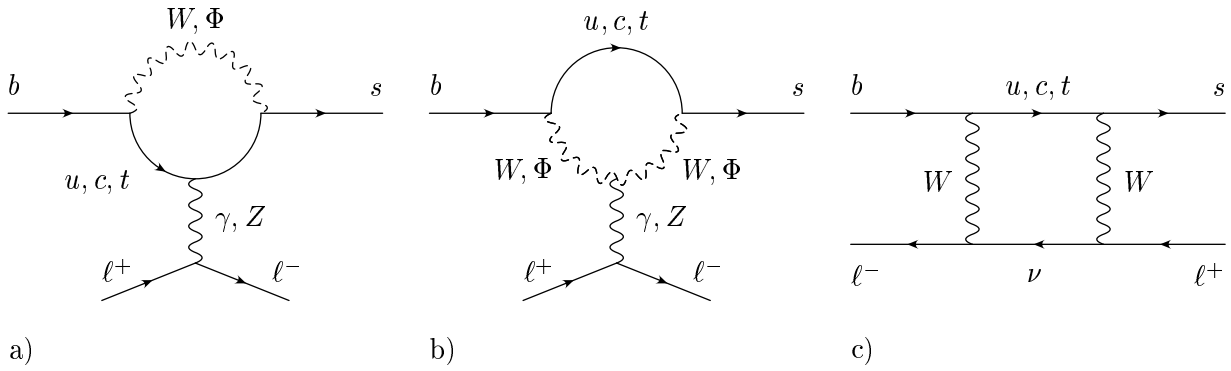

Figure 7.1: Leading order Standard Model Feynman diagrams for the process $b \to s\,\ell^+\ell^-$. a), b) Photonic and Z^0 penguins, c) box diagram.

The operators

$$O_9 = \frac{e^2}{g_s^2}\,(\bar{s}_L\gamma_\mu b_L)\sum_\ell \left(\bar{\ell}\gamma^\mu\ell\right),$$

$$\text{and} \qquad O_{10} = \frac{e^2}{g_s^2}\,(\bar{s}_L\gamma_\mu b_L)\sum_\ell \left(\bar{\ell}\gamma^\mu\gamma_5\ell\right),$$

on the other hand, have non-vanishing tree-level matrix elements contributing to the transition $b \to s\,\ell^+\ell^-$:

$$\langle s\,\ell^+\ell^-|O_9|b\rangle = \frac{e^2}{g_s^2}\big(\bar{u}_s(p')\gamma_\mu L u_b(p)\big) \times \big(\bar{u}_\ell\gamma^\mu v_\ell\big),$$

$$\langle s\,\ell^+\ell^-|O_{10}|b\rangle = \frac{e^2}{g_s^2}\big(\bar{u}_s(p')\gamma_\mu L u_b(p)\big) \times \big(\bar{u}_\ell\gamma^\mu\gamma_5 v_\ell\big).$$

In order to determine the Wilson coefficients C_9 and C_{10}, the amplitude needs to be calculated in the full and in the effective theory. We do not present the calculation of the

individual diagrams and merely give the results, which may be expressed through the following functions:

$$
\begin{aligned}
B_0(x_t) &= \frac{1}{4}\left[\frac{x_t}{1-x_t} + \frac{x_t\,\ln x_t}{(x_t-1)^2}\right], \\
C_0(x_t) &= \frac{x_t}{8}\left[\frac{x_t-6}{x_t-1} + \frac{3\,x_t+2}{(x_t-1)^2}\ln x_t\right], \\
D_0(x_t) &= -\frac{4}{9}\ln x_t - \frac{19\,x_t^3-25\,x_t^2}{36(x_t-1)^3} + \frac{5\,x_t^4-2\,x_t^3-6\,x_t^2}{18(x_t-1)^4}\ln x_t, \\
\widetilde{D}_0(x_t) &= D_0(x_t) - \frac{4}{9},
\end{aligned}
$$

where $x_t = m_t^2/m_W^2$. The function $B_0(x_t)$ results from the evaluation of the box diagrams, $C_0(x_t)$ from the Z^0 penguins and $D_0(x_t)$ from the photon penguins. The basic functions $B_0(x_t)$, $C_0(x_t)$ and $D_0(x_t)$ have been calculated by several authors, mainly by Inami and Lim [12]. At the scale $\mu_W = m_W$, the Wilson coefficients C_9 and C_{10} are given by

$$
C_9(m_W) = \frac{\alpha_s(m_W)}{4\,\pi}\left[4\,C_0(x_t) + \widetilde{D}_0(x_t) + \frac{1}{\sin^2\theta_W}\big(10\,B_0(x_t) - 4\,C_0(x_t)\big)\right],
$$

$$
C_{10}(m_W) = \frac{\alpha_s(m_W)}{4\,\pi}\left[4\,C_0(x_t) + \widetilde{D}_0(x_t)\right].
$$

At the matching scale m_W both C_9 and C_{10} have a vanishing $\mathcal{O}(\alpha_s^0)$ contribution. Evolving the Wilson coefficients to a lower scale, however, yields a non-vanishing contribution C_9^0.

At the scale m_W, the operator O_2 is the only one with a non-vanishing leading contribution, ie $C_i^{(0)}(m_W) = \delta_{i2}$. To get the leading order term of C_9 at a scale μ, it therefore suffices to consider the part of the anomalous dimension matrix describing the mixing between O_2 and O_9. It is given by

$$
\widetilde{\gamma}^{(0)} = \begin{pmatrix} 0 & -\frac{8}{9} \\ 0 & 2\,\beta_0 \end{pmatrix}.
$$

Following the exposition presented in Section 6.2, we find

$$
\widetilde{U}^{(0)}(\mu_b, m_W) = \begin{pmatrix} 1 & 0 \\ -\frac{4}{9\,\beta_0}\,(1-\eta^{-1}) & \eta^{-1} \end{pmatrix}.
$$

From this we readily obtain the leading contribution to C_9:

$$
C_9^{(0)}(\mu_b) = -\frac{4}{9\,\beta_0}\left(1-\eta^{-1}\right) C_2^{(0)}(m_W) = -\frac{4}{9\,\beta_0}\left(1-\eta^{-1}\right).
$$

Note that, because O_2 does not mix into O_{10}, we have $C_{10}^{(0)}(\mu) \equiv 0$.
The formally leading term to the amplitude $b \to s\,\ell^+\ell^-$ is given by

$$A_{\rm LL} = C_9^{(0)}(\mu_b)\langle s\,\ell^+\ell^-|O_9|b\rangle_{\rm tree}$$

and collects all terms of the form $1/g_s^2\big[g_s^2\ln(m_W/\mu)\big]^n$. For the decay $b \to s\,\ell^+\ell^-$, the nomenclature is therefore as follows:

$$\begin{aligned}
\frac{1}{g_s^2}\left[g_s^2\ln\left(\frac{m_W}{\mu_b}\right)\right]^n \quad &\longrightarrow \quad \text{LL} \qquad (n=1,2,3,\ldots)\\
\left[g_s^2\ln\left(\frac{m_W}{\mu_b}\right)\right]^n \quad &\longrightarrow \quad \text{NLL} \qquad (n=0,1,2,\ldots)\\
g_s^2\left[g_s^2\ln\left(\frac{m_W}{\mu_b}\right)\right]^n \quad &\longrightarrow \quad \text{NNLL} \quad (n=0,1,2,\ldots)\\
&\vdots\\
&\cdot
\end{aligned}$$

At next-to-leading order, we get contributions also from other operators, viz $O_7(\mu_b)$ and $O_{10}(\mu_b)$ contribute at tree-level and O_1,...,O_6 at one-loop level. The NLL part to the amplitude is composed as follows

$$\begin{aligned}
A_{\rm NLL} = \sum_{i=1}^{6} C_i^{(0)}\langle O_i\rangle_{\text{1-loop}} + \frac{g_s^2}{16\,\pi^2}\,C_7^{(1)}\langle O_7\rangle_{\rm tree} + C_9^{(0)}\langle O_9\rangle_{\text{1-loop}}\\
+ \frac{g_s^2}{16\,\pi^2}\,C_9^{(1)}\langle O_9\rangle_{\rm tree} + C_{10}^{(1)}\langle O_{10}\rangle_{\rm tree}.
\end{aligned}$$

Because the leading term, $\widetilde{A}_{\rm LL}$, is numerically smaller than the next-to-leading contribution $\big[g_s^2/(16\,\pi^2)\big]C_9^{(1)}\langle O_9\rangle_{\rm tree} + C_9^{(0)}\langle O_9\rangle_{\text{1-loop}}$, we have decided to adapt the systematics to the numerical situation and to treat the LL term as a NLL contribution. The amplitude then starts at NLL only:

$$\widetilde{A}_{\rm LL} = 0, \quad \widetilde{A}_{\rm NLL} = A_{\rm LL} + A_{\rm NLL}.$$

As the Wilson coefficients of the gluonic penguin operators O_3,...,O_6 are much smaller than $C_1(\mu_b)$, $C_2(\mu_b)$ we may safely neglect QCD corrections to their matrix elements in the NNLL approximation. One of the main tasks completed in this thesis is the calculation of the virtual $\mathcal{O}(\alpha_s)$ corrections to the matrix elements of O_1 and O_2. Further NNLL terms arise from the one-loop corrections to O_7, O_8 and O_{10}. A complete NNLL calculation

would also require the two-loop matrix elements to the operator O_9. However, it turned out that numerically the NLL corrections associated with O_9 are of the order of the NNLL corrections to O_1 and O_2. We have therefore omitted the two-loop contributions from O_9 in our analysis. Unfortunately, we have not explicitly communicated this issue in our publications. The following NNLL terms are taken into account in our calculation:

$$\begin{aligned}\widetilde{A}_{\text{NNLL}} = &\sum_{i=1}^{2}\left(C_i^{(0)}\langle O_i\rangle_{\text{2-loop}} + \frac{g_s^2}{16\,\pi^2}\,C_i^{(1)}\langle O_i\rangle_{\text{1-loop}}\right)\\ &+\frac{g_s^2}{16\,\pi^2}\,C_7^{(1)}\langle O_7\rangle_{\text{1-loop}} + \frac{g_s^4}{(16\,\pi^2)^2}\,C_7^{(2)}\langle O_7\rangle_{\text{tree}} + \frac{g_s^2}{16\,\pi^2}\,C_8^{(1)}\langle O_8\rangle_{\text{1-loop}}\\ &+\sum_{i=9}^{10}\left(\frac{g_s^2}{16\,\pi^2}\,C_i^{(1)}\langle O_i\rangle_{\text{1-loop}} + \frac{g_s^4}{(16\,\pi^2)^2}\,C_i^{(2)}\langle O_i\rangle_{\text{tree}}\right).\end{aligned}$$

References

[1] Y. Nir, Lectures given at the **"55$^{\text{th}}$ Scottish Universities Summer School of Physics"** on **"Heavy Flavour Physics"**, hep-ph/0109090.

[2] V. I. Borodulin, R. N. Rogalyov and S. R. Slabospitsky, hep-ph/9507456.

[3] L. Chau and W. Keung, *Phys. Rev. Lett.* **53** (1984) 1802.

[4] L. Wolfenstein, *Phys. Rev. Lett.* **51** (1983) 1945.

[5] CKM fitter home page
http://www.slac.stanford.edu/~laplace/ckmfitter/ckm_wellcome.html.

[6] A. J. Buras, hep-ph/9806471.

[7] C. Bobeth, M. Misiak and J. Urban, *Nucl. Phys.* **B 574** (2000) 291, hep-ph/9910220.

[8] N. Isgur and M. B. Wise,
Phys. Lett. **B 232** (1989) 113, *Phys. Lett.* **B 237** (1990) 527.

[9] M. Neubert, *Adv. Ser. Direct. High Energy Phys.***15** (1998) 239, hep-ph/9702375.

[10] A. Ali, C. Greub, G. Hiller and E. Lunghi, hep-ph/0112300,
to appear in *Phys. Rev.* **D**.

[11] B. Grinstein, R. Springer and M. B. Wise, *Nucl. Phys.* **B 339** (1990) 269.

[12] T. Inami and C. S. Lim,
Prog. Theor. Phys. **65** (1981) 297, *Prog. Theor. Phys.* **65** (1981) 1772 (E).

PART II

Two-loop Virtual Corrections to $B \to X_s \ell^+ \ell^-$ in the Standard Model

published in

Physics Letters B 507 (2001) 162

BUTP–01/6
hep-ph/0103087
Phys. Lett. **B 507** (2001) 162

Two-loop Virtual Corrections to $B \to X_s \ell^+\ell^-$ in the Standard Model [1]

H. H. Asatryan[a], H. M. Asatrian[a], C. Greub[b] and M. Walker[b]

[a] *Yerevan Physics Institute, 2 Alikhanyan Br., 375036 Yerevan, Armenia*
[b] *Institut für Theoretische Physik, Universität Bern, CH–3012 Bern, Switzerland.*

ABSTRACT

We calculate $O(\alpha_s)$ two-loop virtual corrections to the differential decay width $d\Gamma(B \to X_s \ell^+\ell^-)/d\hat{s}$ where $\hat{s}$ is the invariant mass squared of the lepton pair, normalized to m_b^2. We also include those contributions from gluon bremsstrahlung which are needed to cancel infrared and collinear singularities present in the virtual corrections. Our calculation is restricted to the range $0.05 \leq \hat{s} \leq 0.25$ where the effects from resonances are small. The new contributions drastically reduce the renormalization scale dependence of existing results for $d\Gamma(B \to X_s \ell^+\ell^-)/d\hat{s}$. For the corresponding branching ratio (restricted to the above $\hat{s}$ range) the renormalization scale uncertainty gets reduced from $\sim \pm 13\%$ to $\sim \pm 6.5\%$.

[1] Work partially supported by Schweizerischer Nationalfonds and SCOPES program

1 Introduction

After the observation of the penguin-induced decay $B \to X_s\,\gamma$ [1] and the corresponding exclusive channels such as $B \to K^*\gamma$ [2], rare B decays have begun to play an important role in the phenomenology of particle physics. The measured decay rates are in good agreement with the Standard Model (SM) predictions, putting strong constraints on its various extensions. Another interesting decay mode in this context is the inclusive transition $B \to X_s\,\ell^+\ell^-$ ($\ell = e, \mu$). It has not been observed so far [3], but its detection is expected at the B factories which are currently running. It is known that, unlike for $B \to X_s\,\gamma$, large resonant contributions from $\bar{c}c$ intermediate states come into the game when considering $B \to X_s\,\ell^+\ell^-$. When the invariant mass $\sqrt{s}$ of the lepton pair is close to the mass of a resonance, only model dependent predictions for these long distance contributions are available today. It is therefore unclear whether integrating the decay rate over these domains can reduce the theoretical uncertainty below $\pm 20\%$ [4].

However, when restricting to regions of $\sqrt{s}$ below the resonances, the long distance effects are under control. In particular, all the available studies indicate that for the region $0.05 \leq \hat{s} = s/m_b^2 \leq 0.25$ these non–perturbative effects are below 10% [5]–[10]. Consequently, the differential decay rate for $B \to X_s\,\ell^+\ell^-$ can be predicted precisely in this region using renormalization group improved perturbation theory.

It is known that the next-to-leading logarithmic (NLL) result for the $B \to X_s\,\ell^+\ell^-$ decay rate suffers from a relatively large ($\pm 16\%$) matching scale (μ_W) dependence [11, 12]. To reduce it, next-to-next-to leading (NNLL) corrections to the Wilson coefficients were calculated recently by Bobeth et al. [13]. This required a two-loop matching calculation of the effective theory to the full SM theory, followed by a renormalization group treatment of the Wilson coefficients, using up to three-loop anomalous dimensions [13, 14]. Including these NNLL corrections to the Wilson coefficients, the matching scale dependence could be removed to a large extent.

However, this partially NNLL result suffers from a relatively large ($\sim \pm 13\%$) renormalization scale (μ_b) dependence [$\mu_b \sim \mathcal{O}(m_b)$], as pointed out in Ref. [13]. The aim of the current paper is to reduce this dependence by calculating NNLL corrections to the matrix elements of the effective Hamiltonian given in the next section. Our main contribution is the calculation of the $\mathcal{O}(\alpha_s)$ two-loop virtual corrections to the matrix elements of the operators O_1 and O_2, as well as the $\mathcal{O}(\alpha_s)$ one-loop corrections to O_7–O_{10}. Also those bremsstrahlung contributions are included which are needed to cancel infrared and collinear singularities in the virtual corrections. The new contributions reduce the renormalization scale dependence from $\sim \pm 13\%$ to $\sim \pm 6.5\%$.

The remainder of this letter is organized as follows. In Section 2 we review the theoretical framework. Our results for the virtual $\mathcal{O}(\alpha_s)$ corrections to the matrix elements of the operators O_1, O_2, O_7, O_8 and O_9 we present in Section 3. Section 4 is devoted to the bremsstrahlung contributions. The combined corrections (virtual and bremsstrahlung) to $b \to s\,\ell^+\ell^-$ are given in Section 5. Finally, in Section 6, we analyze the invariant mass

distribution of the lepton pair in the range $0.05 \leq \hat{s} \leq 0.25$.

2 Theoretical Framework

The most efficient tool for studying weak decays of B mesons is the effective Hamiltonian technique. For the specific decay channels $b \to s\,\ell^+\ell^-$ ($\ell = \mu, e$), the effective Hamiltonian, derived from the Standard Model (SM) by integrating out the t quark and the W boson, is of the form

$$\mathcal{H}_{\text{eff}} = -\frac{4\,G_F}{\sqrt{2}}\,V_{ts}^* V_{tb} \sum_{i=1}^{10} C_i\,O_i\,, \tag{1}$$

where O_i are dimension six operators and C_i are the corresponding Wilson coefficients. The operators can be chosen as [13]

$$\begin{aligned}
O_1 &= (\bar{s}_L\gamma_\mu T^a c_L)(\bar{c}_L\gamma^\mu T^a b_L), & O_2 &= (\bar{s}_L\gamma_\mu c_L)(\bar{c}_L\gamma^\mu b_L),\\
O_3 &= (\bar{s}_L\gamma_\mu b_L)\textstyle\sum_q(\bar{q}\gamma^\mu q), & O_4 &= (\bar{s}_L\gamma_\mu T^a b_L)\textstyle\sum_q(\bar{q}\gamma^\mu T^a q),\\
O_5 &= (\bar{s}_L\gamma_\mu\gamma_\nu\gamma_\rho b_L)\textstyle\sum_q(\bar{q}\gamma^\mu\gamma^\nu\gamma^\rho q), & O_6 &= (\bar{s}_L\gamma_\mu\gamma_\nu\gamma_\rho T^a b_L)\textstyle\sum_q(\bar{q}\gamma^\mu\gamma^\nu\gamma^\rho T^a q),\\
O_7 &= \tfrac{e}{g_s^2} m_b(\bar{s}_L\sigma^{\mu\nu} b_R)F_{\mu\nu}, & O_8 &= \tfrac{1}{g_s} m_b(\bar{s}_L\sigma^{\mu\nu} T^a b_R)G^a_{\mu\nu},\\
O_9 &= \tfrac{e^2}{g_s^2}(\bar{s}_L\gamma_\mu b_L)\textstyle\sum_\ell(\bar{\ell}\gamma^\mu\ell), & O_{10} &= \tfrac{e^2}{g_s^2}(\bar{s}_L\gamma_\mu b_L)\textstyle\sum_\ell(\bar{\ell}\gamma^\mu\gamma_5\ell),
\end{aligned} \tag{2}$$

where the subscripts L and R refer to left- and right-handed components of the fermion fields. We work in the approximation where the combination $(V_{us}^* V_{ub})$ of the Cabibbo-Kobayashi-Maskawa (CKM) matrix elements is neglected; in this case the CKM structure factorizes, as indicated in Eq. (1).

The factors $1/g_s^2$ in the definition of the operators O_7, O_9 and O_{10}, as well as the factor $1/g_s$ present in O_8 have been chosen by Misiak [11] in order to simplify the organization of the calculation: with these definitions, the one-loop anomalous dimensions (needed for a leading logarithmic (LL) calculation) of the operators O_i are all proportional to g_s^2, while two-loop anomalous dimensions (needed for a next-to-leading logarithmic (NLL) calculation) are proportional to g_s^4, etc.

After this important remark we now outline the principal steps which lead to a LL, NLL, NNLL prediction for the decay amplitude for $b \to s\,\ell^+\ell^-$:

1. A matching calculation between the full SM theory and the effective theory has to be performed in order to determine the Wilson coefficients C_i at the high scale $\mu_W \sim m_W, m_t$. At this scale, the coefficients can be worked out in fixed order

perturbation theory, ie, they can be expanded in g_s^2:

$$C_i(\mu_W) = C_i^{(0)}(\mu_W) + \frac{g_s^2}{16\,\pi^2}\,C_i^{(1)}(\mu_W) + \frac{g_s^4}{(16\,\pi^2)^2}\,C_i^{(2)}(\mu_W) + \mathcal{O}(g_s^6). \tag{3}$$

At LL order, only $C_i^{(0)}$ is needed, at NLL order also $C_i^{(1)}$, etc. While the coefficient $C_7^{(2)}$, which is needed for a NNLL analysis, is known for quite some [15], $C_9^{(2)}$ and $C_{10}^{(2)}$ have been calculated only recently [13] (see also [16]).

2. The renormalization group equation (RGE) has to be solved in order to get the Wilson coefficients at the low scale $\mu_b \sim m_b$. For this RGE step the anomalous dimension matrix to the relevant order in g_s is required, as described above. After these two steps one can decompose the Wilson coefficients $C_i(\mu_b)$ into a LL, NLL and NNLL part according to

$$C_i(\mu_b) = C_i^{(0)}(\mu_b) + \frac{g_s^2(\mu_b)}{16\,\pi^2}\,C_i^{(1)}(\mu_b) + \frac{g_s^4(\mu_b)}{(16\,\pi^2)^2}\,C_i^{(2)}(\mu_b) + \mathcal{O}(g_s^6). \tag{4}$$

3. In order to get the decay amplitude, the matrix elements $\langle s\,\ell^+\ell^-|O_i(\mu_b)|b\rangle$ have to be calculated. At LL precision, only the operator O_9 contributes, as this operator is the only one which at the same time has a Wilson coefficient starting at lowest order and an explicit $1/g_s^2$ factor in the definition. Hence, in the NLL precision QCD corrections (virtual and bremsstrahlung) to the matrix element of O_9 are needed. They have been calculated a few years ago [11, 12]. At NLL precision, also the other operators start contributing, viz $O_7(\mu_b)$ and $O_{10}(\mu_b)$ contribute at tree-level and the four-quark operators $O_1, ..., O_6$ at one-loop level. Accordingly, QCD corrections to the latter matrix elements are needed for a NNLL prediction of the decay amplitude.

As known for a long time [17], the formally leading term $\sim (1/g_s^2)C_9^{(0)}(\mu_b)$ to the amplitude for $b \to s\,\ell^+\ell^-$ is smaller than the NLL term $\sim (1/g_s^2)\big[g_s^2/(16\,\pi^2)\big]\,C_9^{(1)}(\mu_b)$. We adapt our systematics to the numerical situation and treat the sum of these two terms as a NLL contribution. This is, admittedly some abuse of language, because the decay amplitude then starts out with a term which is called NLL.

As pointed out in step 3), $\mathcal{O}(\alpha_s)$ QCD corrections to the matrix elements $\langle s\,\ell^+\ell^-|O_i(\mu_b)|b\rangle$ have to be calculated in order to obtain the NNLL prediction for the decay amplitude. In the present paper we *systematically* evaluate virtual corrections of $\mathcal{O}(\alpha_s)$ to the matrix elements of O_1, O_2, O_7, O_8, O_9 and O_{10}. As the Wilson coefficients of the gluonic penguin operators $O_3, ..., O_6$ are much smaller than those of O_1 and O_2, we neglect QCD corrections to their matrix elements. As discussed in more detail later, we also include those bremsstrahlung diagrams which are needed to cancel infrared and collinear singularities from the virtual contributions. The complete bremsstrahlung corrections, ie, all the finite parts, however, will be given elsewhere [20]. We anticipate that the QCD corrections calculated in the present letter substantially reduce the scale dependence of the NLL result.

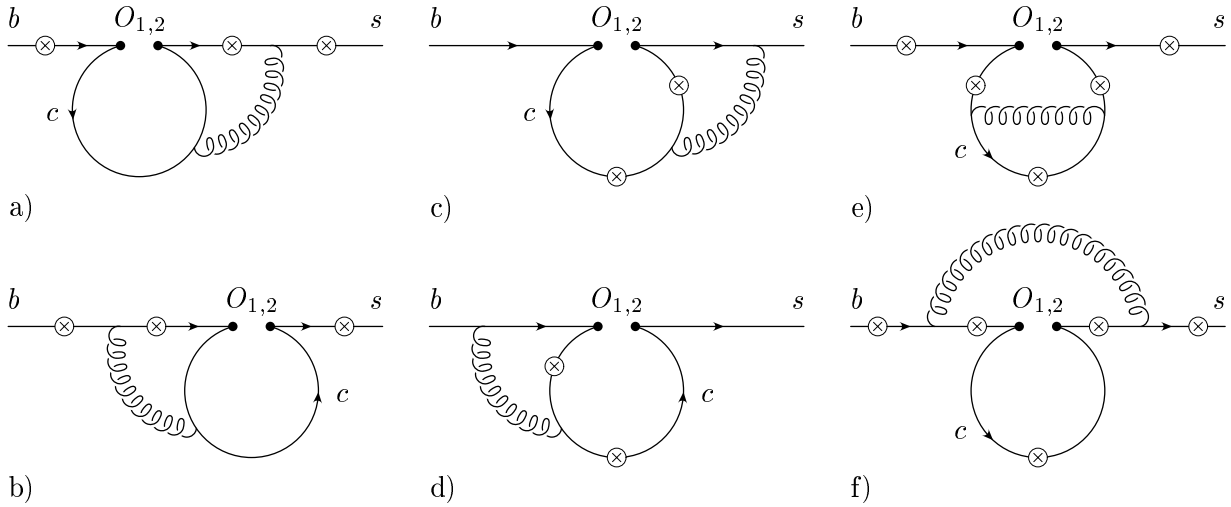

Figure 3.1: Complete list of two-loop Feynman diagrams for $b \to s\gamma^*$ associated with the operators O_1 and O_2. The fermions (b, s and c quarks) are represented by solid lines, whereas the curly lines represent gluons. The circle-crosses denote the possible locations for emission of a virtual photon.

3 Virtual Corrections to O_1, O_2, O_7, O_8 and O_9

In this section we present our results for the virtual $\mathcal{O}(\alpha_s)$ corrections induced by the operators O_1, O_2, O_7, O_8, and O_9. Using the naive dimensional regularization (NDR) scheme in $d = 4 - 2\,\epsilon$ dimensions, both ultraviolet and infrared singularities show up as $1/\epsilon^n$ poles ($n = 1, 2$). The ultraviolet singularities cancel after including the counterterms. Collinear singularities are regularized by retaining a finite strange quark mass m_s. They are cancelled together with the infrared singularities at the level of decay width, taking the bremsstrahlung process $b \to s\,\ell^+\ell^- g$ into account. Gauge invariance implies that the QCD corrected matrix elements of the operators O_i can be written as

$$\langle s\,\ell^+\ell^-|O_i|b\rangle = \hat{F}_i^{(9)}\langle O_9\rangle_{\rm tree} + \hat{F}_i^{(7)}\langle O_7\rangle_{\rm tree}\,, \tag{5}$$

where $\langle O_9\rangle_{\rm tree}$ and $\langle O_7\rangle_{\rm tree}$ are the tree-level matrix elements of O_9 and O_7, respectively.

3.1 Virtual Corrections to O_1 and O_2

The complete list of Feynman diagrams for the two-loop matrix elements of the operators O_1 and O_2 is shown in Fig. 3.1. Our calculation follows the line of [18, 19] where the contributions of O_2 to the processes $B \to X_s\gamma$ and $B \to X_s g$ have been evaluated. There, the results have been found as expansions in terms of powers and logarithms of the small parameter $\hat{m}_c^2 = m_c^2/m_b^2$. The central point of the procedure is to use Mellin-Barnes

representations of certain denominators in the Feynman parameter integrals, as described in detail in Refs. [18, 19]. In the present case, however, we have an additional mass scale: q^2, the invariant mass squared of the lepton pair. For values of q^2 satisfying $\frac{q^2}{m_b^2} < 1$ and $\frac{q^2}{4\,m_c^2} < 1$, most of the diagrams allow a Taylor series expansion in q^2 and can be calculated in combination with a Mellin-Barnes representation. This method does not work for the diagram in Fig. 3.1a) where the photon is emitted from the internal line. Instead, we applied a Mellin-Barnes representation twice. We will explain this procedure in detail in Ref. [20]. The diagrams in Fig. 3.1e) finally, we calculated using the heavy mass expansion technique [21].

Using these methods, the unrenormalized form factors $\hat{F}^{(7,9)}$ of O_1 and O_2, as defined in Eq. (5), are then obtained in the form

$$\hat{F}^{(7,9)} = \sum_{i,j,l,m} c_{ijlm}^{(7,9)}\, \hat{s}^i\, \ln^j(\hat{s})\, \left(\hat{m}_c^2\right)^l \ln^m(\hat{m}_c)\,, \tag{6}$$

where $\hat{s} = q^2/m_b^2$ and $\hat{m}_c = m_c/m_b$. i, j, m are non-negative integers and $l = -i, -i + 1/2, -i + 2/2, \ldots$ .. We keep the terms with i and l up to 3, after checking that higher order terms are small for $0.05 \leq \hat{s} \leq 0.25$, the range considered in this Letter.

The counterterm contributions are of various origin. There are counterterms due to quark field renormalization, renormalization of the strong coupling constant g_s and renormalization of the charm and bottom quark masses. We stress that we use the pole mass definition for both m_c and m_b. Additionally, we also have to take operator mixing into account. The corresponding counterterms to the matrix elements $\langle C_i O_i \rangle$ are of the form

$$\langle C_i O_i \rangle = C_i \sum_j \delta Z_{ij} \langle O_j \rangle, \tag{7}$$

$$\delta Z_{ij} = \frac{\alpha_s}{4\,\pi}\left(a_{ij}^{01} + \frac{1}{\epsilon}\,a_{ij}^{11}\right) + \frac{\alpha_s^2}{(4\,\pi)^2}\left(a_{ij}^{02} + \frac{1}{\epsilon}\,a_{ij}^{12} + \frac{1}{\epsilon^2}\,a_{ij}^{22}\right) + \mathcal{O}(\alpha_s^3). \tag{8}$$

Most of the coefficients a_{ij}^{lm} needed for our calculation are given in Ref. [13]. As some are new, we list those for $i = 1, 2$ and $j = 1, 2, 4, 7, 9, 11, 12$ that are different from zero:

$$\hat{a}^{11} = \begin{pmatrix} -2 & \frac{4}{3} & -\frac{1}{9} & 0 & -\frac{16}{27} & \frac{5}{12} & \frac{2}{9} \\ 6 & 0 & \frac{2}{3} & 0 & -\frac{4}{9} & 1 & 0 \end{pmatrix}, \quad \begin{array}{lll} a_{17}^{12} = -\frac{58}{243}\,, & a_{19}^{12} = -\frac{64}{729}\,, & a_{19}^{22} = \frac{1168}{243}\,, \\ a_{27}^{12} = \frac{116}{81}\,, & a_{29}^{12} = \frac{776}{243}\,, & a_{29}^{22} = \frac{148}{81}\,. \end{array} \tag{9}$$

O_{11} and O_{12}, entering Eq. (7), are evanescent operators, defined as

$$\begin{aligned} O_{11} &= (\bar{s}_L \gamma_\mu \gamma_\nu \gamma_\rho T^a c_L)\,(\bar{c}_L \gamma^\mu \gamma^\nu \gamma^\rho T^a b_L) - 16\, O_1, \\ O_{12} &= (\bar{s}_L \gamma_\mu \gamma_\nu \gamma_\rho c_L)\,(\bar{c}_L \gamma^\mu \gamma^\nu \gamma^\rho b_L) - 16\, O_2. \end{aligned} \tag{10}$$

Before we give the result for the renormalized form factors, we remark that only diagram 3.1f) (and also its renormalized version) suffers from infrared and collinear singularities. As this diagram can easily be combined with diagram 3.2b) associated with the operator O_9, we will take it into account in the next subsection, when discussing virtual corrections to O_9.

We decompose the renormalized matrix elements of O_i $(i = 1, 2)$ as

$$\langle s\,\ell^+\ell^-|C_i^{(0)}O_i|b\rangle = C_i^{(0)}\left(-\frac{\alpha_s}{4\,\pi}\right)\left[F_i^{(9)}\langle\widetilde{O}_9\rangle_{\rm tree} + F_i^{(7)}\langle\widetilde{O}_7\rangle_{\rm tree}\right], \tag{11}$$

with $\widetilde{O}_9 = \frac{\alpha_s}{4\,\pi}\,O_9$ and $\widetilde{O}_7 = \frac{\alpha_s}{4\,\pi}\,O_7$. Using the shorthand notations $L_\mu = \ln(\mu/m_b)$ and $L_s = \ln(\hat{s})$, the form factors $F_i^{(9)}$ and $F_i^{(7)}$ read

$$\begin{aligned} F_1^{(9)} = {} & \left(-\frac{1424}{729} + \frac{16}{243}\,i\pi + \frac{64}{27}\,L_c\right)L_\mu - \frac{16}{243}\,L_\mu\,L_s + \left(\frac{16}{1215} - \frac{32}{135}\,\hat{m}_c^{-2}\right)L_\mu\,\hat{s} \\ & + \left(\frac{4}{2835} - \frac{8}{315}\,\hat{m}_c^{-4}\right)L_\mu\,\hat{s}^2 + \left(\frac{16}{76545} - \frac{32}{8505}\,\hat{m}_c^{-6}\right)L_\mu\,\hat{s}^3 - \frac{256}{243}\,L_\mu^2 + f_1^{(9)}\,, \end{aligned} \tag{12}$$

$$\begin{aligned} F_2^{(9)} = {} & \left(\frac{256}{243} - \frac{32}{81}\,i\pi - \frac{128}{9}\,L_c\right)L_\mu + \frac{32}{81}\,L_\mu\,L_s + \left(-\frac{32}{405} + \frac{64}{45}\,\hat{m}_c^{-2}\right)L_\mu\,\hat{s} \\ & + \left(-\frac{8}{945} + \frac{16}{105}\,\hat{m}_c^{-4}\right)L_\mu\,\hat{s}^2 + \left(-\frac{32}{25515} + \frac{64}{2835}\,\hat{m}_c^{-6}\right)L_\mu\,\hat{s}^3 + \frac{512}{81}\,L_\mu^2 + f_2^{(9)}\,, \end{aligned} \tag{13}$$

$$F_1^{(7)} = -\frac{208}{243}\,L_\mu + f_1^{(7)}\,, \qquad F_2^{(7)} = \frac{416}{81}\,L_\mu + f_2^{(7)}\,. \tag{14}$$

The analytic results for $f_1^{(9)}$, $f_1^{(7)}$, $f_2^{(9)}$, and $f_2^{(7)}$ (expanded up to $\hat{s}^3$ and $(\hat{m}_c^2)^3$) are rather lengthy. The formulas become relatively short, however, if we give the charm quark mass dependence in numerical form (for the characteristic values of $\hat{m}_c$=0.27, 0.29 and 0.31). We write the functions $f_a^{(b)}$ as

$$f_a^{(b)} = \sum_{i,j} k_a^{(b)}(i,j)\,\hat{s}^i\,L_s^j \qquad (a = 1, 2;\; b = 7, 9;\; i = 0, ..., 3;\; j = 0, 1). \tag{15}$$

The numerical values for the quantities $k_a^{(b)}(i, j)$ are given in Tab. 3.1 and 3.2.

3.2 Virtual Corrections to the Matrix Elements of O_7, O_8 and O_9

We first turn to the virtual corrections to the matrix element of the operator O_9, consisting of the vertex correction shown in Fig. 3.2b) and of the quark self-energy contributions.

	$\hat{m}_c = 0.27$	$\hat{m}_c = 0.29$	$\hat{m}_c = 0.31$
$k_1^{(9)}(0,0)$	$-12.327 + 0.13512\,i$	$-11.973 + 0.16371\,i$	$-11.65 + 0.18223\,i$
$k_1^{(9)}(0,1)$	$-0.080505 - 0.067181\,i$	$-0.081271 - 0.059691\,i$	$-0.080959 - 0.051864\,i$
$k_1^{(9)}(1,0)$	$-33.015 - 0.42492\,i$	$-28.432 - 0.25044\,i$	$-24.709 - 0.13474\,i$
$k_1^{(9)}(1,1)$	$-0.041008 + 0.0078685\,i$	$-0.040243 + 0.016442\,i$	$-0.036585 + 0.024753\,i$
$k_1^{(9)}(2,0)$	$-76.2 - 1.5067\,i$	$-57.114 - 0.86486\,i$	$-43.588 - 0.4738\,i$
$k_1^{(9)}(2,1)$	$-0.042685 + 0.015754\,i$	$-0.035191 + 0.027909\,i$	$-0.021692 + 0.036925\,i$
$k_1^{(9)}(3,0)$	$-197.81 - 4.6389\,i$	$-128.8 - 2.5243\,i$	$-86.22 - 1.3542\,i$
$k_1^{(9)}(3,1)$	$-0.039021 + 0.039384\,i$	$-0.017587 + 0.050639\,i$	$0.013282 + 0.052023\,i$
$k_1^{(7)}(0,0)$	$-0.72461 - 0.093424\,i$	$-0.68192 - 0.074998\,i$	$-0.63944 - 0.05885\,i$
$k_1^{(7)}(0,1)$	0	0	0
$k_1^{(7)}(1,0)$	$-0.26156 - 0.15008\,i$	$-0.23935 - 0.12289\,i$	$-0.21829 - 0.10031\,i$
$k_1^{(7)}(1,1)$	$-0.00017705 + 0.02054\,i$	$0.0027424 + 0.019676\,i$	$0.0053227 + 0.018302\,i$
$k_1^{(7)}(2,0)$	$0.023851 - 0.20313\,i$	$-0.0018555 - 0.175\,i$	$-0.022511 - 0.14836\,i$
$k_1^{(7)}(2,1)$	$0.020327 + 0.016606\,i$	$0.022864 + 0.011456\,i$	$0.023615 + 0.0059255\,i$
$k_1^{(7)}(3,0)$	$0.42898 - 0.099202\,i$	$0.28248 - 0.12783\,i$	$0.17118 - 0.12861\,i$
$k_1^{(7)}(3,1)$	$0.031506 + 0.00042591\,i$	$0.029027 - 0.0082265\,i$	$0.022653 - 0.0155\,i$

Table 3.1: Coefficients in the decomposition of $f_1^{(9)}$ and $f_1^{(7)}$ for three different values of $\hat{m}_c$ [Eq. (15)].

The sum of these corrections is ultraviolet finite, but suffers from infrared and collinear singularities. The result can be written as

$$\langle s\,\ell^+\ell^-|C_9 O_9|b\rangle = \widetilde{C}_9^{(0)}\left(-\frac{\alpha_s}{4\,\pi}\right)\left[F_9^{(9)}\langle\widetilde{O}_9\rangle_{\rm tree} + F_9^{(7)}\langle\widetilde{O}_7\rangle_{\rm tree}\right], \tag{16}$$

with

$$\widetilde{O}_9 = \frac{\alpha_s}{4\,\pi}\,O_9 \quad \text{and} \quad \widetilde{C}_9^{(0)} = \frac{4\,\pi}{\alpha_s}\left(C_9^{(0)} + \frac{\alpha_s}{4\,\pi}\,C_9^{(1)}\right).$$

The form factors $F_9^{(9)}$ and $F_9^{(7)}$ read (keeping terms up to order $\hat{s}^3$)

$$F_9^{(9)} = \frac{16}{3} + \frac{20}{3}\,\hat{s} + \frac{16}{3}\,\hat{s}^2 + \frac{116}{27}\,\hat{s}^3 + f_{\rm inf}\,, \tag{17}$$

$$F_9^{(7)} = -\frac{2}{3}\,\hat{s}\left(1 + \frac{1}{2}\,\hat{s} + \frac{1}{3}\,\hat{s}^2\right), \tag{18}$$

	$\hat{m}_c = 0.27$	$\hat{m}_c = 0.29$	$\hat{m}_c = 0.31$
$k_2^{(9)}(0,0)$	$7.9938 - 0.81071\,i$	$6.6338 - 0.98225\,i$	$5.4082 - 1.0934\,i$
$k_2^{(9)}(0,1)$	$0.48303 + 0.40309\,i$	$0.48763 + 0.35815\,i$	$0.48576 + 0.31119\,i$
$k_2^{(9)}(1,0)$	$5.1651 + 2.5495\,i$	$3.3585 + 1.5026\,i$	$1.9061 + 0.80843\,i$
$k_2^{(9)}(1,1)$	$0.24605 - 0.047211\,i$	$0.24146 - 0.098649\,i$	$0.21951 - 0.14852\,i$
$k_2^{(9)}(2,0)$	$-0.45653 + 9.0402\,i$	$-1.1906 + 5.1892\,i$	$-1.8286 + 2.8428\,i$
$k_2^{(9)}(2,1)$	$0.25611 - 0.094525\,i$	$0.21115 - 0.16745\,i$	$0.13015 - 0.22155\,i$
$k_2^{(9)}(3,0)$	$-25.981 + 27.833\,i$	$-17.12 + 15.146\,i$	$-12.113 + 8.1251\,i$
$k_2^{(9)}(3,1)$	$0.23413 - 0.2363\,i$	$0.10552 - 0.30383\,i$	$-0.079692 - 0.31214\,i$
$k_2^{(7)}(0,0)$	$4.3477 + 0.56054\,i$	$4.0915 + 0.44999\,i$	$3.8367 + 0.3531\,i$
$k_2^{(7)}(0,1)$	0	0	0
$k_2^{(7)}(1,0)$	$1.5694 + 0.9005\,i$	$1.4361 + 0.73732\,i$	$1.3098 + 0.60185\,i$
$k_2^{(7)}(1,1)$	$0.0010623 - 0.12324\,i$	$-0.016454 - 0.11806\,i$	$-0.031936 - 0.10981\,i$
$k_2^{(7)}(2,0)$	$-0.14311 + 1.2188\,i$	$0.011133 + 1.05\,i$	$0.13507 + 0.89014\,i$
$k_2^{(7)}(2,1)$	$-0.12196 - 0.099636\,i$	$-0.13718 - 0.068733\,i$	$-0.14169 - 0.035553\,i$
$k_2^{(7)}(3,0)$	$-2.5739 + 0.59521\,i$	$-1.6949 + 0.76698\,i$	$-1.0271 + 0.77168\,i$
$k_2^{(7)}(3,1)$	$-0.18904 - 0.0025554\,i$	$-0.17416 + 0.049359\,i$	$-0.13592 + 0.093\,i$

Table 3.2: Coefficients in the decomposition of $f_2^{(9)}$ and $f_2^{(7)}$ for three different values of $\hat{m}_c$ [Eq. (15)].

where the function $f_{\rm inf}$ contains the infrared and collinear singularities. Its explicit form is [using $r = (m_s/m_b)^2$]

$$f_{\rm inf} = \frac{8}{3\,\epsilon}\left[\frac{\mu}{m_b}\right]^{2\epsilon}\left(1 + \hat{s} + \frac{1}{2}\,\hat{s}^2 + \frac{1}{3}\,\hat{s}^3\right) + \frac{4}{3\,\epsilon}\left[\frac{\mu}{m_b}\right]^{2\epsilon} \ln(r) + \frac{2}{3}\ln(r) - \frac{2}{3}\,\ln^2(r). \qquad (19)$$

At this place, it is convenient to incorporate the renormalized diagram 3.1f), which has not been taken into account so far. It is easy to see that the two loops factorize into two one-loop contributions. The charm loop has the Lorentz structure of O_9 and can therefore be absorbed into an effective Wilson coefficient: diagram 3.1f) is properly included by modifying $\widetilde{C}_9^{(0)}$ in Eq. (16) as follows:

$$\widetilde{C}_9^{(0)} \longrightarrow \widetilde{C}_9^{(0,\rm mod)} = \widetilde{C}_9^{(0)} + \left(C_2^{(0)} + \frac{4}{3}\,C_1^{(0)}\right) H_0, \qquad (20)$$

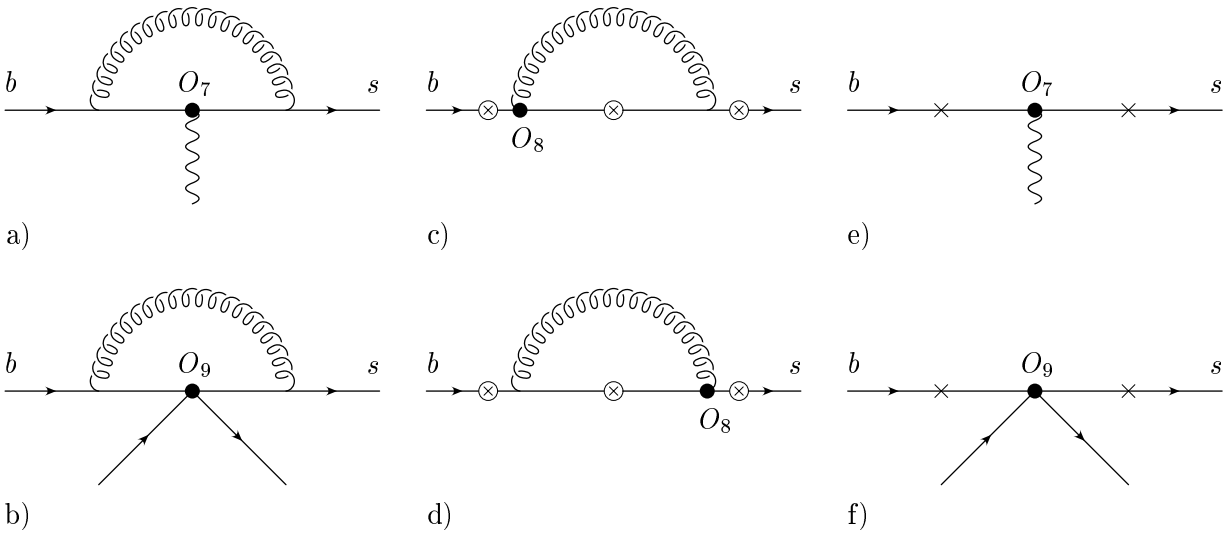

Figure 3.2: Some Feynman diagrams for $b \to s\gamma^*$ or $b \to s\,\ell^+\ell^-$ associated with the operators O_7, O_8 and O_9. The circle-crosses denote the possible locations where the virtual photon is emitted, while the crosses mark the possible locations for gluon bremsstrahlung. See text.

where the charm-loop function H_0 reads (in expanded form)

$$H_0 = \frac{1}{2835}\left[-1260 + 2520\,\ln\left(\frac{\mu}{m_c}\right) + 252\,\frac{\hat{s}}{\hat{m}_c^2} + 27\,\frac{\hat{s}^2}{\hat{m}_c^4} + 4\,\frac{\hat{s}^3}{\hat{m}_c^6}\right]. \tag{21}$$

In the context of virtual corrections also the $\mathcal{O}(\epsilon)$ part of this loop function is needed. We neglect it here since it will drop out in combination with gluon bremsstrahlung. Note that $H_0 = h(\hat{m}_c^2, \hat{s}) + 8/9\,\ln(\mu/m_b)$, with h defined in [12, 13].

We now turn to the virtual corrections to the matrix element of the operator O_7, consisting of the vertex- [Fig. 3.2a)] and self-energy corrections. The sum of these diagrams is ultraviolet singular. After renormalization, the result can be written as

$$\langle\, s\ell^+\ell^-|C_7 O_7|b\rangle = \widetilde{C}_7^{(0)}\left(-\frac{\alpha_s}{4\,\pi}\right)\left[F_7^{(9)}\langle\widetilde{O}_9\rangle_{\rm tree} + F_7^{(7)}\langle\widetilde{O}_7\rangle_{\rm tree}\right], \tag{22}$$

with $\widetilde{O}_7 = \frac{\alpha_s}{4\,\pi}\,O_7$ and $\widetilde{C}_7^{(0)} = C_7^{(1)}$. The form factors $F_7^{(9)}$ and $F_7^{(7)}$ read

$$F_7^{(9)} = -\frac{16}{3}\left(1 + \frac{1}{2}\,\hat{s} + \frac{1}{3}\,\hat{s}^2 + \frac{1}{4}\,\hat{s}^3\right), \tag{23}$$

$$F_7^{(7)} = \frac{32}{3}\,L_\mu + \frac{32}{3} + 8\,\hat{s} + 6\,\hat{s}^2 + \frac{128}{27}\,\hat{s}^3 + f_{\rm inf}\,. \tag{24}$$

Note that for these expressions the *pole mass for* m_b has to be used at lowest order.

Finally, we give the result for the renormalized corrections to the matrix elements of O_8. The corresponding diagrams are shown in Fig. 3.2c) and 3.2d). One obtains:

$$\langle s\,\ell^+\ell^-|C_8 O_8|b\rangle = \widetilde{C}_8^{(0)}\left(-\frac{\alpha_s}{4\,\pi}\right)\left[F_8^{(9)}\langle\widetilde{O}_9\rangle_{\rm tree} + F_8^{(7)}\langle\widetilde{O}_7\rangle_{\rm tree}\right], \tag{25}$$

with $\widetilde{C}_8^{(0)} = C_8^{(1)}$. The form factors $F_8^{(9)}$ and $F_8^{(7)}$ read (in expanded form)

$$\begin{aligned} F_8^{(9)} =& \frac{104}{9} - \frac{32}{27}\,\pi^2 + \left(\frac{1184}{27} - \frac{40}{9}\,\pi^2\right)\hat{s} + \left(\frac{14212}{135} - \frac{32}{3}\,\pi^2\right)\hat{s}^2 \\ &+ \left(\frac{193444}{945} - \frac{560}{27}\,\pi^2\right)\hat{s}^3 + \frac{16}{9}\,L_s\left(1+\hat{s}+\hat{s}^2+\hat{s}^3\right), \end{aligned} \tag{26}$$

$$\begin{aligned} F_8^{(7)} =& -\frac{32}{9}\,L_\mu + \frac{8}{27}\,\pi^2 - \frac{44}{9} - \frac{8}{9}\,i\pi + \left(\frac{4}{3}\,\pi^2 - \frac{40}{3}\right)\hat{s} + \left(\frac{32}{9}\,\pi^2 - \frac{316}{9}\right)\hat{s}^2 \\ &+ \left(\frac{200}{27}\,\pi^2 - \frac{658}{9}\right)\hat{s}^3 - \frac{8}{9}\,L_s\left(\hat{s}+\hat{s}^2+\hat{s}^3\right). \end{aligned} \tag{27}$$

4 Bremsstrahlung Corrections

We stress that in the present Letter only those bremsstrahlung diagrams are taken into account which are needed to cancel the infrared and collinear singularities from the virtual corrections. All other bremsstrahlung contributions (which are finite), will be given elsewhere [20].

It is known [11, 12] that the contribution to the inclusive decay width coming from the interference between the tree-level and the one-loop matrix elements of O_9 [Fig. 3.2b)] and from the corresponding bremsstrahlung corrections [Fig. 3.2f)], can be written in the form

$$\frac{d\Gamma_{99}}{d\hat{s}} = \left(\frac{\alpha_{em}}{4\,\pi}\right)^2 \frac{G_F^2\, m_{b,\rm pole}^5\, |V_{ts}^* V_{tb}|^2}{48\,\pi^3}\,(1-\hat{s})^2\cdot(1+2\,\hat{s})\cdot\left(2\left|\widetilde{C}_9^{(0)}\right|^2\frac{\alpha_s}{\pi}\,\omega_9(\hat{s})\right), \tag{28}$$

where $\widetilde{C}_9^{(0)} = \frac{4\,\pi}{\alpha_s}\left(C_9^{(0)} + \frac{\alpha_s}{4\,\pi}C_9^{(1)}\right)$. The function $\omega_9(\hat{s}) \equiv \omega(\hat{s})$, which contains information on virtual and bremsstrahlung corrections, can be found in [11, 12]. Replacing $\widetilde{C}_9^{(0)}$ by $\widetilde{C}_9^{(0,\rm mod)}$ [see Eq. (20)] in Eq. (28), diagram 3.1f) and the corresponding bremsstrahlung corrections are automatically included.

Similarly, the contribution to the decay width from the interference between the tree-level and the one-loop matrix element of O_7 [Fig. 3.2a)], combined with the corresponding bremsstrahlung corrections shown in Fig. 3.2e), can be written as

$$\frac{d\Gamma_{77}}{d\hat{s}} = \left(\frac{\alpha_{em}}{4\,\pi}\right)^2 \frac{G_F^2\, m_{b,\rm pole}^5\, |V_{ts}^* V_{tb}|^2}{48\,\pi^3}\,(1-\hat{s})^2\cdot 4\,(1+2/\hat{s})\cdot\left(2\left|\widetilde{C}_7^{(0)}\right|^2\frac{\alpha_s}{\pi}\,\omega_7(\hat{s})\right), \tag{29}$$

where $\widetilde{C}_7^{(0)} = C_7^{(1)}$. The function $\omega_7(\hat{s})$, which is new, reads

$$\omega_7(\hat{s}) = -\frac{8}{3}\ln\left(\frac{\mu}{m_b}\right) - \frac{4}{3}\,\mathrm{Li}(\hat{s}) - \frac{2}{9}\,\pi^2 - \frac{2}{3}\,\ln(\hat{s})\ln(1-\hat{s}) - \frac{1}{3}\,\frac{8+\hat{s}}{2+\hat{s}}\ln(1-\hat{s}) - \frac{2}{3}\,\frac{\hat{s}\,(2-2\,\hat{s}-\hat{s}^2)}{(1-\hat{s})^2\,(2+\hat{s})}\ln(\hat{s}) - \frac{1}{18}\,\frac{16-11\,\hat{s}-17\,\hat{s}^2}{(2+\hat{s})\,(1-\hat{s})}\,. \quad (30)$$

Finally, one observes that also the interference between the tree-level matrix element of O_7 and the one-loop matrix element of O_9 (and vice versa) lead to an infrared singular contribution to the decay width. We combined it with the corresponding bremsstrahlung terms coming from the interference of diagrams 3.2e) and 3.2f). The result reads

$$\frac{d\Gamma_{79}}{d\hat{s}} = \left(\frac{\alpha_{em}}{4\,\pi}\right)^2 \frac{G_F^2\,m_{b,\mathrm{pole}}^5\,|V_{ts}^*V_{tb}|^2}{48\,\pi^3}\,(1-\hat{s})^2\cdot 12\cdot\left(2\,\mathrm{Re}\left(\widetilde{C}_7^{(0)}\widetilde{C}_9^{(0)}\right)\frac{\alpha_s}{\pi}\,\omega_{79}(\hat{s})\right). \quad (31)$$

For the function $\omega_{79}(\hat{s})$, which also is new, we obtain

$$\omega_{79}(\hat{s}) = -\frac{4}{3}\ln\left(\frac{\mu}{m_b}\right) - \frac{4}{3}\,\mathrm{Li}(\hat{s}) - \frac{2}{9}\,\pi^2 - \frac{2}{3}\,\ln(\hat{s})\ln(1-\hat{s}) - \frac{1}{9}\,\frac{2+7\,\hat{s}}{\hat{s}}\ln(1-\hat{s}) - \frac{2}{9}\,\frac{\hat{s}\,(3-2\,\hat{s})}{(1-\hat{s})^2}\ln(\hat{s}) + \frac{1}{18}\,\frac{5-9\,\hat{s}}{1-\hat{s}}\,. \quad (32)$$

5 Corrections to the Decay Width

In this section we combine the virtual corrections calculated in Section 3 and the bremsstrahlung contributions discussed in Section 4 and study their influence on the decay width $d\Gamma(b\to s\,\ell^+\ell^-)/d\hat{s}$. In the literature (see eg [13]), this decay width is usually written as

$$\frac{d\Gamma(B\to X_s\,\ell^+\ell^-)}{d\hat{s}} = \left(\frac{\alpha_{em}}{4\,\pi}\right)^2 \frac{G_F^2\,m_{b,\mathrm{pole}}^5\,|V_{ts}^*V_{tb}|^2}{48\,\pi^3}\,(1-\hat{s})^2 \times\left[(1+2\,\hat{s})\left(\left|\widetilde{C}_9^{\mathrm{eff}}\right|^2+\left|\widetilde{C}_{10}^{\mathrm{eff}}\right|^2\right)+4\,(1+2/\hat{s})\left|\widetilde{C}_7^{\mathrm{eff}}\right|^2+12\cdot\mathrm{Re}\left(\widetilde{C}_7^{\mathrm{eff}}\widetilde{C}_9^{\mathrm{eff}*}\right)\right], \quad (33)$$

where the contributions calculated so far have been absorbed into the effective Wilson coefficients $\widetilde{C}_7^{\mathrm{eff}}$, $\widetilde{C}_9^{\mathrm{eff}}$ and $\widetilde{C}_{10}^{\mathrm{eff}}$. It turns out that also the new contributions calculated in the present paper can be absorbed into these coefficients. Following as closely as possible

	$\mu = 2.5$ GeV	$\mu = 5$ GeV	$\mu = 10$ GeV
α_s	0.267	0.215	0.180
$C_1^{(0)}$	-0.697	-0.487	-0.326
$C_2^{(0)}$	1.046	1.024	1.011
$\left(A_7^{(0)},\ A_7^{(1)}\right)$	$(-0.360,\ 0.031)$	$(-0.321,\ 0.019)$	$(-0.287,\ 0.008)$
$A_8^{(0)}$	-0.164	-0.148	-0.134
$\left(A_9^{(0)},\ A_9^{(1)}\right)$	$(4.241,\ -0.170)$	$(4.129,\ 0.013)$	$(4.131,\ 0.155)$
$\left(T_9^{(0)},\ T_9^{(1)}\right)$	$(0.115,\ 0.278)$	$(0.374,\ 0.251)$	$(0.576,\ 0.231)$
$\left(U_9^{(0)},\ U_9^{(1)}\right)$	$(0.045,\ 0.023)$	$(0.032,\ 0.016)$	$(0.022,\ 0.011)$
$\left(W_9^{(0)},\ W_9^{(1)}\right)$	$(0.044,\ 0.016)$	$(0.032,\ 0.012)$	$(0.022,\ 0.009)$
$\left(A_{10}^{(0)},\ A_{10}^{(1)}\right)$	$(-4.372,\ 0.135)$	$(-4.372,\ 0.135)$	$(-4.372,\ 0.135)$

Table 5.1: Coefficients appearing in Eq. (34) for $\mu = 2.5$ GeV, $\mu = 5$ GeV and $\mu = 10$ GeV. For $\alpha_s(\mu)$ (in the $\overline{\text{MS}}$ scheme) we used the two-loop expression with 5 flavors and $\alpha_s(m_Z) = 0.119$. The entries correspond to the pole top quark mass $m_t = 174$ GeV. The superscript (0) refers to lowest order quantities and while the superscript (1) denotes the correction terms of $\mathcal{O}(\alpha_s)$.

the "parameterization" given recently by Bobeth *et al.* [13], we write

$$\begin{aligned}
\widetilde{C}_9^{\text{eff}} &= \left(1 + \frac{\alpha_s(\mu)}{\pi}\,\omega_9(\hat{s})\right)\left(A_9 + T_9\,h(\hat{m}_c^2,\hat{s}) + U_9\,h(1,\hat{s}) + W_9\,h(0,\hat{s})\right) \\
&\quad -\frac{\alpha_s(\mu)}{4\,\pi}\left(C_1^{(0)}F_1^{(9)} + C_2^{(0)}F_2^{(9)} + A_8^{(0)}F_8^{(9)}\right), \qquad (34)\\
\widetilde{C}_7^{\text{eff}} &= \left(1 + \frac{\alpha_s(\mu)}{\pi}\,\omega_7(\hat{s})\right)A_7 - \frac{\alpha_s(\mu)}{4\,\pi}\left(C_1^{(0)}F_1^{(7)} + C_2^{(0)}F_2^{(7)} + A_8^{(0)}F_8^{(7)}\right), \\
\widetilde{C}_{10}^{\text{eff}} &= \left(1 + \frac{\alpha_s(\mu)}{\pi}\,\omega_9(\hat{s})\right)A_{10}\,,
\end{aligned}$$

where the expressions for $h(\hat{m}_c^2,\hat{s})$ and $\omega_9(\hat{s})$ are given in [13]. The quantities $\omega_7(\hat{s})$ and $F_{1,2,8}^{(7,9)}$, on the other hand, have been calculated in the present paper. We take the numerical values for A_7, A_9, A_{10}, T_9, U_9, and W_9 from [13], while $C_1^{(0)}$, $C_2^{(0)}$ and $A_8^{(0)} = \widetilde{C}_8^{(0,\text{eff})}$ are taken from [19]. For completeness we list them in Tab. 5.1.

When calculating the decay width (33), we retain only terms linear in α_s (and thus in ω_9

and ω_7) in $|\widetilde{C}_9^{\rm eff}|^2$ and $|\widetilde{C}_7^{\rm eff}|^2$. In the interference term $\mathrm{Re}\left(\widetilde{C}_7^{\rm eff}\widetilde{C}_9^{\rm eff*}\right)$ too, we keep only terms linear in α_s. By construction, one has to make the replacements $\omega_9 \to \omega_{79}$ and $\omega_7 \to \omega_{79}$ in this term.

Our results include all the relevant virtual corrections and singular bremsstrahlung contributions. There exist additional bremsstrahlung terms coming, eg, from one-loop O_1 and O_2 diagrams in which both the virtual photon and the gluon are emitted from the charm quark line. These contributions do not induce additional renormalization scale dependence as they are ultraviolet finite. Using our experience from $b \to s\gamma$ and $b \to sg$, these contributions are not expected to be large.

6 Numerical Results

The decay width in Eq. (33) has a large uncertainty due to the factor $m_{b,\rm pole}^5$. Following common practice, we consider the ratio

$$R_{\rm quark}(\hat{s}) = \frac{1}{\Gamma(b \to X_c\, e\, \bar{\nu}_e)} \frac{d\Gamma(b \to s\, \ell^+\ell^-)}{d\hat{s}}\,, \tag{35}$$

in which the factor $m_{b,\rm pole}^5$ drops out. The explicit expression for the semileptonic decay width $\Gamma(b \to X_c\, e\, \bar{\nu}_e)$ can be found eg in [13].

We now turn to the numerical results for $R_{\rm quark}(\hat{s})$ for $0.05 \le \hat{s} \le 0.25$. In Fig. 6.1a) we investigate the dependence of $R_{\rm quark}(\hat{s})$ on the renormalization scale μ. The solid lines are obtained by including the new NNLL contributions as explained in detail in Section 5. The three solid lines correspond to $\mu = 2.5$ GeV (lower line), $\mu = 5$ GeV (middle line) and $\mu = 10$ GeV (upper line). The three dashed lines (again $\mu = 2.5$ GeV for the lower, $\mu = 5$ GeV for the middle and $\mu = 10$ GeV for the upper curve), on the other hand, show the results without the new NNLL corrections, ie they include the NLL results combined with the NNLL corrections to the matching conditions as obtained by Bobeth *et al.* [13]. From this figure we conclude that the renormalization scale dependence gets reduced by more than a factor of 2. Only for small values of $\hat{s}$ ($\hat{s} \sim 0.05$), where the NLL μ dependence is small already, the reduction factor is smaller. For the integrated quantity we obtain

$$R_{\rm quark} = \int_{0.05}^{0.25} d\hat{s}\, R_{\rm quark}(\hat{s}) = (1.25 \pm 0.08) \times 10^{-5}\,, \tag{36}$$

where the error is obtained by varying μ between 2.5 GeV and 10 GeV. Before our corrections, the result was $R_{\rm quark} = (1.36 \pm 0.18) \times 10^{-5}$ [13]. In other words, the renormalization scale dependence got reduced from $\sim \pm 13\%$ to $\sim \pm 6.5\%$.

Among the errors on $R_{\rm quark}(\hat{s})$ which are due to the uncertainties in the input parameters, the one induced by $\hat{m}_c = m_c/m_b$ is known to be the largest. We therefore show in Fig. 6.1b)

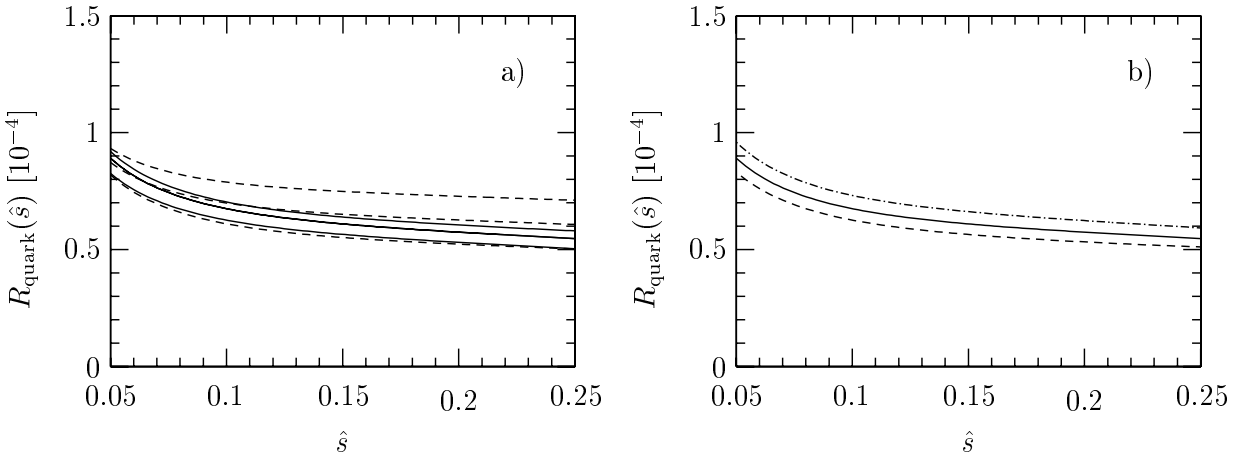

Figure 6.1: a) The three solid lines show the μ dependence of $R_{\rm quark}(\hat{s})$ when including the corrections to the matrix elements calculated in this Letter. The dashed lines are obtained when switching these corrections off. We set $\hat{m}_c = 0.29$. b) $R_{\rm quark}(\hat{s})$ for $\hat{m}_c = 0.27$ (dashed line), $\hat{m}_c = 0.29$ (solid line) and $\hat{m}_c = 0.31$ (dash-dotted line) and $\mu = 5$ GeV. See text.

the dependence of $R_{\rm quark}(\hat{s})$ on $\hat{m}_c$. Comparing Fig. 6.1a) with Fig. 6.1b), we find that the uncertainty due to $\hat{m}_c$ is somewhat larger than the left-over μ dependence at the NNLL level. For the integrated quantity $R_{\rm quark}$ we find an uncertainty of $\pm 7.6\%$ due to $\hat{m}_c$.

To conclude: We have calculated virtual corrections of $\mathcal{O}(\alpha_s)$ to the matrix elements of O_1, O_2, O_7, O_8, O_9 and O_{10}. We also took into account those bremsstrahlung corrections which cancel the infrared and collinear singularities in the virtual corrections. The renormalization scale dependence of $R_{\rm quark}(\hat{s})$ gets reduced by more than a factor of 2. The calculation of the remaining bremsstrahlung contributions (which are expected to be rather small) and a more detailed numerical analysis are in progress [20].

References

[1] R. Ammar *et al.* [CLEO Collaboration], *Phys. Rev. Lett.* **71** (1993) 674.

[2] R. Ammar *et al.* [CLEO Collaboration], *Phys. Rev. Lett.* **74** (1995) 2885.

[3] S. Glenn *et al.* [CLEO Collaboration], *Phys. Rev. Lett.* **80** (1998) 2289.

[4] Z. Ligeti and M. B. Wise, *Phys. Rev.* **D 53** (1996) 4937.

[5] A. F. Falk, M. Luke and M. J. Savage, *Phys. Rev.* **D 49** (1994) 3367.

[6] A. Ali, G. Hiller, L. T. Handoko and T. Morozumi, *Phys. Rev.* **D 55** (1997) 4105, hep-ph/9609449.

[7] J-W. Chen, G. Rupak and M. J. Savage, *Phys. Lett.* **B 410** (1997) 285.

[8] G. Buchalla, G. Isidori and S. J. Rey, *Nucl. Phys.* **B 511** (1998) 594, hep-ph/9705253.

[9] G. Buchalla and G. Isidori, *Nucl. Phys.* **B 525** (1998) 333.

[10] F. Krüger and L.M. Sehgal, *Phys. Lett.* **B 380** (1996) 199.

[11] M. Misiak, *Nucl. Phys.* **B 393** (1993) 23; *Nucl. Phys.* **B 439** (1995) 461 (E).

[12] A. J. Buras and M. Münz, *Phys. Rev.* **D 52** (1995) 186, hep-ph/9501281.

[13] C. Bobeth, M. Misiak and J. Urban, *Nucl. Phys.* **B 574** (2000) 291, hep-ph/9910220.

[14] K. Chetyrkin, M. Misiak and M. Münz, *Phys. Lett.* **B 400** (1997) 206;
Nucl. Phys. **B 518** (1998) 473; *Nucl. Phys.* **B 520** (1998) 279.

[15] K. Adel and Y. P. Yao, *Phys. Rev.* **D 49** (1994) 4945;
C. Greub and T. Hurth *Phys. Rev.* **D 56** (1997) 2934;
A. J. Buras,A. Kwiatkowski and N. Pott, *Nucl. Phys.* **B 517** (1998) 353;
M. Ciuchini, G. Degrassi, P. Gambino and G. F. Giudice,
Nucl. Phys. **B 527** (1998) 21.

[16] G. Buchalla and A. J. Buras, *Nucl. Phys.* **B 548** (1999) 309, hep-ph/9901288.

[17] B. Grinstein, M. J. Savage and M. B. Wise, *Nucl. Phys.* **B 319** (1989) 271.

[18] C. Greub, T. Hurth and D. Wyler, *Phys. Rev.* **D 54** (1996) 3350, hep-ph/9603404.

[19] C. Greub and P. Liniger, *Phys. Lett.* **B 494** (2000) 237, hep-ph/0008071;
Phys. Rev. **D 63** (2001) 054025, hep-ph/0009144.

[20] H. H. Asatryan, H. M. Asatrian, C. Greub and M. Walker, in preparation.

[21] V.A. Smirnov, hep-ph/9412063;
V.A. Smirnov, *Renormalization and Asymptotic Expansions* (Birkhäuser, Basel, 1991).

PART III

Calculation of Two-Loop Virtual Corrections to $b \to s\,\ell^+\ell^-$ in the Standard Model

published in

Physical Review D 65 (2002) 074004

BUTP–01/19
hep-ph/0109140
Phys. Rev. **D 65** (2002) 074004

Calculation of two-loop virtual corrections to $b \to s\,\ell^+\ell^-$ in the Standard Model [1]

H.H. Asatryan[a], H.M. Asatrian[a], C. Greub[b] and M. Walker[b]

[a] *Yerevan Physics Institute, 2 Alikhanyan Br., 375036 Yerevan, Armenia*
[b] *Institut für Theoretische Physik, Universität Bern, CH–3012 Bern, Switzerland.*

ABSTRACT

We present in detail the calculation of the virtual $\mathcal{O}(\alpha_s)$ corrections to the inclusive semileptonic rare decay $b \to s\,\ell^+\ell^-$. We also include those $\mathcal{O}(\alpha_s)$ bremsstrahlung contributions which cancel the infrared and mass singularities showing up in the virtual corrections. In order to avoid large resonant contributions, we restrict the invariant mass squared s of the lepton pair to the range $0.05 \leq s/m_b^2 \leq 0.25$. The analytic results are represented as expansions in the small parameters $\hat{s} = s/m_b^2$, $z = m_c^2/m_b^2$ and $s/(4\,m_c^2)$. The new contributions drastically reduce the renormalization scale dependence of the decay spectrum. For the corresponding branching ratio (restricted to the above $\hat{s}$ range) the renormalization scale uncertainty gets reduced from $\sim \pm 13\%$ to $\sim \pm 6.5\%$.

[1] Work partially supported by Schweizerischer Nationalfonds and SCOPES program

1 Introduction

Rare B decays are an extremely helpful tool for examining the Standard Model (SM) and searching for new physics. Within the SM, they provide checks on the one-loop structure of the theory and allow one to retrieve information on the Cabibbo-Kobayashi-Maskawa (CKM) matrix elements V_{ts} and V_{td}, which cannot be measured directly.

The first measurement of the exclusive rare decay $B \to K^*\gamma$ was obtained in 1992 by the CLEO collaboration [1]. Somewhat later, also the inclusive transition $B \to X_s\gamma$ was observed by the same collaboration [2]. Although challenging for the experimentalists, the inclusive decays are clean from the theoretical point of view, as they are well approximated by the underlying partonic transitions, up to small and calculable power corrections which start at $\mathcal{O}(\Lambda^2_{\rm QCD}/m_b^2)$ [3, 4].

The measured photon energy spectrum [5] and the branching ratio for the decay $B \to X_s\gamma$ [2, 6, 7] are in good agreement with the next-to-leading logarithmic (NLL) Standard Model predictions (see eg [8]–[14]). Consequently, the decay $B \to X_s\gamma$ places stringent constraints on the extensions of the SM, such as two-Higgs doublet models [10, 15, 16], supersymmetric models [17]–[22], etc.

$B \to X_s\,\ell^+\ell^-$ is another interesting rare decay mode which has been extensively considered in the literature in the framework of the SM and its extensions (see eg [23]–[28]). This decay has not been observed so far, but it is expected to be measured at the operating B factories after a few years of data taking (for upper limits on its branching ratio we refer to [29, 30]). The measurement of various kinematical distributions of the decay $B \to X_s\,\ell^+\ell^-$, combined with improved data on $B \to X_s\gamma$, will tighten the constraints on the extensions of the SM or perhaps even reveal some deviations.

The main problem of the theoretical description of $B \to X_s\,\ell^+\ell^-$ is due to the long-distance contributions from $\bar{c}c$ resonant states. When the invariant mass $\sqrt{s}$ of the lepton pair is close to the mass of a resonance, only model dependent predictions for such long distance contributions are available today. It is therefore unclear whether the theoretical uncertainty can be reduced to less than $\pm 20\%$ when integrating over these domains [31].

However, restricting $\sqrt{s}$ to a region below the resonances, the long distance effects are under control. The corrections to the pure perturbative picture can be analyzed within the heavy quark effective theory (HQET). In particular, all available studies indicate that for the region $0.05 < \hat{s} = s/m_b^2 < 0.25$ the non-perturbative effects are below 10% [32]–[37]. Consequently, the differential decay rate for $B \to X_s\,\ell^+\ell^-$ can be precisely predicted in this region using renormalization group improved perturbation theory. It was pointed out in the literature that the differential decay rate and the forward-backward asymmetry are particularly sensitive to new physics in this kinematical window [38]–[40].

Calculations of the next-to-leading logarithmic (NLL) corrections to the process $B \to X_s\,\ell^+\ell^-$ have been performed in Refs. [24] and [28]. It turned out that the NLL result suffers from a relatively large ($\pm 16\%$) dependence on the matching scale μ_W. To reduce it,

next-to-next-to leading (NNLL) corrections to the Wilson coefficients have recently been calculated by Bobeth *et al.* [41]. This required a two-loop matching calculation of the effective theory to the full SM theory, followed by a renormalization group evolution of the Wilson coefficients, using up to three-loop anomalous dimensions [41, 11]. Including these NNLL corrections to the Wilson coefficients, the matching scale dependence is indeed removed to a large extent.

As pointed out in Ref. [41], this partially NNLL result suffers from a relatively large ($\sim \pm 13\%$) renormalization scale (μ_b) dependence [$\mu_b \sim \mathcal{O}(m_b)$] which, interestingly enough, is even larger than that of the pure NLL result. Recently we showed in a letter [42] that the NNLL corrections to the matrix elements of the effective Hamiltonian drastically reduce the renormalization scale dependence. The aim of the current paper is to present a detailed description of the rather involved calculations and to extend the phenomenological part. We will discuss in particular the methods which allowed us to tackle with the most involved part, viz the calculation of the $\mathcal{O}(\alpha_s)$ two-loop virtual corrections to the matrix elements of the operators O_1 and O_2. We also comment on the $\mathcal{O}(\alpha_s)$ one-loop corrections to O_7–O_{10}. Furthermore, we include those bremsstrahlung contributions which are needed to cancel the infrared and collinear singularities in the virtual corrections. As shown already in [42], the new contributions reduce the renormalization scale dependence from $\sim \pm 13\%$ to $\sim \pm 6.5\%$.

The paper is organized as follows: In Section 2 we review the theoretical framework. Our results for the virtual $\mathcal{O}(\alpha_s)$ corrections to the matrix elements of the operators O_1 and O_2 are presented in Section 3, whereas the corresponding corrections to the matrix elements of O_7, O_8, O_9 and O_{10} are given in Section 4. Section 5 is devoted to the bremsstrahlung corrections. The combined corrections (virtual and bremsstrahlung) to $b \to s\,\ell^+\ell^-$ are discussed in Section 6. Finally, in Section 7, we analyze the invariant mass distribution of the lepton pair in the range $0.05 \leq \hat{s} \leq 0.25$.

2 Effective Hamiltonian

The appropriate framework for studying QCD corrections to rare B decays in a systematic way is the effective Hamiltonian technique. For the specific decay channels $b \to s\,\ell^+\ell^-$ ($\ell = \mu,\ e$), the effective Hamiltonian is derived by integrating out the heavy degrees of freedom. In the context of the Standard Model, these are the t quark, the W boson and the Z^0 boson. Because of the unitarity of the CKM matrix, the CKM structure factorizes when neglecting the combination $V_{us}^* V_{ub}$. The effective Hamiltonian then reads

$$\mathcal{H}_{\text{eff}} = -\frac{4\,G_F}{\sqrt{2}}\,V_{ts}^* V_{tb} \sum_{i=1}^{10} C_i(\mu) O_i(\mu)\,. \tag{1}$$

Following Ref. [41], we choose the operator basis as follows:

$$\begin{aligned}
O_1 &= (\bar{s}_L\gamma_\mu T^a c_L)(\bar{c}_L\gamma^\mu T^a b_L)\,, & O_2 &= (\bar{s}_L\gamma_\mu c_L)(\bar{c}_L\gamma^\mu b_L)\,,\\
O_3 &= (\bar{s}_L\gamma_\mu b_L)\textstyle\sum_q(\bar{q}\gamma^\mu q)\,, & O_4 &= (\bar{s}_L\gamma_\mu T^a b_L)\textstyle\sum_q(\bar{q}\gamma^\mu T^a q)\,,\\
O_5 &= (\bar{s}_L\gamma_\mu\gamma_\nu\gamma_\rho b_L)\textstyle\sum_q(\bar{q}\gamma^\mu\gamma^\nu\gamma^\rho q)\,, & O_6 &= (\bar{s}_L\gamma_\mu\gamma_\nu\gamma_\rho T^a b_L)\textstyle\sum_q(\bar{q}\gamma^\mu\gamma^\nu\gamma^\rho T^a q)\,,\\
O_7 &= \tfrac{e}{g_s^2}m_b(\bar{s}_L\sigma^{\mu\nu}b_R)F_{\mu\nu}\,, & O_8 &= \tfrac{1}{g_s}m_b(\bar{s}_L\sigma^{\mu\nu}T^a b_R)G^a_{\mu\nu}\,,\\
O_9 &= \tfrac{e^2}{g_s^2}(\bar{s}_L\gamma_\mu b_L)\textstyle\sum_l(\bar{l}\gamma^\mu l)\,, & O_{10} &= \tfrac{e^2}{g_s^2}(\bar{s}_L\gamma_\mu b_L)\textstyle\sum_l(\bar{l}\gamma^\mu\gamma_5 l)\,,
\end{aligned} \tag{2}$$

where the subscripts L and R refer to left- and right- handed components of the fermion fields.

The factors $1/g_s^2$ in the definition of the operators O_7, O_9 and O_{10}, as well as the factor $1/g_s$ present in O_8 have been chosen by Misiak [24] in order to simplify the organization of the calculation: With these definitions, the one-loop anomalous dimensions [needed for a leading logarithmic (LL) calculation] of the operators O_i are all proportional to g_s^2, while two-loop anomalous dimensions [needed for a next-to-leading logarithmic (NLL) calculation] are proportional to g_s^4, etc.

After this important remark we now outline the principal steps which lead to a LL, NLL, NNLL prediction for the decay amplitude for $b \to s\,\ell^+\ell^-$:

1. A matching calculation between the full SM theory and the effective theory has to be performed in order to determine the Wilson coefficients C_i at the high scale $\mu_W \sim m_W, m_t$. At this scale, the coefficients can be worked out in fixed order perturbation theory, ie they can be expanded in g_s^2:

$$C_i(\mu_W) = C_i^{(0)}(\mu_W) + \frac{g_s^2}{16\,\pi^2}\,C_i^{(1)}(\mu_W) + \frac{g_s^4}{(16\,\pi^2)^2}\,C_i^{(2)}(\mu_W) + \mathcal{O}(g_s^6)\,. \tag{3}$$

   At LL order, only $C_i^{(0)}$ are needed, at NLL order also $C_i^{(1)}$, etc. While the coefficient $C_7^{(2)}$, which is needed for a NNLL analysis, is known for quite some time [9], $C_9^{(2)}$ and $C_{10}^{(2)}$ have been calculated only recently [41] (see also [43]).

2. The renormalization group equation (RGE) has to be solved in order to get the Wilson coefficients at the low scale $\mu_b \sim m_b$. For this RGE step the anomalous dimension matrix to the relevant order in g_s is required, as described above. After these two steps one can decompose the Wilson coefficients $C_i(\mu_b)$ into a LL, NLL and NNLL part according to

$$C_i(\mu_b) = C_i^{(0)}(\mu_b) + \frac{g_s^2(\mu_b)}{16\,\pi^2}\,C_i^{(1)}(\mu_b) + \frac{g_s^4(\mu_b)}{(16\,\pi^2)^2}\,C_i^{(2)}(\mu_b) + \mathcal{O}(g_s^6)\,. \tag{4}$$

3. In order to get the decay amplitude, the matrix elements $\langle s\,\ell^+\ell^-|O_i(\mu_b)|b\rangle$ have to be calculated. At LL precision, only the operator O_9 contributes, as this operator is the only one which at the same time has a Wilson coefficient starting at lowest order and an explicit $1/g_s^2$ factor in the definition. Hence, at NLL precision, QCD corrections (virtual and bremsstrahlung) to the matrix element of O_9 are needed. They have been calculated a few years ago [24, 28]. At NLL precision, also the other operators start contributing, viz $O_7(\mu_b)$ and $O_{10}(\mu_b)$ contribute at tree-level and the four-quark operators $O_1, ..., O_6$ at one-loop level. Accordingly, QCD corrections to the latter matrix elements are needed for a NNLL prediction of the decay amplitude.

The formally leading term $\sim (1/g_s^2)C_9^{(0)}(\mu_b)$ to the amplitude for $b \to s\,\ell^+\ell^-$ is smaller than the NLL term $\sim (1/g_s^2)\left[g_s^2/(16\pi^2)\right] C_9^{(1)}(\mu_b)$ [23]. We adapt our systematics to the numerical situation and treat the sum of these two terms as a NLL contribution. This is, admittedly some abuse of language, because the decay amplitude then starts out with a term which is called NLL.

As pointed out in step 3), $\mathcal{O}(\alpha_s)$ QCD corrections to the matrix elements $\langle s\,\ell^+\ell^-|O_i(\mu_b)|b\rangle$ have to be calculated in order to obtain the NNLL prediction for the decay amplitude. In the present paper we systematically evaluate virtual corrections of $\mathcal{O}(\alpha_s)$ to the matrix elements of O_1, O_2, O_7, O_8, O_9 and O_{10}. As the Wilson coefficients of the gluonic penguin operators $O_3, ..., O_6$ are much smaller than those of O_1 and O_2, we neglect QCD corrections to their matrix elements. As discussed in more detail later, we also include those bremsstrahlung diagrams which are needed to cancel the infrared and collinear singularities from the virtual contributions. The complete bremsstrahlung corrections, ie all the finite parts, will be given elsewhere [44]. We anticipate that the QCD corrections calculated in the present paper substantially reduce the scale dependence of the NLL result.

3 Virtual $\mathcal{O}(\alpha_s)$ Corrections to the Current-Current Operators O_1 and O_2

In this section we present a detailed calculation of the virtual $\mathcal{O}(\alpha_s)$ corrections to the matrix elements of the current-current operators O_1 and O_2. Using the naive dimensional regularization scheme (NDR) in $d = 4 - 2\,\epsilon$ dimensions, both ultraviolet and infrared singularities show up as $1/\epsilon^n$ poles ($n = 1, 2$). The ultraviolet singularities cancel after including the counterterms. Collinear singularities are regularized by retaining a finite strange quark mass m_s. They are cancelled together with the infrared singularities at the level of the decay width, taking the bremsstrahlung process $b \to s\,\ell^+\ell^- g$ into account. Gauge invariance implies that the QCD corrected matrix elements of the operators O_i can be written as

$$\langle s\,\ell^+\ell^-|O_i|b\rangle = \hat{F}_i^{(9)}\langle O_9\rangle_{\rm tree} + \hat{F}_i^{(7)}\langle O_7\rangle_{\rm tree}\,, \tag{5}$$

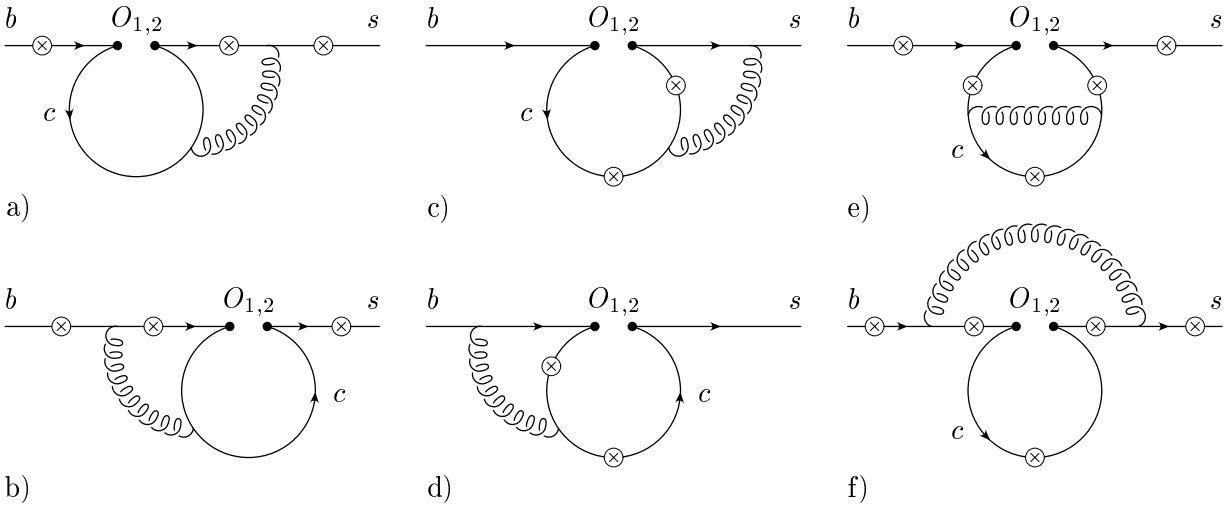

Figure 3.1: Complete list of two-loop Feynman diagrams for $b \to s\gamma^*$ associated with the operators O_1 and O_2. The fermions (b, s and c quarks) are represented by solid lines, whereas the curly lines represent gluons. The circle-crosses denote the possible locations where the virtual photon (which then splits into a lepton pair) is emitted.

where $\langle O_9\rangle_{\rm tree}$ and $\langle O_7\rangle_{\rm tree}$ are the tree-level matrix elements of O_9 and O_7, respectively. Equivalently, we may write

$$\langle s\,\ell^+\ell^-|O_i|b\rangle = -\frac{\alpha_s}{4\,\pi}\left[F_i^{(9)}\langle\widetilde{O}_9\rangle_{\rm tree} + F_i^{(7)}\langle\widetilde{O}_7\rangle_{\rm tree}\right], \tag{6}$$

where the operators $\widetilde{O}_7$ and $\widetilde{O}_9$ are defined as

$$\widetilde{O}_7 = \frac{\alpha_s}{4\,\pi}\,O_7\,, \quad \widetilde{O}_9 = \frac{\alpha_s}{4\,\pi}\,O_9\,. \tag{7}$$

We present the final results for the QCD corrected matrix elements in the form of Eq. (6).

3.1 Regularized $\mathcal{O}(\alpha_s)$ Contribution of O_1 and O_2

The full set of the diagrams contributing to the matrix elements

$$M_i = \langle s\,\ell^+\ell^-|O_i|b\rangle \quad (i = 1, 2) \tag{8}$$

at $\mathcal{O}(\alpha_s)$ is shown in Fig. 3.1. As indicated in this figure, the diagrams associated with O_1 and O_2 are topologically identical. They differ only by the color structure. While the matrix elements of the operator O_2 all involve the color structure

$$\sum_a T^a T^a = C_F\mathbf{1}, \quad C_F = \frac{N_c^2 - 1}{2\,N_c}, \tag{9}$$

there are two possible color structures for the corresponding diagrams of O_1, viz

$$\tau_1 = \sum_{a,b} T^a T^b T^a T^b \quad \text{and} \quad \tau_2 = \sum_{a,b} T^a T^b T^b T^a. \tag{10}$$

The structure τ_1 appears in diagrams 3.1a)-d) and τ_2 in diagrams 3.1e) and 3.1f). Using the relation

$$\sum_a T^a_{\alpha\beta} T^a_{\gamma\delta} = -\frac{1}{2\,N_c}\,\delta_{\alpha\beta}\delta_{\gamma\delta} + \frac{1}{2}\,\delta_{\alpha\delta}\delta_{\beta\gamma},$$

we find that $\tau_1 = C_{\tau_1}\mathbf{1}$ and $\tau_2 = C_{\tau_2}\mathbf{1}$ with

$$C_{\tau_1} = -\frac{N_c^2-1}{4\,N_c^2} \quad \text{and} \quad C_{\tau_2} = \frac{(N_c^2-1)^2}{4\,N_c^2}\,.$$

Inserting $N_c = 3$, the color factors are $C_F = \frac{4}{3}$, $C_{\tau_1} = -\frac{2}{9}$ and $C_{\tau_2} = \frac{16}{9}$. The contributions from O_1 are obtained by multiplying those from O_2 by the appropriate factors, ie by $C_{\tau_1}/C_F = -\frac{1}{6}$ and $C_{\tau_2}/C_F = \frac{4}{3}$, respectively. In the following descriptions of the individual diagrams we therefore restrict ourselves to those associated with the operator O_2.

In the current paper we use the $\overline{\text{MS}}$ renormalization scheme which is technically implemented by introducing the renormalization scale in the form $\overline{\mu}^2 = \mu^2 \exp(\gamma_E)/(4\,\pi)$, followed by minimal subtraction. The precise definition of the evanescent operators, which is necessary to fully specify the renormalization scheme, will be given later. The remainder of this section is divided into 8 subsections. Subsections 3.1.1–3.1.6 deal with the diagrams 3.1a)–d) which are calculated by means of Mellin-Barnes techniques [45]. Subsection 3.1.7 is devoted to the diagrams 3.1e), which are evaluated by using the heavy mass expansion procedure [46]. Among the diagrams 3.1f) only the one where the virtual photon is emitted from the charm quark line is non-zero. As it factorizes into two one-loop diagrams, its calculation is straightforward and does not require to be discussed in detail. It is, however, worth mentioning already at this point that it is convenient to omit this diagram in the discussion of the matrix elements of O_1 and O_2 and to take it into account together with the virtual corrections to O_9. Finally, in Subsection 3.1.8, we give the results for the dimensionally regularized matrix elements $\langle s\,\ell^+\ell^-|O_i|b\rangle$ $(i = 1, 2)$.

3.1.1 The Building Blocks I_β and $J_{\alpha\beta}$

For the calculation of diagrams 3.1a)–d) it is advisable to evaluate the building blocks I_β and $J_{\alpha\beta}$ first. The corresponding diagrams are depicted in Fig. 3.2. After performing a straightforward Feynman parameterization followed by the integration over the loop

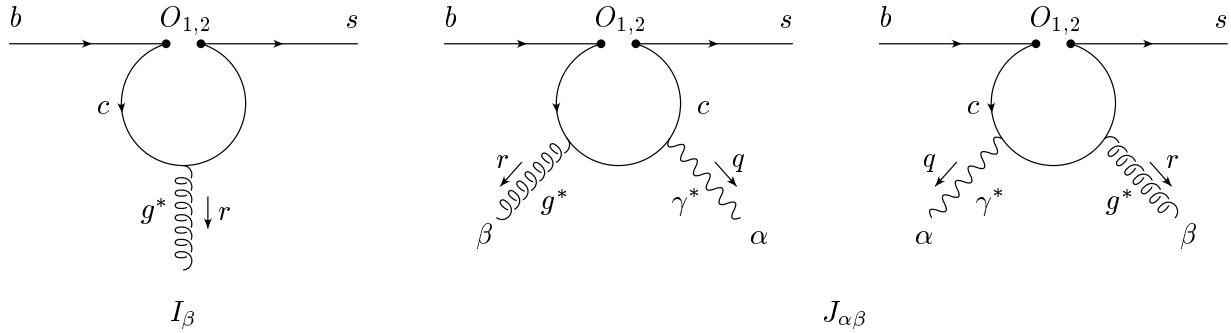

Figure 3.2: The building blocks I_β and $J_{\alpha\beta}$ which are used for the calculation of the two-loop diagrams 3.1a)-d). The curly and wavy lines represent gluons and photons, respectively.

momentum, the analytic expression for the building block I_β reads

$$I_\beta = -\frac{g_s}{4\,\pi^2}\,\Gamma(\epsilon)\,\mu^{2\epsilon}\,\mathrm{e}^{\gamma_E\epsilon}\,(1-\epsilon)\,\mathrm{e}^{i\pi\epsilon}\,\left(r_\beta \not{r} - r^2\gamma_\beta\right)\,L\,\frac{\lambda}{2} \times \int_0^1 dx\,\Big[x(1-x)\Big]^{1-\epsilon}\,\left[r^2 - \frac{m_c^2}{x(1-x)} + i\,\delta\right]^{-\epsilon}, \quad (11)$$

where r is the momentum of the virtual gluon emitted from the c-quark loop. The term $i\,\delta$ is the "$i\,\epsilon$ prescription". In the full two-loop diagrams, the free index β will be contracted with the corresponding gluon propagator. Note that I_β is gauge invariant in the sense that $r^\beta I_\beta = 0$.

The building block $J_{\alpha\beta}$ is somewhat more complicated. Using the notation introduced by Simma and Wyler [47], it reads

$$J_{\alpha\beta} = \frac{e\,g_s\,Q_u}{16\,\pi^2}\,\Big[E(\alpha,\beta,r)\Delta i_5 + E(\alpha,\beta,q)\Delta i_6 - E(\beta,r,q)\frac{r_\alpha}{q\cdot r}\,\Delta i_{23} - E(\alpha,r,q)\frac{r_\beta}{q\cdot r}\,\Delta i_{25} - E(\alpha,r,q)\frac{q_\beta}{q\cdot r}\,\Delta i_{26} - E(\beta,r,q)\frac{q_\alpha}{q\cdot r}\,\Delta i_{27}\Big]\,L\,\frac{\lambda}{2}, \quad (12)$$

where q and r denote the momenta of the (virtual) photon and gluon, respectively. The indices α and β will be contracted with the propagators of the photon and the gluon, respectively. The matrix $E(\alpha,\beta,r)$ is defined as

$$E(\alpha,\beta,r) = \frac{1}{2}(\gamma_\alpha\gamma_\beta \not{r} - \not{r}\gamma_\beta\gamma_\alpha) \quad (13)$$

and the dimensionally regularized quantities Δi_k occurring in Eq. (12) read

$$\begin{aligned}
\Delta i_5 &= 4\,B^+ \int_S dx\,dy\,\big[4(q\cdot r)\,x\,y\,(1-x)\epsilon + r^2\,x\,(1-x)(1-2\,x)\epsilon \\
&\qquad + q^2\,y(2-2\,y+2\,x\,y-x)\epsilon + (1-3\,x)C\big]\;C^{-1-\epsilon}\,, \\
\Delta i_6 &= 4\,B^+ \int_S dx\,dy\,\big[-4(q\cdot r)\,x\,y\,(1-y)\epsilon - q^2\,y\,(1-y)(1-2\,y)\epsilon \\
&\qquad - r^2\,x\,(2-2\,x+2\,x\,y-y)\epsilon - (1-3\,y)C\big]\;C^{-1-\epsilon}\,, \\
\Delta i_{23} &= -\Delta i_{26} = 8\,B^+(q\cdot r)\int_S dx\,dy\,x\,y\,\epsilon\,C^{-1-\epsilon}\,, \\
\Delta i_{25} &= -8\,B^+(q\cdot r)\int_S dx\,dy\,x\,(1-x)\,\epsilon\,C^{-1-\epsilon}\,, \\
\Delta i_{27} &= 8\,B^+(q\cdot r)\int_S dx\,dy\,y\,(1-y)\,\epsilon\,C^{-1-\epsilon}\,,
\end{aligned} \tag{14}$$

where $B^+ = (1+\epsilon)\Gamma(\epsilon)\,\mathrm{e}^{\gamma_E\epsilon}\mu^{2\epsilon}$ and C is given by

$$C = m_c^2 - 2\,x\,y(q\cdot r) - r^2\,x\,(1-x) - q^2\,y\,(1-y).$$

The integration over the Feynman parameters x and y is restricted to the simplex S, ie $y \in [0, 1-x]$, $x \in [0,1]$. Due to Ward identities, the quantities Δi_k are not independent of one another. Namely,

$$q^\alpha J_{\alpha\beta} = 0 \quad \text{and} \quad r^\beta J_{\alpha\beta} = 0$$

imply that Δi_5 and Δi_6 can be expressed as

$$\Delta i_5 = \Delta i_{23} + \frac{q^2}{q\cdot r}\,\Delta i_{27}\,; \quad \Delta i_6 = \frac{r^2}{q\cdot r}\,\Delta i_{25} + \Delta i_{26}. \tag{15}$$

3.1.2 General Remarks

After inserting the above expressions for the building blocks I_β and $J_{\alpha\beta}$ into diagrams 3.1a), b) and 3.1c), d), respectively, and introducing additional Feynman parameters, we can easily perform the integration over the second loop momentum. The remaining Feynman parameter integrals are, however, non-trivial. In Refs. [12] and [48], where the analogous corrections to the processes $b \to s\gamma$ and $b \to sg$ were studied, the strategy used to evaluate these integrals is the following:

- The denominators are represented as complex Mellin-Barnes integrals (see below and Refs. [12, 48]).

- After interchanging the order of integration and appropriate variable transformations, the Feynman parameter integrals reduce to Euler β and Γ functions.
- Finally, by Cauchy's theorem the remaining complex integral over the Mellin variable can be written as a sum over residues taken at certain poles of β and Γ functions. This leads in a natural way to an expansion in the small ratio $z = m_c^2/m_b^2$.

However, this procedure cannot be applied directly in the present case: While the processes $b \to s\gamma$ and $b \to sg$ are characterized by the two mass scales m_b and m_c, a third mass scale, viz q^2, the invariant mass squared of the lepton pair, enters the process $b \to s\,\ell^+\ell^-$. For values of q^2 satisfying

$$\frac{q^2}{m_b^2} < 1 \quad \text{and} \quad \frac{q^2}{4\,m_c^2} < 1,$$

most of the diagrams allow a naive Taylor series expansion in q^2 and the dependence of the charm quark mass can again be calculated by means of Mellin-Barnes representations. This method does not work, however, for the diagram in Fig. 3.1a) where the photon is emitted from the internal s quark line. Instead, we apply a Mellin-Barnes representation twice, as we discuss in detail in Subsection 3.1.4. Using these methods, we get the results for diagrams 3.1a)–d) as an expansion in $\hat{s} = q^2/m_b^2$, $z = m_c^2/m_b^2$ and $\hat{s}/(4\,z)$ as well as $\ln(\hat{s})$ and $\ln(z)$. This implies that our results are meaningful only for small values of $\hat{s}$. Fortunately, this is exactly the range of main theoretical and experimental interest in the phenomenology of the process $b \to s\,\ell^+\ell^-$.

3.1.3 Calculation of Diagram 3.1b)

We describe the basic steps of our calculation of the diagram in Fig. 3.1b) where the photon is emitted from the internal b quark line. Our notations for the momenta are set up in Fig. 3.3a). Inserting the building block I_β yields the following analytic expression for this diagram:

$$M_2[1b] = \frac{i\,\mathrm{e}\,Q_d\,g_s^2}{4\,\pi^2}\,C_F\,\Gamma(\epsilon)\mathrm{e}^{2\gamma_E\epsilon}\mu^{4\epsilon}(1-\epsilon)\,e^{i\pi\epsilon}(4\,\pi)^{-\epsilon}\int_0^1 dx\,\frac{\big[x(1-x)\big]^{1-\epsilon}}{\big[r^2 - m_c^2/[x(1-x)] + i\delta\big]^\epsilon}$$
$$\int\frac{d^dr}{(2\,\pi)^d}\,\bar{u}(p')\left(r_\beta \not{r} - r^2\gamma_\beta\right)\,L\,\frac{\not{p}' + \not{r} + m_b}{(p'+r)^2 - m_b^2}\,\gamma_\alpha\,\frac{\not{p} + \not{r} + m_b}{(p+r)^2 - m_b^2}\,\gamma^\beta\,u(p)\cdot\frac{1}{r^2}\,. \quad (16)$$

Applying a Feynman parameterization according to

$$\frac{1}{D_1\,D_2\,D_3\,D_4^\epsilon} = \frac{\Gamma(3+\epsilon)}{\Gamma(\epsilon)}\int_S \frac{du\,dv\,dy\;y^{\epsilon-1}}{\big[u\,D_1 + vD_2 + (1-u-v-y)D_3 + yD_4\big]^{3+\epsilon}}\,, \quad (17)$$

with

$$D_1 = (p'+r)^2 - m_b^2, \qquad D_2 = (p+r)^2 - m_b^2, \quad (18)$$
$$D_3 = r^2, \qquad D_4 = r^2 - m_c^2/[x(1-x)], \quad (19)$$

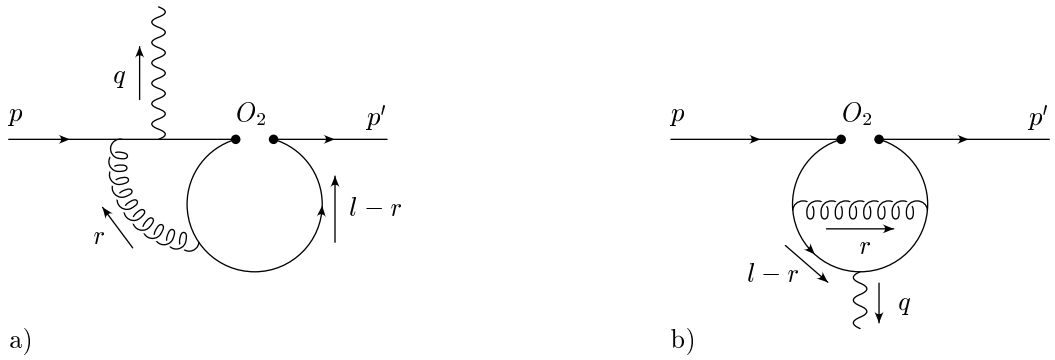

Figure 3.3: a) Momentum flow in diagram 3.1b), where the virtual photon is emitted from the internal b quark line (see Subsection 3.1.3); b) Momentum flow in the vertex correction diagram in Fig. 3.1e) (see Subsection 3.1.7).

and performing the integral over the loop momentum r, we obtain

$$M_2[1b] = -\frac{e\,Q_d\,g_s^2}{64\,\pi^4}(1-\epsilon)C_F\,\Gamma(2\epsilon)\mathrm{e}^{2\gamma_E\epsilon}\mu^{4\epsilon}\times \int_0^1 dx\,\big[x(1-x)\big]^{1-\epsilon}\int_S dv\,du\,dy\,y^{\epsilon-1}\,\bar{u}(p')\left[\frac{P_1}{\Delta_b^{1+2\epsilon}}+\frac{P_2}{\Delta_b^{2\epsilon}}+\frac{P_3\,\Delta_b}{\Delta_b^{2\epsilon}}\right]u(p)\,, \quad (20)$$

where the Feynman parameters u, v and y run over the simplex S, i.e $u, v, y > 0$ and $u+v+y \leq 1$. P_1, P_2 and P_3 are polynomials in the Feynman parameters, and the quantity Δ_b reads

$$\Delta_b = m_b^2(u + u\,v + v^2) - q^2\,u\,v + \frac{m_c^2\,y}{x(1-x)}\,.$$

For $q^2 \leq m_b^2$ it is positive in the integration region. Therefore, one is allowed to do a naive Taylor series expansion of the integrand in q^2. In order to simplify the resulting Feynman parameter integrals, it is convenient to first transform the integration variables x, y, u and v according to

$$u \to \frac{(1-v')(-1+v'+u')}{v'}\,, \quad v \to \frac{(1-v')(1-u')}{v'}\,, \quad x \to x', \quad y \to y'v'.$$

The integration region of the new variables is given by $u' \in [1-v', 1]$ and $v', x', y' \in [0, 1]$. Taking the corresponding Jacobian into account and omitting primes in order to simplify the notation, we find

$$M_2[1b] = -\frac{e\,Q_d\,g_s^2}{64\,\pi^4}(1-\epsilon)C_F\,\Gamma(2\epsilon)\,\mathrm{e}^{2\gamma_E\epsilon}\mu^{4\epsilon}\times \int_0^1 dx\,\big[x(1-x)\big]^{1-\epsilon}\int_0^1 dv\int_{1-v}^1 du\int_0^1 dy\,(v\,y)^{\epsilon-1}\,(1-v)\,\bar{u}(p')\left[\frac{Q_1}{\Delta_b^{1+2\epsilon}}+\frac{Q_2}{\Delta_b^{2\epsilon}}+\frac{Q_3\Delta_b}{\Delta_b^{2\epsilon}}\right]u(p)\,, \quad (21)$$

where, in terms of the new variables, Δ_b reads

$$\Delta_b = m_b^2(1-v)u + q^2\,\frac{(1-v)^2(1-v-u)(1-u)}{v^2} + m_c^2\,\frac{v\,y}{x(1-x)}\,.$$

Q_1, Q_2 and Q_3 are rational functions in the new Feynman parameters. After performing the Taylor series expansion in q^2, the remaining integrals are of the form

$$\int_0^1 dx\,dv\,dy \int_{1-v}^1 du\,\Big[x(1-x)\Big]^{1-\epsilon}(v\,y)^{\epsilon-1}(1-v)\frac{1}{v^m}\frac{P(x,y,u,v)}{\Delta_{b,0}^{n+2\epsilon}}\,, \tag{22}$$

where $P(x,y,u,v)$ is a polynomial in x, y, u and v; $\Delta_{b,0} = \Delta_b(q^2=0)$. n and m are non-negative integers. We further follow the strategy used in [12, 48] and represent the denominators $\Delta_{b,0}^{\lambda}$ as Mellin-Barnes integrals. The Mellin-Barnes representation for $(K^2 - M^2)^{-\lambda}$ reads $(\lambda > 0)$

$$\frac{1}{(K^2-M^2)^{\lambda}} = \frac{1}{(K^2)^{\lambda}}\,\frac{1}{\Gamma(\lambda)}\,\frac{1}{2\,i\pi}\int_{\gamma} ds\,\left(-\frac{M^2}{K^2}\right)^s \Gamma(-s)\,\Gamma(\lambda+s)\,. \tag{23}$$

The integration path γ runs parallel to the imaginary axis and intersects the real axis somewhere between $-\lambda$ and 0. The Mellin-Barnes representation of $\Delta_{b,0}^{\lambda}$ is obtained by making the identifications

$$K^2 \leftrightarrow m_b^2\,u(1-v) \quad \text{and} \quad M^2 \leftrightarrow -m_c^2\,y\,v/[x(1-x)].$$

Interchanging the order of integration, it is now an easy task to perform the Feynman parameter integrals since the most complicated ones are of the form

$$\int_0^1 da\,a^{p(s)}(1-a)^{q(s)} = \beta\big(p(s)+1, q(s)+1\big)\,. \tag{24}$$

The integration path γ has to be chosen in such a way that the Feynman parameter integrals exist for values of $s \in \gamma$. By inspection of the explicit expressions, one finds that this is the case if the path γ is chosen such that Re(s) $> -\epsilon$. (Note that in this paper ϵ is always a positive number). To perform the integration over the Mellin parameter s, we close the integration path in the right half-plane and use the residue theorem to identify the integral with the sum over the residues of the poles located at

$$\begin{aligned}
s &= 0,\ 1,\ 2,\ 3,\ \ldots\,,\\
s &= 1-\epsilon,\ 2-\epsilon,\ 3-\epsilon,\ \ldots\,,\\
s &= 1-2\epsilon,\ 2-2\epsilon,\ 3-2\epsilon,\ \ldots\,,\\
s &= 1/2-2\epsilon,\ 3/2-2\epsilon,\ 5/2-2\epsilon,\ \ldots\,.
\end{aligned} \tag{25}$$

In view of the factor $(m_c^2/m_b^2)^s$, stemming from the Mellin-Barnes formula (23), the evaluation of the residues at the pole positions listed in Eq. (25) corresponds directly to an expansion in $z = m_c^2/m_b^2$. Note that closing the integration contour in the right half-plane yields an overall minus sign due to the clockwise orientation of the integration path. After expanding in ϵ, we get the form factors of $M_2[1b]$ [see Eq. (6)] as an expansion of the form

$$F_2^{(7,9)}[1b] = \sum_{i,l,m} c_{2,ilm}^{(7,9)}\, \hat{s}^i\, z^l\, \ln^m(z), \tag{26}$$

where i and m are non-negative integers and l is a natural multiple of $\frac{1}{2}$ [see Eq. (25)]. Furthermore, the power m of $\ln(z)$ is bounded by four, independent of the values of i and l. This becomes clear if we consider the structure of the poles. There are three poles in s located near any natural number k, viz at $s = k$, $s = k - \epsilon$ and $s = k - 2\epsilon$. Taking the residue at one of them yields a term proportional to $1/\epsilon^2$ from the other two poles. In addition, there can be an explicit $1/\epsilon^2$ term from the integration over the two loop momenta. Therefore, the most singular term can be of order $1/\epsilon^4$ and, after expanding in ϵ, the highest possible power of $\ln(z)$ is four.

3.1.4 Calculation of Diagram 3.1a)

To calculate the diagram in Fig. 3.1a) where the photon is emitted from the internal s quark, we proceed in a similar way as in the previous subsection, ie we insert the building block I_β, introduce three additional Feynman parameters and integrate over the loop momentum r. The characteristic denominator Δ_a is of the form

$$\Delta_a = \left(A\, m_b^2 + B\, q^2 + C\, m_c^2 + i\,\delta\right)$$

and occurs with powers 2ϵ or $1 + 2\epsilon$. The coefficients A, B and C are functions of the Feynman parameters. After suitable transformations, they read

$$A = u\, v(1-v), \quad B = u\, v^2(1-u), \quad C = -\frac{y(1-v)}{x(1-x)}\,,$$

with $u,\ v,\ x,\ y \in [0,1]$. From this we conclude that the result of this diagram is not analytic in q^2. We are therefore not allowed to Taylor expand the integrand. Instead, we apply the Mellin-Barnes representation twice and write

$$\frac{1}{\Delta_a^\lambda} = \frac{1}{(B\,q^2)^\lambda} \int_\gamma ds \int_{\gamma'} ds' \, \frac{\Gamma(s+\lambda)\,\Gamma(-s')\,\Gamma(s'-s)\,\mathrm{e}^{i\pi s'}}{(2\,i\pi)^2\,\Gamma(\lambda)} \left[\frac{A\, m_b^2}{B\, q^2}\right]^s \left[-\frac{C\, m_c^2}{A\, m_b^2}\right]^{s'}. \tag{27}$$

The integration paths γ and γ' are again parallel to the imaginary axis and $-\lambda < \mathrm{Re}(s) < \mathrm{Re}(s') < 0$. λ takes one of the two values 2ϵ and $1 + 2\epsilon$. We have written Eq. (27) in such a way that non-integer powers appear only for positive numbers, ie we made use of the formula

$$(x \pm i\,\delta)^\alpha = \mathrm{e}^{\pm i\pi\alpha}(-x \mp i\,\delta)^\alpha\,.$$

As in the preceding subsection, the exact positions of the integration paths γ and γ' are dictated by the condition that the Feynman parameter integrals exist for values of s and s' lying thereon. For $\lambda = 2\epsilon$, we find that these integrals exist if

$$-\epsilon < \mathrm{Re}(s) < \mathrm{Re}(s') < 0.$$

Closing the integration contour for the s and s' integration in the left and right half-plane, respectively, and applying the residue theorem results in an expansion in $\hat{s}$ and z. As Re(s′) > Re(s), the term $\Gamma(s'-s)$ in Eq. (27) does not generate any poles. For $\lambda = 2\epsilon$, the poles which have to be taken into account are located at

$$\begin{aligned} &s' = 1-\epsilon,\ 2-\epsilon,\ 3-\epsilon,\ \ldots, && s = -\epsilon,\ -1-\epsilon,\ -2-\epsilon,\ \ldots, \\ &s' = 1-2\epsilon,\ 2-2\epsilon,\ 3-2\epsilon,\ \ldots, && s = -2\epsilon,\ -1-2\epsilon,\ -2-2\epsilon,\ \ldots, \\ &s' = 0,\ 1,\ 2,\ \ldots. \end{aligned}$$

For $\lambda = 1 + 2\epsilon$, we find that the Feynman parameter integrals exist if

$$-\epsilon < \mathrm{Re}(s') < 0 \quad \text{and} \quad -1-\epsilon < \mathrm{Re(s)} < -2\epsilon.$$

This condition implies that the poles at $s = -\epsilon, -2\epsilon$ in the above list must not be taken into account when applying the residue theorem.

The final result for the form factors [Eq.(6)] of this diagram is of the form

$$F_2^{(7,9)}[1a] = \sum_{i,j,l,m} c_{i,j,l,m}^{(7,9)}\, \hat{s}^i\, \ln^j(\hat{s})\, z^l\, \ln^m(z), \tag{28}$$

where i, j, l and m all are non-negative integers. The remaining four diagrams in Fig. 3.1a) and b) exhibit no further difficulties.

3.1.5 Calculation of Diagrams 3.1c)

Inserting the building block $J_{\alpha\beta}$ allows us to calculate directly the sum of the two diagrams shown in Fig. 3.1c). After performing the second loop integral, one obtains

$$\begin{aligned} M_2[1c] = {} & \frac{e\,Q_u\,g_s^2\,C_F}{256\,\pi^4}(1+\epsilon)\,\Gamma(2\epsilon)\,\mathrm{e}^{2\gamma_E\epsilon}\mu^{4\epsilon}\mathrm{e}^{2i\pi\epsilon} \\ & \int dx\,dy\,du\,dv\,\frac{v^\epsilon(1-u)^{1+\epsilon}(1-x)}{\big[x(1-x)\big]^{1+\epsilon}}\,\bar{u}(p')\left[\frac{P_1}{\Delta_c^{1+2\epsilon}}+\frac{P_2}{\Delta_c^{2\epsilon}}+\frac{P_3\,\Delta_c}{\Delta_c^{2\epsilon}}\right]u(p)\,, \end{aligned} \tag{29}$$

where P_1, P_2 and P_3 are polynomials in the Feynman parameters, which all run in the interval [0,1]. Δ_c reads [using $v' = v(1-u)$]

$$\Delta_c = m_b^2\,u\,v'\,y - q^2\,y\,v'\,(u + y\,v') - \frac{v'}{x(1-x)}\Big\{m_c^2 - q^2\,y(1-x)\big[1-y(1-x)\big]\Big\}.$$

Note that we do not expand in q^2 at this stage of the calculation. Instead, we use the Mellin-Barnes representation (23) with the identification

$$K^2 \leftrightarrow m_b^2\, u\, v'\, y \quad \text{and} \quad M^2 \leftrightarrow q^2\, y\, v'\, (u + y\, v') + \frac{v'}{x(1-x)} \Big\{ m_c^2 - q^2\, y(1-x)\big[1 - y(1-x)\big] \Big\}\,.$$

This representation does a good job, since $(-M^2/K^2)^s$ turns out to be analytic in q^2 for $\hat{s} < 4\,z$, as in this range M^2/K^2 is positive for all values of the Feynman parameters. We therefore do the Taylor expansion with respect to q^2 only at this level. Evaluating the Feynman parameter integrals as well as the Mellin-Barnes integral, we find the result as an expansion in z and $\hat{s}/(4\,z)$ which can be cast into the general form

$$F_2^{(7,9)}[1c] = \sum_{i,l,m} c_{2,ilm}^{(7,9)}\, \hat{s}^i\, z^l\, \ln^m(z), \tag{30}$$

where i and m are non-negative integers and $l = -i, -i + \frac{1}{2}, -i + 1, \ldots$.

3.1.6 Calculation of Diagrams 3.1d)

After inserting the building block $J_{\alpha\beta}$ and performing the second loop integral, the sum of the diagrams in Fig. 3.1d) yields

$$M_2[1d] = \frac{e\, Q_u\, g_s^2\, C_F}{256\,\pi^4} (1+\epsilon)\, \Gamma(2\epsilon)\, \mathrm{e}^{2\gamma_E \epsilon} \mu^{4\epsilon} \int_S dx\, dy \int_S du\, dv\, \frac{v^\epsilon}{\big[x(1-x)\big]^{1+\epsilon}}\, \bar{u}(p') \left[\frac{P_1}{\Delta_d^{1+2\epsilon}} + \frac{P_2}{\Delta_d^{2\epsilon}} + \frac{P_3\, \Delta_d}{\Delta_d^{2\epsilon}} \right] u(p)\,, \tag{31}$$

where P_1, P_2 and P_3 are polynomials in the Feynman parameters x, y, u and v. The parameters (x, y) and (u, v) run in their respective simplex. The quantity Δ_d reads

$$\Delta_d = m_b^2\, u \left(u + \frac{y\, v}{1-x} \right) + q^2\, y\, v \left[\frac{y\, v}{(1-x)^2} + \frac{u}{1-x} - \frac{(1-y)}{x(1-x)} \right] + \frac{m_c^2\, v}{x(1-x)}\,.$$

Next, we use the Mellin-Barnes representation (23) with the identification

$$K^2 \leftrightarrow m_b^2\, u \left(u + \frac{y\, v}{1-x} \right), \quad M^2 \leftrightarrow q^2\, y\, v \left[\frac{y\, v}{(1-x)^2} + \frac{u}{1-x} - \frac{(1-y)}{x(1-x)} \right] + \frac{m_c^2\, v}{x(1-x)}\,.$$

Again, $(-M^2/K^2)^s$ is analytic in q^2 for $\hat{s} < 4\,z$, which allows us to perform a Taylor series expansion with respect to q^2. In order to perform the integrations over the Feynman parameters, we make suitable substitutions, eg

$$x \to x', \quad y \to \frac{(1-x')\big[y' - (1-v')\big]}{v'}\,, \quad v \to u'v', \quad u \to u'(1-v'). \tag{32}$$

The new variables x', u', v' run in the interval $[0,1]$, while y' varies in $[1-v',1]$. Evaluating the integrals over the Feynman and Mellin parameters, we find the result as an expansion in z and $\hat{s}/(4\,z)$ which can be cast into the general form

$$F_2^{(7,9)}[1d] = \sum_{i,l,m} c_{2,ilm}^{(7,9)}\, \hat{s}^i\, z^l\, \ln^m(z). \tag{33}$$

i and m are non-negative integers and $l = -i, -i+\frac{1}{2}, -i+1, \ldots$.

3.1.7 Calculation of Diagram 3.1e)

We consider one of the diagrams in Fig. 3.1e) in some detail and redraw it in Fig. 3.3b). The matrix element is proportional to $1/\Delta_e$, where

$$\Delta_e = \left[(l-r)^2 - m_c^2\right] \left[(l-q-r)^2 - m_c^2\right] \left[(l-q)^2 - m_c^2\right] \left[l^2 - m_c^2\right] r^2. \tag{34}$$

q is the four-momentum of the off-shell photon, while l and r denote loop momenta. As $q^2 < 4\,m_c^2$ in our application, we use the heavy mass expansion (HME) technique [46] to evaluate this diagram. In the present case, as the gluon is massless, the HME boils down to a naive Taylor series expansion of the diagram (before loop integrations) in the four-momentum q. Expanding $1/\Delta_e$ in q, we obtain

$$\frac{1}{\Delta_e} = \sum_{n,m,i,j,k} C_e(n,m,i,j,k)\, \frac{(q^2)^i\, (q\cdot r)^j\, (q\cdot l)^k}{r^2 \left[l^2 - m_c^2\right]^n \left[(l-r)^2 - m_c^2\right]^m}\,. \tag{35}$$

Using the Feynman parameterization

$$\frac{1}{\left[l^2 - m_c^2\right]^n \left[(l-r)^2 - m_c^2\right]^m} = \frac{\Gamma(n+m)}{\Gamma(n)\,\Gamma(m)} \int_0^1 dv\, \frac{v^{m-1}(1-v)^{n-1}}{\left[l^2 - 2\,v(l\cdot r) - m_c^2 + v\,r^2\right]^{n+m}}\,, \tag{36}$$

we can perform the integration over the loop momentum l. The integral over the loop momentum r can be done using the parameterization

$$\frac{1}{r^2}\left(\frac{1}{r^2 - \frac{m_c^2}{v(1-v)}}\right)^p = \frac{\Gamma(1+p)}{\Gamma(p)} \int_0^1 \frac{u^{p-1}}{\left(r^2 - \frac{u\,m_c^2}{v(1-v)}\right)^{p+1}}\, du\,. \tag{37}$$

The remaining integrals over the Feynman parameters u and v all have the form of Eq. (24) and can be performed easily. The other two diagrams in Fig. 3.1e) where the virtual photon is emitted from the charm quark can be evaluated in a similar way. The diagrams where the photon is radiated from the b quark or the s quark vanish.

As the results for the sum of all the diagrams in Fig. 3.1e) are compact, we explicitly give their contribution to the form factors $F_a^{(j)}$ $(a = 1, 2;\ j = 7, 9)$. We obtain $F_a^{(7)}[1e] = 0$, $F_1^{(9)}[1e] = \frac{4}{3} F_2^{(9)}[1e]$ and

$$\begin{aligned} F_2^{(9)}[1e] \;=\; & \left(\frac{\mu}{m_c}\right)^{4\epsilon} \frac{1}{\epsilon}\left[\frac{8}{3} + \frac{128}{45}\left(\frac{\hat{s}}{4\,z}\right) + \frac{256}{105}\left(\frac{\hat{s}}{4\,z}\right)^2 + \frac{2048}{945}\left(\frac{\hat{s}}{4\,z}\right)^3\right] \\ & - \left[\frac{124}{27} + \frac{12416}{3645}\left(\frac{\hat{s}}{4\,z}\right) + \frac{11072}{42525}\left(\frac{\hat{s}}{4\,z}\right)^2 - \frac{4971776}{4465125}\left(\frac{\hat{s}}{4\,z}\right)^3\right]. \end{aligned} \tag{38}$$

3.1.8 Unrenormalized Form Factors of O_1 and O_2

We stress that the diagram 3.1f) where the virtual photon is emitted from the charm quark line is the only one in Fig. 3.1 which suffers from infrared and collinear singularities. As this diagram can easily be combined with diagram 4.1b) associated with the operator O_9, we take it into account only in Section 4.1, where the virtual corrections to O_9 are discussed. The unrenormalized form factors $F_a^{(7,9)}$ of $\langle s\,\ell^+\ell^-|O_a|b\rangle$ $(a = 1, 2)$, corresponding to diagrams 3.1a)–3.1e), are obtained in the form

$$F_a^{(7,9)} = \sum_{i,j,l,m} c_{a,ijlm}^{(7,9)}\, \hat{s}^i\, \ln^j(\hat{s})\, z^l\, \ln^m(z),$$

where i, j and m are non-negative integers and $l = -i, -i+\frac{1}{2}, -i+1, \ldots$. We keep the terms with i and l up to 3, after checking that higher order terms are small for $0.05 \le \hat{s} \le 0.25$, the range considered in this paper. As we will give the full results for the counterterm contributions to the form factors in Section 3.2 and the renormalized form factors in Section 3.3 and in Appendix B, it is not necessary to explicitly present the somewhat lengthy expressions for the unrenormalized form factors. But, in order to demonstrate the cancellation of ultraviolet singularities in the next section, we list the divergent parts of the unrenormalized form factors: $F_1^{(7)}$, $F_1^{(9)}$, $F_2^{(7)}$ and $F_2^{(9)}$:

$$\begin{aligned} F_{2,\mathrm{div}}^{(9)} = & \frac{128}{81\,\epsilon^2} - \frac{4}{25515\,\epsilon}\left(1890 + 1260\,i\pi + 5040\,L_\mu - 1260\,L_s + 252\,\hat{s} + 27\,\hat{s}^2 + 4\,\hat{s}^3\right) \\ & + \frac{8}{2835\,\epsilon}\left[420 + 2520\,L_\mu - 1260\,L_z + 2016\left(\frac{\hat{s}}{4\,z}\right) + 1296\left(\frac{\hat{s}}{4\,z}\right)^2 + 1024\left(\frac{\hat{s}}{4\,z}\right)^3\right], \end{aligned}$$

$$F_{2,\mathrm{div}}^{(7)} = \frac{92}{81\,\epsilon}, \tag{39a}$$

$$F_{1,\mathrm{div}}^{(9)} = -\frac{64}{243\,\epsilon^2} + \frac{2}{76545\,\epsilon}\left(1890 + 1260\,i\pi + 5040\,L_\mu - 1260\,L_s + 252\,\hat{s} + 27\,\hat{s}^2 + 4\,\hat{s}^3\right) - \frac{4}{8505\,\epsilon}\left[-8085 + 2520\,L_\mu - 1260\,L_z - 7056\left(\frac{\hat{s}}{4\,z}\right) - 6480\left(\frac{\hat{s}}{4\,z}\right)^2 - 5888\left(\frac{\hat{s}}{4\,z}\right)^3\right],$$

$$F_{1,\mathrm{div}}^{(7)} = -\frac{46}{243\,\epsilon}, \tag{39b}$$

where $L_s = \ln(\hat{s})$, $L_z = \ln(z)$, $L_\mu = \ln\left(\frac{\mu}{m_b}\right)$ and $z = \frac{m_c^2}{m_b^2}$.

3.2 $\mathcal{O}(\alpha_s)$ Counterterms to O_1 and O_2

So far, we have calculated the two-loop matrix elements $\langle s\,\ell^+\ell^-|C_i\,O_i|b\rangle$ $(i = 1, 2)$. As the operators mix under renormalization, there are additional contributions proportional to C_i. These counterterms arise from the matrix elements of the operators

$$\sum_{j=1}^{12} \delta Z_{ij} O_j\,, \quad i = 1, 2, \tag{40}$$

where the operators O_1–O_{10} are given in Eq. (2). O_{11} and O_{12} are evanescent operators, ie operators which vanish in $d = 4$ dimensions. In principle, there is some freedom in the choice of the evanescent operators. However, as we want to combine our matrix elements with the Wilson coefficients calculated by Bobeth *et al.* [41], we must use the same definitions:

$$O_{11} = (\bar{s}_L\gamma_\mu\gamma_\nu\gamma_\sigma T^a c_L)\,(\bar{c}_L\gamma^\mu\gamma^\nu\gamma^\sigma T^a b_L) - 16\,O_1\,, \tag{41}$$

$$O_{12} = (\bar{s}_L\gamma_\mu\gamma_\nu\gamma_\sigma c_L)\,(\bar{c}_L\gamma^\mu\gamma^\nu\gamma^\sigma b_L) - 16\,O_2\,. \tag{42}$$

The operator renormalization constants $Z_{ij} = \delta_{ij} + \delta Z_{ij}$ are of the form

$$\delta Z_{ij} = \frac{\alpha_s}{4\,\pi}\left(a_{ij}^{01} + \frac{1}{\epsilon}\,a_{ij}^{11}\right) + \frac{\alpha_s^2}{(4\,\pi)^2}\left(a_{ij}^{02} + \frac{1}{\epsilon}\,a_{ij}^{12} + \frac{1}{\epsilon^2}\,a_{ij}^{22}\right) + \mathcal{O}(\alpha_s^3). \tag{43}$$

Most of the coefficients a_{ij}^{lm} needed for our calculation are given in Ref. [41]. As some are new (or not explicitly given in [41]), we list those for $i = 1, 2$ and $j = 1, ..., 12$:

$$\hat{a}^{11} = \begin{pmatrix} -2 & \frac{4}{3} & 0 & -\frac{1}{9} & 0 & 0 & 0 & 0 & -\frac{16}{27} & 0 & \frac{5}{12} & \frac{2}{9} \\ 6 & 0 & 0 & \frac{2}{3} & 0 & 0 & 0 & 0 & -\frac{4}{9} & 0 & 1 & 0 \end{pmatrix}, \tag{44a}$$

$$
\begin{aligned}
a_{17}^{12} &= -\tfrac{58}{243}\,, \quad a_{19}^{12} = -\tfrac{64}{729}\,, \quad a_{19}^{22} = \tfrac{1168}{243}\,, \\
a_{27}^{12} &= \tfrac{116}{81}\,, \quad\quad a_{29}^{12} = \tfrac{776}{243}\,, \quad\quad a_{29}^{22} = \tfrac{148}{81}\,.
\end{aligned}
\tag{44b}
$$

We denote the counterterm contributions to $b \to s\,\ell^+\ell^-$ which are due to the mixing of O_1 or O_2 into four-quark operators by $F_{i\to 4\text{quark}}^{\text{ct}(7)}$ and $F_{i\to 4\text{quark}}^{\text{ct}(9)}$. They can be extracted from the equation

$$
\sum_j \left(\frac{\alpha_s}{4\,\pi}\right) \frac{1}{\epsilon}\, a_{ij}^{11} \langle s\,\ell^+\ell^-|O_j|b\rangle_{\text{1-loop}} = -\left(\frac{\alpha_s}{4\,\pi}\right) \left[F_{i\to 4\text{quark}}^{\text{ct}(7)} \langle \widetilde{O}_7\rangle_{\text{tree}} + F_{i\to 4\text{quark}}^{\text{ct}(9)} \langle \widetilde{O}_9\rangle_{\text{tree}}\right], \tag{45}
$$

where j runs over the four-quark operators. As certain entries of $\hat{a}^{11}$ are zero, only the one-loop matrix elements of O_1, O_2, O_4, O_{11} and O_{12} are needed. In order to keep the presentation transparent, we relegate their explicit form to Appendix A.

The counterterms which are related to the mixing of O_i $(i = 1, 2)$ into O_9 can be split into two classes: The first class consists of the one-loop mixing $O_i \to O_9$, followed by taking the one-loop corrected matrix element of O_9. It is obvious that this class contributes to the renormalization of diagram 3.1f). As we decided to treat diagram 3.1f) only in Section 4.1 (when discussing virtual corrections to O_9), we proceed in the same way with the counterterm just mentioned. There is, however, a second class of counterterm contributions due to $O_i \to O_9$ mixing. These contributions are generated by two-loop mixing of O_2 into O_9 as well as by one-loop mixing and one-loop renormalization of the g_s factor in the definition of the operator O_9. We denote the corresponding contribution to the counterterm form factors by $F_{i\to 9}^{\text{ct}(7)}$ and $F_{i\to 9}^{\text{ct}(9)}$. We obtain

$$
F_{i\to 9}^{\text{ct}(9)} = -\left(\frac{a_{i9}^{22}}{\epsilon^2} + \frac{a_{i9}^{12}}{\epsilon}\right) - \frac{a_{i9}^{11}\,\beta_0}{\epsilon^2}\,, \quad F_{i\to 9}^{\text{ct}(7)} = 0, \tag{46}
$$

where we made use of the renormalization constant Z_{g_s} given by

$$
Z_{g_s} = 1 - \frac{\alpha_s}{4\pi}\,\frac{\beta_0}{2}\,\frac{1}{\epsilon}\,, \quad \beta_0 = 11 - \frac{2}{3}N_f\,, \quad N_f = 5. \tag{47}
$$

Besides the contribution from operator mixing, there are ordinary QCD counterterms. The renormalization of the charm quark mass is taken into account by replacing m_c through $Z_{m_c} \cdot m_c$ in the one-loop matrix elements of O_1 and O_2 (see Appendix A). We denote the corresponding contribution to the counterterm form factors by $F_{i,m_c\text{ren}}^{\text{ct}(7)}$ and $F_{i,m_c\text{ren}}^{\text{ct}(9)}$. We

obtain

$$
\begin{aligned}
F^{\mathrm{ct}(7)}_{1,m_c\mathrm{ren}} &= F^{\mathrm{ct}(7)}_{2,m_c\mathrm{ren}} = 0, \\
F^{\mathrm{ct}(9)}_{1,m_c\mathrm{ren}} &= \frac{4}{3}\, F^{\mathrm{ct}(9)}_{2,m_c\mathrm{ren}}\,, \\
F^{\mathrm{ct}(9)}_{2,m_c\mathrm{ren}} &= -\frac{32}{945\,\epsilon}\left[105 + 84\left(\frac{\hat{s}}{4\,z}\right) + 72\left(\frac{\hat{s}}{4\,z}\right)^2 + 64\left(\frac{\hat{s}}{4\,z}\right)^3\right] \\
&\quad - \frac{32}{2835}\left[105 + 1260\ln\frac{\mu}{m_c} + \left(\frac{\hat{s}}{4\,z}\right)\left(336 + 1008\ln\frac{\mu}{m_c}\right)\right. \\
&\quad \left. + \left(\frac{\hat{s}}{4\,z}\right)^2\left(396 + 864\ln\frac{\mu}{m_c}\right) + \left(\frac{\hat{s}}{4\,z}\right)^3\left(416 + 768\ln\frac{\mu}{m_c}\right)\right], \qquad (48)
\end{aligned}
$$

where we have used the pole mass definition of m_c which is characterized by the renormalization constant

$$
Z_m = 1 - \frac{\alpha_s}{4\,\pi}\,\frac{4}{3}\left[\frac{3}{\epsilon} + 6\ln\left(\frac{\mu}{m}\right) + 4\right]. \qquad (49)
$$

If one wishes to express the results for $F^{\mathrm{ct}(9)}_{i,m_c\mathrm{ren}}$ in terms of the $\overline{\mathrm{MS}}$ definition of the charm quark mass, the expressions in Eqs. (48) get changed according to

$$
F^{\mathrm{ct}(9)}_{i,m_c\mathrm{ren}} \to F^{\mathrm{ct}(9)}_{i,m_c\mathrm{ren}} + \Delta F^{\mathrm{ct}(9)}_{i,m_c\mathrm{ren}}\,, \qquad (50)
$$

where $\Delta F^{\mathrm{ct}(9)}_{i,m_c\mathrm{ren}}$ reads

$$
\begin{aligned}
\Delta F^{\mathrm{ct}(9)}_{1,m_c\mathrm{ren}} &= \frac{4}{3}\,\Delta F^{\mathrm{ct}(9)}_{2,m_c\mathrm{ren}}\,, \qquad (51) \\
\Delta F^{\mathrm{ct}(9)}_{2,m_c\mathrm{ren}} &= \frac{64}{945}\left[105 + 84\left(\frac{\hat{s}}{4\,z}\right) + 72\left(\frac{\hat{s}}{4\,z}\right)^2 + 64\left(\frac{\hat{s}}{4\,z}\right)^3\right]\left(\ln\frac{\mu}{m_c} + \frac{2}{3}\right).
\end{aligned}
$$

We stress at this point that we always use the pole mass definition in the following, ie Eqs. (48) for $F^{\mathrm{ct(j)}}_{i,m_c\mathrm{ren}}$.

The total counterterms $F^{\mathrm{ct(j)}}_i$ $(i = 1, 2;\ j = 7, 9)$ which renormalize diagrams 3.1a)–3.1e) are given by

$$
F^{\mathrm{ct(j)}}_i = F^{\mathrm{ct(j)}}_{i\to 4\mathrm{quark}} + F^{\mathrm{ct(j)}}_{i\to 9} + F^{\mathrm{ct(j)}}_{i,m_c\mathrm{ren}}\,. \qquad (52)
$$

Explicitly, they read

$$
\begin{aligned}
F_2^{\mathrm{ct}(9)} =& - F_{2,\,\mathrm{div}}^{(9)} - \frac{4}{25515}\Bigg[5740 + 2520\,\pi^2 - 840\,i\pi \\
&+ 840\,L_\mu\,(19 - 3\,i\pi - 54\,L_z + 48\,L_\mu) + 3780\,L_z(-2 + 3\,L_z) \\
&+ 420\,L_s\,(3\,i\pi + 2 + 6\,L_\mu) - 630\,L_s^2 + 252\,\hat{s}\,(1 - 2\,L_\mu) - 54\,L_\mu\,\hat{s}^2 - 2\,\hat{s}^3\,(1 + 4\,L_\mu) \\
&+ 6048\left(\frac{\hat{s}}{4\,z}\right)(18\,L_\mu - 9\,L_z - 1) + 7776\left(\frac{\hat{s}}{4\,z}\right)^2(10\,L_\mu - 5\,L_z + 3) \\
&+ 1536\left(\frac{\hat{s}}{4\,z}\right)^3(42\,L_\mu - 21\,L_z + 19)\Bigg],
\end{aligned}
$$

$$
F_2^{\mathrm{ct}(7)} = - F_{2,\,\mathrm{div}}^{(7)} + \frac{2}{2835}\left(840\,L_\mu + 70\,\hat{s} + 7\,\hat{s}^2 + \hat{s}^3\right),
$$

$$
\begin{aligned}
F_1^{\mathrm{ct}(9)} =& - F_{1,\,\mathrm{div}}^{(9)} + \frac{2}{76545}\Bigg[- 62300 - 840\,i\pi + 2520\,\pi^2 \\
&+ 840\,L_\mu(-3\,i\pi - 54\,L_z + 48\,L_\mu - 791) + 3780\,L_z(3\,L_z + 88) \\
&+ 420\,L_s(3\,i\pi + 2 + 6\,L_\mu) - 630\,L_s^2 + \hat{s}(252 - 504\,L_\mu) - 54\,\hat{s}^2\,L_\mu - 2\,\hat{s}^3(1 + 4\,L_\mu) \\
&- 6048\left(\frac{\hat{s}}{4\,z}\right)(28 + 90\,L_\mu - 45\,L_z) - 7776\left(\frac{\hat{s}}{4\,z}\right)^2(27 + 62\,L_\mu - 31\,L_z) \\
&- 768\left(\frac{\hat{s}}{4\,z}\right)^3(295 + 564\,L_\mu - 282\,L_z)\Bigg],
\end{aligned}
$$

$$
F_1^{\mathrm{ct}(7)} = -F_{1,\,\mathrm{div}}^{(7)} - \frac{1}{8505}\left(840\,L_\mu + 70\,\hat{s} + 7\,\hat{s}^2 + \hat{s}^3\right). \tag{53}
$$

The divergent parts of these counterterms are, up to a sign, identical to those of the unrenormalized matrix elements given in Eq. (39a), which proves the cancellation of ultraviolet singularities.

As mentioned before, we will take diagram 3.1f) into account only in Section 4.1. The same holds for the counterterms associated with the b and s quark wave function renormalization and, as mentioned earlier in this subsection, the $\mathcal{O}(\alpha_s)$ correction to the matrix element of $\delta Z_{i9} O_9$. The sum of these contributions is

$$
\delta\bar{Z}_\psi\langle O_i\rangle_{\text{1-loop}} + \frac{\alpha_s}{4\,\pi}\,\frac{a_{i9}^{11}}{\epsilon}\left[\delta\bar{Z}_\psi\langle O_9\rangle_{\text{tree}} + \langle O_9\rangle_{\text{1-loop}}\right], \quad \delta\bar{Z}_\psi = \sqrt{Z_\psi(m_b)Z_\psi(m_s)} - 1,
$$

and provides the counterterm that renormalizes diagram 3.1f). We use on-shell renormalization for the external b and s quark. In this scheme the field strength renormalization

constants are given by

$$Z_\psi(m) = 1 - \frac{\alpha_s}{4\,\pi}\,\frac{4}{3}\,\left(\frac{\mu}{m}\right)^{2\epsilon}\left(\frac{1}{\epsilon} + \frac{2}{\epsilon_{\rm IR}} + 4\right). \tag{54}$$

So far, we have discussed the counterterms which renormalize the $\mathcal{O}(\alpha_s)$ corrected matrix elements $\langle s\,\ell^+\ell^-|O_i|b\rangle$ $(i = 1, 2)$. The corresponding one-loop matrix elements [of $\mathcal{O}(\alpha_s^0)$] are renormalized by adding the counterterms

$$\frac{\alpha_s}{4\,\pi}\,\frac{a_{i9}^{11}}{\epsilon}\,\langle O_9\rangle_{\rm tree}\,.$$

3.3 Renormalized Form Factors of O_1 and O_2

We decompose the renormalized matrix elements of O_i $(i = 1, 2)$ as

$$\langle s\,\ell^+\ell^-|C_i^{(0)}O_i|b\rangle = C_i^{(0)}\left(-\frac{\alpha_s}{4\,\pi}\right)\left[F_i^{(9)}\langle\widetilde{O}_9\rangle_{\rm tree} + F_i^{(7)}\langle\widetilde{O}_7\rangle_{\rm tree}\right], \tag{55}$$

where $\widetilde{O}_9 = \frac{\alpha_s}{4\,\pi}\,O_9$ and $\widetilde{O}_7 = \frac{\alpha_s}{4\,\pi}\,O_7$. The form factors $F_i^{(9)}$ and $F_i^{(7)}$, expanded up to $\hat{s}^3$ and z^3, of the renormalized sum of diagrams 3.1a)–e) read [$L_c = \ln(m_c/m_b) = \ln(\hat{m}_c) = L_c/2$]

$$\begin{aligned} F_1^{(9)} = {} & \left(-\frac{1424}{729} + \frac{16}{243}\,i\pi + \frac{64}{27}\,L_c\right)L_\mu - \frac{16}{243}\,L_\mu\,L_s + \left(\frac{16}{1215} - \frac{32}{135}\,z^{-1}\right)L_\mu\,\hat{s} \\ & + \left(\frac{4}{2835} - \frac{8}{315}\,z^{-2}\right)L_\mu\,\hat{s}^2 + \left(\frac{16}{76545} - \frac{32}{8505}\,z^{-3}\right)L_\mu\,\hat{s}^3 - \frac{256}{243}\,L_\mu^2 + f_1^{(9)}\,, \end{aligned} \tag{56}$$

$$\begin{aligned} F_2^{(9)} = {} & \left(\frac{256}{243} - \frac{32}{81}\,i\pi - \frac{128}{9}\,L_c\right)L_\mu + \frac{32}{81}\,L_\mu\,L_s + \left(-\frac{32}{405} + \frac{64}{45}\,z^{-1}\right)L_\mu\,\hat{s} \\ & + \left(-\frac{8}{945} + \frac{16}{105}\,z^{-2}\right)L_\mu\,\hat{s}^2 + \left(-\frac{32}{25515} + \frac{64}{2835}\,z^{-3}\right)L_\mu\,\hat{s}^3 + \frac{512}{81}\,L_\mu^2 + f_2^{(9)}\,, \end{aligned} \tag{57}$$

$$F_1^{(7)} = -\frac{208}{243}\,L_\mu + f_1^{(7)}, \qquad F_2^{(7)} = \frac{416}{81}\,L_\mu + f_2^{(7)}\,. \tag{58}$$

The analytic results for $f_1^{(9)}$, $f_1^{(7)}$, $f_2^{(9)}$, and $f_2^{(7)}$ are rather lengthy. We decompose them as follows:

$$f_a^{(b)} = \sum_{i,j,l,m}\kappa_{a,ijlm}^{(b)}\,\hat{s}^i\,L_s^j\,z^l\,L_c^m + \sum_{i,j}\rho_{a,ij}^{(b)}\,\hat{s}^i\,L_s^j. \tag{59}$$

	$\hat{m}_c = 0.25$	$\hat{m}_c = 0.29$	$\hat{m}_c = 0.33$
$k_1^{(9)}(0,0)$	$-12.715 + 0.094699\,i$	$-11.973 + 0.16371\,i$	$-11.355 + 0.19217\,i$
$k_1^{(9)}(0,1)$	$-0.078830 - 0.074138\,i$	$-0.081271 - 0.059691\,i$	$-0.079426 - 0.043950\,i$
$k_1^{(9)}(1,0)$	$-38.742 - 0.67862\,i$	$-28.432 - 0.25044\,i$	$-21.648 - 0.063493\,i$
$k_1^{(9)}(1,1)$	$-0.039301 - 0.00017258\,i$	$-0.040243 + 0.016442\,i$	$-0.029733 + 0.031803\,i$
$k_1^{(9)}(2,0)$	$-103.83 - 2.5388\,i$	$-57.114 - 0.86486\,i$	$-33.788 - 0.24902\,i$
$k_1^{(9)}(2,1)$	$-0.044702 + 0.0026283\,i$	$-0.035191 + 0.027909\,i$	$-0.0020505 + 0.040170\,i$
$k_1^{(9)}(3,0)$	$-313.75 - 8.4554\,i$	$-128.80 - 2.5243\,i$	$-59.105 - 0.72977\,i$
$k_1^{(9)}(3,1)$	$-0.051133 + 0.022753\,i$	$-0.017587 + 0.050639\,i$	$0.052779 + 0.038212\,i$
$k_1^{(7)}(0,0)$	$-0.76730 - 0.11418\,i$	$-0.68192 - 0.074998\,i$	$-0.59736 - 0.044915\,i$
$k_1^{(7)}(0,1)$	0	0	0
$k_1^{(7)}(1,0)$	$-0.28480 - 0.18278\,i$	$-0.23935 - 0.12289\,i$	$-0.19850 - 0.081587\,i$
$k_1^{(7)}(1,1)$	$-0.0032808 + 0.020827\,i$	$0.0027424 + 0.019676\,i$	$0.0074152 + 0.016527\,i$
$k_1^{(7)}(2,0)$	$0.056108 - 0.23357\,i$	$-0.0018555 - 0.17500\,i$	$-0.039209 - 0.12242\,i$
$k_1^{(7)}(2,1)$	$0.016370 + 0.020913\,i$	$0.022864 + 0.011456\,i$	$0.022282 + 0.00062522\,i$
$k_1^{(7)}(3,0)$	$0.62438 - 0.027438\,i$	$0.28248 - 0.12783\,i$	$0.085946 - 0.11020\,i$
$k_1^{(7)}(3,1)$	$0.030536 + 0.0091424\,i$	$0.029027 - 0.0082265\,i$	$0.012166 - 0.019772\,i$

Table 3.1: Coefficients in the decomposition of $f_1^{(9)}$ and $f_1^{(7)}$ for three different values of $\hat{m}_c$. See Eq. (60).

The quantities $\rho_{a,ij}^{(b)}$ collect the half-integer powers of $z = m_c^2/m_b^2 = \hat{m}_c^2$. This way, the summation indices in the above equation run over integers only. We list the coefficients $\kappa_{a,ijlm}^{(b)}$ and $\rho_{a,ij}^{(b)}$ in Appendix B.

If we give the charm quark mass dependence in numerical form, the formulas become simpler. For this purpose, we write the functions $f_a^{(b)}$ as

$$f_a^{(b)} = \sum_{i,j} k_a^{(b)}(i,j)\,\hat{s}^i\,L_s^j \quad (a = 1,2;\; b = 7,9;\; i = 0,...,3;\; j = 0,1)\,. \tag{60}$$

The numerical values for the quantities $k_a^{(b)}(i,j)$ are given in Table 3.1 and 3.2 for $\hat{m}_c = 0.25$, 0.29, 0.33. For numerical values corresponding to $\hat{m}_c = 0.27$, 0.29, 0.31 we refer to Tables I and II (Tables 3.1 and 3.2 in Part II of this thesis) in the letter version [42].

	$\hat{m}_c = 0.25$	$\hat{m}_c = 0.29$	$\hat{m}_c = 0.33$
$k_2^{(9)}(0,0)$	$9.5042 - 0.56819\,i$	$6.6338 - 0.98225\,i$	$4.3035 - 1.1530\,i$
$k_2^{(9)}(0,1)$	$0.47298 + 0.44483\,i$	$0.48763 + 0.35815\,i$	$0.47656 + 0.26370\,i$
$k_2^{(9)}(1,0)$	$7.4238 + 4.0717\,i$	$3.3585 + 1.5026\,i$	$0.73780 + 0.38096\,i$
$k_2^{(9)}(1,1)$	$0.23581 + 0.0010355\,i$	$0.24146 - 0.098649\,i$	$0.17840 - 0.19082\,i$
$k_2^{(9)}(2,0)$	$0.33806 + 15.233\,i$	$-1.1906 + 5.1892\,i$	$-2.3570 + 1.4941\,i$
$k_2^{(9)}(2,1)$	$0.26821 - 0.015770\,i$	$0.21115 - 0.16745\,i$	$0.012303 - 0.24102\,i$
$k_2^{(9)}(3,0)$	$-42.085 + 50.732\,i$	$-17.120 + 15.146\,i$	$-9.2008 + 4.3786\,i$
$k_2^{(9)}(3,1)$	$0.30680 - 0.13652\,i$	$0.10552 - 0.30383\,i$	$-0.31667 - 0.22927\,i$
$k_2^{(7)}(0,0)$	$4.6038 + 0.68510\,i$	$4.0915 + 0.44999\,i$	$3.5842 + 0.26949\,i$
$k_2^{(7)}(0,1)$	0	0	0
$k_2^{(7)}(1,0)$	$1.7088 + 1.0967\,i$	$1.4361 + 0.73732\,i$	$1.1910 + 0.48952\,i$
$k_2^{(7)}(1,1)$	$0.019685 - 0.12496\,i$	$-0.016454 - 0.11806\,i$	$-0.044491 - 0.099160\,i$
$k_2^{(7)}(2,0)$	$-0.33665 + 1.4014\,i$	$0.011133 + 1.0500\,i$	$0.23525 + 0.73452\,i$
$k_2^{(7)}(2,1)$	$-0.098219 - 0.12548\,i$	$-0.13718 - 0.068733\,i$	$-0.13369 - 0.0037513\,i$
$k_2^{(7)}(3,0)$	$-3.7463 + 0.16463\,i$	$-1.6949 + 0.76698\,i$	$-0.51568 + 0.66118\,i$
$k_2^{(7)}(3,1)$	$-0.18321 - 0.054854\,i$	$-0.17416 + 0.049359\,i$	$-0.072997 + 0.11863\,i$

Table 3.2: Coefficients in the decomposition of $f_2^{(9)}$ and $f_2^{(7)}$ for three different values of $\hat{m}_c$. See Eq. (60).

4 Virtual Corrections to the Matrix Elements of the Operators O_7, O_8, O_9 and O_{10}

4.1 Virtual Corrections to the Matrix Element of O_9 and O_{10}

As the hadronic parts of the operators O_9 and O_{10} are identical, the QCD corrected matrix element of O_{10} can easily be obtained from the one of O_9. We therefore present only the calculation for $\langle s\,\ell^+\ell^-|O_9|b\rangle$ in some detail. The virtual corrections to this matrix element consist of the vertex correction shown in Fig. 4.1b) and of the quark self-energy contributions. The result can be written as

$$\langle s\,\ell^+\ell^-|C_9 O_9|b\rangle = \widetilde{C}_9^{(0)}\left(-\frac{\alpha_s}{4\,\pi}\right)\left[F_9^{(9)}\langle\widetilde{O}_9\rangle_{\rm tree} + F_9^{(7)}\langle\widetilde{O}_7\rangle_{\rm tree}\right], \tag{61}$$

with $\widetilde{O}_9 = \frac{\alpha_s}{4\,\pi}\,O_9$ and $\widetilde{C}_9^{(0)} = \frac{4\,\pi}{\alpha_s}\left(C_9^{(0)} + \frac{\alpha_s}{4\,\pi}\,C_9^{(1)}\right)$.

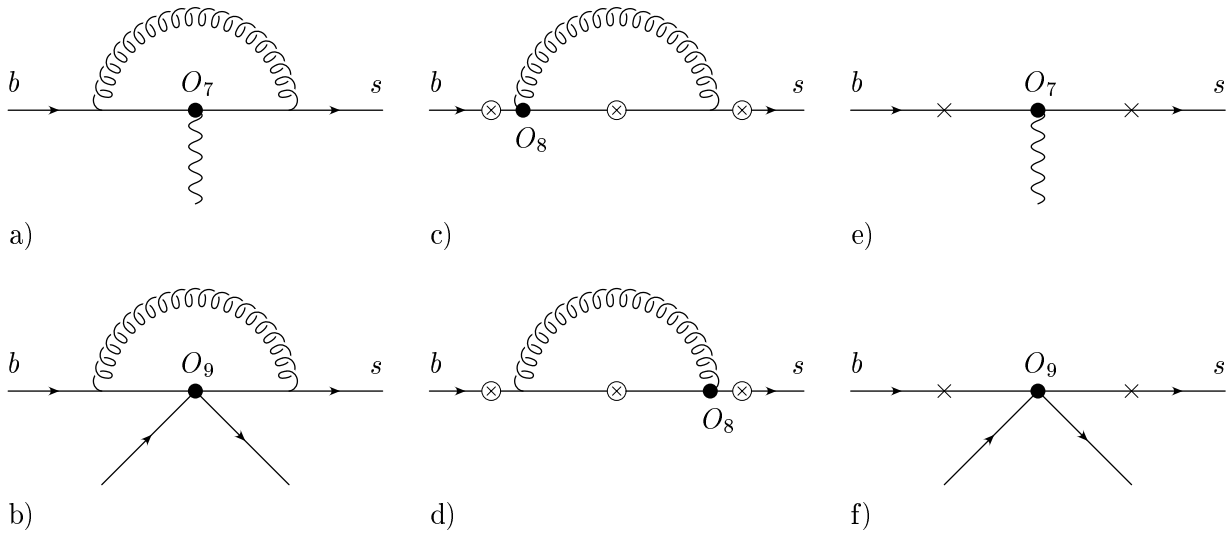

Figure 4.1: Some Feynman diagrams for $b \to s\gamma^*$ or $b \to s\,\ell^+\ell^-$ associated with the operators O_7, O_8 and O_9. The circle-crosses denote the possible locations where the virtual photon is emitted, while the crosses mark the possible locations for gluon bremsstrahlung. See text.

We evaluate diagram 4.1b) keeping the strange quark mass m_s as a regulator of collinear singularities. The unrenormalized contributions of diagram 4.1b) to the form factors $F_9^{(7)}$ and $F_9^{(9)}$ read

$$\begin{aligned} F_9^{(9)}[4b] &= -\frac{\left[\frac{\mu}{m_b}\right]^{2\epsilon}}{\epsilon}\,\frac{4}{3} + \frac{\left[\frac{\mu}{m_b}\right]^{2\epsilon}}{\epsilon_{\rm IR}}\,\frac{8}{3}\left(\hat{s} + \frac{1}{2}\,\hat{s}^2 + \frac{1}{3}\,\hat{s}^3 + \frac{1}{2}\ln(r)\right) \\ &\quad + \frac{8}{3}\ln(r) - \frac{2}{3}\ln^2(r) + \frac{16}{3} + \frac{20}{3}\,\hat{s} + \frac{16}{3}\,\hat{s}^2 + \frac{116}{27}\,\hat{s}^3\,, \\ F_9^{(7)}[4b] &= -\frac{2}{3}\,\hat{s}\left(1 + \frac{1}{2}\,\hat{s} + \frac{1}{3}\,\hat{s}^2\right), \end{aligned} \tag{62}$$

where we kept all terms up to $\hat{s}^3$. $\epsilon_{\rm IR}$ and $r = (m_s^2/m_b^2)$ regularize the infrared and collinear singularities in Eq. (62).

The b and s quark self-energy contributions are obtained by multiplying the tree level matrix element of O_9 by the quark field renormalization factor $\delta\bar{Z}_\psi = \sqrt{Z_\psi(m_b)Z_\psi(m_s)} - 1$, where the explicit form for $Z_\psi(m)$ (in the on-shell scheme) is given in Eq. (54).

Adding the self-energy contributions and the vertex correction, we get the ultraviolet finite

results

$$F_9^{(9)} = \frac{16}{3} + \frac{20}{3}\,\hat{s} + \frac{16}{3}\,\hat{s}^2 + \frac{116}{27}\,\hat{s}^3 + f_{\rm inf}\,, \tag{63}$$

$$f_{\rm inf} = \frac{\left[\frac{\mu}{m_b}\right]^{2\epsilon}}{\epsilon_{\rm IR}}\,\frac{8}{3}\left(1+\hat{s}+\frac{1}{2}\,\hat{s}^2+\frac{1}{3}\,\hat{s}^3\right) + \frac{\left[\frac{\mu}{m_b}\right]^{2\epsilon}}{\epsilon_{\rm IR}}\,\frac{4}{3}\,\ln(r) + \frac{2}{3}\ln(r) - \frac{2}{3}\ln^2(r), \tag{64}$$

$$F_9^{(7)} = -\frac{2}{3}\,\hat{s}\left(1+\frac{1}{2}\,\hat{s}+\frac{1}{3}\,\hat{s}^2\right). \tag{65}$$

At this place, it is convenient to incorporate diagram 3.1f) together with its counterterms discussed in Section 3.2.

It is easy to see that the two loops in diagram 3.1f) factorize into two one-loop contributions. The charm loop has the Lorentz structure of O_9 and can therefore be absorbed into a modified Wilson coefficient: The renormalized diagram 3.1f) is properly included by modifying $\widetilde{C}_9^{(0)}$ in Eq. (61) as follows:

$$\widetilde{C}_9^{(0)} \longrightarrow \widetilde{C}_9^{(0,\rm mod)} = \widetilde{C}_9^{(0)} + \left(C_2^{(0)} + \frac{4}{3}\,C_1^{(0)}\right) H_0\,, \tag{66}$$

where the charm-loop function H_0 reads (in expanded form)

$$H_0 = \frac{1}{2835}\left[-1260 + 2520\ln\left(\frac{\mu}{m_c}\right) + 1008\left(\frac{\hat{s}}{4\,z}\right) + 432\left(\frac{\hat{s}}{4\,z}\right)^2 + 256\left(\frac{\hat{s}}{4\,z}\right)^3\right]. \tag{67}$$

In the context of virtual corrections also the $\mathcal{O}(\epsilon)$ part of this loop function is needed. We neglect it here since it will drop out in combination with gluon bremsstrahlung. Note that $H_0 = h(z,\hat{s}) + 8/9\,\ln(\mu/m_b)$, with h defined in [41].

4.2 Virtual Corrections to the Matrix Element of O_7

We now turn to the virtual corrections to the matrix element of the operator O_7, consisting of the vertex- [see Fig. 4.1a)] and self-energy corrections. The ultraviolet singularities of the sum of these diagrams are cancelled when adding the counterterm amplitude

$$C_7\left[Z_{77}\,Z_{m_b}/Z_{g_s}^2 - 1\right]\langle s\,\ell^+\ell^-|O_7|b\rangle_{\rm tree}\,, \quad \text{where} \quad Z_{77} = 1 - \frac{\alpha_s}{4\,\pi}\frac{7}{3\,\epsilon}\,. \tag{68}$$

The expressions for Z_{m_b} and Z_{g_s} are given in Eqs. (49) and (47), respectively. The renormalized result for the contribution proportional to C_7 can be written as

$$\langle s\,\ell^+\ell^-|C_7 O_7|b\rangle = \widetilde{C}_7^{(0)}\left(-\frac{\alpha_s}{4\,\pi}\right)\left[F_7^{(9)}\langle\widetilde{O}_9\rangle_{\rm tree} + F_7^{(7)}\langle\widetilde{O}_7\rangle_{\rm tree}\right], \tag{69}$$

with $\widetilde{O}_7 = \frac{\alpha_s}{4\pi} O_7$ and $\widetilde{C}_7^{(0)} = C_7^{(1)}$. The expanded form factors $F_7^{(9)}$ and $F_7^{(7)}$ read

$$F_7^{(9)} = -\frac{16}{3}\left(1 + \frac{1}{2}\,\hat{s} + \frac{1}{3}\,\hat{s}^2 + \frac{1}{4}\,\hat{s}^3\right), \tag{70}$$

$$F_7^{(7)} = \frac{32}{3}\,L_\mu + \frac{32}{3} + 8\,\hat{s} + 6\,\hat{s}^2 + \frac{128}{27}\,\hat{s}^3 + f_{\rm inf}\,, \tag{71}$$

where the infrared and collinear singular part $f_{\rm inf}$ is identical to the one of $F_9^{(9)}$ in Eq. (64). Note that the on-shell value for the renormalization factor Z_{m_b} was used in Eq. (68). Therefore, when using the expression for $F_7^{(7,9)}$ in the form given above, the pole mass for m_b has to be used at lowest order.

4.3 Virtual Corrections to the Matrix Element of O_8

Finally, we present our results for the corrections to the matrix elements of O_8. The corresponding diagrams are shown in Fig. 4.1c) and d). Including the counterterm

$$C_8\,\delta Z_{87}\,\langle s\,\ell^+\ell^-|O_7|b\rangle_{\rm tree}\,, \quad \text{where} \quad \delta Z_{87} = -\frac{\alpha_s}{4\pi}\frac{16}{9\,\epsilon}\,,$$

yields the ultraviolet and infrared finite result

$$\langle s\,\ell^+\ell^-|C_8 O_8|b\rangle = \widetilde{C}_8^{(0)}\left(-\frac{\alpha_s}{4\pi}\right)\left[F_8^{(9)}\langle\widetilde{O}_9\rangle_{\rm tree} + F_8^{(7)}\langle\widetilde{O}_7\rangle_{\rm tree}\right], \tag{72}$$

with $\widetilde{C}_8^{(0)} = C_8^{(1)}$. The expanded form factors $F_8^{(9)}$ and $F_8^{(7)}$ read

$$\begin{aligned} F_8^{(9)} = {} & \frac{104}{9} - \frac{32}{27}\,\pi^2 + \left(\frac{1184}{27} - \frac{40}{9}\,\pi^2\right)\hat{s} + \left(\frac{14212}{135} - \frac{32}{3}\,\pi^2\right)\hat{s}^2 \\ & + \left(\frac{193444}{945} - \frac{560}{27}\,\pi^2\right)\hat{s}^3 + \frac{16}{9}\,L_s\left(1 + \hat{s} + \hat{s}^2 + \hat{s}^3\right), \end{aligned} \tag{73}$$

$$\begin{aligned} F_8^{(7)} = {} & -\frac{32}{9}\,L_\mu + \frac{8}{27}\,\pi^2 - \frac{44}{9} - \frac{8}{9}\,i\pi + \left(\frac{4}{3}\,\pi^2 - \frac{40}{3}\right)\hat{s} + \left(\frac{32}{9}\,\pi^2 - \frac{316}{9}\right)\hat{s}^2 \\ & + \left(\frac{200}{27}\,\pi^2 - \frac{658}{9}\right)\hat{s}^3 - \frac{8}{9}\,L_s\left(\hat{s} + \hat{s}^2 + \hat{s}^3\right). \end{aligned} \tag{74}$$

5 Bremsstrahlung Corrections

First of all, we remark that in the present paper only those bremsstrahlung diagrams are taken into account which are needed to cancel the infrared and collinear singularities

appearing in the virtual corrections. All other bremsstrahlung contributions (which are finite), will be given elsewhere [44].

It is known [24, 28] that the contribution to the inclusive decay width coming from the interference between the tree-level and the one-loop matrix elements of O_9 [Fig. 4.1b)] and from the corresponding bremsstrahlung corrections [Fig. 4.1f)] can be written in the form

$$\begin{aligned}\frac{d\Gamma_{99}}{d\hat{s}} &= \frac{d\Gamma_{99}^{\rm virt}}{d\hat{s}} + \frac{d\Gamma_{99}^{\rm brems}}{d\hat{s}}\,,\\ \frac{d\Gamma_{99}}{d\hat{s}} &= \left(\frac{\alpha_{em}}{4\,\pi}\right)^2 \frac{G_F^2\, m_{b,\rm pole}^5\, |V_{ts}^* V_{tb}|^2}{48\,\pi^3}\,(1-\hat{s})^2\,(1+2\hat{s})\left[2\left|\widetilde{C}_9^{(0)}\right|^2 \frac{\alpha_s}{\pi}\,\omega_9(\hat{s})\right], \qquad (75)\end{aligned}$$

where $\widetilde{C}_9^{(0)} = \frac{4\,\pi}{\alpha_s}\left(C_9^{(0)} + \frac{\alpha_s}{4\,\pi}\,C_9^{(1)}\right)$. This procedure corresponds to encapsulating the virtual and bremsstrahlung corrections in the tree-level calculation by the replacement

$$\langle O_9\rangle_{\rm tree} \to \left(1 + \frac{\alpha_s}{\pi}\,\omega_9(\hat{s})\right)\langle O_9\rangle_{\rm tree}.$$

The function $\omega_9(\hat{s}) \equiv \omega(\hat{s})$, which contains all information on virtual and bremsstrahlung corrections, can be found in [24, 28] and is given by

$$\begin{aligned}\omega_9(\hat{s}) &= -\frac{4}{3}\,{\rm Li}(\hat{s}) - \frac{2}{3}\ln(1-\hat{s})\ln(\hat{s}) - \frac{2}{9}\,\pi^2 - \frac{5+4\,\hat{s}}{3(1+2\,\hat{s})}\ln(1-\hat{s})\\ &\quad -\frac{2\,\hat{s}(1+\hat{s})(1-2\,\hat{s})}{3(1-\hat{s})^2(1+2\,\hat{s})}\ln(\hat{s}) + \frac{5+9\,\hat{s}-6\,\hat{s}^2}{6(1-\hat{s})(1+2\,\hat{s})}\,. \qquad (76)\end{aligned}$$

Replacing $\widetilde{C}_9^{(0)}$ by $\widetilde{C}_9^{(0,{\rm mod})}$ [see Eq. (66)] in Eq. (75), diagram 3.1f) and the corresponding bremsstrahlung corrections are automatically included.

For the combination of the interference terms between the tree-level and the one-loop matrix element of O_7 [Fig. 4.1a)] and the corresponding bremsstrahlung corrections [Fig. 4.1e)] we make the ansatz

$$\begin{aligned}\frac{d\Gamma_{77}}{d\hat{s}} &= \frac{d\Gamma_{77}^{\rm virt}}{d\hat{s}} + \frac{d\Gamma_{77}^{\rm brems}}{d\hat{s}}\,,\\ \frac{d\Gamma_{77}}{d\hat{s}} &= \left(\frac{\alpha_{em}}{4\,\pi}\right)^2 \frac{G_F^2\, m_{b,\rm pole}^5\, |V_{ts}^* V_{tb}|^2}{48\,\pi^3}\,(1-\hat{s})^2\,4\,(1+2/\hat{s})\left[2\left|\widetilde{C}_7^{(0)}\right|^2 \frac{\alpha_s}{\pi}\,\omega_7(\hat{s})\right], \qquad (77)\end{aligned}$$

where $\widetilde{C}_7^{(0)} = C_7^{(1)}$. This time, the encapsulation of virtual and bremsstrahlung corrections is provided by the replacement

$$\langle O_7\rangle_{\rm tree} \to \left(1 + \frac{\alpha_s}{\pi}\,\omega_7(\hat{s})\right)\langle O_7\rangle_{\rm tree}.$$

In order to simplify the calculation of $\omega_7(\hat{s})$, we make the important observation that the form factors $F_7^{(7)}$ and $F_9^{(9)}$ have the same infrared divergent part $f_{\rm inf}$ [cf Eqs. (70) and (63)],

whereas $F_7^{(9)}$ and $F_9^{(7)}$ are finite. Taking into account that in d dimensions the decay width $d\Gamma(b \to s\,\ell^+\ell^-)/d\hat{s}$ corresponding to the matrix element

$$M(b \to s\,\ell^+\ell^-) = \left\langle s\,\ell^+\ell^- \left| \widetilde{C}_7^{(0)}\,\widetilde{O}_7^{(0)} + \widetilde{C}_9^{(0)}\,\widetilde{O}_9^{(0)} + \widetilde{C}_{10}^{(0)}\,\widetilde{O}_{10}^{(0)} \right| b \right\rangle_{\text{tree}} \tag{78}$$

is given by

$$\begin{aligned}\frac{d\Gamma(b \to X_s\,\ell^+\ell^-)}{d\hat{s}} &= \left(\frac{\alpha_{em}}{4\,\pi}\right)^2 \frac{G_F^2\, m_{b,\text{pole}}^5\, |V_{ts}^* V_{tb}|^2}{48\,\pi^3}\,(1-\hat{s})^2\left[1+\mathcal{O}(d-4)\right] \\ &\quad \times \Big\{\big[1+(d-2)\hat{s}\big]\left(\left|\widetilde{C}_9^{(0)}\right|^2 + \left|\widetilde{C}_{10}^{(0)}\right|^2\right) + 4\big[1+(d-2)/\hat{s}\big]\left|\widetilde{C}_7^{(0)}\right|^2 \\ &\quad + 4(d-1)\,\text{Re}\Big(\widetilde{C}_7^{(0)}\widetilde{C}_9^{(0)*}\Big)\Big\}\,,\end{aligned} \tag{79}$$

one concludes that the combination

$$\Delta\Gamma^{\text{virt}} = \frac{\left|\widetilde{C}_9^{(0)}\right|^{-2}}{1+(d-2)\hat{s}}\,\frac{d\Gamma_{99}^{\text{virt}}}{d\hat{s}} - \frac{\left|\widetilde{C}_7^{(0)}\right|^{-2}}{4\big[1+(d-2)/\hat{s}\big]}\,\frac{d\Gamma_{77}^{\text{virt}}}{d\hat{s}} \tag{80}$$

is free of infrared and collinear singularities. Defining analogously

$$\Delta\Gamma^{\text{brems}} = \frac{\left|\widetilde{C}_9^{(0)}\right|^{-2}}{1+(d-2)\hat{s}}\,\frac{d\Gamma_{99}^{\text{brems}}}{d\hat{s}} - \frac{\left|\widetilde{C}_7^{(0)}\right|^{-2}}{4\big[1+(d-2)/\hat{s}\big]}\,\frac{d\Gamma_{77}^{\text{brems}}}{d\hat{s}} \tag{81}$$

and using the identity

$$\frac{\left|\widetilde{C}_9^{(0)}\right|^{-2}}{1+(d-2)\hat{s}}\,\frac{d\Gamma_{99}}{d\hat{s}} - \frac{\left|\widetilde{C}_7^{(0)}\right|^{-2}}{4\big[1+(d-2)/\hat{s}\big]}\,\frac{d\Gamma_{77}}{d\hat{s}} = \Delta\Gamma^{\text{virt}} + \Delta\Gamma^{\text{brems}}\,, \tag{82}$$

one concludes that also $\Delta\Gamma^{\text{brems}}$ is finite. This is because $d\Gamma_{99}/d\hat{s}$ and $d\Gamma_{77}/d\hat{s}$ are finite due to the Kinoshita-Lee-Nauenberg theorem and because $\Delta\Gamma^{\text{virt}}$ is finite as mentioned above. The calculation of $\Delta\Gamma^{\text{brems}}$ is straightforward, as the integrand, expanded in ϵ, leads to unproblematic integrals. Using the explicit results for $\Delta\Gamma^{\text{virt}}$, $\Delta\Gamma^{\text{brems}}$ and $\omega_9(\hat{s})$, one can readily extract $\omega_7(\hat{s})$ from Eq. (82):

$$\begin{aligned}\omega_7(\hat{s}) \;=\; & -\frac{8}{3}\ln\left(\frac{\mu}{m_b}\right) - \frac{4}{3}\,\text{Li}(\hat{s}) - \frac{2}{9}\,\pi^2 - \frac{2}{3}\,\ln(\hat{s})\ln(1-\hat{s}) - \frac{1}{3}\,\frac{8+\hat{s}}{2+\hat{s}}\ln(1-\hat{s}) \\ & -\frac{2}{3}\,\frac{\hat{s}\,(2-2\,\hat{s}-\hat{s}^2)}{(1-\hat{s})^2(2+\hat{s})}\ln(\hat{s}) - \frac{1}{18}\,\frac{16-11\,\hat{s}-17\,\hat{s}^2}{(2+\hat{s})(1-\hat{s})}\,.\end{aligned} \tag{83}$$

The reasoning for the interference terms between the tree-level matrix element of O_7 and the one-loop matrix element of O_9 and vice versa is analogous: We may combine this

contribution with the corresponding bremsstrahlung terms coming from the interference of diagrams 4.1e) and 4.1f) making the ansatz

$$\begin{aligned}\frac{d\Gamma_{79}}{d\hat{s}} &= \frac{d\Gamma_{79}^{\rm virt}}{d\hat{s}} + \frac{d\Gamma_{79}^{\rm brems}}{d\hat{s}}\,,\\ \frac{d\Gamma_{79}}{d\hat{s}} &= \left(\frac{\alpha_{em}}{4\,\pi}\right)^2 \frac{G_F^2\, m_{b,\rm pole}^5\, |V_{ts}^* V_{tb}|^2}{48\,\pi^3}\,(1-\hat{s})^2 \cdot 12\left[2\,{\rm Re}\Big(\widetilde{C}_7^{(0)}\widetilde{C}_9^{(0)*}\Big)\,\frac{\alpha_s}{\pi}\,\omega_{79}(\hat{s})\right]. \quad (84)\end{aligned}$$

The corresponding encapsulation is realized by the replacement

$$\langle O_{7,9}\rangle_{\rm tree} \to \left(1+\frac{\alpha_s}{\pi}\omega_{79}(\hat{s})\right)\langle O_{7,9}\rangle_{\rm tree}.$$

This time, we make use of the fact that the quantities

$$\Delta\Gamma_{\rm mixed}^{\rm virt} = \frac{\left|\widetilde{C}_9^{(0)}\right|^{-2}}{1+(d-2)\hat{s}}\,\frac{d\Gamma_{99}^{\rm virt}}{d\hat{s}} - \frac{{\rm Re}\left[\widetilde{C}_7^{(0)}\widetilde{C}_9^{(0)*}\right]^{-1}}{4(d-1)}\,\frac{d\Gamma_{79}^{\rm virt}}{d\hat{s}} \quad (85)$$

and

$$\Delta\Gamma_{\rm mixed}^{\rm brems} = \frac{\left|\widetilde{C}_9^{(0)}\right|^{-2}}{1+(d-2)\hat{s}}\,\frac{d\Gamma_{99}^{\rm brems}}{d\hat{s}} - \frac{{\rm Re}\left[\widetilde{C}_7^{(0)}\widetilde{C}_9^{(0)*}\right]^{-1}}{4(d-1)}\,\frac{d\Gamma_{79}^{\rm brems}}{d\hat{s}} \quad (86)$$

are finite. For the function $\omega_{79}(\hat{s})$ we obtain

$$\begin{aligned}\omega_{79}(\hat{s}) &= -\frac{4}{3}\,\ln\left(\frac{\mu}{m_b}\right) - \frac{4}{3}\,{\rm Li}(\hat{s}) - \frac{2}{9}\,\pi^2 - \frac{2}{3}\,\ln(\hat{s})\ln(1-\hat{s}) - \frac{1}{9}\,\frac{2+7\,\hat{s}}{\hat{s}}\,\ln(1-\hat{s})\\ &\quad -\frac{2}{9}\,\frac{\hat{s}\,(3-2\,\hat{s})}{(1-\hat{s})^2}\,\ln(\hat{s}) + \frac{1}{18}\,\frac{5-9\,\hat{s}}{1-\hat{s}}\,. \quad (87)\end{aligned}$$

Note that the procedure described here does work only if one of the functions $\omega_7(\hat{s})$, $\omega_9(\hat{s})$ or $\omega_{79}(\hat{s})$ is known already.

Finally, we remark that the combined virtual and bremsstrahlung corrections to the operator O_{10} (which has the same hadronic structure as O_9) is described by the function $\omega_9(\hat{s})$, too:

$$\begin{aligned}\frac{d\Gamma_{10,10}}{d\hat{s}} &= \frac{d\Gamma_{10,10}^{\rm virt}}{d\hat{s}} + \frac{d\Gamma_{10,10}^{\rm brems}}{d\hat{s}}\,,\\ \frac{d\Gamma_{10,10}}{d\hat{s}} &= \left(\frac{\alpha_{em}}{4\,\pi}\right)^2 \frac{G_F^2\, m_{b,\rm pole}^5\, |V_{ts}^* V_{tb}|^2}{48\,\pi^3}\,(1-\hat{s})^2\,(1+2\hat{s})\left[2\left|\widetilde{C}_{10}^{(0)}\right|^2\,\frac{\alpha_s}{\pi}\,\omega_9(\hat{s})\right], \quad (88)\end{aligned}$$

where $\widetilde{C}_{10}^{(0)} = C_{10}^{(1)}$.

6 Corrections to the Decay Width for $B \to X_s\,\ell^+\ell^-$

In this section we combine the virtual corrections calculated in Sections 3, 4 and the bremsstrahlung contributions discussed in Section 5 and study their influence on the decay width $d\Gamma(b \to X_s\,\ell^+\ell^-)/d\hat{s}$. In the literature (see eg [41]), this decay width is usually written as

$$\begin{aligned}\frac{d\Gamma(b \to X_s\,\ell^+\ell^-)}{d\hat{s}} &= \left(\frac{\alpha_{em}}{4\,\pi}\right)^2 \frac{G_F^2\, m_{b,\rm pole}^5\, |V_{ts}^* V_{tb}|^2}{48\,\pi^3}\,(1-\hat{s})^2 \\ &\times \left\{(1+2\hat{s})\left(\left|\widetilde{C}_9^{\rm eff}\right|^2 + \left|\widetilde{C}_{10}^{\rm eff}\right|^2\right) + 4(1+2/\hat{s})\left|\widetilde{C}_7^{\rm eff}\right|^2 + 12\,{\rm Re}\left(\widetilde{C}_7^{\rm eff}\widetilde{C}_9^{\rm eff*}\right)\right\}, \quad (89)\end{aligned}$$

where the contributions calculated so far have been absorbed into the effective Wilson coefficients $\widetilde{C}_7^{\rm eff}$, $\widetilde{C}_9^{\rm eff}$ and $\widetilde{C}_{10}^{\rm eff}$. It turns out that also the new contributions calculated in the present paper can be absorbed into these coefficients. Following as closely as possible the 'parameterization' given recently by Bobeth *et al.* [41], we write

$$\begin{aligned}\widetilde{C}_9^{\rm eff} &= \left(1+\frac{\alpha_s(\mu)}{\pi}\,\omega_9(\hat{s})\right)\left(A_9 + T_9\,h(z,\hat{s}) + U_9\,h(1,\hat{s}) + W_9\,h(0,\hat{s})\right) \\ &\quad -\frac{\alpha_s(\mu)}{4\,\pi}\left(C_1^{(0)}F_1^{(9)} + C_2^{(0)}F_2^{(9)} + A_8^{(0)}F_8^{(9)}\right), \quad (90)\\ \widetilde{C}_7^{\rm eff} &= \left(1+\frac{\alpha_s(\mu)}{\pi}\omega_7(\hat{s})\right)A_7 - \frac{\alpha_s(\mu)}{4\,\pi}\left(C_1^{(0)}F_1^{(7)} + C_2^{(0)}F_2^{(7)} + A_8^{(0)}F_8^{(7)}\right), \\ \widetilde{C}_{10}^{\rm eff} &= \left(1+\frac{\alpha_s(\mu)}{\pi}\omega_9(\hat{s})\right)A_{10}\,,\end{aligned}$$

where the expressions for $h(z,\hat{s})$ and $\omega_9(\hat{s})$ [see Eqs. (67) and (76)] were already available in the literature [24, 28, 41]. The quantities $\omega_7(\hat{s})$ and $F_{1,2,8}^{(7,9)}$, on the other hand, have been calculated in the present paper. We take the numerical values for A_7, A_9, A_{10}, T_9, U_9, and W_9 from [41], while $C_1^{(0)}$, $C_2^{(0)}$ and $A_8^{(0)} = \widetilde{C}_8^{(0,\rm eff)}$ can be found in [48]. For completeness we list them in Table 6.1.

In Fig. 6.1 we illustrate the renormalization scale dependence of ${\rm Re}\left[\widetilde{C}_7^{\rm eff}(\hat{s})\right]$. The dashed curves are obtained by neglecting the corrections calculated in this paper, ie $\omega_7(\hat{s})$, $F_1^{(7)}$, $F_2^{(7)}$ and $F_8^{(7)}$ are put equal to zero in Eq. (90). The three curves correspond to the values $\mu = 2.5$ GeV (lower curve), $\mu = 5$ GeV (middle curve) and $\mu = 10$ GeV (upper curve) of the renormalization scale. The solid curves are obtained by taking into account the new corrections. In this case, the lowest, middle and uppermost curve correspond to $\mu = 10$ GeV, 5 GeV and 2.5 GeV, respectively. We conclude that the new corrections significantly reduce the renormalization scale dependence of ${\rm Re}\left[\widetilde{C}_7^{\rm eff}(\hat{s})\right]$.

Fig. 6.2 shows the renormalization scale dependence of ${\rm Re}\left[\widetilde{C}_9^{\rm eff}(\hat{s})\right]$. Again, the dashed

	$\mu = 2.5$ GeV	$\mu = 5$ GeV	$\mu = 10$ GeV
α_s	0.267	0.215	0.180
$C_1^{(0)}$	-0.697	-0.487	-0.326
$C_2^{(0)}$	1.046	1.024	1.011
$\left(A_7^{(0)},\ A_7^{(1)}\right)$	$(-0.360,\ 0.031)$	$(-0.321,\ 0.019)$	$(-0.287,\ 0.008)$
$A_8^{(0)}$	-0.164	-0.148	-0.134
$\left(A_9^{(0)},\ A_9^{(1)}\right)$	$(4.241,\ -0.170)$	$(4.129,\ 0.013)$	$(4.131,\ 0.155)$
$\left(T_9^{(0)},\ T_9^{(1)}\right)$	$(0.115,\ 0.278)$	$(0.374,\ 0.251)$	$(0.576,\ 0.231)$
$\left(U_9^{(0)},\ U_9^{(1)}\right)$	$(0.045,\ 0.023)$	$(0.032,\ 0.016)$	$(0.022,\ 0.011)$
$\left(W_9^{(0)},\ W_9^{(1)}\right)$	$(0.044,\ 0.016)$	$(0.032,\ 0.012)$	$(0.022,\ 0.009)$
$\left(A_{10}^{(0)},\ A_{10}^{(1)}\right)$	$(-4.372,\ 0.135)$	$(-4.372,\ 0.135)$	$(-4.372,\ 0.135)$

Table 6.1: Coefficients appearing in Eq. (90) for $\mu = 2.5$ GeV, $\mu = 5$ GeV and $\mu = 10$ GeV. For $\alpha_s(\mu)$ (in the $\overline{\rm MS}$ scheme) we used the two-loop expression with 5 flavors and $\alpha_s(m_Z) = 0.119$. The entries correspond to the pole top quark mass $m_t = 174$ GeV. The superscript (0) refers to lowest order quantities while the superscript (1) denotes the correction terms of order α_s.

curves are obtained by neglecting the new corrections in Eq. (90), ie $F_1^{(9)}$, $F_2^{(9)}$ and $F_8^{(9)}$ are put to zero. We stress that $\omega_9(\hat{s})$ is retained, as this function has been known before. The three curves correspond to the values $\mu = 2.5$ GeV (lower curve), $\mu = 5$ GeV (middle curve) and $\mu = 10$ GeV (upper curve) of the renormalization scale. The solid curves take the new corrections into account. Now, the lowest, middle and uppermost curve correspond to $\mu = 2.5$ GeV, 5 GeV and 10 GeV, respectively. We conclude that the new corrections significantly reduce the renormalization scale dependence of $\mathrm{Re}\left[\widetilde{C}_9^{\rm eff}(\hat{s})\right]$, too.

When calculating the decay width (89), we retain only terms linear in α_s (and thus in ω_7, ω_9) in the expressions for $|\widetilde{C}_7^{\rm eff}|^2$, $|\widetilde{C}_9^{\rm eff}|^2$ and $|\widetilde{C}_{10}^{\rm eff}|^2$. In the interference term $\mathrm{Re}\left[\widetilde{C}_7^{\rm eff}\widetilde{C}_9^{\rm eff*}\right]$ too, we keep only linear contributions in α_s. By construction, one has to make the replacements $\omega_9 \to \omega_{79}$ and $\omega_7 \to \omega_{79}$ in this term.

Our results include all the relevant virtual corrections and those bremsstrahlung diagrams which generate infrared and collinear singularities. There exist additional bremsstrahlung terms coming, for example, from one-loop O_1 and O_2 diagrams in which both the virtual photon and the gluon are emitted from the charm quark line. These contributions do not

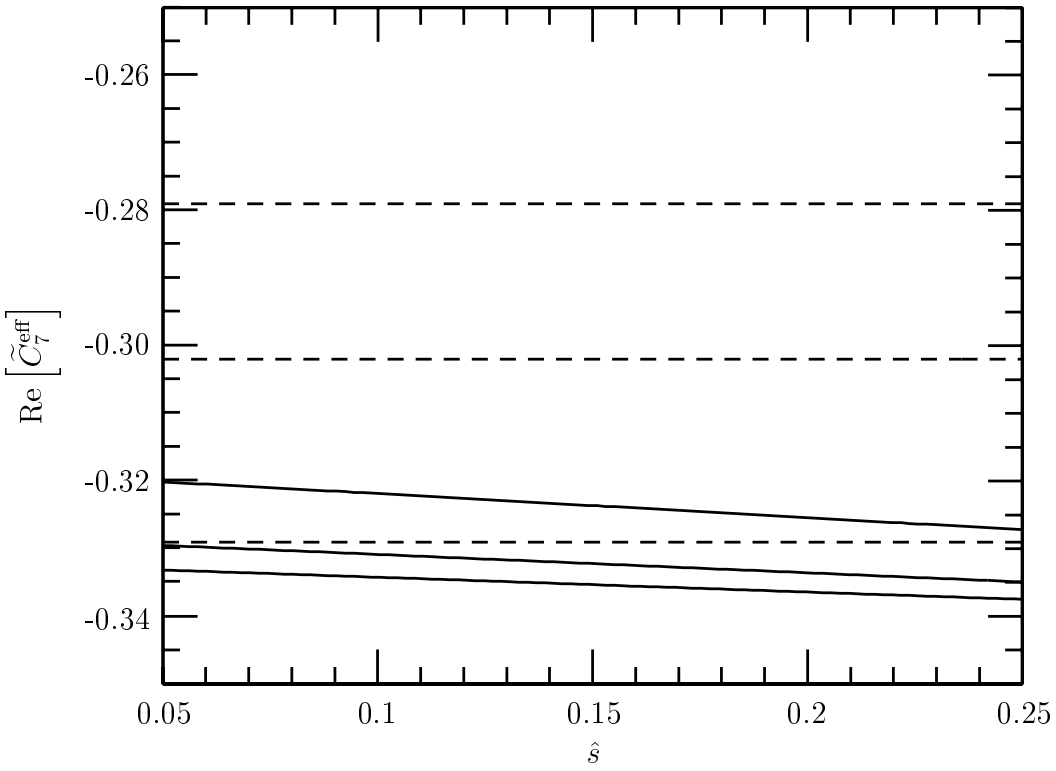

Figure 6.1: The three solid curves illustrate the μ dependence of $\mathrm{Re}\left[\widetilde{C}_7^{\rm eff}(\hat{s})\right]$ when the new corrections are included. The dashed curves are obtained when switching off these corrections. We set $\hat{m}_c = 0.29$. See text.

induce additional renormalization scale dependence as they are ultraviolet finite. Using our experience from $b \to s\gamma$ and $b \to sg$, these contributions are not expected to be large, but to give a definitive answer concerning their size they have to be calculated [44].

7 Numerical Results for $R_{\rm quark}(\hat{s})$

The decay width in Eq. (89) has a large uncertainty due to the factor $m_{b,\rm pole}^5$. Following common practice, we consider the ratio

$$R_{\rm quark}(\hat{s}) = \frac{1}{\Gamma(b \to X_c\, e\, \bar{\nu}_e)} \frac{d\Gamma(b \to X_s\, \ell^+\ell^-)}{d\hat{s}}\,, \tag{91}$$

in which the factor $m_{b,\rm pole}^5$ drops out. The explicit expression for the semileptonic decay width $\Gamma(b \to X_c\, e\, \bar{\nu}_e)$ reads

$$\Gamma(b \to X_c\, e\, \bar{\nu}_e) = \frac{G_F^2\, m_{b,\rm pole}^5}{192\,\pi^3}\, |V_{cb}|^2 \cdot g\left(\frac{m_{c,\rm pole}^2}{m_{b,\rm pole}^2}\right) \cdot K\left(\frac{m_c^2}{m_b^2}\right), \tag{92}$$

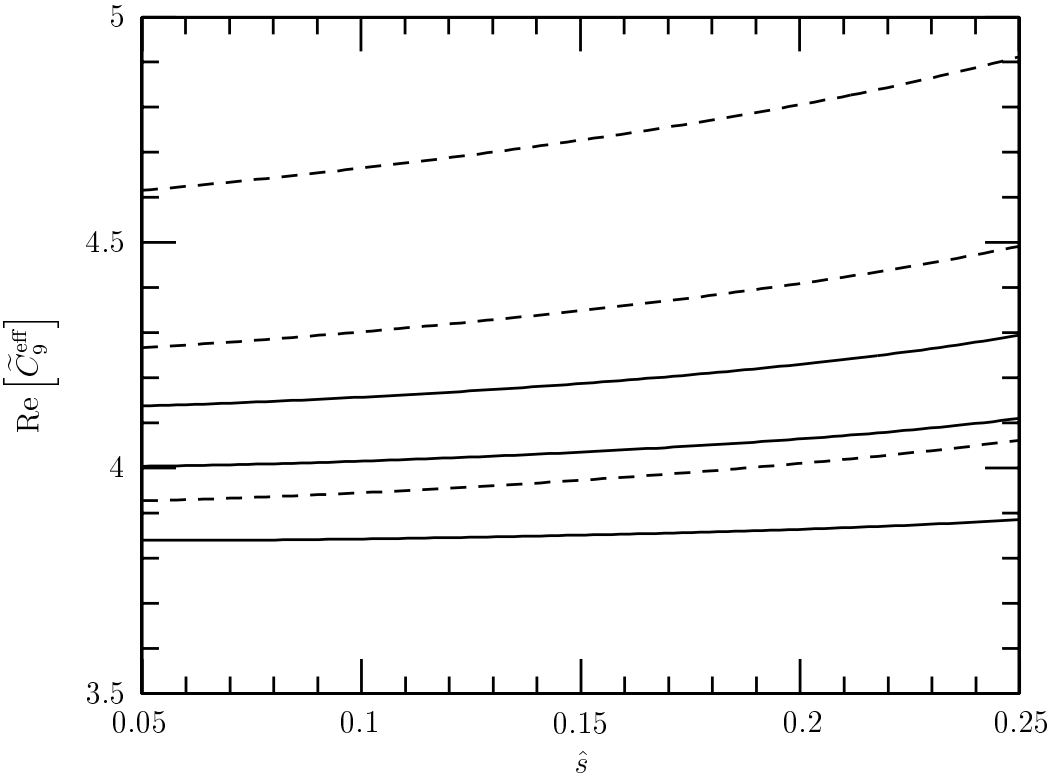

Figure 6.2: The three solid curves illustrate the μ dependence of $\mathrm{Re}\left[\widetilde{C}_9^{\mathrm{eff}}(\hat{s})\right]$ when the new corrections are included. The dashed curves are obtained when switching off these corrections. We set $\hat{m}_c = 0.29$. See text.

where $g(z) = 1 - 8\,z + 8\,z^3 - z^4 - 12\,z^2\,\ln(z)$ is the phase space factor, and

$$K(z) = 1 - \frac{2\,\alpha_s(m_b)}{3\,\pi}\,\frac{f(z)}{g(z)} \tag{93}$$

incorporates the next-to-leading QCD correction to the semileptonic decay [49]. The function $f(z)$ has been given analytically in Ref. [50]:

$$\begin{aligned} f(z) = &-(1-z^2)\left(\frac{25}{4} - \frac{239}{3}\,z + \frac{25}{4}\,z^2\right) + z\,\ln(z)\left(20 + 90\,z - \frac{4}{3}\,z^2 + \frac{17}{3}\,z^3\right) \\ &+ z^2\,\ln^2(z)\left(36 + z^2\right) + \left(1-z^2\right)\left(\frac{17}{3} - \frac{64}{3}\,z + \frac{17}{3}\,z^2\right)\ln(1-z) \\ &- 4\left(1 + 30\,z^2 + z^4\right)\ln(z)\ln(1-z) - \left(1 + 16\,z^2 + z^4\right)\left(6\,\mathrm{Li}(z) - \pi^2\right) \\ &- 32\,z^{3/2}(1+z)\left[\pi^2 - 4\,\mathrm{Li}(\sqrt{z}) + 4\,\mathrm{Li}(-\sqrt{z}) - 2\ln(z)\,\ln\left(\frac{1-\sqrt{z}}{1+\sqrt{z}}\right)\right]. \end{aligned} \tag{94}$$

We now turn to the numerical results for $R_{\mathrm{quark}}(\hat{s})$ for $0.05 \le \hat{s} \le 0.25$. In Fig. 7.1 we investigate the dependence of $R_{\mathrm{quark}}(\hat{s})$ on the renormalization scale μ. The solid lines

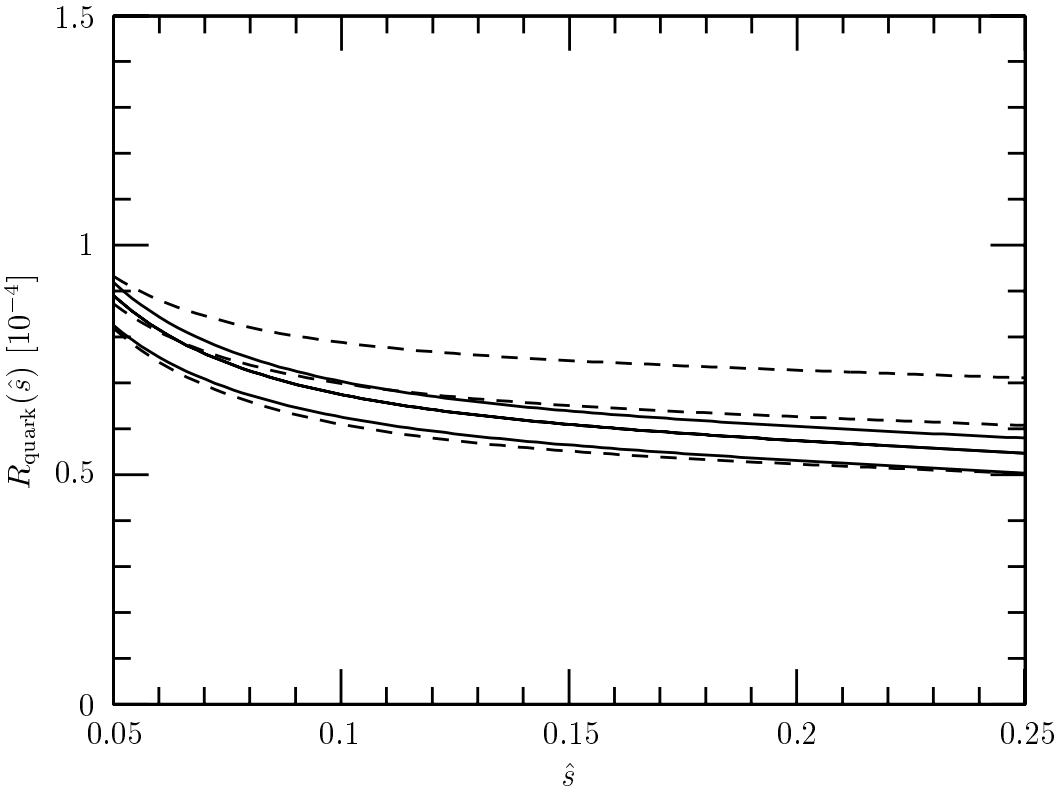

Figure 7.1: The three solid lines show the μ dependence of $R_{\rm quark}(\hat{s})$ when including the corrections to the matrix elements calculated in this paper. The dashed lines are obtained when switching off these corrections. We set $\hat{m}_c = 0.29$. See text.

are obtained by including the new NNLL contributions, as explained in Section 6. The three solid curves correspond to $\mu = 2.5$ GeV (lowest line), $\mu = 5$ GeV (middle line) and $\mu = 10$ GeV (uppermost line). The three dashed curves (again $\mu = 2.5$ GeV for the lowest, $\mu = 5$ GeV for the middle and $\mu = 10$ GeV for the uppermost line), on the other hand, show the results without the new NNLL corrections, ie they include the NLL results combined with the NNLL corrections to the matching conditions as obtained by Bobeth *et al.* [41]. From this figure we conclude that the renormalization scale dependence gets reduced by more than a factor of 2. Only for low values of $\hat{s}$ ($\hat{s} \sim 0.05$), where the NLL μ dependence is small already, the reduction factor is smaller. For the integrated quantity we obtain

$$R_{\rm quark} = \int_{0.05}^{0.25} d\hat{s}\, R_{\rm quark}(\hat{s}) = \big(1.25 \pm 0.08(\mu)\big) \times 10^{-5}\,, \tag{95}$$

where the error is obtained by varying μ between 2.5 GeV and 10 GeV. Before our corrections, the result was $R_{\rm quark} = (1.36 \pm 0.18) \times 10^{-5}$ [41]. In other words, the renormalization scale dependence got reduced from $\sim \pm 13\%$ to $\sim \pm 6.5\%$.

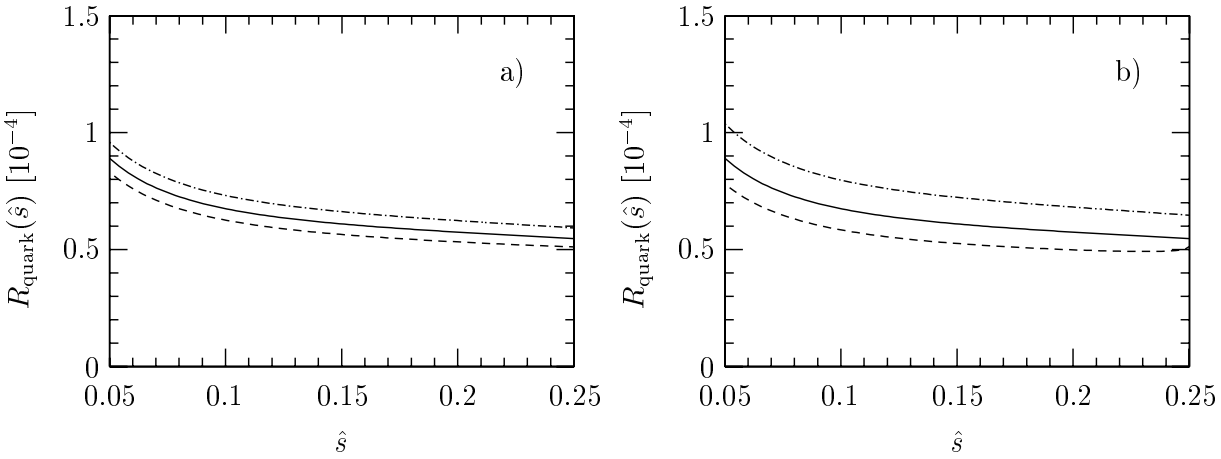

Figure 7.2: a) $R_{\rm quark}(\hat{s})$ for $\hat{m}_c = 0.27$ (dashed line), $\hat{m}_c = 0.29$ (solid line) and $\hat{m}_c = 0.31$ (dash-dotted line) and $\mu = 5$ GeV. b) $R_{\rm quark}(\hat{s})$ for $\hat{m}_c = 0.25$ (dashed line), $\hat{m}_c = 0.29$ (solid line) and $\hat{m}_c = 0.33$ (dash-dotted line) and $\mu = 5$ GeV. See text.

Among the errors on $R_{\rm quark}(\hat{s})$ which are due to the uncertainties in the input parameters, the one induced by $\hat{m}_c = m_c/m_b$ is known to be the largest. We repeat at this point that m_c enters (unlike in $B \to X_s\,\gamma$) already the one-loop diagrams associated with O_1 and O_2. We did the renormalization of the charm quark mass in such a way that m_c has the meaning of the pole mass in the one-loop expressions. The meaning of m_c in the corresponding two-loop matrix elements, on the other hand, is not fixed (for a discussion of this issue for $B \to X_s\,\gamma$, see Ref. [14]). As the running charm mass at a scale of $\mathcal{O}(m_b)$ is smaller than the pole mass, it numerically makes a difference whether one inserts a pole mass- or a running mass value for m_c in the two-loop contributions. In a thorough phenomenological analysis this issue should certainly be included when estimating the theoretical error. We decide, however, to postpone the quantitative discussion of this point and will take it up when also the finite bremsstrahlung contributions, which complete the NNLL calculation of $R_{\rm quark}(\hat{s})$, are available [44]. For the time being, we interpret m_c to be the pole mass in the two-loop contributions. In Fig. 7.2a) we vary $\hat{m}_c$ between 0.27 and 0.31, while in Fig. 7.2b) the more conservative range $0.25 \le \hat{m}_c \le 0.33$ is considered. Comparing Fig. 7.1 with Figs. 7.2a) and b), we find that at the NNLL level the uncertainty due to $\hat{m}_c$ is larger than the leftover μ dependence, even for the less conservative range of $\hat{m}_c$. For the integrated quantity $R_{\rm quark}$ we have an uncertainty of $\pm 7.6\%$ when $\hat{m}_c$ is varied between 0.27 and 0.31. Varying $\hat{m}_c$ in the more conservative range, the corresponding uncertainty amounts to $\pm 15\%$.

A more detailed numerical analysis for $R_{\rm quark}(\hat{s})$ and $R_{\rm quark}$, including the errors which are due to uncertainties in other input parameters as well as non-perturbative effects, will be given together with the complete bremsstrahlung terms in Ref. [44].

To conclude: We have calculated virtual corrections of $\mathcal{O}(\alpha_s)$ to the matrix elements of O_1,

O_2, O_7, O_8, O_9 and O_{10}. We also took into account those bremsstrahlung corrections which cancel the infrared and collinear singularities in the virtual corrections. The renormalization scale dependence of $R_{\rm quark}(\hat{s})$ gets reduced by more than a factor of 2. The calculation of the remaining bremsstrahlung contributions (which are expected to be rather small) and a more detailed numerical analysis are in progress [44].

Acknowledgements:
C.G. would like to thank the members of the Yerevan Physics Institute for the kind hospitality extended to him when this paper was finalized. We thank K. Bieri and P. Liniger for helpful discussions. This work was partially supported by Schweizerischer Nationalfonds and SCOPES program.

A One-loop Matrix Elements of the Four-Quark Operators

In order to fix the counterterms $F_{i\to 4\text{quark}}^{\text{ct}(7,9)}$ $(i = 1, 2)$ in Eq. (45), we need the one-loop matrix elements $\langle s\,\ell^+\ell^-|O_j|b\rangle_{\text{1-loop}}$ of the four-quark operators O_1, O_2, O_4, O_{11} and O_{12}. Due to the $1/\epsilon$ factor in Eq. (45), they are needed up to $\mathcal{O}(\epsilon^1)$. The explicit results (in expanded form) read

$$\begin{aligned}\langle s\,\ell^+\ell^-|O_2|b\rangle_{\text{1-loop}} = &\left(\frac{\mu}{m_c}\right)^{2\epsilon}\times\\ &\left\{\frac{4}{9\,\epsilon}+\frac{4}{2835}\left[-315+252\left(\frac{\hat{s}}{4\,z}\right)+108\left(\frac{\hat{s}}{4\,z}\right)^2+64\left(\frac{\hat{s}}{4\,z}\right)^3\right]\right.\\ &\left.+\frac{\epsilon}{2835}\left[105\,\pi^2-1008\left(\frac{\hat{s}}{4\,z}\right)+128\left(\frac{\hat{s}}{4\,z}\right)^3\right]\right\}\langle\widetilde{O}_9\rangle_{\text{tree}}\,,\end{aligned}\tag{96}$$

$$\langle s\,\ell^+\ell^-|O_1|b\rangle_{\text{1-loop}} = \frac{4}{3}\,\langle s\,\ell^+\ell^-|O_2|b\rangle_{\text{1-loop}}\,,\tag{97}$$

$$\begin{aligned}\langle s\,\ell^+\ell^-|O_4|b\rangle_{\text{1-loop}} = &-\left(\frac{\mu}{m_b}\right)^{2\epsilon}\left\{\left[\frac{4}{9}+\frac{\epsilon}{945}\left(70\,\hat{s}+7\,\hat{s}^2+\hat{s}^3\right)\right]\langle\widetilde{O}_7\rangle_{\text{tree}}\right.\\ &+\left[\frac{16}{27\,\epsilon}+\frac{2}{8505}\left(-420+1260\,i\pi-1260\,L_s+252\,\hat{s}+27\,\hat{s}^2+4\,\hat{s}^3\right)\right.\\ &+\frac{4\,\epsilon}{8505}\left(420\,i\pi+910-630\,i\,L_s\,\pi-420\,L_s-315\,\pi^2\right.\\ &\left.\left.\left.+\,315\,L_s^2-126\,\hat{s}+\hat{s}^3\right)\right]\langle\widetilde{O}_9\rangle_{\text{tree}}\right\},\end{aligned}\tag{98}$$

$$\begin{aligned}\langle s\,\ell^+\ell^-|O_{11}|b\rangle_{\text{1-loop}} = &-\frac{64}{27}\times\\ &\left(\frac{\mu}{m_c}\right)^{2\epsilon}\left\{1+\frac{4\,\epsilon}{5}\left[\frac{\hat{s}}{4\,z}+\frac{3}{7}\left(\frac{\hat{s}}{4\,z}\right)^2+\frac{16}{63}\left(\frac{\hat{s}}{4\,z}\right)^3\right]\right\}\langle\widetilde{O}_9\rangle_{\text{tree}}\,,\end{aligned}\tag{99}$$

$$\langle s\,\ell^+\ell^-|O_{12}|b\rangle_{\text{1-loop}} = \frac{3}{4}\,\langle s\,\ell^+\ell^-|O_{11}|b\rangle_{\text{1-loop}}\,.\tag{100}$$

B Full $\hat{s}$ and z Dependence of the Form Factors $F_{1,2}^{(7,9)}$

In this appendix we give the dependence of $f_a^{(b)}$ $(a = 1, 2;\ b = 7, 9)$ [see Eq. (59)] on $\hat{s}$ and z. We decompose them as follows:

$$f_a^{(b)} = \sum_{i,j,l,m} \kappa_{a,ijlm}^{(b)}\, \hat{s}^i\, L_s^j\, z^l\, L_c^m + \sum_{i,j} \rho_{a,ij}^{(b)}\, \hat{s}^i\, L_s^j\,.$$

The quantities $\rho_{a,ij}^{(b)}$ collect the half-integer powers of $z = m_c^2/m_b^2 = \hat{m}_c^2$. This way, the summation indices in the above equation run over integers only. On the following pages, we list the numerical values of $\kappa_{a,ijlm}^{(b)}$ and $\rho_{a,ij}^{(b)}$ for

$$i = 0, ..., 3; \quad j = 0, 1; \quad l = -3, ..., 3 \quad \text{and} \quad m = 0, ..., 4\,.$$

Coefficients not explicitly mentioned below vanish.

Coefficients $\kappa_{1,ijlm}^{(9)}$ and $\rho_{1,ij}^{(9)}$ for the decomposition of $f_1^{(9)}$

$$\rho_{1,00}^{(9)} = 3.8991\,\hat{m}_c^3 \qquad \rho_{1,10}^{(9)} = -23.3946\,\hat{m}_c$$
$$\rho_{1,20}^{(9)} = -140.368\,\hat{m}_c \qquad \rho_{1,30}^{(9)} = 7.79821\,\hat{m}_c^{-1} - 319.726\,\hat{m}_c$$

$$\kappa_{1,00lm}^{(9)} = \begin{pmatrix} 0 & 0 & 0 & 0 & 0 \\ 0 & 0 & 0 & 0 & 0 \\ 0 & 0 & 0 & 0 & 0 \\ -4.61812 + 3.67166\,i & 5.62963 + 1.86168\,i & 0 & 0 & 0 \\ 14.4621 - 16.2155\,i & 9.59321 - 11.1701\,i & -1.18519 - 7.44674\,i & -0.790123 & 0 \\ -16.0864 + 26.7517\,i & 54.2439 - 14.8935\,i & -15.4074 - 29.787\,i & -3.95062 & 0 \\ -14.73 - 23.6892\,i & -28.5761 + 34.7514\,i & 20.1481 & 0 & 0 \end{pmatrix}$$

$$\kappa_{1,01lm}^{(9)} = \begin{pmatrix} 0 & 0 & 0 & 0 & 0 \\ 0 & 0 & 0 & 0 & 0 \\ 0 & 0 & 0 & 0 & 0 \\ -0.0493827 - 0.103427\,i & 0 & 0 & 0 & 0 \\ -0.592593 & 0 & 0 & 0 & 0 \\ 4.95977 - 1.86168\,i & -1.18519 - 7.44674\,i & -2.37037 & 0 & 0 \\ -9.20287 - 1.65483\,i & -1.0535 + 9.92898\,i & 3.16049 & 0 & 0 \end{pmatrix}$$

$$\kappa_{1,10lm}^{(9)} = \begin{pmatrix} 0 & 0 & 0 & 0 & 0 \\ 0 & 0 & 0 & 0 & 0 \\ -2.48507 - 0.186168\,i & 0 & 0 & 0 & 0 \\ 4.47441 - 0.310281\,i & 1.48148 - 1.86168\,i & 0 & 0 & 0 \\ 71.3855 - 30.7987\,i & 8.47677 - 33.5103\,i & 12.5389 - 7.44674\,i & -0.790123 & 0.790123 \\ -18.1301 + 66.1439\,i & 149.596 - 67.0206\,i & -49.1852 - 81.9141\,i & -11.0617 & 0 \\ -72.89 - 63.7828\,i & -68.135 + 134.041\,i & 63.6049 & 0 & 0 \end{pmatrix}$$

$$\kappa_{1,11lm}^{(9)} = \begin{pmatrix} 0 & 0 & 0 & 0 & 0 \\ 0 & 0 & 0 & 0 & 0 \\ 0 & 0 & 0 & 0 & 0 \\ 0 & 0 & 0 & 0 & 0 \\ -2.66667 - 1.86168\,i & -1.18519 & 0 & 0 & 0 \\ 18.6539 - 7.44674\,i & -4.74074 - 29.787\,i & -9.48148 & 0 & 0 \\ -41.6104 - 3.72337\,i & -2.37037 + 44.6804\,i & 14.2222 & 0 & 0 \end{pmatrix}$$

$$\kappa^{(9)}_{1,20lm} = \begin{pmatrix} 0 & 0 & 0 & 0 & 0 \\ -0.403158 - 0.0199466\,i & 0 & 0 & 0 & 0 \\ -0.0613169 + 0.0620562\,i & 0 & 0 & 0 & 0 \\ 37.1282 - 1.36524\,i & 22.0621 - 1.86168\,i & 5.33333 & 0.790123 & 0 \\ 212.74 - 52.2081\,i & -21.9215 - 52.1272\,i & 57.1724 - 7.44674\,i & -2.37037 & 2.37037 \\ -44.6829 + 108.713\,i & 272.015 - 163.828\,i & -119.111 - 156.382\,i & -21.3333 & 0 \\ -137.203 - 106.832\,i & -99.437 + 330.139\,i & 168.889 & 0 & 0 \end{pmatrix}$$

$$\kappa^{(9)}_{1,21lm} = \begin{pmatrix} 0 & 0 & 0 & 0 & 0 \\ 0 & 0 & 0 & 0 & 0 \\ 0 & 0 & 0 & 0 & 0 \\ 0.0164609 & 0 & 0 & 0 & 0 \\ -5.33333 - 3.72337\,i & -2.37037 & 0 & 0 & 0 \\ 40.786 - 22.3402\,i & -14.2222 - 67.0206\,i & -21.3333 & 0 & 0 \\ -111.356 & 119.148\,i & 37.9259 & 0 & 0 \end{pmatrix}$$

$$\kappa^{(9)}_{1,30lm} = \begin{pmatrix} -0.0759415 - 0.00295505\,i & 0 & 0 & 0 & 0 \\ -0.00480894 + 0.00369382\,i & 0 & 0 & 0 & 0 \\ -1.81002 + 0.0871741\,i & -0.919459 & -0.197531 & 0 & 0 \\ 79.7475 - 1.72206\,i & 57.3171 - 1.86168\,i & 11.2593 & 2.37037 & 0 \\ 425.579 - 76.6479\,i & -68.8016 - 69.5029\,i & 129.357 - 7.44674\,i & -5.53086 & 4.74074 \\ -87.8946 + 148.481\,i & 417.612 - 311.522\,i & -227.16 - 253.189\,i & -34.7654 & 0 \\ -279.268 - 135.118\,i & -146.853 + 652.831\,i & 331.259 & 0 & 0 \end{pmatrix}$$

$$\kappa^{(9)}_{1,31lm} = \begin{pmatrix} 0 & 0 & 0 & 0 & 0 \\ 0 & 0 & 0 & 0 & 0 \\ 0 & 0 & 0 & 0 & 0 \\ 0.0219479 & 0 & 0 & 0 & 0 \\ -8.2963 - 5.58505\,i & -3.55556 & 0 & 0 & 0 \\ 70.2698 - 49.6449\,i & -31.6049 - 119.148\,i & -37.9259 & 0 & 0 \\ -231.893 + 18.6168\,i & 11.8519 + 248.225\,i & 79.0123 & 0 & 0 \end{pmatrix}$$

Coefficients $\kappa^{(7)}_{1,ijlm}$ and $\rho^{(7)}_{1,ij}$ for the decomposition of $f^{(7)}_1$

$$\rho^{(7)}_{1,00} = 1.94955\,\hat{m}_c^3 \qquad \rho^{(7)}_{1,10} = 11.6973\,\hat{m}_c$$
$$\rho^{(7)}_{1,20} = 70.1839\,\hat{m}_c \qquad \rho^{(7)}_{1,30} = -3.8991\,\hat{m}_c^{-1} + 159.863\,\hat{m}_c$$

$$\kappa^{(7)}_{1,00lm} = \begin{pmatrix} 0 & 0 & 0 & 0 & 0 \\ 0 & 0 & 0 & 0 & 0 \\ 0 & 0 & 0 & 0 & 0 \\ -1.14266 - 0.517135\,i & 0 & 0 & 0 & 0 \\ -2.20356 + 1.59186\,i & -5.21743 + 1.86168\,i & 0.592593 + 3.72337\,i & 0.395062 & 0 \\ 1.86366 - 3.06235\,i & -4.66347 & 3.72337\,i & 0.395062 & 0 \\ -1.21131 + 2.89595\,i & 2.99588 - 2.48225\,i & -4.14815 & 0 & 0 \end{pmatrix}$$

$$\kappa^{(7)}_{1,01lm} = 0$$

$$\kappa^{(7)}_{1,10lm} = \begin{pmatrix} 0 & 0 & 0 & 0 & 0 \\ 0 & 0 & 0 & 0 & 0 \\ 0 & 0 & 0 & 0 & 0 \\ -2.07503 + 1.39626\,i & -0.444444 + 0.930842\,i & 0 & 0 & 0 \\ -25.9259 + 5.78065\,i & -3.40101 + 13.0318\,i & -4.4917 + 3.72337\,i & 0.395062 & -0.395062 \\ 11.4229 - 15.2375\,i & -34.0806 + 11.1701\,i & 10.3704 + 18.6168\,i & 2.37037 & 0 \\ 11.7509 + 15.6984\,i & 18.9564 - 24.8225\,i & -14.6173 & 0 & 0 \end{pmatrix}$$

$$\kappa^{(7)}_{1,11lm} = \begin{pmatrix} 0 & 0 & 0 & 0 & 0 \\ 0 & 0 & 0 & 0 & 0 \\ 0 & 0 & 0 & 0 & 0 \\ -0.0164609 & 0 & 0 & 0 & 0 \\ 1.03704 + 0.930842\,i & 0.592593 & 0 & 0 & 0 \\ -4.66347 & 7.44674\,i & 2.37037 & 0 & 0 \\ 6.73754 + 1.86168\,i & 1.18519 - 7.44674\,i & -2.37037 & 0 & 0 \end{pmatrix}$$

$$\kappa^{(7)}_{1,20lm} = \begin{pmatrix} 0 & 0 & 0 & 0 & 0 \\ 0 & 0 & 0 & 0 & 0 \\ 0.00555556 & 0 & 0 & 0 & 0 \\ -19.4691 + 1.59019\,i & -11.6779 + 0.930842\,i & -2.96296 & -0.395062 & 0 \\ -90.4953 + 14.7788\,i & 14.9329 + 22.3402\,i & -24.438 + 3.72337\,i & 1.18519 & -1.18519 \\ 23.8816 - 32.8021\,i & -82.7915 + 39.0954\,i & 32.2963 + 44.6804\,i & 5.92593 & 0 \\ 38.1415 + 34.8683\,i & 38.6436 - 80.673\,i & -41.5802 & 0 & 0 \end{pmatrix}$$

$$\kappa^{(7)}_{1,21lm} = \begin{pmatrix} 0 & 0 & 0 & 0 & 0 \\ 0 & 0 & 0 & 0 & 0 \\ 0 & 0 & 0 & 0 & 0 \\ -0.0164609 & 0 & 0 & 0 & 0 \\ 2.37037 + 1.86168\,i & 1.18519 & 0 & 0 & 0 \\ -13.9904 + 3.72337\,i & 2.37037 + 22.3402\,i & 7.11111 & 0 & 0 \\ 27.5428 + 3.72337\,i & 2.37037 - 29.787\,i & -9.48148 & 0 & 0 \end{pmatrix}$$

$$\kappa^{(7)}_{1,30lm} = \begin{pmatrix} 0 & 0 & 0 & 0 & 0 \\ -0.00010778 + 0.00258567\,i & 0 & 0 & 0 & 0 \\ 0.946811 - 0.0258567\,i & 0.488889 & 0.0987654 & 0 & 0 \\ -41.9952 + 1.63673\,i & -30.2091 + 0.930842\,i & -6.22222 & -1.18519 & 0 \\ -189.354 + 25.8196\,i & 42.6566 + 31.0281\,i & -57.765 + 3.72337\,i & 2.76543 & -2.37037 \\ 45.1784 - 52.4207\,i & -145.181 + 88.7403\,i & 70.9136 + 81.9141\,i & 11.0617 & 0 \\ 77.3602 + 54.2499\,i & 58.4491 - 184.927\,i & -96.0988 & 0 & 0 \end{pmatrix}$$

$$\kappa^{(7)}_{1,31lm} = \begin{pmatrix} 0 & 0 & 0 & 0 & 0 \\ 0 & 0 & 0 & 0 & 0 \\ 0 & 0 & 0 & 0 & 0 \\ -0.0164609 & 0 & 0 & 0 & 0 \\ 3.85185 + 2.79253\,i & 1.77778 & 0 & 0 & 0 \\ -27.3882 + 13.0318\,i & 8.2963 + 44.6804\,i & 14.2222 & 0 & 0 \\ 69.4495 + 1.86168\,i & 1.18519 - 74.4674\,i & -23.7037 & 0 & 0 \end{pmatrix}$$

Coefficients $\kappa^{(9)}_{2,ijlm}$ and $\rho^{(9)}_{2,ij}$ for the decomposition of $f_2^{(9)}$

$$\rho^{(9)}_{2,00} = -23.3946\,\hat{m}_c^3 \qquad \rho^{(9)}_{2,10} = 140.368\,\hat{m}_c$$
$$\rho^{(9)}_{2,20} = 842.206\,\hat{m}_c \qquad \rho^{(9)}_{2,30} = -46.7892\,\hat{m}_c^{-1} + 1918.36\,\hat{m}_c$$

$$\kappa^{(9)}_{2,00lm} = \begin{pmatrix} 0 & 0 & 0 & 0 & 0 \\ 0 & 0 & 0 & 0 & 0 \\ 0 & 0 & 0 & 0 & 0 \\ -24.2913 - 22.0299\,i & -23.1111 - 11.1701\,i & 0 & 0 & 0 \\ -86.7723 + 97.2931\,i & -57.5593 + 67.0206\,i & 7.11111 + 44.6804\,i & 4.74074 & 0 \\ 96.5187 - 160.51\,i & -325.463 + 89.3609\,i & 92.4444 + 178.722\,i & 23.7037 & 0 \\ 88.3801 + 142.135\,i & 171.457 - 208.509\,i & -120.889 & 0 & 0 \end{pmatrix}$$

$$\kappa^{(9)}_{2,01lm} = \begin{pmatrix} 0 & 0 & 0 & 0 & 0 \\ 0 & 0 & 0 & 0 & 0 \\ 0 & 0 & 0 & 0 & 0 \\ 0.296296 + 0.620562\,i & 0 & 0 & 0 & 0 \\ 3.55556 & 0 & 0 & 0 & 0 \\ -29.7586 + 11.1701\,i & 7.11111 + 44.6804\,i & 14.2222 & 0 & 0 \\ 55.2172 + 9.92898\,i & 6.32099 - 59.5739\,i & -18.963 & 0 & 0 \end{pmatrix}$$

$$\kappa^{(9)}_{2,10lm} = \begin{pmatrix} 0 & 0 & 0 & 0 & 0 \\ 0 & 0 & 0 & 0 & 0 \\ 0.8462 + 1.11701\,i & 0 & 0 & 0 & 0 \\ -26.8464 + 1.86168\,i & -8.88889 + 11.1701\,i & 0 & 0 & 0 \\ -428.313 + 184.792\,i & -50.8606 + 201.062\,i & -75.2337 + 44.6804\,i & 4.74074 & -4.74074 \\ 108.781 - 396.864\,i & -897.575 + 402.124\,i & 295.111 + 491.485\,i & 66.3704 & 0 \\ 437.34 + 382.697\,i & 408.81 - 804.248\,i & -381.63 & 0 & 0 \end{pmatrix}$$

$$\kappa^{(9)}_{2,11lm} = \begin{pmatrix} 0 & 0 & 0 & 0 & 0 \\ 0 & 0 & 0 & 0 & 0 \\ 0 & 0 & 0 & 0 & 0 \\ 0 & 0 & 0 & 0 & 0 \\ 16. + 11.1701\,i & 7.11111 & 0 & 0 & 0 \\ -111.923 + 44.6804\,i & 28.4444 + 178.722\,i & 56.8889 & 0 & 0 \\ 249.663 + 22.3402\,i & 14.2222 - 268.083\,i & -85.3333 & 0 & 0 \end{pmatrix}$$

$$\kappa^{(9)}_{2,20lm} = \begin{pmatrix} 0 & 0 & 0 & 0 & 0 \\ -0.0132191 + 0.11968\,i & 0 & 0 & 0 & 0 \\ 0.367901 - 0.372337\,i & 0 & 0 & 0 & 0 \\ -222.769 + 8.19141\,i & -132.372 + 11.1701\,i & -32.0 & -4.74074 & 0 \\ -1276.44 + 313.249\,i & 131.529 + 312.763\,i & -343.034 + 44.6804\,i & 14.2222 & -14.2222 \\ 268.098 - 652.279\,i & -1632.09 + 982.969\,i & 714.667 + 938.289\,i & 128.0 & 0 \\ 823.218 + 640.989\,i & 596.622 - 1980.83\,i & -1013.33 & 0 & 0 \end{pmatrix}$$

$$\kappa^{(9)}_{2,21lm} = \begin{pmatrix} 0 & 0 & 0 & 0 & 0 \\ 0 & 0 & 0 & 0 & 0 \\ 0 & 0 & 0 & 0 & 0 \\ -0.0987654 & 0 & 0 & 0 & 0 \\ 32.0 + 22.3402\,i & 14.2222 & 0 & 0 & 0 \\ -244.716 + 134.041\,i & 85.3333 + 402.124\,i & 128 & 0 & 0 \\ 668.137 & -714.887\,i & -227.556 & 0 & 0 \end{pmatrix}$$

$$\kappa^{(9)}_{2,30lm} = \begin{pmatrix} -0.0142243 + 0.0177303\,i & 0 & 0 & 0 & 0 \\ 0.0288536 - 0.0221629\,i & 0 & 0 & 0 & 0 \\ 10.8601 - 0.523045\,i & 5.51675 & 1.18519 & 0 & 0 \\ -478.485 + 10.3323\,i & -343.902 + 11.1701\,i & -67.5556 & -14.2222 & 0 \\ -2553.47 + 459.887\,i & 412.809 + 417.017\,i & -776.143 + 44.6804\,i & 33.1852 & -28.4444 \\ 527.368 - 890.889\,i & -2505.67 + 1869.13\,i & 1362.96 + 1519.13\,i & 208.593 & 0 \\ 1675.61 + 810.709\,i & 881.117 - 3916.98\,i & -1987.56 & 0 & 0 \end{pmatrix}$$

$$\kappa^{(9)}_{2,31lm} = \begin{pmatrix} 0 & 0 & 0 & 0 & 0 \\ 0 & 0 & 0 & 0 & 0 \\ 0 & 0 & 0 & 0 & 0 \\ -0.131687 & 0 & 0 & 0 & 0 \\ 49.7778 + 33.5103\,i & 21.3333 & 0 & 0 & 0 \\ -421.619 + 297.87\,i & 189.63 + 714.887\,i & 227.556 & 0 & 0 \\ 1391.36 - 111.701\,i & -71.1111 - 1489.35\,i & -474.074 & 0 & 0 \end{pmatrix}$$

Coefficients $\kappa^{(7)}_{2,ijlm}$ and $\rho^{(7)}_{2,ij}$ for the decomposition of $f_2^{(7)}$

$$\rho^{(7)}_{2,00} = -\,11.6973\,\hat{m}_c^3 \qquad \rho^{(7)}_{2,10} = -\,70.1839\,\hat{m}_c$$
$$\rho^{(7)}_{2,20} = -\,421.103\,\hat{m}_c \qquad \rho^{(7)}_{2,30} = 23.3946\,\hat{m}_c^{-1} - 959.179\,\hat{m}_c$$

$$\kappa^{(7)}_{2,00lm} = \begin{pmatrix} 0 & 0 & 0 & 0 & 0 \\ 0 & 0 & 0 & 0 & 0 \\ 0 & 0 & 0 & 0 & 0 \\ 6.85597 + 3.10281\,i & 0 & 0 & 0 & 0 \\ 13.2214 - 9.55118\,i & 31.3046 - 11.1701\,i & -3.55556 - 22.3402\,i & -2.37037 & 0 \\ -11.182 + 18.3741\,i & 27.9808 & -22.3402\,i & -2.37037 & 0 \\ 7.26787 - 17.3757\,i & -17.9753 + 14.8935\,i & 24.8889 & 0 & 0 \end{pmatrix}$$

$$\kappa^{(7)}_{2,01lm} = 0$$

$$\kappa^{(7)}_{2,10lm} = \begin{pmatrix} 0 & 0 & 0 & 0 & 0 \\ 0 & 0 & 0 & 0 & 0 \\ 0 & 0 & 0 & 0 & 0 \\ 12.4502 - 8.37758\,i & 2.66667 - 5.58505\,i & 0 & 0 & 0 \\ 155.555 - 34.6839\,i & 20.4061 - 78.1908\,i & 26.9502 - 22.3402\,i & -2.37037 & 2.37037 \\ -68.5374 + 91.4251\,i & 204.484 - 67.0206\,i & -62.2222 - 111.701\,i & -14.2222 & 0 \\ -70.5057 - 94.1903\,i & -113.738 + 148.935\,i & 87.7037 & 0 & 0 \end{pmatrix}$$

$$\kappa^{(7)}_{2,11lm} = \begin{pmatrix} 0 & 0 & 0 & 0 & 0 \\ 0 & 0 & 0 & 0 & 0 \\ 0 & 0 & 0 & 0 & 0 \\ 0.0987654 & 0 & 0 & 0 & 0 \\ -6.22222 - 5.58505\,i & -3.55556 & 0 & 0 & 0 \\ 27.9808 & -44.6804\,i & -14.2222 & 0 & 0 \\ -40.4253 - 11.1701\,i & -7.11111 + 44.6804\,i & 14.2222 & 0 & 0 \end{pmatrix}$$

$$\kappa^{(7)}_{2,20lm} = \begin{pmatrix} 0 & 0 & 0 & 0 & 0 \\ 0 & 0 & 0 & 0 & 0 \\ -0.0333333 & 0 & 0 & 0 & 0 \\ 116.815 - 9.54113\,i & 70.0677 - 5.58505\,i & 17.7778 & 2.37037 & 0 \\ 542.972 - 88.6728\,i & -89.5971 - 134.041\,i & 146.628 - 22.3402\,i & -7.11111 & 7.11111 \\ -143.29 + 196.813\,i & 496.749 - 234.572\,i & -193.778 - 268.083\,i & -35.5556 & 0 \\ -228.849 - 209.21\,i & -231.862 + 484.038\,i & 249.481 & 0 & 0 \end{pmatrix}$$

$$\kappa^{(7)}_{2,21lm} = \begin{pmatrix} 0 & 0 & 0 & 0 & 0 \\ 0 & 0 & 0 & 0 & 0 \\ 0 & 0 & 0 & 0 & 0 \\ 0.0987654 & 0 & 0 & 0 & 0 \\ -14.2222 - 11.1701\,i & -7.11111 & 0 & 0 & 0 \\ 83.9424 - 22.3402\,i & -14.2222 - 134.041\,i & -42.6667 & 0 & 0 \\ -165.257 - 22.3402\,i & -14.2222 + 178.722\,i & 56.8889 & 0 & 0 \end{pmatrix}$$

$$\kappa^{(7)}_{2,30lm} = \begin{pmatrix} 0 & 0 & 0 & 0 & 0 \\ 0.000646678 - 0.015514\,i & 0 & 0 & 0 & 0 \\ -5.68087 + 0.15514\,i & -2.93333 & -0.592593 & 0 & 0 \\ 251.971 - 9.82039\,i & 181.255 - 5.58505\,i & 37.3333 & 7.11111 & 0 \\ 1136.13 - 154.918\,i & -255.94 - 186.168\,i & 346.59 - 22.3402\,i & -16.5926 & 14.2222 \\ -271.07 + 314.524\,i & 871.089 - 532.442\,i & -425.481 - 491.485\,i & -66.3704 & 0 \\ -464.161 - 325.499\,i & -350.695 + 1109.56\,i & 576.593 & 0 & 0 \end{pmatrix}$$

$$\kappa^{(7)}_{2,31lm} = \begin{pmatrix} 0 & 0 & 0 & 0 & 0 \\ 0 & 0 & 0 & 0 & 0 \\ 0 & 0 & 0 & 0 & 0 \\ 0.0987654 & 0 & 0 & 0 & 0 \\ -23.1111 - 16.7552\,i & -10.6667 & 0 & 0 & 0 \\ 164.329 - 78.1908\,i & -49.7778 - 268.083\,i & -85.3333 & 0 & 0 \\ -416.697 - 11.1701\,i & -7.11111 + 446.804\,i & 142.222 & 0 & 0 \end{pmatrix}$$

References

[1] R. Ammar *et al.* [CLEO Collaboration], *Phys. Rev. Lett.* **71** (1993) 674.

[2] M. S. Alam *et al.* [CLEO Collaboration], *Phys. Rev. Lett.* **74** (1995) 2885;
T. E. Coan *et al.* [CLEO Collaboration], Report CLNS 00/1697, CLEO 00-21.

[3] I. Bigi *et al.*, *Phys. Rev. Lett.* **71** (1993) 496;
A. Manohar and M.B. Wise, *Phys. Rev.* **D 49** (1994) 1310;
B. Blok *et al.*, *Phys. Rev.* **D 49** (1994) 3356;
T. Mannel, *Nucl. Phys.* **B 413** (1994) 396;
A. Falk, M. Luke, and M. Savage, *Phys. Rev.* **D 49** (1994) 3367.

[4] I. Bigi et al., *Phys. Lett.* **B 293** (1992) 430; *Phys. Lett.* **B 297** (1993) 477 (E).

[5] S. Chen *et al.* [CLEO Collaboration], `hep-ex/0108032`.

[6] R. Barate *et al.* [ALEPH collaboration], *Phys. Lett.* **B 429** (1998) 169.

[7] A. Abashian *et al.* [BELLE collaboration], BELLE-CONF-0003.

[8] A. Ali and C. Greub, *Z. Physik* **C 49** (1991) 431; *Phys. Lett.* **B 259** (1991) 182;
Phys. Lett. **B 361** (1995) 146.
A.L. Kagan and M. Neubert, *Eur. Phys. J.* **C 7** (1999) 5.

[9] K. Adel and Y. P. Yao, *Phys. Rev.* **D 49** (1994) 4945;
C. Greub and T. Hurth *Phys. Rev.* **D 56** (1997) 2934;
A. J. Buras, A. Kwiatkowski and N. Pott, *Nucl. Phys.* **B 517** (1998) 353.

[10] M. Ciuchini, G. Degrassi, P. Gambino and G.F. Giudice,
Nucl. Phys. **B 527** (1998) 21.

[11] K. Chetyrkin, M. Misiak and M. Münz, *Phys. Lett.* **B 400** (1997) 206.

[12] C. Greub, T. Hurth and D. Wyler, *Phys. Rev.* **D 54** (1996) 3350.

[13] A. J. Buras, A. Czarnecki, M. Misiak, J. Urban, `hep-ph/0105160`.

[14] P. Gambino and M. Misiak, `hep-ph/0104034`.

[15] F. Borzumati and C. Greub, *Phys. Rev.* **D 58** (1998) 074004;
Phys. Rev. **D 59** (1999) 057501.

[16] H. H. Asatryan, H. M. Asatrian, G. K. Yeghiyan and G. K. Savvidy,
Int. J. Mod. Phys. **A 16** (2001) 3805, `hep-ph/0012085`.

[17] S. Bertolini, F. Borzumati, A. Masiero and G. Ridolfi, *Nucl. Phys.* **B 353** (1991) 591.

[18] M. Ciuchini, G. Degrassi, P. Gambino and G.F. Giudice, *Nucl. Phys.* **B 534** (1998) 3.

[19] C. Bobeth, M. Misiak and J. Urban, *Nucl. Phys.* **B 567** (2000) 153.

[20] F. Borzumati, C. Greub, T. Hurth and D. Wyler, *Phys. Rev.* **D 62** (2000) 075005.

[21] T. Besmer, C. Greub and T. Hurth, *Nucl. Phys.* **B 609** (2001) 359.

[22] H. H. Asatrian and H. M. Asatrian, *Phys. Lett.* **B 460** (1999) 148, hep-ph/9906221.

[23] B. Grinstein, M. J. Savage and M. B. Wise, *Nucl. Phys.* **B 319** (1989) 271.

[24] M. Misiak, *Nucl. Phys.* **B 393** (1993) 23, *Nucl. Phys.* **B 439** (1995) 461 (E).

[25] A. Ali, G. F. Guidice, T. Mannel, *Z. Physik* **C 67** (1995) 417.

[26] N. Desphande, J. Trampetic, K. Pancrose, *Phys. Rev.* **D 39** (1989) 1461; C. S. Lim, T. Morozumi, A. I. Sanda, *Phys. Lett.* **B 218** (1989) 343.

[27] P. Cho, M. Misiak, D. Wyler, *Phys. Rev.* **D 54** (1996) 3329.

[28] A. J. Buras and M. Münz, *Phys. Rev.* **D 52** (1995) 186.

[29] S. Glenn *et al.* [CLEO Collaboration], *Phys. Rev. Lett.* **80** (1998) 2289.

[30] K. Abe *et al.* [BELLE Collaboration], BELLE-CONF-0110, hep-ex/0107072.

[31] Z. Ligeti and M. B. Wise, *Phys. Rev.* **D 53** (1996) 4937.

[32] A. F. Falk, M. Luke and M. J. Savage, *Phys. Rev.* **D 49** (1994) 3367.

[33] A. Ali, G. Hiller, L. T. Handoko and T. Morozumi, *Phys. Rev.* **D 55** (1997) 4105.

[34] J-W. Chen, G. Rupak and M. J. Savage, *Phys. Lett.* **B 410** (1997) 285.

[35] G. Buchalla, G. Isidori and S. J. Rey, *Nucl. Phys.* **B 511** (1998) 594.

[36] G. Buchalla and G. Isidori, *Nucl. Phys.* **B 525** (1998) 333.

[37] F. Krüger and L.M. Sehgal, *Phys. Lett.* **B 380** (1996) 199.

[38] A. Ali, P. Ball, L.T. Handoko, G. Hiller, *Phys. Rev.* **D 61** (2000) 074024.

[39] E. Lunghi and I. Scimemi, *Nucl. Phys.* **B 574** (2000) 43.

[40] E. Lunghi, A. Masiero, I. Scimemi and L. Silvestrini, *Nucl. Phys.* **B 568** (2000) 120.

[41] C. Bobeth, M. Misiak and J. Urban, *Nucl. Phys.* **B 574** (2000) 291.

[42] H. H. Asatryan, H. M. Asatrian, C. Greub and M. Walker, *Phys. Lett.* **B 507** (2001) 162, hep-ph/0103087.

[43] G. Buchalla and A. J. Buras, *Nucl. Phys.* **B 548** (1999) 309.

[44] H. H. Asatryan, H. M. Asatrian, C. Greub and M. Walker, in preparation.

[45] V. A. Smirnov, *Renormalization and Asymptotic Expansions* (Birkhäuser, Basel, 1991).

[46] V. A. Smirnov, *Mod. Phys. Lett.* **A 10** (1995) 1485, hep-th/9412063.

[47] H. Simma and D. Wyler, *Nucl. Phys.* **B 344** (1990) 283.

[48] C. Greub and P. Liniger, *Phys. Lett.* **B 494** (2000) 237; *Phys. Rev.* **D 63** (2001) 054025.

[49] N. Cabibbo and L. Maiani, *Phys. Lett.* **B 79** (1978) 109.

[50] Y. Nir, *Phys. Lett.* **B 221** (1989) 184.

PART IV

JHEP Conference Proceedings

hep-ph/0110388
Budapest 2001, High energy physics, hep2001/091

PROCEEDINGS

International Europhysics Conference on HEP

Results of the $\mathcal{O}(\alpha_s)$ Two-Loop Virtual Corrections to $B \to X_s \ell^+\ell^-$ in the Standard Model [1]

C. Greub[a] and M. Walker[a]

[a] *Institut für Theoretische Physik, Universität Bern, CH–3012 Bern, Switzerland.*

ABSTRACT

We present the results of the $\mathcal{O}(\alpha_s)$ two-loop virtual corrections to the differential decay width $d\Gamma(B \to X_s \ell^+\ell^-)/d\hat{s}$, where $\hat{s}$ is the invariant mass squared of the lepton pair, normalized to m_b^2. Those contributions from gluon bremsstrahlung which are needed to cancel infrared and collinear singularities are also included. Our calculation is restricted to the range $0.05 \leq \hat{s} \leq 0.25$ where the effects from resonances are small. The new contributions drastically reduce the renormalization scale dependence of existing results for $d\Gamma(B \to X_s \ell^+\ell^-)/d\hat{s}$. The renormalization scale uncertainty of the corresponding branching ratio (restricted to $0.05 \leq \hat{s} \leq 0.25$) gets reduced from $\sim \pm 13\%$ to $\sim \pm 6.5\%$.

[1]Work partially supported by Schweizerischer Nationalfonds and SCOPES program

1 Introduction

After the observation of the penguin-induced decay $B \to X_s\gamma$ [1] and corresponding exclusive channels such as $B \to K^*\gamma$ [2], rare B decays have begun to play an important role in the phenomenology of particle physics. They put strong constraints on various extensions of the Standard Model. The inclusive decay $B \to X_s\,\ell^+\ell^-$ has not been observed so far, but is expected to be detected at the currently running B factories.

The next-to-leading logarithmic (NLL) result for $B \to X_s\,\ell^+\ell^-$ suffers from a relatively large ($\pm 16\%$) dependence on the matching scale μ_W [3, 4]. The NNLL corrections to the Wilson coefficients remove the matching scale dependence to a large extent [5], but leave a $\pm 13\%$-dependence on the renormalization scale μ_b, which is of $\mathcal{O}(m_b)$. In order to further improve the result, we have recently calculated the $\mathcal{O}(\alpha_s)$ two-loop corrections to the matrix elements of the operators O_1 and O_2 as well as the $\mathcal{O}(\alpha_s)$ one-loop corrections to O_7,..., O_{10} [6]. Because of large resonant contributions from $\bar{c}c$ intermediate states, we restrict the invariant lepton mass squared s to the region $0.05 \le \hat{s} \le 0.25$, where $\hat{s} = s/m_b^2$. In the following we present a summary of the results of these calculations.

2 Theoretical Framework

The appropriate tool for studies on weak B mesons decays is the effective Hamiltonian technique. The effective Hamiltonian is derived from the Standard Model by integrating out the t quark, the Z_0 and the W boson. For the decay channels $b \to s\,\ell^+\ell^-$ ($\ell = \mu, e$) it reads

$$\mathcal{H}_{\rm eff} = -\frac{4\,G_F}{\sqrt{2}}\,V_{ts}^*\,V_{tb}\sum_{i=1}^{10} C_i\,O_i,$$

where O_i are dimension six operators and C_i denote the corresponding Wilson coefficients. The operators can be chosen as [5]

$$\begin{aligned}
O_1 &= (\bar{s}_L\gamma_\mu T^a c_L)(\bar{c}_L\gamma^\mu T^a b_L), & O_2 &= (\bar{s}_L\gamma_\mu c_L)(\bar{c}_L\gamma^\mu b_L),\\
O_3 &= (\bar{s}_L\gamma_\mu b_L)\textstyle\sum_q(\bar{q}\gamma^\mu q), & O_4 &= (\bar{s}_L\gamma_\mu T^a b_L)\textstyle\sum_q(\bar{q}\gamma^\mu T^a q),\\
O_5 &= (\bar{s}_L\gamma_\mu\gamma_\nu\gamma_\sigma b_L)\textstyle\sum_q(\bar{q}\gamma^\mu\gamma^\nu\gamma^\sigma q), & O_6 &= (\bar{s}_L\gamma_\mu\gamma_\nu\gamma_\sigma T^a b_L)\textstyle\sum_q(\bar{q}\gamma^\mu\gamma^\nu\gamma^\sigma T^a q),\\
O_7 &= \tfrac{e}{g_s^2}m_b(\bar{s}_L\sigma^{\mu\nu}b_R)F_{\mu\nu}, & O_8 &= \tfrac{1}{g_s}m_b(\bar{s}_L\sigma^{\mu\nu}T^a b_R)G^a_{\mu\nu},\\
O_9 &= \tfrac{e^2}{g_s^2}(\bar{s}_L\gamma_\mu b_L)\textstyle\sum_\ell(\bar{\ell}\gamma^\mu\ell), & O_{10} &= \tfrac{e^2}{g_s^2}(\bar{s}_L\gamma_\mu b_L)\textstyle\sum_\ell(\bar{\ell}\gamma^\mu\gamma_5\ell).
\end{aligned}$$

The subscripts L and R refer to left- and right-handed fermion fields. We work in the approximation where the combination $(V_{us}^*V_{ub})$ of Cabibbo-Kobayashi-Maskawa (CKM) matrix elements is neglected. The CKM structure factorizes therefore.

3 Virtual Corrections to the Operators O_1, O_2, O_7, O_8, O_9 and O_{10}

Using the naive dimensional regularization scheme in $d = 4-2\,\epsilon$ dimensions, ultraviolet and infrared singularities both show up as $1/\epsilon^n$ poles ($n = 1, 2$). The ultraviolet singularities cancel after including the counterterms. Collinear singularities are regularized by retaining a finite strange quark mass m_s. They are cancelled together with the infrared singularities at the level of the decay width, when taking the bremsstrahlung process $b \to s\,\ell^+\ell^- g$ into account. Gauge invariance implies that the QCD-corrected matrix elements of the operators O_i can be written as

$$\langle s\,\ell^+\ell^-|O_i|b\rangle = \hat{F}_i^{(9)}\langle O_9\rangle_{\rm tree} + \hat{F}_i^{(7)}\langle O_7\rangle_{\rm tree}\,,$$

where $\langle O_9\rangle_{\rm tree}$ and $\langle O_7\rangle_{\rm tree}$ are the tree-level matrix elements of O_9 and O_7, respectively.

3.1 Virtual Corrections to O_1 and O_2

For the calculation of the two-loop diagrams associated with O_1 and O_2 we mainly used a combination of Mellin-Barnes technique [6, 7] and of Taylor series expansion in s. For $s < m_b^2$ and $s < 4\,m_c^2$, most diagrams allow the latter. The unrenormalized form factors $\hat{F}^{(7,9)}$ of O_1 and O_2 are then obtained in the form

$$\hat{F}^{(7,9)} = \sum_{i,j,l,m} c_{ijlm}^{(7,9)}\,\hat{s}^i\,\ln^j(\hat{s})\,\left(\hat{m}_c^2\right)^l\,\ln^m(\hat{m}_c)\,,$$

where $\hat{m}_c = \frac{m_c}{m_b}$. The indices i, j, m are non-negative integers and $l = -i, -i+\frac{1}{2}, -i+1, \ldots.$.

Besides the counterterms from quark field, quark mass and coupling constant (g_s) renormalization, there are counterterms induced by operator mixing. They are of the form

$$C_i \cdot \sum_j \delta Z_{ij}\langle O_j\rangle \quad \text{with} \quad \delta Z_{ij} = \frac{\alpha_s}{4\,\pi}\left[a_{ij}^{01} + \frac{a_{ij}^{11}}{\epsilon}\right] + \frac{\alpha_s^2}{(4\,\pi)^2}\left[a_{ij}^{02} + \frac{a_{ij}^{12}}{\epsilon} + \frac{a_{ij}^{22}}{\epsilon^2}\right] + \mathcal{O}\big(\alpha_s^3\big)\,.$$

A complete list of the coefficients a_{ij}^{lm} used for our calculation can be found in [6]. The operator mixing involves also the evanescent operators

$$\begin{aligned} O_{11} &= (\bar{s}_L\gamma_\mu\gamma_\nu\gamma_\sigma T^a c_L)\,(\bar{c}_L\gamma^\mu\gamma^\nu\gamma^\sigma T^a b_L) - 16\,O_1 \quad \text{and} \\ O_{12} &= (\bar{s}_L\gamma_\mu\gamma_\nu\gamma_\sigma c_L)\,(\bar{c}_L\gamma^\mu\gamma^\nu\gamma^\sigma b_L) - 16\,O_2. \end{aligned}$$

3.2 Virtual Corrections to O_7, O_8, O_9 and O_{10}

The renormalized contributions from the operators O_7, O_8 and O_9 can all be written in the form

$$\langle s\,\ell^+\ell^-|C_iO_i|b\rangle = \widetilde{C}_i^{(0)}\left(-\frac{\alpha_s}{4\,\pi}\right)\left[F_i^{(9)}\langle\widetilde{O}_9\rangle_{\rm tree} + F_i^{(7)}\langle\widetilde{O}_7\rangle_{\rm tree}\right],$$

with $\widetilde{O}_i = \frac{\alpha_s}{4\pi} O_i$, $\widetilde{C}_{7,8}^{(0)} = C_{7,8}^{(1)}$ and $\widetilde{C}_9^{(0)} = \frac{4\pi}{\alpha_s}\left(C_9^{(0)} + \frac{\alpha_s}{4\pi} C_9^{(1)}\right)$.

The formally leading term $\sim g_s^{-2} C_9^{(0)}(\mu_b)$ to the amplitude for $b \to s\,\ell^+\ell^-$ is smaller than the NLL term $\sim g_s^{-2}\left[g_s^2/(16\pi^2)\right] C_9^{(1)}(\mu_b)$ [8]. We therefore adapt our systematics to the numerical situation and treat the sum of these two terms as a NLL contribution, as indicated by the expression for $\widetilde{C}_9^{(0)}$. The decay amplitude then starts out with a NLL term.

The contribution from O_8 is finite, whereas those from O_7 and O_9 are not, ie $F_7^{(7)}$ and $F_9^{(9)}$ suffer from the same infrared divergent part $f_{\rm inf}$.

As the hadronic parts of the operators O_9 and O_{10} are identical, the QCD corrected matrix element of O_{10} can easily be obtained from that of O_9.

4 Bremsstrahlung Corrections

It is known [3, 4] that the contribution to the inclusive decay width from the interference between the tree-level and the one-loop matrix elements of O_9 and from the corresponding bremsstrahlung corrections can be written as

$$\frac{d\Gamma_{99}}{d\hat{s}} = \left(\frac{\alpha_{em}}{4\pi}\right)^2 \frac{G_F^2\, m_{b,\rm pole}^5\, |V_{ts}^* V_{tb}|^2}{48\pi^3} (1-\hat{s})^2\,(1+2\,\hat{s}) \left[2\left|\widetilde{C}_9^{(0)}\right|^2 \frac{\alpha_s}{\pi}\,\omega_9(\hat{s})\right].$$

Analogous formulas hold true for the contributions from O_7 and the interference terms between the matrix elements of O_7 and O_9:

$$\frac{d\Gamma_{77}}{d\hat{s}} = \left(\frac{\alpha_{em}}{4\pi}\right)^2 \frac{G_F^2\, m_{b,\rm pole}^5\, |V_{ts}^* V_{tb}|^2}{48\pi^3} (1-\hat{s})^2\, 4\,(1+2/\hat{s}) \left[2\left|\widetilde{C}_7^{(0)}\right|^2 \frac{\alpha_s}{\pi}\,\omega_7(\hat{s})\right],$$

$$\frac{d\Gamma_{79}}{d\hat{s}} = \left(\frac{\alpha_{em}}{4\pi}\right)^2 \frac{G_F^2\, m_{b,\rm pole}^5\, |V_{ts}^* V_{tb}|^2}{48\pi^3} (1-\hat{s})^2\, 12\cdot 2\,\frac{\alpha_s}{\pi}\,\omega_{79}(\hat{s})\,{\rm Re}\left[\widetilde{C}_7^{(0)}\widetilde{C}_9^{(0)}\right].$$

The function $\omega_9(\hat{s}) \equiv \omega(\hat{s})$ can be found eg in [3, 4]. For $\omega_7(\hat{s})$ and $\omega_{79}(\hat{s})$ see [6]. All other bremsstrahlung corrections are finite and will be given in [9].

5 Corrections to the Decay Width for $B \to X_s\,\ell^+\ell^-$

Combining the virtual corrections discussed in Section 3 with the bremsstrahlung contributions considered in Section 4, we find for the decay width

$$\frac{d\Gamma(b\to X_s\ell^+\ell^-)}{d\hat{s}} = \left(\frac{\alpha_{em}}{4\pi}\right)^2 \frac{G_F^2\, m_{b,\rm pole}^5\, |V_{ts}^* V_{tb}|^2}{48\pi^3} (1-\hat{s})^2$$
$$\times \left\{(1+2\,\hat{s})\left[\left|\widetilde{C}_9^{\rm eff}\right|^2 + \left|\widetilde{C}_{10}^{\rm eff}\right|^2\right] + 4\,(1+2/\hat{s})\left|\widetilde{C}_7^{\rm eff}\right|^2 + 12\,{\rm Re}\left[\widetilde{C}_7^{\rm eff}\widetilde{C}_9^{\rm eff*}\right]\right\}, \quad (1)$$

where the effective Wilson coefficients $\widetilde{C}_7^{\rm eff}$, $\widetilde{C}_9^{\rm eff}$ and $\widetilde{C}_{10}^{\rm eff}$ can be written as

$$\begin{aligned}
\widetilde{C}_9^{\rm eff} &= \left[1+\frac{\alpha_s(\mu)}{\pi}\,\omega_9(\hat{s})\right]\Big(A_9+T_9\,h(\hat{m}_c^2,\hat{s})+U_9\,h(1,\hat{s})+W_9\,h(0,\hat{s})\Big) \\
&\qquad -\frac{\alpha_s(\mu)}{4\,\pi}\Big(C_1^{(0)}F_1^{(9)}+C_2^{(0)}F_2^{(9)}+A_8^{(0)}F_8^{(9)}\Big)\,, \\
\widetilde{C}_7^{\rm eff} &= \left[1+\frac{\alpha_s(\mu)}{\pi}\,\omega_7(\hat{s})\right]A_7-\frac{\alpha_s(\mu)}{4\,\pi}\Big(C_1^{(0)}F_1^{(7)}+C_2^{(0)}F_2^{(7)}+A_8^{(0)}F_8^{(7)}\Big)\,, \\
\widetilde{C}_{10}^{\rm eff} &= \left[1+\frac{\alpha_s(\mu)}{\pi}\,\omega_9(\hat{s})\right]A_{10}\,.
\end{aligned}$$

The function $h(\hat{m}_c^2,\hat{s})$ is defined in [5], where also the values of A_7, A_9, A_{10}, T_9, U_9 and W_9 can be found. $C_1^{(0)}$, $C_2^{(0)}$ and $A_8^{(0)}=\widetilde{C}_8^{(0,\rm eff)}$ are taken from [7].

6 Numerical Results

The decay width in Eq. (1) has a large uncertainty due to the factor $m_{b,\rm pole}^5$. Following common practice, we consider the ratio

$$R_{\rm quark}(\hat{s})=\frac{1}{\Gamma(b\to X_c\,e\,\bar{\nu}_e)}\frac{d\Gamma(b\to X_s\,\ell^+\ell^-)}{d\hat{s}}\,,$$

in which the factor $m_{b,\rm pole}^5$ drops out. $\Gamma(b\to X_c\,e\,\bar{\nu}_e)$ can be found eg in [5].

In Fig. 6.1(a) we investigate the dependence of $R_{\rm quark}(\hat{s})$ on the renormalization scale μ_b for $0.05\le\hat{s}\le 0.25$. The solid lines take the new NNLL contributions into account, whereas the dashed lines include the NLL results combined with the NNLL corrections to the matching conditions [5], only. The lower, middle and upper line each correspond to $\mu_b=2.5,\ 5$ and 10 GeV, respectively, and $\hat{m}_c=0.29$. From this figure we conclude that the renormalization scale dependence gets reduced by more than a factor of two. For the integrated quantity we get

$$R_{\rm quark}=\int_{0.05}^{0.25}d\hat{s}\,R_{\rm quark}(\hat{s})=(1.25\pm0.08)\times10^{-5}\,,$$

where the error is obtained by varying μ_b between 2.5 GeV and 10 GeV. Not including our corrections, one finds $R_{\rm quark}=(1.36\pm0.18)\times10^{-5}$ [5]. In other words, the renormalization scale dependence got reduced from $\sim\pm13\%$ to $\sim\pm6.5\%$. The largest uncertainty due to the input parameters is induced by $\hat{m}_c$. Fig. 6.1(b) illustrates the dependence of $R_{\rm quark}(\hat{s})$ on $\hat{m}_c$. The dashed, solid and dash-dotted lines correspond to $\hat{m}_c=0.27$, $\hat{m}_c=0.29$ and $\hat{m}_c=0.31$, respectively, and $\mu_b=5$ GeV. We find an uncertainty of $\pm7.6\%$ due to $\hat{m}_c$.

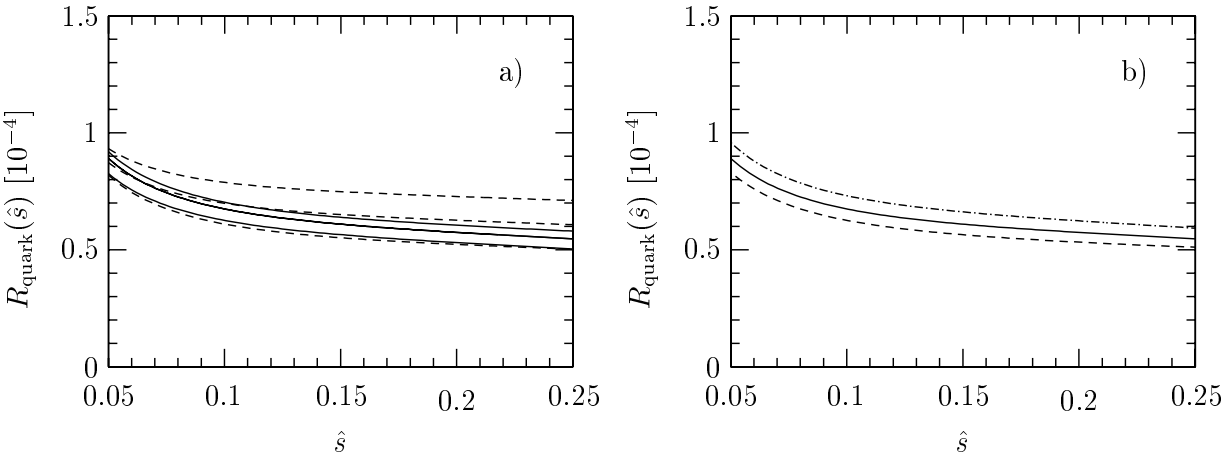

(a) Dependence of $R_{\rm quark}(\hat{s})$ on μ_b.

(b) Dependence of $R_{\rm quark}(\hat{s})$ on $\hat{m}_c$.

We conclude with the remark that the results presented in this exposition have recently been included in a systematic description of the corresponding exclusive decay mode $B \to K^* \ell^+ \ell^-$ [10, 11].

References

[1] M. S. Alam et al. [CLEO Collaboration], *Phys. Rev. Lett.* **74** (1995) 2885.

[2] R. Ammar et al. [CLEO Collaboration], *Phys. Rev. Lett.* **71** (1993) 674.

[3] M. Misiak, *Nucl. Phys.* **B 393** (1993) 23, *Nucl. Phys.* **B 439** (1995) 461 (E).

[4] A. J. Buras and M. Münz, *Phys. Rev.* **D 52** (1995) 186, hep-ph/9501281.

[5] C. Bobeth, M. Misiak and J. Urban, *Nucl. Phys.* **B 574** (2000) 291, hep-ph/9910220.

[6] H. H. Asatryan, H. M. Asatrian, C. Greub and M. Walker, *Phys. Lett.* **B 507** (2001) 162, hep-ph/0103087; H. H. Asatryan, H. M. Asatrian, C. Greub and M. Walker, hep-ph/0109140.

[7] C. Greub and P. Liniger, *Phys. Lett.* **B 494** (2000) 237, hep-ph/0008071; C. Greub and P. Liniger, *Phys. Rev.* **D 63** (2001) 054025, hep-ph/0009144.

[8] B. Grinstein, M. J. Savage and M. B. Wise, *Nucl. Phys.* **B 319** (1989) 271.

[9] H. H. Asatryan, H. M. Asatrian, C. Greub and M. Walker, in preparation.

[10] M. Beneke, Th. Feldmann and D. Seidel, *Nucl. Phys.* **B 612** (2001) 25.

[11] Th. Feldmann, these proceedings, hep-ph/0108142.

PART V

Complete Gluon Bremsstrahlung Corrections to the Process $b \to s\,\ell^+\ell^-$

accepted for publication in

Physical Review D

BUTP–02/06
hep-ph/0204341

Complete Gluon Bremsstrahlung Corrections to the Process $b \to s\,\ell^+\ell^-$ [1]

H. H. Asatryan[a], H. M. Asatrian[a], C. Greub[b] and M. Walker[b]

[a] *Yerevan Physics Institute, 2 Alikhanyan Br., 375036 Yerevan, Armenia*
[b] *Institut für Theoretische Physik, Universität Bern, CH–3012 Bern, Switzerland.*

ABSTRACT

In a recent paper [1], we presented the calculation of the $\mathcal{O}(\alpha_s)$ virtual corrections to $b \to s\,\ell^+\ell^-$ and of those bremsstrahlung terms which are needed to cancel the infrared divergences. In the present paper we work out the remaining $\mathcal{O}(\alpha_s)$ bremsstrahlung corrections to $b \to s\,\ell^+\ell^-$, which do not suffer from infrared and collinear singularities. These new contributions turn out to be small numerically. In addition, we also investigate the impact of the definition of m_c on the numerical results.

[1]Work partially supported by Schweizerischer Nationalfonds and SCOPES program

1 Introduction

The inclusive rare decay $B \to X_s\,\ell^+\ell^-$ has not been observed so far, but is expected to be measured at the operating B factories after a few years of data taking. The measurement of its various kinematical distributions, combined with improved data on $B \to X_s\,\gamma$, will imply tight constraints on the extensions of the Standard Model and perhaps even reveal some new physics.

The main problem of the theoretical description of $B \to X_s\,\ell^+\ell^-$ is due to the long-distance contributions from $\bar{c}c$ resonant states. When the invariant mass $\sqrt{s}$ of the lepton pair is close to the mass of a resonance, only model dependent predictions for these long distance contributions are available today. It is therefore unclear whether the theoretical uncertainty can be reduced to less than $\pm 20\%$ when integrating over these domains [2].

However, when restricting $\sqrt{s}$ to a region below the resonances, the long distance effects are under control. The corrections to the pure perturbative picture can be analyzed within the heavy quark effective theory (HQET). In particular, all available studies indicate that for the region $0.05 < \hat{s} = s/m_b^2 < 0.25$ the non-perturbative effects are below 10% [3]–[8]. Consequently, the differential decay rate for $B \to X_s\,\ell^+\ell^-$ can be precisely predicted in this region using renormalization group improved perturbation theory. It was pointed out in the literature that the differential decay rate and the forward-backward asymmetry are particularly sensitive to new physics in this kinematical window [9]–[13].

The next-to-leading logarithmic (NLL) result for $B \to X_s\,\ell^+\ell^-$ suffers from a relatively large ($\pm 16\%$) dependence on the matching scale μ_W [14, 15]. The NNLL corrections to the Wilson coefficients remove the matching scale dependence to a large extent [16], but leave a $\pm 13\%$-dependence on the renormalization scale μ_b, which is of $\mathcal{O}(m_b)$. In order to further improve the theoretical prediction, we have recently calculated the $\mathcal{O}(\alpha_s)$ virtual two-loop corrections to the matrix elements $\langle s\,\ell^+\ell^-|O_i|b\rangle$ $(i = 1, 2)$ as well as the virtual $\mathcal{O}(\alpha_s)$ one-loop corrections to O_7,...,O_{10} [1]. As some of these corrections suffer from infrared and collinear singularities, we have added those bremsstrahlung corrections needed to cancel these singularities. This improvement reduced the renormalization scale dependence by a factor of 2.

In the present paper we complete the calculation of the bremsstrahlung corrections associated with the operators O_1, O_2, O_7,...,O_{10}, ie we add those bremsstrahlung terms which are purely finite and have therefore been omitted in Ref. [1]. We anticipate that the additional terms have a small impact on the phenomenology of $b \to s\,\ell^+\ell^-$.

The paper is organized as follows: In Section 2, we briefly specify the theoretical framework, before, in Section 3, we discuss the organization of the calculation of the finite bremsstrahlung corrections and review the structure of the virtual corrections and singular bremsstrahlung contributions, calculated in Ref. [1]. The finite bremsstrahlung corrections are worked out in Section 4 and Section 5. In Section 6, finally, we investigate the numerical impact of the new corrections on the invariant mass spectrum of the lepton pair. We

also illustrate the dependence of our results on the definition of the charm quark mass.

2 Effective Hamiltonian

The appropriate tool for studies on weak B mesons decays is the effective Hamiltonian technique. The effective Hamiltonian is derived from the Standard Model by integrating out the t quark, the Z_0 and the W boson. For the decay channels $b \to s\,\ell^+\ell^-$ ($\ell = \mu, e$) it reads

$$\mathcal{H}_{\rm eff} = -\frac{4\,G_F}{\sqrt{2}}\,V_{ts}^*\,V_{tb}\sum_{i=1}^{10} C_i\,O_i\,,$$

where O_i are dimension six operators and C_i denote the corresponding Wilson coefficients. The operators we choose as in [16]:

$$\begin{aligned}
O_1 &= (\bar{s}_L\gamma_\mu T^a c_L)(\bar{c}_L\gamma^\mu T^a b_L), & O_2 &= (\bar{s}_L\gamma_\mu c_L)(\bar{c}_L\gamma^\mu b_L),\\
O_3 &= (\bar{s}_L\gamma_\mu b_L)\textstyle\sum_q(\bar{q}\gamma^\mu q), & O_4 &= (\bar{s}_L\gamma_\mu T^a b_L)\textstyle\sum_q(\bar{q}\gamma^\mu T^a q),\\
O_5 &= (\bar{s}_L\gamma_\mu\gamma_\nu\gamma_\sigma b_L)\textstyle\sum_q(\bar{q}\gamma^\mu\gamma^\nu\gamma^\sigma q), & O_6 &= (\bar{s}_L\gamma_\mu\gamma_\nu\gamma_\sigma T^a b_L)\textstyle\sum_q(\bar{q}\gamma^\mu\gamma^\nu\gamma^\sigma T^a q),\\
O_7 &= \tfrac{e}{g_s^2}m_b(\bar{s}_L\sigma^{\mu\nu}b_R)F_{\mu\nu}, & O_8 &= \tfrac{1}{g_s}m_b(\bar{s}_L\sigma^{\mu\nu}T^a b_R)G^a_{\mu\nu},\\
O_9 &= \tfrac{e^2}{g_s^2}(\bar{s}_L\gamma_\mu b_L)\textstyle\sum_\ell(\bar{\ell}\gamma^\mu\ell), & O_{10} &= \tfrac{e^2}{g_s^2}(\bar{s}_L\gamma_\mu b_L)\textstyle\sum_\ell(\bar{\ell}\gamma^\mu\gamma_5\ell).
\end{aligned}$$

The subscripts L and R refer to left- and right-handed fermion fields. We work in the approximation where the combination $(V_{us}^*V_{ub})$ of Cabibbo-Kobayashi-Maskawa (CKM) matrix elements is neglected and the CKM structure factorizes.

In the following it is convenient to define the operators $\widetilde{O}_7$,...,$\widetilde{O}_{10}$ according to

$$\widetilde{O}_j = \frac{\alpha_s}{4\,\pi}\,O_j\,, \quad (j = 7, ..., 10), \tag{1}$$

with the corresponding coefficients

$$\widetilde{C}_j = \frac{4\,\pi}{\alpha_s}\,C_j\,, \quad (j = 7, ..., 10). \tag{2}$$

3 Organization of the Calculation and Previous Results

In this section we comment on the organization of the calculation of the virtual and bremsstrahlung corrections to the process $b \to s\,\ell^+\ell^-$ and repeat the results obtained in Ref. [1].

The one-loop diagrams in Fig. 3.1, associated with the four-quark operators O_1,...,O_6, lead to contributions which are proportional to the tree level matrix elements of the operators

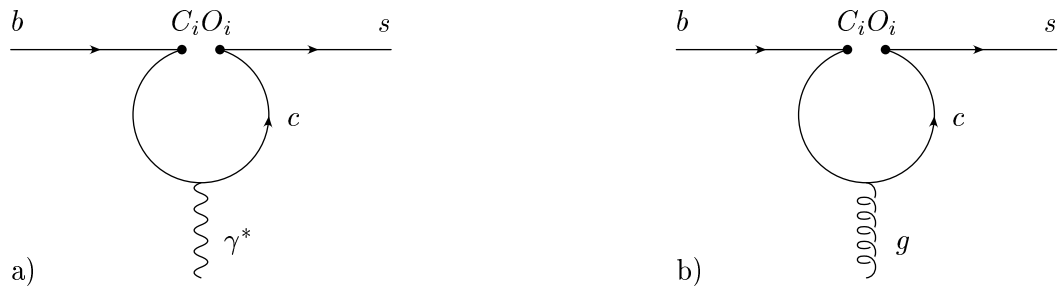

Figure 3.1: Diagram a) can be absorbed by replacing the Wilson coefficients $\widetilde{C}_7$ and $\widetilde{C}_9$ through $\widetilde{C}_7^{\rm mod}$ and $\widetilde{C}_9^{\rm mod}$, respectively. γ^* denotes an off-shell photon which subsequently decays into a $(\ell^+\ell^-)$ pair. Similarly, diagram b) is absorbed through the replacement $\widetilde{C}_8 \to \widetilde{C}_8^{\rm mod}$. g denotes an on-shell gluon. The index i runs from 1 to 6. See text for details.

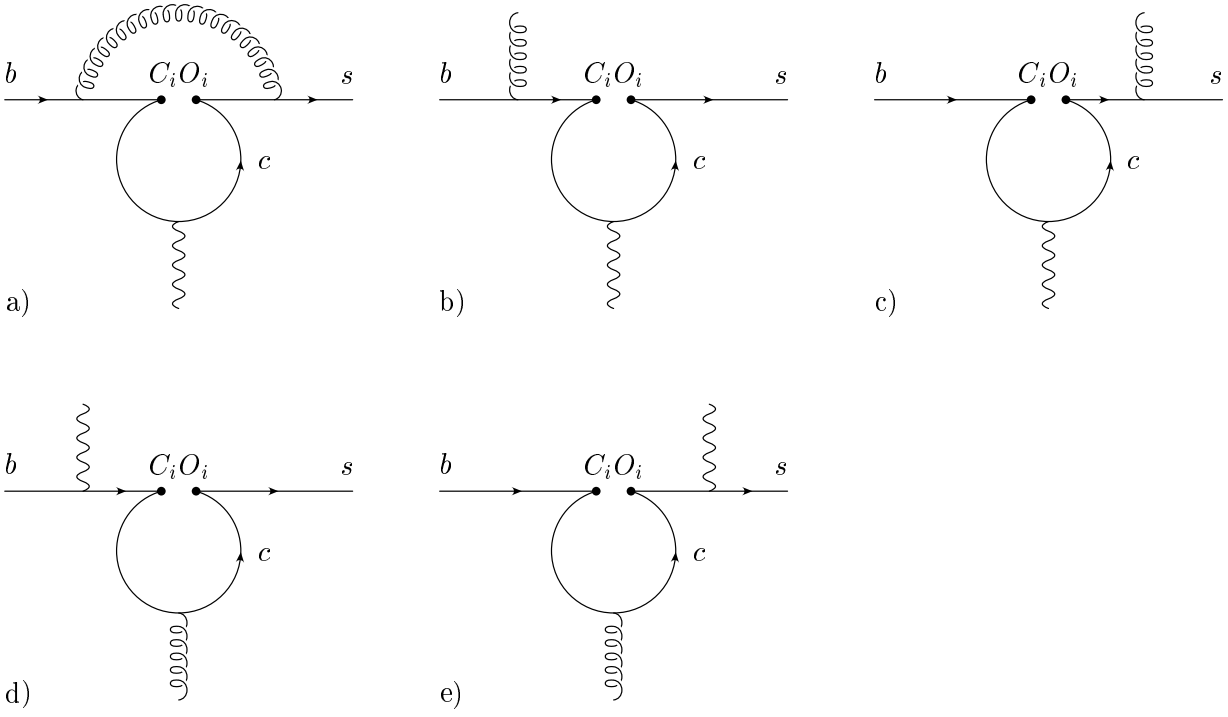

Figure 3.2: Diagrams which are automatically taken into account when calculating corrections to $\widetilde{C}_7^{(0,{\rm mod})}\widetilde{O}_7$, $\widetilde{C}_8^{(0,{\rm mod})}\widetilde{O}_8$ and $\widetilde{C}_9^{(0,{\rm mod})}\widetilde{O}_9$.

$\widetilde{O}_7$, $\widetilde{O}_8$ and $\widetilde{O}_9$. Therefore, they can be absorbed by appropriately modifying the Wilson

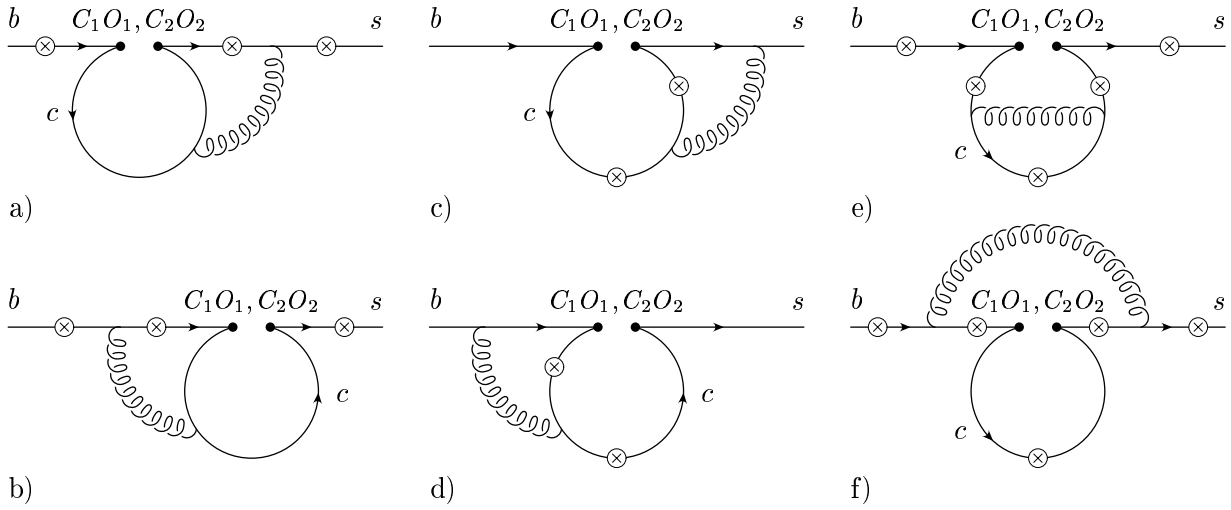

Figure 3.3: The two-loop virtual diagrams induced by O_1 and O_2 that cannot be absorbed into the $\widetilde{O}_{7,8,9}$ contributions by weighing them with the modified Wilson coefficients. The circle-crosses denote the possible locations where the virtual photon is emitted. The curly lines represent gluons.

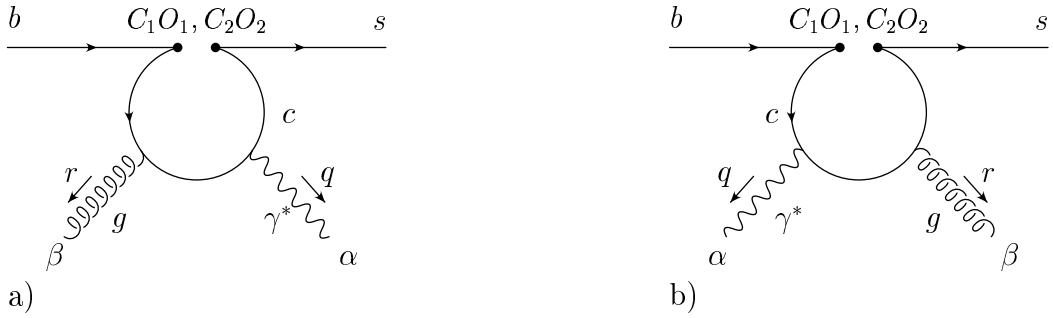

Figure 3.4: The only two bremsstrahlung diagrams induced by O_1 and O_2 that cannot be absorbed into the $\widetilde{O}_{7,8,9}$ contributions by weighing them with the modified Wilson coefficients.

coefficients $\widetilde{C}_7$, $\widetilde{C}_8$ and $\widetilde{C}_9$. The modified coefficients we write as

$$\begin{aligned} \widetilde{C}_7^{\text{mod}} &= A_7, \\ \widetilde{C}_8^{\text{mod}} &= A_8, \\ \widetilde{C}_9^{\text{mod}} &= A_9 + T_9\, h(z,\hat{s}) + U_9\, h(1,\hat{s}) + W_9\, h(0,\hat{s})\,. \end{aligned} \tag{3}$$

The auxiliary quantities A_i, T_9, U_9 and W_9 are linear combinations of the Wilson coefficients $C_i(\mu)$. Their explicit form is relegated to the appendix. The one-loop function $h(z,\hat{s})$ is

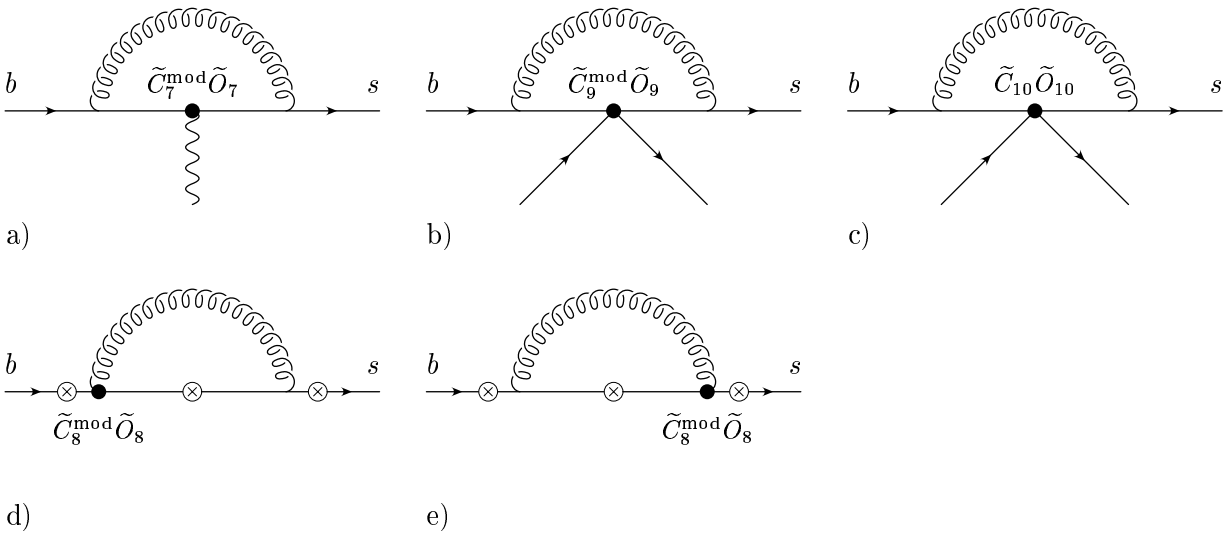

Figure 3.5: One-loop virtual $\mathcal{O}(\alpha_s)$ corrections induced by $\widetilde{C}_7^{(0,\rm mod)}\widetilde{O}_7$, $\widetilde{C}_8^{(0,\rm mod)}\widetilde{O}_8$, $\widetilde{C}_9^{(0,\rm mod)}\widetilde{O}_9$ and $\widetilde{C}_{10}^{(0)}\widetilde{O}_{10}$. The circle-crosses denote the possible locations for emission of a virtual photon.

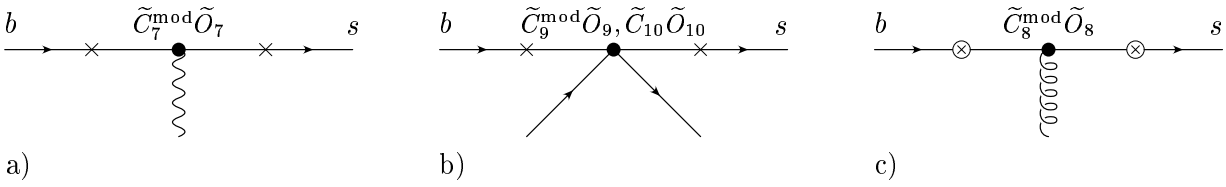

Figure 3.6: The $\mathcal{O}(\alpha_s)$ bremsstrahlung diagrams induced by $\widetilde{O}_7$, $\widetilde{O}_9$, $\widetilde{O}_{10}$ and $\widetilde{O}_8$. Weighing the contributions of $\widetilde{O}_7$, $\widetilde{O}_8$ and $\widetilde{O}_9$ with the corresponding modified Wilson coefficients accounts for the bremsstrahlung diagrams depicted in Fig. 3.2b)–e). The crosses and circle-crosses denote the possible locations for emission of a bremsstrahlung gluon and a virtual photon, respectively.

given by [16]

$$h(z,\hat{s}) = -\frac{4}{9}\ln(z) + \frac{8}{27} + \frac{16}{9}\frac{z}{\hat{s}} - \frac{2}{9}\left(2+\frac{4\,z}{\hat{s}}\right)\sqrt{\left|\frac{4\,z-\hat{s}}{\hat{s}}\right|}\cdot\begin{cases} 2\arctan\sqrt{\frac{\hat{s}}{4\,z-\hat{s}}}\,, & \hat{s} < 4\,z \\ \ln\left(\frac{\sqrt{\hat{s}}+\sqrt{\hat{s}-4\,z}}{\sqrt{\hat{s}}-\sqrt{\hat{s}-4\,z}}\right) - i\,\pi, & \hat{s} > 4\,z \end{cases}. \quad (4)$$

It is obvious that the modification of the Wilson coefficients automatically accounts also for the diagrams in Fig. 3.2 when calculating the corresponding corrections to the matrix

elements

$$\langle s\,\ell^+\ell^-|\widetilde{C}_i^{(0,\mathrm{mod})}\widetilde{O}_i|b\rangle \quad (i=7,8,9),$$

where $\widetilde{C}_i^{(0,\mathrm{mod})}$ are the leading order terms of the modified Wilson coefficients, ie

$$\begin{aligned}
\widetilde{C}_7^{(0,\mathrm{mod})} &= A_7^{(0)},\\
\widetilde{C}_8^{(0,\mathrm{mod})} &= A_8^{(0)},\\
\widetilde{C}_9^{(0,\mathrm{mod})} &= A_9^{(0)} + T_9^{(0)}\,h(z,\hat{s}) + U_9^{(0)}\,h(1,\hat{s}) + W_9^{(0)}\,h(0,\hat{s})\,.
\end{aligned} \tag{5}$$

For the explicit expressions of the quantities $A_i^{(0)}$, $T_9^{(0)}$, $U_9^{(0)}$ and $W_9^{(0)}$ we refer to the appendix.

Notice that the virtual and bremsstrahlung corrections of the four-quark operators with topologies shown in Figs. 3.3 and 3.4, however, have to be calculated explicitly. As the Wilson coefficients C_1 and C_2 are much larger than C_3,...,C_6 we retain the contributions of these topologies only for O_1 and O_2 insertions.

In the previous work [1], we systematically calculated the virtual corrections to the matrix elements of $C_1^{(0)}O_1$, $C_2^{(0)}O_2$, shown in Fig. 3.3, as well as to those of $\widetilde{C}_j^{(0,\mathrm{mod})}\widetilde{O}_j$ $(j=7,...,9)$ and $\widetilde{C}_{10}^{(0)}\widetilde{O}_{10}$ (cf Fig. 3.5). Furthermore, we also took into account the corrections to the Wilson coefficients calculated in Refs. [16, 17].

We found that the matrix elements of the operators $\widetilde{O}_7$, $\widetilde{O}_9$ and $\widetilde{O}_{10}$ [cf Fig. 3.5a)–c)] suffer from infrared and collinear singularities. Consequently, on decay width level the interferences $(\widetilde{O}_j,\widetilde{O}_k)$ $(j,k=7,9,10)$ are singular, too. We therefore included the gluon bremsstrahlung corrections associated with $(\widetilde{O}_j,\widetilde{O}_k)$ $(j,k=7,9,10)$ in order to get an infrared finite result for the decay width [cf Fig. 3.6a) and b)].

Taking into account the virtual and bremsstrahlung contributions discussed so far, we obtain the result presented in Ref. [1]:

$$\begin{aligned}
\frac{d\Gamma(b\to X_s\,\ell^+\ell^-)}{d\hat{s}} &= \left(\frac{\alpha_{em}}{4\,\pi}\right)^2 \frac{G_F^2\,m_{b,\mathrm{pole}}^5\,|V_{ts}^*V_{tb}|^2}{48\,\pi^3}\,(1-\hat{s})^2\\
&\times\left\{(1+2\,\hat{s})\left(\left|\widetilde{C}_9^{\mathrm{eff}}\right|^2+\left|\widetilde{C}_{10}^{\mathrm{eff}}\right|^2\right)+4\,(1+2/\hat{s})\left|\widetilde{C}_7^{\mathrm{eff}}\right|^2+12\cdot\mathrm{Re}\left(\widetilde{C}_7^{\mathrm{eff}}\widetilde{C}_9^{\mathrm{eff}*}\right)\right\},
\end{aligned} \tag{6}$$

where the effective Wilson coefficients $\widetilde{C}_7^{\mathrm{eff}}$, $\widetilde{C}_9^{\mathrm{eff}}$ and $\widetilde{C}_{10}^{\mathrm{eff}}$ are given by [1]

$$\widetilde{C}_7^{\rm eff} = \left(1 + \frac{\alpha_s(\mu)}{\pi}\,\omega_7(\hat{s})\right) A_7 - \frac{\alpha_s(\mu)}{4\,\pi}\left(C_1^{(0)} F_1^{(7)}(\hat{s}) + C_2^{(0)} F_2^{(7)}(\hat{s}) + A_8^{(0)} F_8^{(7)}(\hat{s})\right), \tag{7}$$

$$\widetilde{C}_9^{\rm eff} = \left(1 + \frac{\alpha_s(\mu)}{\pi}\,\omega_9(\hat{s})\right)\left(A_9 + T_9\,h(\hat{m}_c^2,\hat{s}) + U_9\,h(1,\hat{s}) + W_9\,h(0,\hat{s})\right) - \frac{\alpha_s(\mu)}{4\,\pi}\left(C_1^{(0)} F_1^{(9)}(\hat{s}) + C_2^{(0)} F_2^{(9)}(\hat{s}) + A_8^{(0)} F_8^{(9)}(\hat{s})\right), \tag{8}$$

$$\widetilde{C}_{10}^{\rm eff} = \left(1 + \frac{\alpha_s(\mu)}{\pi}\,\omega_9(\hat{s})\right) A_{10}. \tag{9}$$

The quantities $C_1^{(0)}$, $C_2^{(0)}$, A_7, $A_8^{(0)}$, A_9, A_{10}, T_9, U_9 and W_9 are Wilson coefficients or linear combinations thereof. We give their analytical expressions and numerical values in the appendix. The one-loop function $h(\hat{m}_c^2,\hat{s})$ is given in Eq. (4), while the two-loop functions $F_{1,2}^{(7),(9)}$, accounting for the diagrams in Fig. 3.3, and the one-loop functions $F_8^{(7),(9)}$, corresponding to the diagrams 3.5d) and e), are given in Ref. [1]. The functions ω_7 and ω_9, finally, include both virtual and bremsstrahlung corrections associated with $\widetilde{O}_7$, $\widetilde{O}_9$ and $\widetilde{O}_{10}$. For details on their construction we again refer to [1].

When calculating the decay width (6), we retain only terms linear in α_s (and thus in ω_7, ω_9) in the expressions for $|\widetilde{C}_7^{\rm eff}|^2$, $|\widetilde{C}_9^{\rm eff}|^2$ and $|\widetilde{C}_{10}^{\rm eff}|^2$. In the interference term $\mathrm{Re}\left[\widetilde{C}_7^{\rm eff}\widetilde{C}_9^{\rm eff*}\right]$ too, we keep only linear contributions in α_s. By construction one has to make the replacements $\omega_9 \to \omega_{79}$ and $\omega_7 \to \omega_{79}$ in this term.

The functions ω_7, ω_9 and ω_{79} read

$$\omega_7(\hat{s}) = -\frac{8}{3}\ln\left(\frac{\mu}{m_b}\right) - \frac{4}{3}\,\mathrm{Li}(\hat{s}) - \frac{2}{9}\,\pi^2 - \frac{2}{3}\,\ln(\hat{s})\ln(1-\hat{s}) - \frac{1}{3}\,\frac{8+\hat{s}}{2+\hat{s}}\ln(1-\hat{s}) - \frac{2}{3}\,\frac{\hat{s}\,(2-2\,\hat{s}-\hat{s}^2)}{(1-\hat{s})^2\,(2+\hat{s})}\ln(\hat{s}) - \frac{1}{18}\,\frac{16-11\,\hat{s}-17\,\hat{s}^2}{(2+\hat{s})\,(1-\hat{s})}, \tag{10}$$

$$\omega_9(\hat{s}) = -\frac{4}{3}\,\mathrm{Li}(\hat{s}) - \frac{2}{3}\ln(1-\hat{s})\ln(\hat{s}) - \frac{2}{9}\pi^2 - \frac{5+4\,\hat{s}}{3(1+2\,\hat{s})}\ln(1-\hat{s}) - \frac{2\,\hat{s}\,(1+\hat{s})(1-2\,\hat{s})}{3\,(1-\hat{s})^2(1+2\,\hat{s})}\ln(\hat{s}) + \frac{5+9\,\hat{s}-6\,\hat{s}^2}{6\,(1-\hat{s})(1+2\,\hat{s})}, \tag{11}$$

$$\omega_{79}(\hat{s}) = -\frac{4}{3}\ln\left(\frac{\mu}{m_b}\right) - \frac{4}{3}\,\mathrm{Li}(\hat{s}) - \frac{2}{9}\,\pi^2 - \frac{2}{3}\,\ln(\hat{s})\ln(1-\hat{s}) \\ - \frac{1}{9}\,\frac{2+7\,\hat{s}}{\hat{s}}\ln(1-\hat{s}) - \frac{2}{9}\,\frac{\hat{s}\,(3-2\,\hat{s})}{(1-\hat{s})^2}\ln(\hat{s}) + \frac{1}{18}\,\frac{5-9\,\hat{s}}{1-\hat{s}}\,. \quad (12)$$

Summary
The bremsstrahlung corrections associated with the interferences

$$\left(\widetilde{C}_j^{(0,\mathrm{mod})}\widetilde{O}_j, \widetilde{C}_k^{(0,\mathrm{mod})}\widetilde{O}_k\right), \quad (j,k=7,9,10),$$

are already included in formula (6). The remaining bremsstrahlung corrections, which are infrared finite, we derive in Section 4 and 5. In Section 4 we discuss the contributions of the interferences

$$\left(\widetilde{C}_8^{(0,\mathrm{mod})}\widetilde{O}_8, \widetilde{C}_k^{(0,\mathrm{mod})}\widetilde{O}_k\right), \quad (k=7,8,9,10)\,,$$

which we call to be of type A. There is no contribution from $k=10$ because of the Dirac structures of the involved operators. Section 5 is devoted to the interferences

$$\left(C_i^{(0)}O_i, C_j^{(0)}O_j\right), \quad (i,j=1,2) \quad \text{and} \quad \left(C_i^{(0)}O_i, \widetilde{C}_k^{(0,\mathrm{mod})}\widetilde{O}_k\right), \quad (i=1,2;\ k=7,8,9,10).$$

Accordingly, we call these the type B terms. Again, the contributions for $k=10$ vanish due to the Dirac structures of the operators involved.

4 Finite Bremsstrahlung Contributions of Type A

The bremsstrahlung contributions taken into account by introducing the functions $\omega_i(\hat{s})$ cancel the infrared divergences associated with the virtual corrections. All other bremsstrahlung terms are finite. This allows us to perform their calculation directly in $d=4$ dimensions.

The bremsstrahlung contributions from $\widetilde{O}_7-\widetilde{O}_8$ and $\widetilde{O}_8-\widetilde{O}_9$ interference terms as well as the $\widetilde{O}_8-\widetilde{O}_8$ term oppose no difficulties. The sum of these three parts can be written as

$$\frac{d\Gamma^{\mathrm{Brems,A}}}{d\hat{s}} = \frac{d\Gamma_{78}^{\mathrm{Brems}}}{d\hat{s}} + \frac{d\Gamma_{89}^{\mathrm{Brems}}}{d\hat{s}} + \frac{d\Gamma_{88}^{\mathrm{Brems}}}{d\hat{s}} = \\ \left(\frac{\alpha_{em}}{4\,\pi}\right)^2\left(\frac{\alpha_s}{4\,\pi}\right)\frac{m_{b,\mathrm{pole}}^5\,|V_{ts}^*\,V_{tb}|^2\,G_F^2}{48\,\pi^3} \times \Big(2\,\mathrm{Re}\big[c_{78}\,\tau_{78}+c_{89}\,\tau_{89}\big]+c_{88}\,\tau_{88}\Big). \quad (13)$$

The coefficients c_{ij} are given by

$$c_{78} = C_F\cdot\widetilde{C}_7^{(0,\mathrm{eff})}\widetilde{C}_8^{(0,\mathrm{eff})*}, \quad c_{89} = C_F\cdot\widetilde{C}_8^{(0,\mathrm{eff})}\widetilde{C}_9^{(0,\mathrm{eff})*}, \quad c_{88} = C_F\cdot\left|\widetilde{C}_8^{(0,\mathrm{eff})}\right|^2, \quad (14)$$

while the quantities τ_{ij} read

$$\begin{aligned}\tau_{78} = \frac{8}{9\,\hat{s}}\Bigg\{ & 25 - 2\,\pi^2 - 27\,\hat{s} + 3\,\hat{s}^2 - \hat{s}^3 + 12\left(\hat{s} + \hat{s}^2\right)\,\ln(\hat{s}) \\ & + 6\left(\frac{\pi}{2} - \arctan\left[\frac{2 - 4\,\hat{s} + \hat{s}^2}{(2-\hat{s})\sqrt{\hat{s}}\,\sqrt{4-\hat{s}}}\right]\right)^2 - 24\,\mathrm{Re}\left(\mathrm{Li}\left[\frac{\hat{s} - i\sqrt{\hat{s}}\,\sqrt{4-\hat{s}}}{2}\right]\right) \\ & - 12\left((1-\hat{s})\sqrt{\hat{s}}\,\sqrt{4-\hat{s}} - 2\arctan\left[\frac{\sqrt{\hat{s}}\,\sqrt{4-\hat{s}}}{2-\hat{s}}\right]\right) \\ & \times\left(\arctan\left[\sqrt{\frac{4-\hat{s}}{\hat{s}}}\right] - \arctan\left[\frac{\sqrt{\hat{s}}\,\sqrt{4-\hat{s}}}{2-\hat{s}}\right]\right)\Bigg\}, \quad (15)\end{aligned}$$

$$\begin{aligned}\tau_{88} = \frac{4}{27\,\hat{s}}\Bigg\{ & -8\,\pi^2 + (1-\hat{s})\left(77 - \hat{s} - 4\,\hat{s}^2\right) - 24\,\mathrm{Li}(1-\hat{s}) \\ & + 3\left(10 - 4\,\hat{s} - 9\,\hat{s}^2 + 8\ln\left[\frac{\sqrt{\hat{s}}}{1-\hat{s}}\right]\right)\ln(\hat{s}) + 48\,\mathrm{Re}\left(\mathrm{Li}\left[\frac{3-\hat{s}}{2} + i\,\frac{(1-\hat{s})\sqrt{4-\hat{s}}}{2\sqrt{\hat{s}}}\right]\right) \\ & - 6\left(\frac{20\,\hat{s} + 10\,\hat{s}^2 - 3\,\hat{s}^3}{\sqrt{\hat{s}}\,\sqrt{4-\hat{s}}} - 8\,\pi + 8\arctan\left[\sqrt{\frac{4-\hat{s}}{\hat{s}}}\right]\right) \\ & \times\left(\arctan\left[\sqrt{\frac{4-\hat{s}}{\hat{s}}}\right] - \arctan\left[\frac{\sqrt{\hat{s}}\,\sqrt{4-\hat{s}}}{2-\hat{s}}\right]\right)\Bigg\}, \quad (16)\end{aligned}$$

$$\begin{aligned}\tau_{89} = \frac{2}{3}\Bigg\{ & \hat{s}\,(4-\hat{s}) - 3 - 4\,\ln(\hat{s})\left(1 - \hat{s} - \hat{s}^2\right) \\ & - 8\,\mathrm{Re}\left(\mathrm{Li}\left[\frac{\hat{s}}{2} + i\,\frac{\sqrt{\hat{s}}\,\sqrt{4-\hat{s}}}{2}\right] - \mathrm{Li}\left[\frac{-2 + \hat{s}(4-\hat{s})}{2} + i\,\frac{(2-\hat{s})\sqrt{\hat{s}}\,\sqrt{4-\hat{s}}}{2}\right]\right) \\ & + 4\left(\hat{s}^2\sqrt{\frac{4-\hat{s}}{\hat{s}}} + 2\,\arctan\left[\frac{\sqrt{\hat{s}}\,\sqrt{4-\hat{s}}}{2-\hat{s}}\right]\right) \\ & \times\left(\arctan\left[\sqrt{\frac{4-\hat{s}}{\hat{s}}}\right] - \arctan\left[\frac{\sqrt{\hat{s}}\,\sqrt{4-\hat{s}}}{2-\hat{s}}\right]\right)\Bigg\}. \quad (17)\end{aligned}$$

5 Finite Bremsstrahlung Contributions of Type B

In this section we consider the bremsstrahlung contributions from O_1 and O_2 and interference terms with $\widetilde{O}_7$, $\widetilde{O}_8$, $\widetilde{O}_9$ and $\widetilde{O}_{10}$. As mentioned before, interferences with $\widetilde{O}_{10}$ vanish due to the Dirac structures of the operators.

The bremsstrahlung contributions discussed in this section all involve the matrix elements associated with the two diagrams depicted in Fig. 3.4. Their sum, $\bar{J}_{\alpha\beta}$, is given by

$$\bar{J}_{\alpha\beta} = \frac{e\, g_s\, Q_u}{16\,\pi^2}\left[E(\alpha,\beta,r)\,\bar{\Delta}i_5 + E(\alpha,\beta,q)\,\bar{\Delta}i_6 - E(\beta,r,q)\frac{r_\alpha}{q\cdot r}\,\bar{\Delta}i_{23} - E(\alpha,r,q)\frac{q_\beta}{q\cdot r}\,\bar{\Delta}i_{26} - E(\beta,r,q)\frac{q_\alpha}{q\cdot r}\,\bar{\Delta}i_{27}\right] L\,\frac{\lambda}{2}\,, \quad (18)$$

where q and r denote the momenta of the virtual photon and of the gluon, respectively. The index α will be contracted with the photon propagator, whereas β is contracted with the polarization vector $\epsilon^\beta(r)$ of the gluon. $\bar{J}_{\alpha\beta}$ and $\bar{\Delta}i_k$ are obtained from $J_{\alpha\beta}$ and Δi_k [1], respectively, by setting $r^2 = 0$ and dropping terms proportional to r_β. The matrix $E(\alpha,\beta,r)$ is defined as

$$E(\alpha,\beta,r) = \frac{1}{2}(\gamma_\alpha\gamma_\beta\not{r} - \not{r}\gamma_\beta\gamma_\alpha). \quad (19)$$

Due to Ward identities, the quantities $\bar{\Delta}i_k$ are not independent of one another. Namely,

$$q^\alpha \bar{J}_{\alpha\beta} = 0 \quad \text{and} \quad r^\beta \bar{J}_{\alpha\beta} = 0$$

imply that $\bar{\Delta}i_5$ and $\bar{\Delta}i_6$ can be expressed as

$$\bar{\Delta}i_5 = \bar{\Delta}i_{23} + \frac{q^2}{q\cdot r}\bar{\Delta}i_{27}\,, \quad \bar{\Delta}i_6 = \bar{\Delta}i_{26}\,. \quad (20)$$

As in addition $\bar{\Delta}i_{26} = -\bar{\Delta}i_{23}$, the bremsstrahlung matrix elements depend on $\bar{\Delta}i_{23}$ and $\bar{\Delta}i_{27}$, only. In $d = 4$ dimensions we find

$$\begin{aligned}\bar{\Delta}i_{23} &= 8\,(q\cdot r)\int_0^1 dx\,dy\,\frac{x\,y(1-y)^2}{C}\,,\\ \bar{\Delta}i_{27} &= 8\,(q\cdot r)\int_0^1 dx\,dy\,\frac{y\,(1-y)^2}{C}\,,\end{aligned} \quad (21)$$

where

$$C = m_c^2 - 2\,x\,y(1-y)(q\cdot r) - q^2\,y\,(1-y) - i\,\delta.$$

In the rest frame of the b quark and for fixed $\hat{s} = q^2/m_b^2$, the phase space integrals which one encounters in the calculation of $d\Gamma^{\rm Brems,B}/d\hat{s}$ can be reduced to a two-dimensional integral over $\hat{E}_r = E_r/m_b$ and $\hat{E}_s = E_s/m_b$, where E_r and E_s are the energy of the gluon

and the s quark, respectively. In the following it is useful to introduce the integration variable $w = 1 - 2\hat{E}_s$ instead of $\hat{E}_s$. The integration limits are then given by

$$\hat{E}_r \in \left[\frac{w-\hat{s}}{2}, \frac{w-\hat{s}}{2\,w}\right] \quad \text{and} \quad w \in [\hat{s}, 1].$$

For fixed values of $\hat{s}$, the quantities $\bar{\Delta}i_{23}$ and $\bar{\Delta}i_{27}$ depend only on the scalar product $q{\cdot}r$, which, in the rest frame of the b quark, is given by $(w-\hat{s})\,m_b^2/2$. The integration over $\hat{E}_r$ turns out to be of rational kind and can be performed analytically. The remaining integration over w, however, is more complicated and is done numerically. The result can be written as

$$\frac{d\Gamma^{\text{Brems,B}}}{d\hat{s}} = \left(\frac{\alpha_{\text{em}}}{4\,\pi}\right)^2 \left(\frac{\alpha_s}{4\,\pi}\right) \frac{G_F^2\, m_{b,\text{pole}}^5\, |V_{ts}^*\, V_{tb}|^2}{48\,\pi^3} \times$$
$$\int_{\hat{s}}^{1} dw \left[(c_{11}+c_{12}+c_{22})\,\tau_{22} + 2\,\text{Re}\big[\,(c_{17}+c_{27})\,\tau_{27} + (c_{18}+c_{28})\,\tau_{28} + (c_{19}+c_{29})\,\tau_{29}\big]\right]. \quad (22)$$

The quantities τ_{ij}, expressed in terms of $\bar{\Delta}i_{23}$ and $\bar{\Delta}i_{27}$, read

$$\tau_{22} = \frac{8}{27}\frac{(w-\hat{s})(1-w)^2}{\hat{s}\,w^3} \times \Big\{\Big[3\,w^2 + 2\,\hat{s}^2(2+w) - \hat{s}\,w\,(5-2\,w)\Big]\,\big|\bar{\Delta}i_{23}\big|^2 +$$
$$\Big[2\,\hat{s}^2\,(2+\,w) + \hat{s}\,w\,(1+2\,w)\Big]\,\big|\bar{\Delta}i_{27}\big|^2 + 4\,\hat{s}\Big[w\,(1-w) - \hat{s}\,(2+w)\Big]\cdot \text{Re}\left[\bar{\Delta}i_{23}\bar{\Delta}i_{27}^*\right]\Big\}, \quad (23)$$

$$\tau_{27} = \frac{8}{3}\frac{1}{\hat{s}\,w} \times \Big\{\Big[(1-w)\left(4\,\hat{s}^2 - \hat{s}\,w + w^2\right) + \hat{s}\,w\,(4+\hat{s}-w)\ln(w)\Big]\bar{\Delta}i_{23}$$
$$- \Big[4\,\hat{s}^2\,(1-w) + \hat{s}\,w\,(4+\hat{s}-w)\,\ln(w)\Big]\bar{\Delta}i_{27}\Big\}, \quad (24)$$

$$\tau_{28} = \frac{8}{9}\frac{1}{\hat{s}\,w\,(w-\hat{s})} \times \Big\{\Big[(w-s)^2(2\,\hat{s}-w)(1-w)\Big]\bar{\Delta}i_{23} - \Big[2\,\hat{s}\,(w-\hat{s})^2(1-w)\Big]\bar{\Delta}i_{27}$$
$$+ \hat{s}\,w\Big[(1+2\,\hat{s}-2\,w)\bar{\Delta}i_{23} - 2\,(1+\hat{s}-w)\bar{\Delta}i_{27}\Big]\cdot\ln\left[\frac{\hat{s}}{(1+\hat{s}-w)(w^2+\hat{s}\,(1-w))}\right]\Big\}, \quad (25)$$

$$\tau_{29} = \frac{4}{3}\frac{1}{w} \times \Big\{\Big[2\,\hat{s}(1-w)(\hat{s}+w) + 4\,\hat{s}\,w\ln(w)\Big]\bar{\Delta}i_{23} -$$
$$\Big[2\,\hat{s}(1-w)(\hat{s}+w) + w(3\,\hat{s}+w)\ln(w)\Big]\bar{\Delta}i_{27}\Big\}. \quad (26)$$

The coefficients c_{ij} in Eq. (22) include the dependence on the Wilson coefficients and the color factors. Explicitly, they read

$$\begin{aligned}
c_{11} &= C_{\tau_1} \cdot \left|C_1^{(0)}\right|^2, & c_{17} &= C_{\tau_2} \cdot C_1^{(0)} \widetilde{C}_7^{(0,\text{eff})*}, & c_{27} &= C_F \cdot C_2^{(0)} \widetilde{C}_7^{(0,\text{eff})*}, \\
c_{12} &= C_{\tau_2} \cdot 2\,\text{Re}\Big[C_1^{(0)} C_2^{(0)*}\Big], & c_{18} &= C_{\tau_2} \cdot C_1^{(0)} \widetilde{C}_8^{(0,\text{eff})*}, & c_{28} &= C_F \cdot C_2^{(0)} \widetilde{C}_8^{(0,\text{eff})*}, \\
c_{22} &= C_F \cdot \left|C_2^{(0)}\right|^2, & c_{19} &= C_{\tau_2} \cdot C_1^{(0)} \widetilde{C}_9^{(0,\text{eff})*}, & c_{29} &= C_F \cdot C_2^{(0)} \widetilde{C}_9^{(0,\text{eff})*},
\end{aligned} \tag{27}$$

where the color factors C_F, C_{τ_1} and C_{τ_2} arise from the following color structures:

$$\sum_a T^a T^a = C_F \mathbf{1}, \quad C_F = \frac{N_c^2 - 1}{2\,N_c},$$

$$\sum_{a,b,c} T^a T^c T^a T^b T^c T^b = C_{\tau_1} \mathbf{1}, \quad C_{\tau_1} = \frac{N_c^2 - 1}{8\,N_c^3},$$

and

$$\sum_{a,b} T^a T^b T^a T^b = C_{\tau_2} \mathbf{1}, \quad C_{\tau_2} = -\frac{N_c^2 - 1}{4\,N_c^2}.$$

Finally, we list the explicit formulas for $\bar{\Delta} i_{23}$ and $\bar{\Delta} i_{27}$ expressed as a function of $\hat{s}$ and the integration variable w. We obtain

$$\bar{\Delta} i_{23} = -2 + \frac{4}{w - \hat{s}} \left[z\, G_{-1}\Big(\frac{\hat{s}}{z}\Big) - z\, G_{-1}\Big(\frac{w}{z}\Big) - \frac{\hat{s}}{2}\, G_0\Big(\frac{\hat{s}}{z}\Big) + \frac{\hat{s}}{2}\, G_0\Big(\frac{w}{z}\Big) \right], \tag{28}$$

$$\bar{\Delta} i_{27} = 2 \left[G_0\Big(\frac{\hat{s}}{z}\Big) - G_0\Big(\frac{w}{z}\Big) \right], \tag{29}$$

where the functions $G_k(t)$ $(k \geq -1)$ are defined through the integral

$$G_k(t) = \int_0^1 dx\, x^k\, \ln\big[1 - t\,x(1-x) - i\,\delta\big], \quad G_1(t) = \frac{1}{2} G_0(t).$$

Explicitly, the functions $G_{-1}(t)$ and $G_0(t)$ read

$$G_{-1}(t) = \begin{cases} 2\,\pi\, \arctan\Big(\sqrt{\frac{4-t}{t}}\Big) - \frac{\pi^2}{2} - 2\, \arctan^2\Big(\sqrt{\frac{4-t}{t}}\Big), & t < 4 \\ -2\,i\pi\, \ln\Big(\frac{\sqrt{t}+\sqrt{t-4}}{2}\Big) - \frac{\pi^2}{2} + 2\, \ln^2\Big(\frac{\sqrt{t}+\sqrt{t-4}}{2}\Big), & t > 4 \end{cases}, \tag{30}$$

$$G_0(t) = \begin{cases} \pi \sqrt{\frac{4-t}{t}} - 2 - 2 \sqrt{\frac{4-t}{t}}\, \arctan\Big(\sqrt{\frac{4-t}{t}}\Big), & t < 4 \\ -i\pi \sqrt{\frac{t-4}{t}} - 2 + 2 \sqrt{\frac{t-4}{t}}\, \ln\Big(\frac{\sqrt{t}+\sqrt{t-4}}{2}\Big), & t > 4 \end{cases}. \tag{31}$$

6 Numerical Results

First, we investigate the numerical impact of the finite bremsstrahlung corrections [see Eqs. (13) and (22)] on the dilepton invariant mass spectrum. Following common practice, we consider the ratio

$$R_{\rm quark}(\hat{s}) = \frac{1}{\Gamma(b \to X_c\, e\, \bar{\nu}_e)} \frac{d\Gamma(b \to s\,\ell^+\ell^-)}{d\hat{s}}\,, \tag{32}$$

in which the factor $m_{b,\rm pole}^5$ drops out. The explicit expression for the semileptonic decay width $\Gamma(b \to X_c\, e\, \bar{\nu}_e)$ reads

$$\Gamma(b \to X_c\, e\, \bar{\nu}_e) = \frac{G_F^2\, m_{b,\rm pole}^5}{192\,\pi^3}\, |V_{cb}|^2 \cdot g\left(\frac{m_{c,\rm pole}^2}{m_{b,\rm pole}^2}\right) \cdot K\left(\frac{m_c^2}{m_b^2}\right)\,, \tag{33}$$

where $g(z) = 1 - 8\,z + 8\,z^3 - z^4 - 12\,z^2\,\ln(z)$ is the phase space factor, and

$$K(z) = 1 - \frac{2\,\alpha_s(m_b)}{3\,\pi}\,\frac{f(z)}{g(z)} \tag{34}$$

incorporates the next-to-leading QCD correction to the semi-leptonic decay [18]. The function $f(z)$ has been calculated analytically in Ref. [19]. It reads

$$\begin{aligned} f(z) = &-(1-z^2)\left(\frac{25}{4} - \frac{239}{3}\,z + \frac{25}{4}\,z^2\right) + z\,\ln(z)\left(20 + 90\,z - \frac{4}{3}\,z^2 + \frac{17}{3}\,z^3\right) \\ &+ z^2\,\ln^2(z)\,\left(36 + z^2\right) + \left(1 - z^2\right)\left(\frac{17}{3} - \frac{64}{3}\,z + \frac{17}{3}\,z^2\right)\ln(1-z) \\ &- 4\,\left(1 + 30\,z^2 + z^4\right)\ln(z)\ln(1-z) - \left(1 + 16\,z^2 + z^4\right)\left(6\,{\rm Li}(z) - \pi^2\right) \\ &- 32\,z^{3/2}(1+z)\left[\pi^2 - 4\,{\rm Li}(\sqrt{z}) + 4\,{\rm Li}(-\sqrt{z}) - 2\ln(z)\,\ln\left(\frac{1-\sqrt{z}}{1+\sqrt{z}}\right)\right]. \end{aligned} \tag{35}$$

We stress that the function $f(z)$ refers to on-shell renormalization of the charm quark mass.

In Fig. 6.1 we consider the contribution $\Delta R_{\rm quark}(\hat{s})$, which is due to the finite bremsstrahlung corrections in Eqs. (13) and (22), for three values of the renormalization scale ($\mu = 2.5$, 5 and 10 GeV) and for fixed value $m_c/m_b = 0.29$. The values of all the other input parameters are as in Ref. [1]. In Fig. 6.2 we combine the new corrections with the previous results. The solid lines show the ratio $R_{\rm quark}(\hat{s})$, including the new corrections, for the values $\mu = 10$ GeV (uppermost curve), $\mu = 5$ GeV (middle curve) and $\mu = 2.5$ GeV (lowest curve) and for fixed value $m_c/m_b = 0.29$. The dashed lines represent the corresponding results without the new corrections. We find that for $\hat{s} = 0.05$ the new corrections increase the ratio $R_{\rm quark}(\hat{s})$ by $\sim 3\%$, while for larger values of $\hat{s}$ their impact is even smaller. When

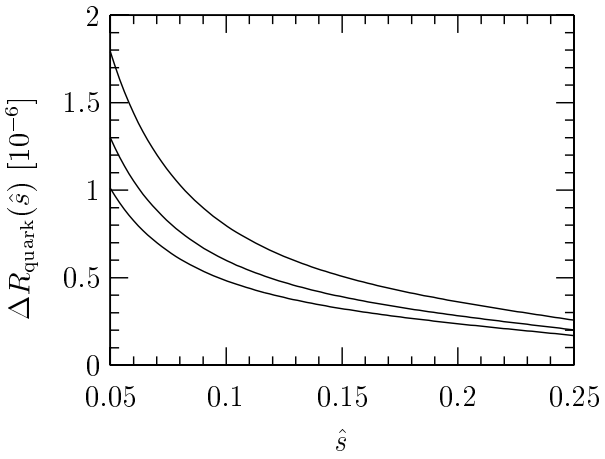

Figure 6.1: The new contribution $\Delta R_{\rm quark}(\hat{s})$ due to finite bremsstrahlung corrections for $\mu = 2.5$ GeV (uppermost curve), $\mu = 5$ GeV (middle curve) and $\mu = 10$ GeV (lowest curve) and $m_c/m_b = 0.29$.

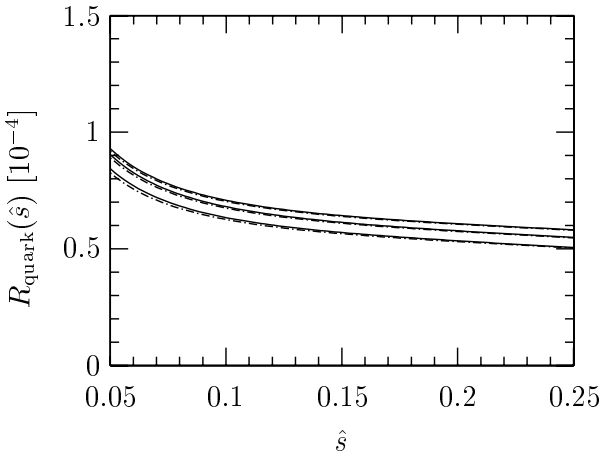

Figure 6.2: The solid curves show the ratio $R_{\rm quark}(\hat{s})$ including the finite bremsstrahlung corrections while the dash-dotted curves show the corresponding results without the new corrections. The uppermost curves (solid and dash-dotted) correspond to $\mu = 10$ GeV, the middle curves to $\mu = 5$ GeV and the lowest curves to $\mu = 2.5$ GeV. $m_c/m_b = 0.29$.

including the finite bremsstrahlung corrections we obtain

$$R_{\rm quark} = \int_{0.05}^{0.25} d\hat{s}\, R_{\rm quark}(\hat{s}) = \big(1.27 \pm 0.08(\mu)\big) \times 10^{-5}$$

for the integrated quantity $R_{\rm quark}$. The error is obtained by varying μ between 2.5 GeV and 10 GeV. For comparison, the corresponding result without the finite bremsstrahlung correction is $R_{\rm quark}(\hat{s}) = \big(1.25 \pm 0.08(\mu)\big) \times 10^{-5}$ [1].

Among the errors on $R_{\rm quark}(\hat{s})$ due to uncertainties in the input parameters, the one related to the charm quark mass is by far the largest. We therefore only comment on this error. In principle, the uncertainties induced by the charm quark mass have two sources. First, it is unclear whether m_c in the virtual- and bremsstrahlung corrections should be interpreted as the pole mass or the $\overline{\rm MS}$ mass (at an appropriate scale). Secondly, the question arises what the numerical value of m_c is, once a choice concerning the definition of m_c has been made.

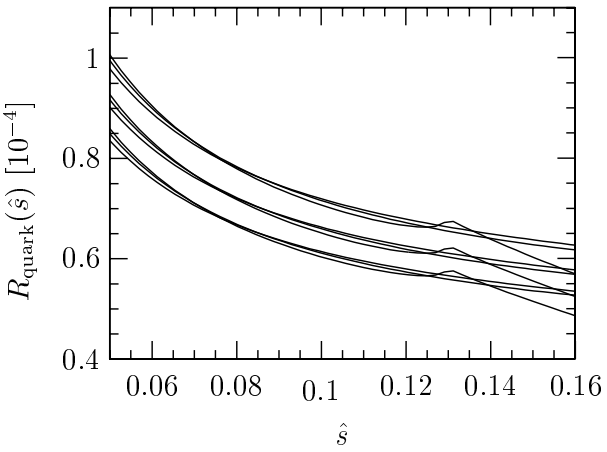

Figure 6.3: $R_{\rm quark}(\hat{s})$ for various values and definitions of m_c: The three bands are obtained by setting $m_c^{\rm pole}/m_b^{\rm pole}$=0.31 (uppermost), 0.29 (middle) and 0.27 (lowest) in $\Gamma(b \to X_c\, e\, \bar\nu_e)$. In the rare decay $b \to X_s\,\ell^+\ell^-$ we set $m_c^{\overline{\rm MS}}/m_b^{\rm pole} = 0.18, 0.22, 0.26$. This leads to three curves all within a narrow band. See text.

To illustrate these problems more clearly, it is useful to first consider the process $B \to X_s\gamma$. There, the one-loop matrix elements of O_1 and O_2 vanish, implying that the charm quark mass dependence only enters at $\mathcal{O}(\alpha_s)$. Formally, one can interpret m_c in these $\mathcal{O}(\alpha_s)$ expressions to be the pole mass or the $\overline{\rm MS}$ mass because the difference is of higher order in α_s. Nevertheless, it has been argued in the literature [20] that the choice $m_c^{\overline{\rm MS}}(\mu)$ with $\mu \in [m_c, m_b]$ seems more reasonable than $m_c^{\rm pole}$ (which was used in all the previous analysis) due to the fact that the largest charm quark mass dependence comes from the real part of the two-loop matrix elements of O_1 and O_2, where the charm quarks are usually off-shell, with a momentum scale set by $m_b^{\rm pole}$ (or some seizable fraction of it). It was shown in Ref. [20] that the definition of the charm quark mass leads to a relatively large uncertainty in the branching ratio: Changing m_c/m_b in $\Gamma(B \to X_s\gamma)$ from 0.29 ± 0.02 to 0.22 ± 0.04, ie from $m_c^{\rm pole}/m_b^{\rm pole}$ to $m_c^{\overline{\rm MS}}/m_b^{\rm pole}$ (with $\mu \in [m_c, m_b]$), causes an enhancement of ${\rm BR}(B \to X_s\gamma)$ by $\sim 11\%$.

In the process $B \to X_s\,\ell^+\ell^-$ this problem is less severe because m_c enters already the one-loop diagrams [ie at $\mathcal{O}(\alpha_s^0)$] associated with O_1 and O_2. As the two-loop calculation requires the renormalization of m_c, the definition of m_c has to be specified. Therefore, the two-loop result explicitly depends on the definition of the charm quark mass. This can be seen from [1]. For the pole mass definition, the results for the two-loop matrix elements of O_1 and O_2, encoded in $F_{1,2}^{(7),(9)}$, are given in Eqs. (54)–(56), while those corresponding to the $\overline{\rm MS}$ definition are obtained by adding the terms $\Delta F_{1,2,m_c{\rm ren}}^{{\rm ct}(9)}$ given in Eq. (49).

In the following, we investigate the impact of pole- vs $\overline{\rm MS}$ definition of m_c in the rare decay $b \to X_s\,\ell^+\ell^-$ on the ratio $R_{\rm quark}(\hat{s})$. In the semileptonic decay $b \to X_c\, e\, \bar\nu_e$ the charm quark is basically on-shell. Therefore, we always use the pole mass definition for the charm quark mass in $\Gamma(b \to X_c\, e\, \bar\nu_e)$, which enters $R_{\rm quark}(\hat{s})$. In Fig. 6.3 we set $m_c^{\rm pole}/m_b^{\rm pole}$ equal to 0.31, 0.29 and 0.27 in the decay width $\Gamma(b \to X_c\, e\, \bar\nu_e)$. In the rare decay $b \to X_s\,\ell^+\ell^-$, on the other hand, we use the $\overline{\rm MS}$ definition for m_c, and put $m_c^{\overline{\rm MS}}/m_b^{\rm pole} = 0.18, 0.22$ and 0.26 (independently of $m_c^{\rm pole}/m_b^{\rm pole}$, to be on the conservative side). This leads, for a given value of $m_c^{\rm pole}/m_b^{\rm pole}$, to three curves which form a narrow band. The uppermost band

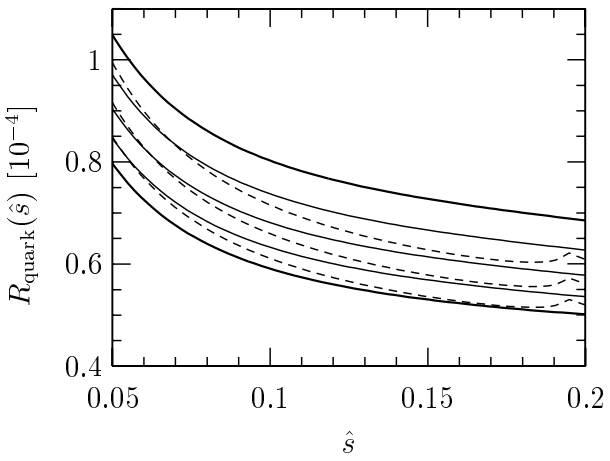

Figure 6.4: $R_{\rm quark}(\hat{s})$ for various values and definitions of m_c: The solid curves are obtained by setting $m_c^{\rm pole}/m_b^{\rm pole} = 0.33$ (uppermost), 0.31, 0.29, 0.27 and 0.25 (lowest) in the rare- and the semileptonic decay. The dashed lines are obtained by taking $m_c^{\overline{\rm MS}}/m_b^{\rm pole} = 0.22$ in the rare decay and $m_c^{\rm pole}/m_b^{\rm pole} = 0.31$, 0.29 and 0.27 in $\Gamma(b \to X_c\, e\, \bar{\nu}_e)$. See text.

corresponds to $m_c^{\rm pole}/m_b^{\rm pole} = 0.31$, the middle to 0.29 and the lowest to 0.27. The curves with the strange behavior for $\hat{s} > 0.13$ all belong to the lowest value $m_c^{\overline{\rm MS}}/m_b^{\rm pole} = 0.18$. As the result for the two-loop corrections was derived in expanded form, which only holds for $\hat{s} < 4\, m_c^2/m_b^2$, the strange behavior illustrates that, for $m_c/m_b = 0.18$, the result is not valid for $\hat{s} > 0.13$. In Fig. 6.4 the three middle solid curves are obtained by adopting the pole mass definition of m_c, both in the rare and in the semileptonic decay. They correspond to $m_c^{\rm pole}/m_b^{\rm pole} = 0.31$, 0.29, 0.27. The dashed curves, on the other hand, are obtained when the $\overline{\rm MS}$ definition with $m_c^{\overline{\rm MS}}/m_b^{\rm pole} = 0.22$ is used in the rare decay width. One finds that for $\hat{s} > 0.06$ the results for $R_{\rm quark}(\hat{s})$ are somewhat larger when using the pole mass definition of m_c in the rare decay. For values below $\hat{s} < 0.06$ the situation is reversed and thus the same as for $b \to X_s\gamma$ [20]. Again, the strange behavior of the dashed curves indicates that, for $m_c/m_b = 0.22$, the expanded formulas become unreliable for values of $\hat{s} > 0.19$. The thick solid lines are obtained by adopting the pole mass definition on the whole and correspond to $m_c/m_b = 0.33$ (upper) and 0.25 (lower). In summary, the figure shows that the quark mass uncertainties can effectively be estimated by working with the pole mass definition throughout, provided one takes the rather conservative range $0.25 \le m_c^{\rm pole}/m_b^{\rm pole} \le 0.33$. Finally, in Fig. 6.5 we show $R_{\rm quark}(\hat{s})$ in the full range $\hat{s} \in [0.05, 0.25]$ for $m_c^{\rm pole}/m_b^{\rm pole} \in [0.25, 0.33]$. Note that for these values of m_c/m_b the expanded formulas hold just up to $\hat{s} = 0.25$.

Comparing Fig. 6.2 with Fig. 6.5, we find that the uncertainty due to m_c/m_b is clearly larger than the leftover μ dependence. Varying m_c/m_b between 0.25 and 0.33, the corresponding uncertainty amounts to $\pm 15\%$.

To conclude: We have calculated the finite gluon bremsstrahlung corrections of $\mathcal{O}(\alpha_s)$ to $\Gamma(b \to s\,\ell^+\ell^-)$, taking into account the contributions of the operators O_1, O_2, O_7, O_8, O_9 and O_{10}. We have worked out the numerical impact of the new corrections on the invariant mass spectrum of the lepton pair in the range $\hat{s} \in [0.05, 0.25]$ and found an increase of about 3% for $\hat{s} = 0.05$ and even less for larger values of $\hat{s}$. Furthermore, we investigated the uncertainties of $R_{\rm quark}(\hat{s})$ due to the definition and numerical uncertainties of the

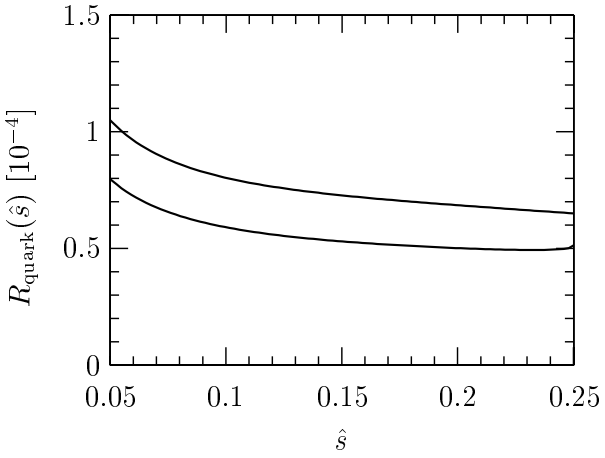

Figure 6.5: $R_{\rm quark}(\hat{s})$ for $m_c^{\rm pole}/m_b^{\rm pole}$=0.33 (uppermost), 0.31, 0.29, 0.27 and 0.25 (lowest) in the rare- and the semileptonic decay in the full range $\hat{s} \in [0.05, 0.25]$.

charm quark mass. We found that these errors can be reliably estimated when working with the pole mass definition of m_c, provided one takes the rather conservative range $0.25 \leq m_c^{\rm pole}/m_b^{\rm pole} \leq 0.33$.

Acknowledgements:
The work of H.M.A. was partially supported by NATO Grant PST.CLG.978154.

A Auxiliary Quantities A_i, T_9, U_9 and W_9

The auxiliary quantities A_i, T_9, U_9 and W_9, appearing in the modified Wilson coefficients in Eq. (3) and in the effective Wilson coefficients in Eqs. (7)–(9) are the following linear combinations of the Wilson coefficients $C_i(\mu)$ [12, 16]:

$$\begin{aligned}
A_7 &= \frac{4\,\pi}{\alpha_s(\mu)}\,C_7(\mu) - \frac{1}{3}\,C_3(\mu) - \frac{4}{9}\,C_4(\mu) - \frac{20}{3}\,C_5(\mu) - \frac{80}{9}\,C_6(\mu)\,,\\
A_8 &= \frac{4\,\pi}{\alpha_s(\mu)}\,C_8(\mu) + C_3(\mu) - \frac{1}{6}\,C_4(\mu) + 20\,C_5(\mu) - \frac{10}{3}\,C_6(\mu)\,,\\
A_9 &= \frac{4\pi}{\alpha_s(\mu)}\,C_9(\mu) + \sum_{i=1}^{6} C_i(\mu)\,\gamma_{i9}^{(0)}\,\ln\!\left(\frac{m_b}{\mu}\right) + \frac{4}{3}\,C_3(\mu) + \frac{64}{9}\,C_5(\mu) + \frac{64}{27}\,C_6(\mu)\,,\\
A_{10} &= \frac{4\pi}{\alpha_s(\mu)}\,C_{10}(\mu)\,,\\
T_9 &= \frac{4}{3}\,C_1(\mu) + C_2(\mu) + 6\,C_3(\mu) + 60\,C_5(\mu)\,,\\
U_9 &= -\frac{7}{2}\,C_3(\mu) - \frac{2}{3}\,C_4(\mu) - 38\,C_5(\mu) - \frac{32}{3}\,C_6(\mu)\,,\\
W_9 &= -\frac{1}{2}\,C_3(\mu) - \frac{2}{3}\,C_4(\mu) - 8\,C_5(\mu) - \frac{32}{3}\,C_6(\mu)\,.
\end{aligned} \tag{36}$$

The elements $\gamma_{i9}^{(0)}$ can be found in [16], while the loop-function $h(z,\hat{s})$ is given in Eq. (4).

In the contributions which explicitly involve virtual or bremsstrahlung corrections only the leading order coefficients $A_i^{(0)}$, $T_9^{(0)}$, $U_9^{(0)}$ and $W_9^{(0)}$ enter. They are given by

$$\begin{aligned}
A_7^{(0)} &= C_7^{(1)} - \frac{1}{3}\,C_3^{(0)} - \frac{4}{9}\,C_4^{(0)} - \frac{20}{3}\,C_5^{(0)} - \frac{80}{9}\,C_6^{(0)}\,,\\
A_8^{(0)} &= C_8^{(1)} + C_3^{(0)} - \frac{1}{6}\,C_4^{(0)} + 20\,C_5^{(0)} - \frac{10}{3}\,C_6^{(0)}\,,\\
A_9^{(0)} &= \frac{4\,\pi}{\alpha_s}\left(C_9^{(0)} + \frac{\alpha_s}{4\,\pi}\,C_9^{(1)}\right) + \sum_{i=1}^{6} C_i^{(0)}\,\gamma_{i9}^{(0)}\,\ln\!\left(\frac{m_b}{\mu}\right) + \frac{4}{3}\,C_3^{(0)} + \frac{64}{9}\,C_5^{(0)} + \frac{64}{27}\,C_6^{(0)}\,,\\
A_{10}^{(0)} &= C_{10}^{(1)}\,,\\
T_9^{(0)} &= \frac{4}{3}\,C_1^{(0)} + C_2^{(0)} + 6\,C_3^{(0)} + 60\,C_5^{(0)}\,,\\
U_9^{(0)} &= -\frac{7}{2}\,C_3^{(0)} - \frac{2}{3}\,C_4^{(0)} - 38\,C_5^{(0)} - \frac{32}{3}\,C_6^{(0)}\,,\\
W_9^{(0)} &= -\frac{1}{2}\,C_3^{(0)} - \frac{2}{3}\,C_4^{(0)} - 8\,C_5^{(0)} - \frac{32}{3}\,C_6^{(0)}\,.
\end{aligned} \tag{37}$$

We list the leading and next-to-leading order contributions to the quantities A_i, T_9, U_9 and W_9 in Tab. A.1.

μ	2.5 GeV	5 GeV	10 GeV
α_s	0.267	0.215	0.180
$C_1^{(0)}$	-0.697	-0.487	-0.326
$C_2^{(0)}$	1.046	1.024	1.011
$\left(A_7^{(0)},\ A_7^{(1)}\right)$	$(-0.360,\ 0.031)$	$(-0.321,\ 0.019)$	$(-0.287,\ 0.008)$
$A_8^{(0)}$	-0.164	-0.148	-0.134
$\left(A_9^{(0)},\ A_9^{(1)}\right)$	$(4.241,\ -0.170)$	$(4.129,\ 0.013)$	$(4.131,\ 0.155)$
$\left(T_9^{(0)},\ T_9^{(1)}\right)$	$(0.115,\ 0.278)$	$(0.374,\ 0.251)$	$(0.576,\ 0.231)$
$\left(U_9^{(0)},\ U_9^{(1)}\right)$	$(0.045,\ 0.023)$	$(0.032,\ 0.016)$	$(0.022,\ 0.011)$
$\left(W_9^{(0)},\ W_9^{(1)}\right)$	$(0.044,\ 0.016)$	$(0.032,\ 0.012)$	$(0.022,\ 0.009)$
$\left(A_{10}^{(0)},\ A_{10}^{(1)}\right)$	$(-4.372,\ 0.135)$	$(-4.372,\ 0.135)$	$(-4.372,\ 0.135)$

Table A.1: Coefficients appearing Eqs. (7)–(9) for $\mu = 2.5$ GeV, $\mu = 5$ GeV and $\mu = 10$ GeV. For $\alpha_s(\mu)$ (in the $\overline{\rm MS}$ scheme) we used the two-loop expression with five flavors and $\alpha_s(m_Z) = 0.119$. The entries correspond to the pole top quark mass $m_t = 174$ GeV. The superscript (0) refers to lowest order quantities.

References

[1] H. H. Asatryan, H. M. Asatrian, C. Greub and M. Walker, *Phys. Lett.* **B 507** (2001) 162, hep-ph/0103087; H. H. Asatryan, H. M. Asatrian, C. Greub and M. Walker, *Phys. Rev.* **D 65** (2002) 074004, hep-ph/0109140.

[2] Z. Ligeti and M. B. Wise, *Phys. Rev.* **D 53** (1996) 4937.

[3] A. F. Falk, M. Luke and M. J. Savage, *Phys. Rev.* **D 49** (1994) 3367.

[4] A. Ali, G. Hiller, L. T. Handoko and T. Morozumi, *Phys. Rev.* **D 55** (1997) 4105.

[5] J-W. Chen, G. Rupak and M. J. Savage, *Phys. Lett.* **B 410** (1997) 285.

[6] G. Buchalla, G. Isidori and S. J. Rey, *Nucl. Phys.* **B 511** (1998) 594.

[7] G. Buchalla and G. Isidori, *Nucl. Phys.* **B 525** (1998) 333.

[8] F. Krüger and L.M. Sehgal, *Phys. Lett.* **B 380** (1996) 199.

[9] A. Ali, P. Ball, L.T. Handoko, G. Hiller, *Phys. Rev.* **D 61** (2000) 074024.

[10] E. Lunghi and I. Scimemi, *Nucl. Phys.* **B 574** (2000) 43.

[11] E. Lunghi, A. Masiero, I. Scimemi and L. Silvestrini, *Nucl. Phys.* **B 568** (2000) 120.

[12] A. Ali, E. Lunghi, C. Greub and G. Hiller, hep-ph/0112300.

[13] H. H. Asatryan, H. M. Asatrian, G. K. Yeghiyan and G. K. Savvidy, *Int. J. Mod. Phys.* **A 16** (2001) 3805.

[14] M. Misiak, *Nucl. Phys.* **B 393** (1993) 23; *Nucl. Phys.* **B 439** (1995) 461 (E).

[15] A. J. Buras and M. Münz, *Phys. Rev.* **D 52** (1995) 186.

[16] C. Bobeth, M. Misiak and J. Urban, *Nucl. Phys.* **B 574** (2000) 291.

[17] K. Chetyrkin, M. Misiak and M. Münz, *Phys. Lett.* **B 400** (1997) 206.

[18] N. Cabibbo and L. Maiani, *Phys. Lett.* **B 79** (1978) 109.

[19] Y. Nir, *Phys. Lett.* **B 221** (1989) 184.

[20] P. Gambino and M. Misiak, *Nucl. Phys.* **B 611** (2001) 338, hep-ph/0104034.

PART VI

QCD Corrections to $b \to d\,\ell^+\ell^-$

QCD Corrections to $b \to d\,\ell^+\ell^-$ in the Standard Model

ABSTRACT

We present the calculation of the virtual $\mathcal{O}(\alpha_s)$ corrections to the inclusive semileptonic rare decay $b \to d\,\ell^+\ell^-$. The calculation of these contributions is an extension to the $b \to s\,\ell^+\ell^-$ corrections [1], ie the diagrams induced by the four-quark operators O_1 and O_2 with an u quark running in the quark loop are no longer Cabibbo suppressed. We discuss in detail the calculation of the corresponding matrix elements. The analytic results for the process $b \to d\,\ell^+\ell^-$ are represented as expansions in the small parameters $\hat{s} = s/m_b^2$, $z = m_c^2/m_b^2$ and $s/(4\,m_c^2)$, where s is the invariant mass squared of the lepton pair. We also include the complete set of $\mathcal{O}(\alpha_s)$ bremsstrahlung contributions.

1 Introduction

For the transition $b \to s\,\ell^+\ell^-$ the contributions with an u quark running in the fermion loop is Cabibbo suppressed, ie $|\lambda'_u| \ll |\lambda'_c|, |\lambda'_t|$, where $\lambda'_q = V^*_{qs}V_{qb}$. It is a save approximation to set $|\lambda'_u| = 0$. In the case of $b \to d\,\ell^+\ell^-$, this is no longer true, and we have to calculate the u quark diagrams as well: $|\lambda_u| \approx |\lambda_c| \approx |\lambda_t|$, $\lambda_q = V^*_{qd}V_{qb}$. Setting $m_u = 0$ seems to be a substantial simplification of the calculations because they involve one scale less than c quark diagrams. This is definitely true for some of the diagrams. Others, however, get quite more involved because the techniques we used for their counterparts [1], where we could use the ratio $\hat{s}/(4\,z)$ as an expansion parameter, fail. The quantities $\hat{s}$ and z are given by $\hat{s} = s/m_b^2$ and $z = m_c^2/m_b^2$, where s denotes the invariant mass squared of the lepton pair.

Another problem arising in the analysis of $b \to d\,\ell^+\ell^-$ are the large resonant contributions due to $\bar{u}u$ intermediate states. Unlike in the $b \to s\,\ell^+\ell^-$ case, the threshold of these resonances lies rather low. Therefore, we may no longer evade integrating over these domains, where only model dependent predictions are available.

A big part of the work for $b \to d\,\ell^+\ell^-$ has been completed by now. However, the results can not yet be presented in paper form. Therefore, in this part, we merely give an account on what has been done so far and introduce two methods used to solve some of the integrals.

2 Effective Hamiltonian

The effective Hamiltonian mediating the transition $b \to d\,\ell^+\ell^-$ or $b \to d\,\gamma^*$, respectively, is given by

$$\mathcal{H}_{\text{eff}} = \frac{4\,G_F}{\sqrt{2}}\left[\sum_{i=1}^{2} C_i(\lambda_c\,O_i^c + \lambda_u O_i^u) - \lambda_t \sum_{i=3}^{10} C_i\,O_i\right],$$

with $\lambda_q = V^*_{qd}V_{qb}$. The operator basis we choose accordingly to [12]

$$\begin{aligned}
O_1^u &= (\bar{d}_L\gamma_\mu T^a u_L)(\bar{u}_L\gamma^\mu T^a b_L), & O_2^u &= (\bar{d}_L\gamma_\mu u_L)(\bar{u}_L\gamma^\mu b_L),\\
O_1^c &= (\bar{d}_L\gamma_\mu T^a c_L)(\bar{c}_L\gamma^\mu T^a b_L), & O_2^c &= (\bar{d}_L\gamma_\mu c_L)(\bar{c}_L\gamma^\mu b_L),\\
O_3 &= (\bar{d}_L\gamma_\mu b_L)\textstyle\sum_q(\bar{q}\gamma^\mu q), & O_4 &= (\bar{d}_L\gamma_\mu T^a b_L)\textstyle\sum_q(\bar{q}\gamma^\mu T^a q),\\
O_5 &= (\bar{d}_L\gamma_\mu\gamma_\nu\gamma_\rho b_L)\textstyle\sum_q(\bar{q}\gamma^\mu\gamma^\nu\gamma^\rho q), & O_6 &= (\bar{d}_L\gamma_\mu\gamma_\nu\gamma_\rho T^a b_L)\textstyle\sum_q(\bar{q}\gamma^\mu\gamma^\nu\gamma^\rho T^a q),\\
O_7 &= \tfrac{e}{g_s^2}m_b(\bar{d}_L\sigma^{\mu\nu}b_R)F_{\mu\nu}, & O_8 &= \tfrac{1}{g_s}m_b(\bar{d}_L\sigma^{\mu\nu}T^a b_R)G^a_{\mu\nu},\\
O_9 &= \tfrac{e^2}{g_s^2}(\bar{d}_L\gamma_\mu b_L)\textstyle\sum_\ell(\bar{\ell}\gamma^\mu\ell), & O_{10} &= \tfrac{e^2}{g_s^2}(\bar{d}_L\gamma_\mu b_L)\textstyle\sum_\ell(\bar{\ell}\gamma^\mu\gamma_5\ell),
\end{aligned} \tag{1}$$

where the subscripts L and R refer to left- and right-handed components of the fermion fields, respectively.

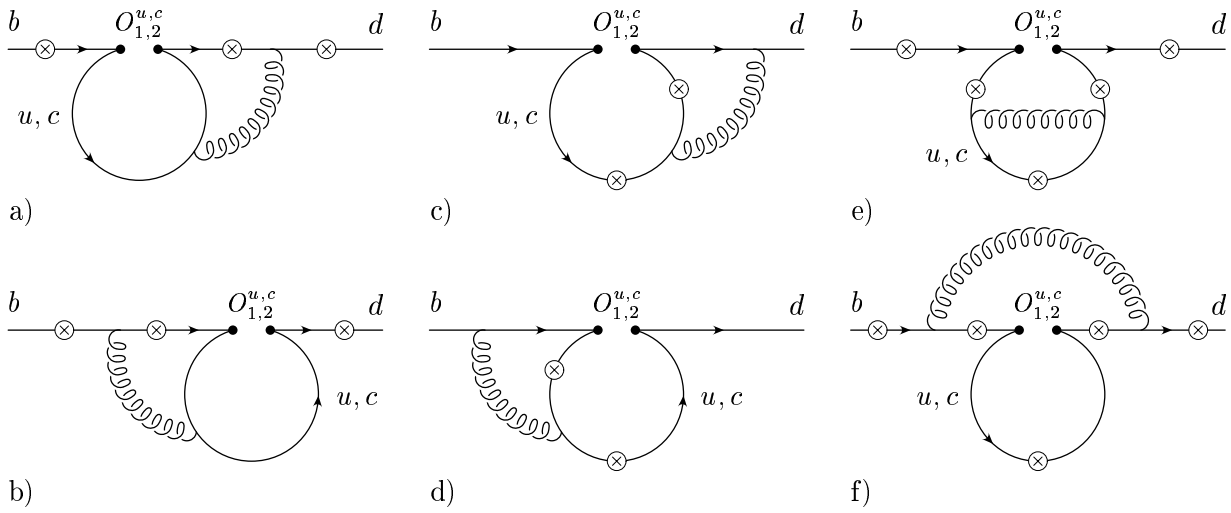

Figure 3.1: Complete list of two-loop Feynman diagrams for $b \to d\,\gamma^*$ associated with the operators $O_1^{u,c}$ and $O_2^{u,c}$. The fermions (b, d, u and c quarks) are represented by solid lines, whereas the curly lines represent gluons. The circle-crosses denote the possible locations where the virtual photon (which then splits into a lepton pair) is emitted.

The factors $1/g_s^2$ in the definition of the operators O_7, O_9 and O_{10} as well as the factor $1/g_s$ present in O_8 have been chosen by Misiak [2] in order to simplify the organization of the calculation. With these definitions, the one-loop anomalous dimensions [needed for a leading logarithmic (LL) calculation] of the operators O_i are all proportional to g_s^2, while two-loop anomalous dimensions [needed for a next-to-leading logarithmic (NLL) calculation] are proportional to g_s^4, etc.

The formally leading term $\sim (1/g_s^2)\, C_9^{(0)}(\mu_b)$ to the amplitude for $b \to d\,\ell^+\ell^-$ is smaller than the NLL term $\sim (1/g_s^2)\big[g_s^2/(16\,\pi^2)\big]\, C_9^{(1)}(\mu_b)$ [3]. We adapt our systematics to the numerical situation and treat the sum of these two terms as a NLL contribution. This is, admittedly some abuse of language, because the decay amplitude then starts out with a term which is called NLL.

3 Virtual $\mathcal{O}(\alpha_s)$ Corrections to the Current-Current Operators $O_1^{u,c}$ and $O_2^{u,c}$

In this section we present the calculation of the virtual $\mathcal{O}(\alpha_s)$ corrections to the matrix elements of the current-current operators $O_1^{u,c}$ and $O_2^{u,c}$. Using the naive dimensional regularization scheme (NDR) in $d = 4 - 2\,\epsilon$ dimensions, both ultraviolet and infrared singularities show up as $1/\epsilon^n$ poles ($n = 1, 2$). The ultraviolet singularities cancel after including the counterterms. Collinear singularities are regularized by retaining a finite

down quark mass m_d. They are cancelled together with the infrared singularities at the level of the decay width when taking the bremsstrahlung process $b \to d\,\ell^+\ell^- g$ into account. Gauge invariance implies that the QCD corrected matrix elements of the operators O_i can be written as

$$\langle d\,\ell^+\ell^-|O_i|b\rangle = \hat{F}_i^{(9)}\langle O_9\rangle_{\rm tree} + \hat{F}_i^{(7)}\langle O_7\rangle_{\rm tree}\,, \tag{2}$$

where $\langle O_9\rangle_{\rm tree}$ and $\langle O_7\rangle_{\rm tree}$ are the tree-level matrix elements of O_9 and O_7, respectively. Equivalently, we may write

$$\langle d\,\ell^+\ell^-|O_i|b\rangle = -\frac{\alpha_s}{4\,\pi}\,\left[F_i^{(9)}\langle\widetilde{O}_9\rangle_{\rm tree} + F_i^{(7)}\langle\widetilde{O}_7\rangle_{\rm tree}\right], \tag{3}$$

where the operators $\widetilde{O}_7$ and $\widetilde{O}_9$ are defined as

$$\widetilde{O}_7 = \frac{\alpha_s}{4\,\pi}\,O_7, \quad \widetilde{O}_9 = \frac{\alpha_s}{4\,\pi}\,O_9. \tag{4}$$

We present the final results for the QCD corrected matrix elements in the form of Eq. (3). The full set of the diagrams contributing at $\mathcal{O}(\alpha_s)$ to the matrix elements

$$M_i^q = \langle d\,\ell^+\ell^-|O_i^q|b\rangle \quad (i = 1, 2;\ q = u, c) \tag{5}$$

is shown in Fig. 3.1. As indicated, the diagrams associated with $O_1^{u,c}$ and $O_2^{u,c}$ are topologically identical. They differ only by the color structure. While the matrix elements of the operator $O_2^{u,c}$ all involve the color structure

$$\sum_a T^a T^a = C_F\mathbf{1}, \quad C_F = \frac{N_c^2 - 1}{2\,N_c}\,,$$

there are two possible color structures for the corresponding diagrams of $O_1^{u,c}$, viz

$$\tau_1 = \sum_{a,b} T^a T^b T^a T^b \quad \text{and} \quad \tau_2 = \sum_{a,b} T^a T^b T^b T^a.$$

The structure τ_1 appears in diagrams 3.1a)-d), and τ_2 enters diagrams 3.1e) and 3.1f). Using the relation

$$\sum_a T^a_{\alpha\beta} T^a_{\gamma\delta} = -\frac{1}{2\,N_c}\,\delta_{\alpha\beta}\delta_{\gamma\delta} + \frac{1}{2}\,\delta_{\alpha\delta}\delta_{\beta\gamma},$$

we find that $\tau_1 = C_{\tau_1}\mathbf{1}$ and $\tau_2 = C_{\tau_2}\mathbf{1}$, with

$$C_{\tau_1} = -\frac{N_c^2 - 1}{4\,N_c^2} \quad \text{and} \quad C_{\tau_2} = \frac{(N_c^2 - 1)^2}{4\,N_c^2}\,.$$

Inserting $N_c = 3$, the color factors are $C_F = \frac{4}{3}, C_{\tau_1} = -\frac{2}{9}$ and $C_{\tau_2} = \frac{16}{9}$. The contributions from $O_1^{u,c}$ are obtained by multiplying those from $O_2^{u,c}$ by the appropriate factors, ie by $C_{\tau_1}/C_F = -\frac{1}{6}$ and $C_{\tau_2}/C_F = \frac{4}{3}$, respectively. The regularized $\mathcal{O}(\alpha_s)$ contributions of the

operators O_1^c and O_2^c are discussed in detail in Ref. [1] (cf Part III of this thesis). In the following exposition we therefore focus on the discussion of the contributions from O_2^u to the individual diagrams.

We use the $\overline{\text{MS}}$ renormalization scheme, ie we introduce the renormalization scale in the form $\overline{\mu}^2 = \mu^2 \exp(\gamma_E)/(4\pi)$ followed by minimal subtraction. The precise definition of the evanescent operators, which is necessary to fully specify the renormalization scheme, will be given later.

3.1 Tensor Integrals and Irreducible Numerators

We follow [4] and derive a method that allows to express tensor integrals of generic dimension d in terms of scalar integrals of higher dimension.

An arbitrary L loop tensor integral with N internal and E external lines can be written as a linear combination of integrals of the form

$$G^{(d)}\Big(\{s_u\},\{m_v^2\}\Big) = \int \left(\prod_{i=1}^{L} \frac{d^d k_i}{(2\pi)^d}\right) \prod_{j=1}^{N} \prod_{l=1}^{n_j} \bar{k}_j^{\mu_{jl}} P^{\nu_j}_{\bar{k}_j,m_j}\,, \tag{6}$$

where

$$P^{\nu}_{k,m} = \frac{1}{\left(k^2 - m^2 + i\,\epsilon\right)^{\nu}} \quad \text{and} \quad \bar{k}_j = \sum_{n=1}^{L} \omega_{jn}\, k_n + \sum_{m=1}^{E} \eta_{jm}\, q_m\,.$$

k_i and q_j denote the loop and external momenta, respectively. The matrices of incidences of the diagram, ω and η, have matrix elements $\omega_{ij}, \eta_{ij} \in \{-1, 0, 1\}$. $\{s_u\}$, finally, denotes a set of scalar invariants formed from the external momenta q_j. In principle, the exponents ν_i would generically be equal to 1. However, often two or more internal lines are equipped with the same propagator. This may be taken into account by reducing N to $N^{\text{eff}} < N$, thus increasing some of the exponents ν_i. Applying the integral representations

$$\frac{1}{\left(k^2 - m^2 + i\,\epsilon\right)^{\nu}} = \frac{(-i)^{\nu}}{\Gamma(\nu)} \int_0^{\infty} d\alpha\, \alpha^{\nu-1} \exp\Big[i\,\alpha\left(k^2 - m^2 + i\,\epsilon\right)\Big] \tag{7}$$

and

$$\prod_{l=1}^{n_j} \bar{k}_j^{\mu_{il}} = (-i)^{n_j} \prod_{l=1}^{n_j} \frac{\partial}{\partial (a_j)_{\mu_{jl}}} \exp\Big[i(a_j \bar{k}_j)\Big]\Big|_{a_j=0}\,, \tag{8}$$

allows us to easily perform the integration over the loop momenta by using the d dimensional Gaussian integration formula

$$\int d^d k\, \exp\Big[i\left(A\,k^2 + 2(p\,k)\right)\Big] = i\left(\frac{\pi}{i\,A}\right)^{\frac{d}{2}} \exp\left[-\frac{i\,p^2}{A}\right].$$

We find the following parametric representation:

$$G^{(d)} = i^L \left(\frac{1}{4\,i\pi}\right)^{\frac{d\,L}{2}} \prod_{j=1}^{N} \frac{(-i)^{n_j+\nu_j}}{\Gamma(\nu_j)} \times \prod_{l=1}^{n_j} \frac{\partial}{\partial (a_j)_{\mu_{jl}}} \times \int_0^\infty \ldots \int_0^\infty \frac{d\alpha_j\, \alpha_j^{\nu_j-1}}{\left[D(\alpha)\right]^{\frac{d}{2}}} \exp\left[\frac{i\,Q\big(\{s_u\},\alpha,a\big)}{D(\alpha)} - i\sum_{r=1}^{N} \alpha_r \left(m_r^2 - i\,\epsilon\right)\right]\Bigg|_{a_j=0} . \quad (9)$$

The differentiation with respect to a_j generates products of external momenta, metric tensors $g_{\mu\nu}$ and polynomials $R(\alpha)$ and provides an additional factor $D(\alpha)^{-1}$. Because of

$$R(\alpha) \exp\left[-i\sum_{r=1}^{N} \alpha_r m_r^2\right] = R(i\partial) \exp\left[-i\sum_{r=1}^{N} \alpha_r m_r^2\right], \quad \text{with} \quad \partial_j = \frac{\partial}{\partial m_j^2},$$

we may replace the polynomials $R(\alpha)$ with $R(i\partial)$. The additional factor of $1/D(\alpha)$ can be absorbed by a redefinition of d, ie by shifting d to $d+2$ and multiplying with a factor $(4\,i\pi)^L$. The crucial point is, that this way all factors generated by differentiation with respect to a_j may be written as an operator which does not depend on the integral representations we have introduced in Eqs. (7), (8). Therefore, it is possible to write tensor integrals in momentum space in terms of scalar ones without direct appeal to the parametric representation (9):

$$\int \left(\prod_{i=1}^{L} \frac{d^d k_i}{(2\,\pi)^d}\right) \prod_{j=1}^{N} \prod_{l=1}^{n_j} \bar{k}_j^{\mu_{jl}} P^{\nu_j}_{\bar{k}_j,m_j} = T\big(q,\partial,\boldsymbol{d}^+\big) \int \left(\prod_{i=1}^{L} \frac{d^d k_i}{(2\,\pi)^d}\right) \prod_{l=1}^{n_j} P^{\nu_j}_{\bar{k}_j,m_j}, \quad (10)$$

where the tensor operator T is given by

$$T\big(q,\partial,\boldsymbol{d}^+\big) = \exp\Big[-i\,Q\big(\{\bar{s}_i\},\alpha,a\big)\,(4\,i\pi)^L\,\boldsymbol{d}^+\Big] \times \prod_{j=1}^{N} \prod_{l=1}^{n_j} \frac{\partial}{\partial (a_j)_{\mu_{jl}}} \exp\Big[i\,Q\big(\{\bar{s}_i\},\alpha,a\big)\,(4\,i\pi)^L\,\boldsymbol{d}^+\Big]\Bigg|_{\substack{a_j=0\\ \alpha_j=i\partial_j}} . \quad (11)$$

The operator $\boldsymbol{d}^+$ shifts the space-time dimension of the integral by two units:

$$\boldsymbol{d}^+\, G^{(d)}\Big(\big\{s_i\big\},\big\{m_j^2\big\}\Big) = G^{(d+2)}\Big(\big\{s_i\big\},\big\{m_j^2\big\}\Big).$$

The quantities $\bar{s}_i$ are scalar invariants formed out of external momenta q_i and auxiliary momenta a_i. Notice that throughout the derivation of the tensor operator T the masses m_j must be kept as parameters. They are set to their original values only in the very end. In Eq. (6), the product over $\bar{k}_i$ is very often replaced by a product over k_i. This slightly complicates the notation of the derivation of Eqs. (10) and (11). The result will be of the same form, however.

3.2 Integration by Parts

According to general rules of d dimensional integration, integrals of the form

$$\int d^d k_i \, \frac{\partial}{\partial k_i^\mu} \, \frac{\bar{k}_l^\mu}{\prod_{j=1}^N \left(\bar{k}_j^2 - m_j^2 + i\,\epsilon\right)^{\nu_j}}$$

vanish. There may exist suitable linear combinations

$$\int d^d k_i \, \frac{\partial}{\partial k_i^\mu} \, \frac{\sum_l c_l \bar{k}_l^\mu}{\prod_{j=1}^N \left(\bar{k}_j^2 - m_j^2 + i\,\epsilon\right)^{\nu_j}}$$

that lead to recurrence relations connecting the original integral to more simple ones. The task of finding such recurrence relations, however, is in general a non-trivial one. A criterion for irreducibility of multi-loop Feynman integrals is presented in [5]. In [4], the method of partial integration is combined with the technique of reducing tensor integrals by means of shifting the space-time dimension (cf preceding section).

The integral

$$F^{(d)}_{\nu_1\nu_2\nu_3\nu_4\nu_5} = \int d^d l \, d^d r \, I_{\nu_1\nu_2\nu_3\nu_4\nu_5} = \int d^d l \, d^d r \, \frac{1}{\left[l^2\right]^{\nu_1}\left[r^2\right]^{\nu_2}\left[(l+r)^2\right]^{\nu_3}\left[(l+q)^2\right]^{\nu_4}\left[(r+p')^2\right]^{\nu_5}} \tag{12}$$

enters the calculation of diagrams 3.1c) ($p'^2 = 0$). At the same time it is a very good example to illustrate the integration by parts method. The operators $\mathbf{1}^\pm$, $\mathbf{2}^\pm$,... are defined through

$$\mathbf{1}^\pm f_{\nu_1\nu_2\nu_3\nu_4\nu_5} := f_{\nu_1\pm 1\,\nu_2\nu_3\nu_4\nu_5}, \quad \ldots \, .$$

The present case is especially simple because we only need to calculate one derivative. Using the shorthand notation $I_{\nu_1\nu_2\nu_3\nu_4\nu_5} = I_{\{\nu_i\}}$ we get

$$\frac{\partial}{\partial r_\mu} \, r^\mu \, I_{\{\nu_i\}} = \Big[d - 2\,\nu_2\, r^2\, \mathbf{2}^+ - 2\,\nu_3\, r(l+r)\, \mathbf{3}^+ - 2\,\nu_5\, r(r+p')\, \mathbf{5}^+\Big] I_{\{\nu_i\}}.$$

Scalar products of the form $a \cdot b$ we write as $\left[a^2 + b^2 - (a-b)^2\right]/2$ and find

$$\frac{\partial}{\partial r_\mu} \, r^\mu \, I_{\{\nu_i\}} = \Big[d - 2\,\nu_2 - \nu_3 - \nu_5 - \nu_3(\mathbf{2}^- - \mathbf{1}^-)\, \mathbf{3}^+ - \nu_5\, \mathbf{2}^-\, \mathbf{5}^+\Big] I_{\{\nu_i\}}.$$

At this stage we might also reduce some of the scalar products by shifting the dimension. The corresponding procedure is presented eg in [4]. In the present case, however, the pure integration by parts approach suffices. The identity

$$\int d^d r \, \frac{\partial}{\partial r_\mu} \, r^\mu \, I_{\{\nu_i\}} \equiv 0$$

yields directly the desired recurrence relation for the integral $F^{(d)}_{\nu_1\nu_2\nu_3\nu_4\nu_5}$ [Eq. (12)]:

$$F^{(d)}_{\nu_1\nu_2\nu_3\nu_4\nu_5} = \frac{\nu_3(\mathbf{2}^- - \mathbf{1}^-)\,\mathbf{3}^+ + \nu_5\,\mathbf{2}^-\,\mathbf{5}^+}{d - 2\,\nu_2 - \nu_3 - \nu_5}\, F^{(d)}_{\nu_1\nu_2\nu_3\nu_4\nu_5}. \tag{13}$$

Subsequent application of this relation allows to express any integral $F^{(d)}\{\nu_i\}$ with indices $\nu_i \in \mathbb{N}^+$ as a sum over integrals $F^{(d)}\{\nu_i\}$ with at least $\nu_1 = 0$ or $\nu_2 = 0$. The same recurrence relation as for $F^{(d)}_{\{\nu_i\}}$ applies for the integral $\widetilde{F}^{(d)}_{\{\nu_i\}}$:

$$\widetilde{F}^{(d)}_{\nu_1\nu_2\nu_3\nu_4\nu_5} = \int d^dl\, d^dr\, \frac{1}{\left[l^2\right]^{\nu_1}\left[r^2\right]^{\nu_2}\left[(l+r)^2\right]^{\nu_3}\left[(l-q)^2\right]^{\nu_4}\left[(r+p)^2 - m_b^2\right]^{\nu_5}},$$

$$\widetilde{F}^{(d)}_{\nu_1\nu_2\nu_3\nu_4\nu_5} = \frac{\nu_3(\mathbf{2}^- - \mathbf{1}^-)\,\mathbf{3}^+ + \nu_5\,\mathbf{2}^-\,\mathbf{5}^+}{d - 2\,\nu_2 - \nu_3 - \nu_5}\, \widetilde{F}^{(d)}_{\nu_1\nu_2\nu_3\nu_4\nu_5}, \tag{14}$$

where $p^2 = m_b^2$. This relation will come in handy when evaluating the diagrams 3.1d).

The general procedure is the following:

- We express, as far as possible, all scalar products in the numerator of a given Feynman integrand in terms of inverse propagators $P_{\bar{k},m}$ and cancel them down.
- We write the integral as a sum over tensor integrals of the form (6), possibly with products over k_i^μ instead of $\bar{k}_i^\mu$. For each of those integrals the tensor operator T is determined in order to reduce the problem to scalar integrals with shifted space-time dimension.
- We apply appropriate recurrence relations to reduce the number of propagators in the integrals – and hope that we can solve the remaining integrals.

It is worth mentioning that, sometimes, recurrence relations obtained by combining integration by parts and dimension shifting can help, too. In general, however, this will only allow us to find a set of master integrals that are all of generic dimension d. Unfortunately it will not help to lower the power of a propagator to zero. In [6] an algorithm for calculating two-loop propagator type Feynman diagrams with arbitrary masses is proposed. The combined method allows to reduce the problem to a set of 15 essentially two-loop and 15 essentially one-loop master integrals.

3.3 Unrenormalized Form Factors of O_1^c and O_2^c

The matrix elements of O_1^c and O_2^c are discussed in detail in Ref. [1], where the unrenormalized form factors $F_{a,c}^{(7,9)}$ of $\langle d\,\ell^+\ell^-|O_a^c|b\rangle$ $(a = 1, 2)$, corresponding to diagrams 3.1a)–3.1e),

are given in the form

$$F_{a,c}^{(7,9)} = \sum_{i,j,l,m} c_{a,ijlm}^{(7,9)}\, \hat{s}^i\, \ln^j(\hat{s})\, z^l\, \ln^m(z),$$

where i, j and m are non-negative integers and $l = -i, -i+\frac{1}{2}, -i+1, \ldots$, $\hat{s} = s/m_b^2$ and $z = m_c^2/m_b^2$. Because of the lengthy result, we cite it only in parts in this paper.

We use the abbreviations $L_s = \ln(\hat{s})$, $L_\mu = \ln(\mu/m_b)$ and $L_c = \ln(z)/2$. The renormalized form factors $F_{i,u}^{(9)}$ and $F_{i,u}^{(7)}$ of the sum of diagrams 3.1a)-e) are

$$\begin{aligned} F_{1,c}^{(9)} = {} & \left(-\frac{1424}{729} + \frac{16}{243}\, i\pi + \frac{64}{27}\, L_c\right) L_\mu - \frac{16}{243}\, L_\mu\, L_s + \left(\frac{16}{1215} - \frac{32}{135}\, z^{-1}\right) L_\mu\, \hat{s} \\ & + \left(\frac{4}{2835} - \frac{8}{315}\, z^{-2}\right) L_\mu\, \hat{s}^2 + \left(\frac{16}{76545} - \frac{32}{8505}\, z^{-3}\right) L_\mu\, \hat{s}^3 - \frac{256}{243}\, L_\mu^2 + f_1^{(9)}\,, \end{aligned} \tag{15}$$

$$\begin{aligned} F_{2,c}^{(9)} = {} & \left(\frac{256}{243} - \frac{32}{81}\, i\pi - \frac{128}{9}\, L_c\right) L_\mu + \frac{32}{81}\, L_\mu\, L_s + \left(-\frac{32}{405} + \frac{64}{45}\, z^{-1}\right) L_\mu\, \hat{s} \\ & + \left(-\frac{8}{945} + \frac{16}{105}\, z^{-2}\right) L_\mu\, \hat{s}^2 + \left(-\frac{32}{25515} + \frac{64}{2835}\, z^{-3}\right) L_\mu\, \hat{s}^3 + \frac{512}{81}\, L_\mu^2 + f_2^{(9)}\,, \end{aligned} \tag{16}$$

$$F_{1,c}^{(7)} = -\frac{208}{243}\, L_\mu + f_1^{(7)}, \qquad F_{2,c}^{(7)} = \frac{416}{81}\, L_\mu + f_2^{(7)}\,. \tag{17}$$

The analytic results for $f_1^{(9)}$, $f_1^{(7)}$, $f_2^{(9)}$, and $f_2^{(7)}$ are decomposed as follows:

$$f_a^{(b)} = \sum_{i,j,l,m} \kappa_{a,ijlm}^{(b)}\, \hat{s}^i\, L_s^j\, z^l\, L_c^m + \sum_{i,j} \rho_{a,ij}^{(b)}\, \hat{s}^i\, L_s^j. \tag{18}$$

For the quantities $\rho_{a,ij}^{(b)}$, which collect the half-integer powers of z, and the coefficients $\kappa_{a,ijlm}^{(b)}$ we refer to Appendix B of Ref. [1].

3.4 Unrenormalized Form Factors of O_1^u and O_2^u

The remainder of this section is organized as follows: we first give the results for diagrams 3.1a) and b), which are calculated by means of the Mellin-Barnes approach [7]. We then turn to the calculation of diagrams 3.1c). We have used both the Mellin-Barnes technique and the techniques presented in Sections 3.1 and 3.2. Both approaches are discussed in detail. Subsequently, we comment on the problems arising with diagram 3.1d). Up to now, the corresponding integral has withstood our attempts to solve it. We then give the form factors of diagram 3.1e). Among the diagrams in Fig. 3.1f), only those where the virtual photon is emitted from the up or charm quark line, respectively, are non-zero. As they factorize into two one-loop diagrams, their calculation is straightforward. We already

mention at this point that it is convenient to omit these diagrams in the discussion of the matrix elements of O_1 and O_2. We take them into account together with the virtual corrections to O_9.

In the following, p and p' denote the momenta of the b and s quark, respectively, whereas q is given by $q = p - p'$.

3.4.1 Diagrams 3.1a) and b)

The calculation of the contribution from diagrams 3.1a) and b) opposes no difficulties. The diagram where the photon is emitted from the internal s quark line can be treated by the Mellin-Barnes approach. Alternatively, we may get the result directly from the corresponding form factors of the $b \to s\,\ell^+\ell^-$ transition by taking the limit $m_c \to 0$. Up to $\mathcal{O}(\hat{s}^3)$, the form factors for the contribution of the sum of the three diagrams in Fig. 3.1a) are given by

$$\begin{aligned} F_{2,u}^{(9)}[a] = C_F \cdot \Bigg[& -\frac{2}{27\,\epsilon^2} + \left(\frac{1}{\epsilon} + 4\,L_\mu\right)\left(-\frac{19}{81} + \frac{4}{27}\,L_s - \frac{4}{27}\,i\pi\right) - \frac{8}{27\,\epsilon}\,L_\mu - \frac{16}{27}\,L_\mu^2 \\ & + \left(-\frac{463}{486} - \frac{38\,i\pi}{81} + \frac{5\,\pi^2}{27}\right) - \frac{4}{27}\,\hat{s} + \left(-\frac{1}{27} - \frac{2}{27}\,L_s\right)\hat{s}^2 \\ & + \left(-\frac{4}{243} - \frac{8}{81}\,L_s\right)\hat{s}^3 + \frac{26}{81}\,L_s + \frac{8}{27}\,i\pi\,L_s - \frac{2}{27}\,L_s^2\Bigg], \end{aligned} \tag{19}$$

$$F_{2,u}^{(7)}[a] = C_F \cdot \left[\frac{1}{27}\left(\frac{1}{\epsilon} + 4\,L_\mu\right) + \frac{37}{162} + \frac{2}{27}\,i\pi + \frac{2}{27}\,\hat{s}\left(1 + \hat{s} + \hat{s}^2\right)L_s\right],$$

where

$$L_s = \ln(\hat{s}) \quad \text{and} \quad L_\mu = \ln\left(\frac{\mu}{m_b}\right).$$

C_F denotes the colour factor. For the sum of the diagrams in Fig. 3.1b) we find

$$\begin{aligned} F_{2,u}^{(9)}[b] = C_F \cdot \Bigg[& -\frac{2}{27\,\epsilon^2} + \left(\frac{1}{\epsilon} + 4\,L_\mu\right)\left(\frac{1}{81} - \frac{4}{135}\,\hat{s} - \frac{1}{315}\,\hat{s}^2 - \frac{4}{8505}\,\hat{s}^3\right) - \frac{8}{27\,\epsilon}\,L_\mu - \frac{16}{27}\,L_\mu^2 \\ & + \left(\frac{917}{486} - \frac{19\,\pi^2}{81}\right) + \left(\frac{172}{225} - \frac{2\,\pi^2}{27}\right)\hat{s} + \left(-\frac{871057}{396900} + \frac{2\,\pi^2}{9}\right)\hat{s}^2 \\ & + \left(-\frac{83573783}{10716300} + \frac{64\,\pi^2}{81}\right)\hat{s}^3\Bigg], \end{aligned} \tag{20}$$

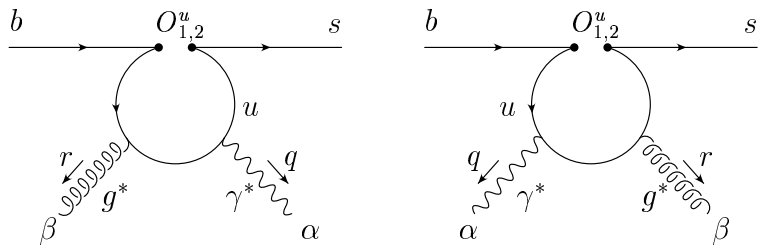

Figure 3.2: The two diagrams contributing to the building block $J^u_{\alpha\beta}$. The curly and wavy lines represent gluons and photons, respectively.

$$F^{(7)}_{2,u}[b] = C_F \cdot \left[-\frac{5}{27\,\epsilon} - \frac{20}{27}\,L_\mu + \frac{13}{162} + \left(\frac{25}{81} - \frac{\pi^2}{27}\right)\hat{s} + \left(\frac{118}{81} - \frac{4\,\pi^2}{27}\right)\hat{s}^2 + \left(\frac{10361}{2835} - \frac{10\,\pi^2}{27}\right)\hat{s}^3 \right].$$

3.4.2 Diagrams 3.1c), part 1

The diagram 3.1c) may be calculated in two ways, which we elucidate both. We first present how to calculate diagram 3.1c) by pure Mellin-Barnes methods. We discuss this approach for two reasons. First, it differs in some way from the calculation of diagram 1a) in Ref. [1], where we used a double Mellin-Barnes representation, too. Secondly, it is the much more complicated one of the two ways and thus points out the elegance of the techniques introduced in Sections 3.1 and 3.2. The second solution we will demonstrate in the following section. Both approaches yield the same result, which is, needless to say, an excellent consistency check.

It is advisable to first evaluate the building block $J^u_{\alpha\beta}$, shown in Fig. 3.2. Using the notation introduced by Simma and Wyler [8], it reads

$$J^u_{\alpha\beta} = \frac{e\,g_s\,Q_u}{16\,\pi^2}\left[E(\alpha,\beta,r)\Delta i^{(u)}_5 + E(\alpha,\beta,q)\Delta i^{(u)}_6 - E(\beta,r,q)\frac{r_\alpha}{q\cdot r}\,\Delta i^{(u)}_{23} - E(\alpha,r,q)\frac{r_\beta}{q\cdot r}\,\Delta i^{(u)}_{25} - E(\alpha,r,q)\frac{q_\beta}{q\cdot r}\,\Delta i^{(u)}_{26} - E(\beta,r,q)\frac{q_\alpha}{q\cdot r}\,\Delta i^{(u)}_{27}\right] L\,\frac{\lambda}{2}\,, \quad (21)$$

where q and r denote the momenta of the (virtual) photon and gluon. The indices α and β will be contracted with the propagators of the photon and the gluon, respectively. The matrix $E(\alpha,\beta,r)$ is defined as

$$E(\alpha,\beta,r) = \frac{1}{2}(\gamma_\alpha\gamma_\beta\not{r} - \not{r}\gamma_\beta\gamma_\alpha) \quad (22)$$

and the dimensionally regularized quantities $\Delta i_k^{(u)}$ occurring in Eq. (12) read

$$\begin{aligned}
\Delta i_5^{(u)} &= 4\,B^+ \int_S dx\,dy \left[4(q\cdot r)\,x\,y\,(1-x)\epsilon + r^2\,x\,(1-x)(1-2\,x)\epsilon \right.\\
&\qquad \left. + q^2\,y(2-2\,y+2\,x\,y-x)\epsilon + (1-3\,x)C\right]\,C^{-1-\epsilon}\,,\\
\Delta i_6^{(u)} &= 4\,B^+ \int_S dx\,dy \left[-4(q\cdot r)\,x\,y\,(1-y)\epsilon - q^2\,y\,(1-y)(1-2\,y)\epsilon \right.\\
&\qquad \left. - r^2\,x\,(2-2\,x+2\,x\,y-y)\epsilon - (1-3\,y)C\right]\,C^{-1-\epsilon}\,,\\
\Delta i_{23}^{(u)} &= -\Delta i_{26} = 8\,B^+(q\cdot r)\int_S dx\,dy\,x\,y\,\epsilon\,C^{-1-\epsilon}\,,\\
\Delta i_{25}^{(u)} &= -8\,B^+(q\cdot r)\int_S dx\,dy\,x\,(1-x)\,\epsilon\,C^{-1-\epsilon}\,,\\
\Delta i_{27}^{(u)} &= 8\,B^+(q\cdot r)\int_S dx\,dy\,y\,(1-y)\,\epsilon\,C^{-1-\epsilon}\,,
\end{aligned} \tag{23}$$

where $B^+ = (1+\epsilon)\Gamma(\epsilon)\,\mathrm{e}^{\gamma_E\epsilon}\mu^{2\epsilon}$ and C is given by

$$C = -2\,x\,y(q\cdot r) - r^2\,x\,(1-x) - q^2\,y\,(1-y) + i\,\delta.$$

The integration over the Feynman parameters x and y is restricted to the simplex S, ie $y \in [0, 1-x]$, $x \in [0,1]$. Due to Ward identities, the quantities $\Delta i_k^{(u)}$ are not independent of one another. Namely,

$$q^\alpha J_{\alpha\beta} = 0 \quad \text{and} \quad r^\beta J_{\alpha\beta} = 0$$

imply that $\Delta i_5^{(u)}$ and $\Delta i_6^{(u)}$ can be expressed as

$$\Delta i_5^{(u)} = \Delta i_{23}^{(u)} + \frac{q^2}{q\cdot r}\,\Delta i_{27}^{(u)}\,, \quad \Delta i_6^{(u)} = \frac{r^2}{q\cdot r}\,\Delta i_{25}^{(u)} + \Delta i_{26}^{(u)}\,. \tag{24}$$

After the variable transformation $y \to y'(1-x)$, the quantity C may be written as

$$C = -x(1-x)\left[(r+y\,q)^2 + \frac{y(1-y)}{x}\,q^2\right] + i\,\delta,$$

where we have omitted the prime to ease the notation. The variable transformation provides the Jacobian $(1-x)$ and maps the integration region from the simplex on to the unit square, ie $x, y \in [0,1]$. The idea is, to apply a Mellin-Barnes representation directly on $C^{-\lambda}$, ie before performing the loop integral over r. This is in contrast to the procedure followed in [1, 9]. The Mellin-Barnes representation for the propagator $(K^2-M^2)^{-\lambda}$ reads $(\lambda > 0)$

$$\mathcal{M}_{\gamma,s}(K^2,M^2,\lambda) := \frac{1}{(K^2-M^2)^\lambda} = \frac{1}{(K^2)^\lambda}\,\frac{1}{\Gamma(\lambda)}\,\frac{1}{2\,i\pi}\int_\gamma ds\,\left(-\frac{M^2}{K^2}\right)^s \Gamma(-s)\,\Gamma(\lambda+s)\,. \tag{25}$$

The integration path γ runs parallel to the imaginary axis and intersects the real axis somewhere between $-\lambda$ and 0. The Mellin-Barnes representation of $C^{-\lambda}$ is obtained by making the identifications

$$K^2 \leftrightarrow (r + y\,q)^2 \quad \text{and} \quad M^2 \leftrightarrow \frac{y(1-y)}{x}\,q^2.$$

The corresponding Mellin integral is given by

$$C^{-\lambda} = \frac{\mathrm{e}^{i\pi\,\lambda}}{2\,i\pi} \int\limits_\gamma dt\, x^{-t-\lambda}\,(1-x)^{-\lambda}\,y^t\,(1-y)^t\,\frac{\Gamma(-t)\,\Gamma(t+\lambda)}{\Gamma(\lambda)}\,\frac{(q^2)^t}{\left[(r+y\,q)^2\right]^{t+\lambda}}\,.$$

We have got rid of non-integer powers of negative numbers by use of the formula

$$(x \pm i\,\delta)^\alpha = \mathrm{e}^{\pm i\pi\delta}(-x \mp i\,\delta)^\alpha.$$

The variable λ takes the value $1+\epsilon$ throughout the present calculation. Inserting the building block, we get the following analytical expression corresponding to diagram 3.1c)

$$M_2^u[c] = -i\,g_s\,\bar{\mu}^{4\epsilon} \int \frac{d^dr}{(2\,\pi)^d}\,\bar{u}(p')\frac{\gamma^\beta(\not{p}' - \not{r})\,R\,J_{\alpha\beta}(r,q)\gamma_\beta}{r^2(r-p')^2}\,u(p)\,\frac{\lambda}{2}\,.$$

We use the Mellin-Barnes representation for $C^{-\lambda}$, entering via $J_{\alpha\beta}$. The propagator structure of the integrand is then given by

$$P = \frac{1}{r^2\,(r-p')^2\,\left[(r+y\,q)^2\right]^{t+1+\epsilon}}\,.$$

We may apply an ordinary Feynman parameterization for P according to

$$\frac{1}{D_1\,D_2\,D_3^{t+1+\epsilon}} = \int\limits_0^1 du\,dv\,\frac{u^{t+\epsilon}\,(1-u)\Gamma(3+t+\epsilon)}{\Gamma(1+t+\epsilon)} \times \frac{1}{\left[(1-u)(1-v)D_1 + (1-u)v\,D_2 + u\,D_3\right]^{3+t+\epsilon}}\,,$$

with $D_1 = r^2$, $D_2 = (r-p')^2$ and $D_3 = (r+y\,q)^2$. Subsequently shifting the loop momentum r to $r + (1-u)v\,p' - u\,y\,q$, we find

$$P = \int\limits_0^1 du\,dv\,\frac{u^{t+\epsilon}(1-u)\,\Gamma(3+t+\epsilon)}{\Gamma(1+t+\epsilon)} \cdot \frac{1}{(r^2-\Delta)^{3+t+\epsilon}}\,,$$

where

$$\Delta = -u\,v\,y(1-u)\left(m_b^2 - q^2\right) - u\,y^2(1-u)q^2.$$

After changing the order of integration and performing the integral over the loop momentum r, we arrive at

$$M_2^u[c] = e\,Q_u\,g_s^2\,C_F\bar{\mu}^{4\epsilon}\frac{\mathrm{e}^{i\pi(1+\epsilon)}}{2\,i\pi}\int\limits_\gamma dt\int\limits_0^1 dx\,dy\,du\,dv\,x^{-t-1-\epsilon}\,(1-x)^{-1-\epsilon}\,y^t\,(1-y)^t$$
$$\Gamma(-t)\,\Gamma(3+t+\epsilon)\,(q^2)^t\,u^{t+\epsilon}\,\bar{u}(p')\left[\frac{P_1}{\Delta^{t+1+2\epsilon}}+\frac{P_2}{\Delta^{t+2\epsilon}}\right]u(p), \quad (26)$$

where P_1 and P_2 are polynomials in the Feynman parameters. We apply a second Mellin-Barnes representation to the quantities $\Delta^{-\lambda}$:

$$\Delta^{-\lambda} = \mathrm{e}^{i\pi\,\lambda}\mathcal{M}_{\gamma',t'}\big(m_b^2\,u\,v\,y(1-u)(1-\hat{s}), m_b^2\,u\,y^2(1-u)\hat{s}, \lambda\big).$$

There are two values λ can take here, namely $t+1+2\epsilon$ and $t+2\epsilon$. Correspondingly, the integration path γ' has to satisfy

$$-\mathrm{Re}(t)-1-2\epsilon < \mathrm{Re}(t') < 0 \quad \text{and} \quad -\mathrm{Re}(t)-2\epsilon < \mathrm{Re}(t') < 0,$$

respectively. We change the order of integration once more and do the integrals over the Feynman parameters x, y , u and v, which all are of the form

$$\int\limits_0^1 x^{p(t,t')}(1-x)^{q(t,t')} = \beta\big[p(t,t')+1, q(t,t')+1\big].$$

The integration paths γ and γ' have to be chosen such that all Feynman parameter integrals exist for values of $t \in \gamma$, $t' \in \gamma'$, ie $\mathrm{Re}[p(t,t')]$, $\mathrm{Re}[q(t,t')] > -1$. The dependence of $M_2^u[c]$ on $\hat{s}$ is of the form

$$M_2^u[c] = \frac{1}{(1-\hat{s})^{1+\epsilon}}\int\limits_\gamma dt\int\limits_\gamma dt'\,\hat{s}^t\left(\frac{\hat{s}}{1-\hat{s}}\right)^{t'}\left[F_0(t,t')+\hat{s}\,F_1(t,t')+\hat{s}^2F_1(t,t')\right]. \quad (27)$$

The remaining Mellin-Barnes integrals we perform by closing both γ and γ' in the right half-plane and identifying the integrals with the sum over the residues of the poles enclosed by the paths. This leads directly to an expansion in $\hat{s}$. In the following we just give the locations of all poles that have to be taken into account, but refrain from mentioning every technical detail. We first care about the t' integration. At this point is important not to keep the t integration at the back of our mind. It turns out that some of the residues we need to calculate depend on t and t'. We consider 'coupled' and 'un-coupled' residues separately.

Un-coupled residues

We find that we have to take into account the series of poles located at

$$t' = 0,\ 1,\ 2,\ 3,\ \ldots\ ,$$

in order to do the t' integral. We sum the residues up to the desired order in $\hat{s}$. As what concerns the t integration, we need the residues

- of the series' of poles at

$$t = 0,\, 1,\, 2,\, 3,\, \dots\,,$$
$$t = -\epsilon,\, 1-\epsilon,\, 2-\epsilon \dots\,;$$

- and of the two single poles at

$$t = 1 - 2\,\epsilon \quad \text{and} \quad t = 2 - 2\,\epsilon.$$

Again we need only to sum the residues up to the desired order in $\hat{s}$.

Coupled residues
The coupled residues are somewhat more involved. They are associated with the poles in t' situated at

$$\begin{aligned} t' = {} & 1 - t - 2\,\epsilon,\, 2 - t - 2\,\epsilon \quad \text{(for type A terms)}, \\ t' = {} & -t - 2\,\epsilon, 1 - t - 2\,\epsilon,\, 2 - t - 2\,\epsilon \quad \text{(for type B terms)}. \end{aligned}$$

Here we have to distinguish between terms associated with $\Delta^{-t-2\,\epsilon}$ (type A) and $\Delta^{-1-t-2\,\epsilon}$ (type B) [cf Eq. (26)]. In view of Eq. (27) it becomes immediately clear that in this case the integration over t will lead to contributions of fixed order in $\hat{s}$, ie we have to take into account all poles enclosed by the integration path γ to get the contributions of the corresponding orders. We need the residues

- of the series' of poles at

$$t = 0, 1, 2, 3, \dots\,,$$
$$t = -\epsilon, 1-\epsilon, 2-\epsilon, \dots\,,$$
$$t = 2 - 4\,\epsilon, 3 - 4\,\epsilon, 4 - 4\,\epsilon, \dots\,;$$

- and of the two single poles at

$$t = 1 - 2\,\epsilon \quad \text{and} \quad t = 2 - 2\,\epsilon.$$

We give the result of the calculation in the next section and make only a concluding comment on the evaluation of the infinite sums. It is straightforward to write down the explicit expression for the residues at $t = n$ ($n \in \mathbb{N}$), etc. The summation over n then yields hypergeometric functions as eg

$${}_3H_2\left(\left.\begin{matrix} 1,\, -2+2\,\epsilon,\, -3-3\,\epsilon \\ \epsilon,\, -3+4\,\epsilon \end{matrix}\right| 1\right).$$

It is rather tricky to find the corresponding ϵ expansions. Sometimes, it is easier to do the Taylor series expansion in ϵ before the summation. However, for the first few terms the expansion of the general addends is usually not valid and has to be done explicitly. Only the remaining terms are summed up analytically. In our calculation we have chosen to avoid explicit hypergeometrical functions.

3.4.3 Diagrams 3.1c), part 2

To calculate diagrams 3.1c), there exists a more elegant way, which might prove very useful for the calculation of other diagrams, too. In the following we present this alternative approach.

The contribution of the sum of diagrams 3.1c) is given by a combination of integrals of the form

$$\int d^dl\, d^dr\, \frac{\prod_{i=1}^{n_l} l^{\mu_i} \prod_{j=1}^{n_r} r^{\rho_j}}{\left[l^2\right]^{\nu_1} \left[r^2\right]^{\nu_2} \left[(l+r)^2\right]^{\nu_3} \left[(l+q)^2\right]^{\nu_4} \left[(r+p')^2\right]^{\nu_5}}\,.$$

The function $D(\alpha)$, which we do not need to find the tensor operators, is independent of n_l and n_r. We give it as an illustration:

$$D(\alpha) = (\alpha_1+\alpha_4)\,(\alpha_2+\alpha_5) + \alpha_3\,(\alpha_1+\alpha_2+\alpha_4+\alpha_5)\,.$$

The function $Q\big(\{\bar{s}_i\},\alpha,a\big)$, however, must be recalculated for each type of tensor integral. The expressions get quickly rather lengthy. As an example we give $Q(\{\bar{s}_i\},\alpha,a\}$ for $n_l=0$, $n_r=1$:

$$\begin{aligned} Q\big(\{s_i\},\alpha,a\big) = &-(\alpha_1+\alpha_3+\alpha_4)\,\alpha_5\,(a_1\cdot p') + \alpha_4\big(\alpha_2+\alpha_3+\alpha_1\,(\alpha_2+\alpha_3+\alpha_5)\,\big)q^2 + \\ &m_b^2\,\alpha_3\,\alpha_4\,\alpha_5 + \alpha_3\,\alpha_4(a_1\cdot q) - \frac{1}{4}\,(\alpha_1+\alpha_3+\alpha_4)\,a_1^2\,. \end{aligned} \quad (28)$$

The tensor operator T (cf Section 3.1) for the ($n_l=0$, $n_r=1$) integral, finally, reads

$$T = 16\,\pi^2\,\boldsymbol{d}^+\Big[q^{\rho_1}\partial_3\,\partial_4 - p'^{\rho_1}\,(\partial_1+\partial_3+\partial_4)\,\partial_5\Big].$$

The action of an operator ∂_i on the integral $F^{(d)}_{\{\nu\}}$ is

$$\partial_1^n\, F^{(d)}_{\nu_1\nu_2\nu_3\nu_4\nu_5} = \frac{\Gamma(\nu_1+n)}{\Gamma(n)}\, F^{(d)}_{\nu_1+n\,\nu_2\nu_3\nu_4\nu_5},$$

ie ∂_i acts similar to the operators $\boldsymbol{i}^+$. The next step is to use the recurrence relation (13). Notice that it must only be applied to integrals with $\nu_1,\nu_2>0$. As mentioned before, we are left with integrals that have at least $\nu_1=0$ or $\nu_2=0$. Hence, the remaining task is the calculation of the two integrals

$$F^{(d)}_{0\nu_2\nu_3\nu_4\nu_5} \quad \text{and} \quad F^{(d)}_{\nu_1 0\nu_3\nu_4\nu_5}.$$

In the present calculation d may take the values

$$d = 4-2\epsilon,\; 6-2\epsilon,\; 8-2\epsilon \quad \text{or} \quad 10-2\epsilon.$$

We start with the discussion of the integral $F^{(d)}_{0\nu_2\nu_3\nu_4\nu_5}$ and arbitrary indices $\nu_i \in \mathbb{N}^+$. After straightforward Feynman parametrizations and integration over the loop momenta l and r we get

$$F^{(d)}_{0\nu_2\nu_3\nu_4\nu_5} = \frac{(-1)^\Sigma}{(4\,\pi)^d} \int_0^1\int_0^1\int_0^1 du\,dx\,dy\,\frac{\Gamma\left(\Sigma - d\right)}{\Gamma(\nu_2)\,\Gamma(\nu_3)\,\Gamma(\nu_4)\,\Gamma(\nu_4)}$$

$$\times\, D^{d-\Sigma}\,u^{d/2-\nu_4-1}\,x^{\nu_5-1}\,y^{\nu_3+\nu_4-3-1-d/2}\,(1-u)^{d/2-\nu_3-1}\,(1-x)^{\nu_2-1}\,(1-y)^{\nu_2+\nu_5-2}, \quad (29)$$

where we have introduced the shorthand notation

$$\Sigma = \sum_{i=2}^{5} \nu_i.$$

The Feynman denominator D is given by

$$D = -m_b^2\,y\,(1-y)\left[x + (1-x)\hat{s}\right] - i\,\delta.$$

We represent $D^{-\lambda}$ $(\lambda > 0)$ as a Mellin-Barnes integral:

$$D^{-\lambda} = \frac{1}{2\,i\pi}\int_\gamma dt\,\mathrm{e}^{i\pi\,\lambda}\,m_b^{-2\,\lambda}\,\hat{s}^t\,x^{-\lambda-t}\,y^{-\lambda}\,(1-x)^t\,(1-y)^{-\lambda}\,\frac{\Gamma(-t)\,\Gamma(t+\lambda)}{\Gamma(\lambda)}\,.$$

All Feynman parameter integrals are now of the form

$$\int_0^1 x^{p(t)}(1-x)^{q(t)} = \beta\big[p(t)+1, q(t)+1\big].$$

Again, the integration path γ has to be chosen such that all Feynman parameter integrals exist for values of $t \in \gamma$, ie $\mathrm{Re}\big[p(t)\big]$, $\mathrm{Re}\big[q(t)\big] > -1$. The expression for $F^{(d)}_{0\nu_2\nu_3\nu_4\nu_5}$ now reads

$$F^{(d)}_{0\nu_2\nu_3\nu_4\nu_5} = -\hat{s}^t\,\frac{\mathrm{e}^{-id\,\pi}m_b^{2(d-\Sigma)}}{(4\,\pi)^d}\,\Gamma\left(\frac{d}{2}-\nu_2-\nu_5\right)\Gamma\left(d-t-\sum_{i=2}^{4}\nu_i\right)\Gamma(t-d+\Sigma)\times$$

$$\frac{\Gamma(-t)\,\Gamma(\nu_2+t)\,\Gamma\left(\frac{d}{2}-\nu_3\right)\Gamma\left(\frac{d}{2}-\nu_4\right)}{\Gamma(\nu_2)\,\Gamma(\nu_3)\,\Gamma(\nu_4)\,\Gamma(\nu_5)\,\Gamma(d-\nu_3-\nu_4)\,\Gamma(3\,d/2-\Sigma)}\,. \quad (30)$$

By inspection of the explicit expressions, we get the following conditions for $\mathrm{Re}(t)$:

$$\mathrm{Re}(t) > -\nu_2, \quad \mathrm{Re}(t) < d-\nu_2-\nu_3-\nu_4. \quad (31)$$

To perform the integration over the Mellin parameter t, we close the integration path in the right half-plane and use the residue theorem to identify the integral with the sum over the residues of the poles located at

$$\begin{aligned} &t = 0,\ 1,\ 2, \dots\,, \\ &t = d - \nu_2 - \nu_3 - \nu_4,\ d - \nu_2 - \nu_3 - \nu_4 + 1,\ d - \nu_2 - \nu_3 - \nu_4 + 2, \dots\,. \end{aligned} \tag{32}$$

The constraints (31) ensure that the path γ separates the series of poles that extends to the right from the series extending to the left, ie we have to take into account none of the poles located at $t = -\nu_2, -\nu_2 - 1, \dots$ or $t = d - \Sigma, d - \Sigma - 1, \dots$. In view of the factor $\hat{s}^t$ in Eq. (30), the evaluation of the residues at the pole positions listed in Eq. (32) corresponds directly to an expansion in $\hat{s}$. Notice that closing the integration path in the right half-plane yields an overall minus sign due the clockwise orientation of the integration contour. The evaluation of the integrals $F^{(d)}_{\nu_1 0 \nu_3 \nu_4 \nu_5}$ is completely analogous and needs not to be discussed further.

Reducing tensor integrals to scalar ones and applying recurrence relations proves, in the present case, to be quite efficient. The form factors of diagrams 3.1c) we find to be

$$\begin{aligned} F^{(9)}_{2,u}[c] = C_F \cdot \Bigg[&\frac{2}{3\,\epsilon^2} + \frac{1}{\epsilon}\left(\frac{5}{3} - \frac{4\,L_s}{3} + \frac{8}{3}\,L_\mu + \frac{4\,i\pi}{3}\right) + \frac{16}{3}\,L_\mu^2 \\ &+ \frac{1}{2} - 6\,L_s + \frac{2}{3}\,L_s^2 + \frac{10\,i\pi}{3} - \frac{8\,i\pi}{3}\,L_s - \frac{5\,\pi^2}{3} \\ &+ \left(\frac{4}{3} - 4\,L_s + \frac{2}{3}\,L_s^2 + \frac{2\,\pi^2}{9}\right)\hat{s} + \left(-1 - 2\,L_s + \frac{2}{3}\,L_s^2 + \frac{2\,\pi^2}{9}\right)\hat{s}^2 \\ &+ \left(-\frac{41}{27} - \frac{10}{9}\,L_s + \frac{2}{3}\,L_s^2 + \frac{2\,\pi^2}{9}\right) + \left(\frac{20}{3} + \frac{16\,i\pi}{3} - \frac{16}{3}\,L_s\right)L_\mu \Bigg], \end{aligned} \tag{33}$$

$$\begin{aligned} F^{(7)}_{2,u}[c] = C_F \cdot \Bigg[&\frac{1}{3\,\epsilon} + \frac{5}{2} + \frac{2\,i\pi}{3} + \left(\frac{2\,L_s}{3} - \frac{L_s^2}{3} - \frac{\pi^2}{9}\right)\hat{s} + \left(\frac{2}{3} - \frac{L_s^2}{3} - \frac{\pi^2}{9}\right)\hat{s}^2 \\ &+ \left(\frac{5}{6} - \frac{L_s}{3} - \frac{L_s^2}{3} - \frac{\pi^2}{9}\right)\hat{s}^3 + \frac{4}{3}\,L_\mu \Bigg]. \end{aligned} \tag{34}$$

As stated before, the pure Mellin-Barnes approach yields the same result.

3.4.4 Diagrams 3.1d)

In the case of diagrams 3.1d), neither of the two methods used to evaluate diagrams 3.1c) has been crowned with success so far. From my point of view, the most promising approach is nevertheless shifting the space-time dimension and subsequent application of recurrence

relations. We therefore comment in a few words on the present stage of the corresponding calculation.

After reducing the tensor integrals to scalar ones, we are left with integrals $\widetilde{F}^{(d)}_{\nu_1\nu_2\nu_3\nu_4\nu_5}$, for which the same recurrence relation as for $F^{(d)}_{\nu_1\nu_2\nu_3\nu_4\nu_5}$ holds [cf Eq. (14)]. The problem can thus be reduced to the two integrals $\widetilde{F}^{(d)}_{0\nu_2\nu_3\nu_4\nu_5}$ and $\widetilde{F}^{(d)}_{\nu_1 0\nu_3\nu_4\nu_5}$. The first one is readily solved in the same way as $F^{(d)}_{0\nu_2\nu_3\nu_4\nu_5}$ and $F^{(d)}_{\nu_1 0\nu_3\nu_4\nu_5}$ whereas the second one has not been cracked up to now.

To illustrate the difficulties, we explicitly consider the integral

$$\widetilde{F}_{10111} = \frac{1}{(4\,\pi^2)^d}\,\widetilde{F}^{(d=4-2\epsilon)}_{10111} = \frac{1}{(4\,\pi^2)^d}\int d^d l\, d^d r\, \frac{1}{l^2\,(l+r)^2\,(l-q)^2\,\left[(r+p)^2-m_b^2\right]}\,.$$

It is more promising to perform the integration over r before the integration over l. This way it is straightforward to find

$$\widetilde{F}_{10111} = \frac{\Gamma(\epsilon)}{(4\,\pi)^{4-2\epsilon}}\int\limits_0^1 dx\,dy\,du\,\frac{u^{-\epsilon}\,(1-u)^{-\epsilon}\,(1-x)^{-1-\epsilon}\,(1-y)^{\epsilon}}{\Delta^{2\epsilon}},$$

where

$$\Delta = m_b^2(1-x)(1-y)\frac{(1-u\,y)}{u} - q^2 x\,y(1-y).$$

We may use again a Mellin-Barnes representation for $\Delta^{-2\epsilon}$ with the hope of finding a natural expansion in terms of $\hat{s} = q^2/m_b^2$. We get

$$\begin{aligned}\widetilde{F}_{10111} = -\frac{1}{2\,i\pi}\int\limits_\gamma dt \int\limits_0^1 dx\,dy\,du\,\frac{\mathrm{e}^{-i\pi\,t}}{(4\,\pi)^{4-2\epsilon}}\,m_b^{-4\epsilon}\,\hat{s}^t \\ \times\, u^{t+\epsilon}\,(1-u)^{-\epsilon}\,x^t\,(1-x)^{-1-t-\epsilon}\,y^t\,(1-y)^{-\epsilon}\,(1-u\,y)^{-t-2\epsilon}\,\Gamma(-t)\,\Gamma(t+2\epsilon).\end{aligned}$$

The integration over the Feynman parameter x yields Euler Γ functions. However, the term $(1-u\,y)^{-s-2\epsilon}$ complicates the evaluation of the y and u integrals. Performing the integral over u brings in the hypergeometric function

$${}_2H_1\left(\left.\begin{matrix}1+t+\epsilon,\,t+2\,\epsilon\\ 2+t\end{matrix}\right|\,y\right) = \sum_{n=0}^{\infty}\frac{\Gamma(1+t+\epsilon+n)\,\Gamma(t+2\epsilon+n)\,\Gamma(2+t)}{\Gamma(1+t+\epsilon)\,\Gamma(t+2\epsilon)\,\Gamma(2+t+n)}\,\frac{y^n}{\Gamma(n+1)}\,.$$

It is now possible to do the remaining Feynman parameter integral over y and to perform the sum over n. This yields

$$\begin{aligned}\widetilde{F}_{10111} = -\frac{1}{2\,i\pi}\int\limits_\gamma \frac{dt\,\mathrm{e}^{-i\pi\,t}}{(4\,\pi)^{4-2\epsilon}}\,m_b^{-4\epsilon}\,\hat{s}^t\,\frac{\Gamma(-t)\,\Gamma(1+t)\,\Gamma(-t-\epsilon)\,\Gamma(1+t+\epsilon)\,\Gamma(t+2\,\epsilon)\,\Gamma(1-\epsilon)}{(1+t)\,\Gamma(2+t-\epsilon)} \\ \times\,{}_3H_2\left(\left.\begin{matrix}1+t,\,1+t+\epsilon,\,t+2\epsilon\\ 2+t,\,2+t-\epsilon\end{matrix}\right|1\right).\end{aligned}$$

Of course one is now tempted to express the hypergeometric function as an infinite sum, to close the integration contour in the right half-plane, to calculate the residues that contribute to the desired orders in $\hat{s}$ and afterwards to calculate the infinite sum again. However, there is a problem with the above hypergeometric function, viz it is only defined for

$$\mathrm{Re}\big[(2+t)+(2+t-\epsilon)-(1+t)-(1+t+\epsilon)-(t+2\epsilon)\big] = \mathrm{Re}(2-t-4\epsilon) > 0.$$

From this it becomes evident that we will run into difficulties when closing the integration path in the right half-plane. Indeed, naively summing up all residues contributing at $\mathcal{O}\left(\hat{s}^m\right)$ $(m = 2, 3, 4, ...)$ yields divergent results. At the moment I see two ways out:

- Close the integration contour in the left half-plane. This is certainly allowed, but results in an expansion in $1/\hat{s}$. In other words, this requires to take into account all residues lying on the left side of γ what, let it be noted, yields the exact result, which we may then expand in terms of $\hat{s}$.
- Introduce an additional regulator, ie replace $\int_0^1 dy$ by $\int_0^{1-\epsilon_W} dy$. This yields a hypergeometric function with argument $1-\epsilon_W$ instead of 1. We may not, however, expect the integral over the semi-circle, introduced to close the integration contour, to be harmless.

To follow up these ideas requires some more time because they comprise additional technical difficulties. I have also tried to find other recurrence relations and applied Mellin-Barnes representations in other ways, however without being rewarded. We stress that the integrals $\widetilde{F}^{(d)}_{\nu_1 0 \nu_3 \nu_4 \nu_5}$ are the missing puzzle to complete the NNLL calculation of the process $b \to d\,\ell^+\ell^-$.

3.4.5 Diagrams 3.1e)

The diagrams in 3.1e) finally, may again be solved in two ways. The first way is to use the heavy external momentum expansion technique [7]. The second possibility is to apply the dimension-shifting-and-integration-by-parts procedure also for this diagram. The structure of the integral is of propagator type, ie depends only on *one* external momentum. Hence, we might even use the algorithm presented in [6] to boil the problem down to two essentially two-loop and two essentially one-loop integrals in the generic dimension. It is, however, not necessary to reduce the problem that far because the integrals get solvable immediately after applying a first recurrence relation. We do without presenting the calculation of diagram 3.1e) and merely give the results for the form factors.

$$\begin{aligned} F^{(9)}_{2,u}[e] &= \frac{2}{3}\left(\frac{1}{\epsilon} + 4\,L_\mu\right) + \frac{49}{9} + \frac{4\,i\pi}{3} - \frac{4}{3}\,L_s - \frac{16}{3}\,\zeta(3), \\ F^{(7)}_{2,u}[e] &= 0. \end{aligned} \tag{35}$$

3.5 $\mathcal{O}(\alpha_s)$ Counterterms to O_1^u and O_2^u

So far, we have calculated the two-loop matrix elements $\langle d\,\ell^+\ell^-|C_i\,O_i^q|b\rangle$ ($i=1,2$; $q=u,d$). As the operators mix under renormalization, there are additional contributions proportional to C_i. These counterterms arise from the matrix elements of the operators

$$\sum_{j=1}^{2}\delta Z_{ij}(O_j^u+O_j^c)+\sum_{j=3}^{10}\delta Z_{ij}O_j+\sum_{j=11}^{12}\delta Z_{ij}(O_j^u+O_j^c),\quad i=1,2, \tag{36}$$

where the operators O_1–O_{10} are given in Eq. (1). $O_{11}^{u,c}$ and $O_{12}^{u,c}$ are evanescent operators, ie operators which vanish in $d=4$ dimensions. In principle, there is some freedom in the choice of the evanescent operators. However, as we want to combine our matrix elements with the Wilson coefficients calculated by Bobeth *et al.* [10], we have to use the same definitions:

$$\begin{aligned}
O_{11}^u &= \left(\bar d_L\gamma_\mu\gamma_\nu\gamma_\sigma T^a u_L\right)\left(\bar u_L\gamma^\mu\gamma^\nu\gamma^\sigma T^a b_L\right)-16\,O_1^u\,,\\
O_{12}^u &= \left(\bar d_L\gamma_\mu\gamma_\nu\gamma_\sigma u_L\right)\left(\bar u_L\gamma^\mu\gamma^\nu\gamma^\sigma b_L\right)-16\,O_2^u\,,\\
O_{11}^c &= \left(\bar d_L\gamma_\mu\gamma_\nu\gamma_\sigma T^a c_L\right)\left(\bar c_L\gamma^\mu\gamma^\nu\gamma^\sigma T^a b_L\right)-16\,O_1^c\,,\\
O_{12}^c &= \left(\bar d_L\gamma_\mu\gamma_\nu\gamma_\sigma c_L\right)\left(\bar c_L\gamma^\mu\gamma^\nu\gamma^\sigma b_L\right)-16\,O_2^c\,.
\end{aligned} \tag{37}$$

The operator renormalization constants $Z_{ij}=\delta_{ij}+\delta Z_{ij}$ are of the form

$$\delta Z_{ij}=\frac{\alpha_s}{4\,\pi}\left(a_{ij}^{01}+\frac{1}{\epsilon}\,a_{ij}^{11}\right)+\frac{\alpha_s^2}{(4\,\pi)^2}\left(a_{ij}^{02}+\frac{1}{\epsilon}\,a_{ij}^{12}+\frac{1}{\epsilon^2}\,a_{ij}^{22}\right)+\mathcal{O}(\alpha_s^3). \tag{38}$$

The coefficients a_{ij}^{lm} needed for our calculation we take from Refs. [1, 10] and list them for $i=1,2$ and $j=1,...,12$:

$$\hat a^{11}=\begin{pmatrix} -2 & \frac{4}{3} & 0 & -\frac{1}{9} & 0 & 0 & 0 & 0 & -\frac{16}{27} & 0 & \frac{5}{12} & \frac{2}{9}\\[2ex] 6 & 0 & 0 & \frac{2}{3} & 0 & 0 & 0 & 0 & -\frac{4}{9} & 0 & 1 & 0\end{pmatrix}, \tag{39}$$

$$\begin{aligned}
a_{17}^{12}&=-\tfrac{58}{243}\,, & a_{19}^{12}&=-\tfrac{64}{729}\,, & a_{19}^{22}&=\tfrac{1168}{243}\,,\\
a_{27}^{12}&=\tfrac{116}{81}\,, & a_{29}^{12}&=\tfrac{776}{243}\,, & a_{29}^{22}&=\tfrac{148}{81}\,.
\end{aligned} \tag{40}$$

We denote the counterterm contributions to $b\to d\,\ell^+\ell^-$ which are due to the mixing of O_1^u or O_2^u into four-quark operators by $F_{i,u\to 4\text{quark}}^{\text{ct}(7)}$ and $F_{i,u\to 4\text{quark}}^{\text{ct}(9)}$. They can be extracted from the equation

$$\sum_j\left(\frac{\alpha_s}{4\,\pi}\right)\frac{1}{\epsilon}\,a_{ij}^{11}\langle d\,\ell^+\ell^-|O_j^u|b\rangle_{\text{1-loop}}=-\left(\frac{\alpha_s}{4\,\pi}\right)\left[F_{i,u\to 4\text{quark}}^{\text{ct}(7)}\langle\widetilde O_7\rangle_{\text{tree}}+F_{i,u\to 4\text{quark}}^{\text{ct}(9)}\langle\widetilde O_9\rangle_{\text{tree}}\right], \tag{41}$$

where j runs over the four-quark operators. As certain entries of $\hat{a}^{11}$ are zero, only the one-loop matrix elements of $O_1^{u,c}$, $O_2^{u,c}$, $O_4^{u,c}$, $O_{11}^{u,c}$ and $O_{12}^{u,c}$ are needed. In order to keep the presentation transparent, we relegate their explicit form to Appendix A. We do not repeat the renormalization of the O_1^c and O_2^c contributions in this place and refer to [1].

The counterterms which are related to the mixing of O_i^u $(i = 1, 2)$ into O_9 can be split into two classes: The first class consists of the one-loop mixing $O_i^u \to O_9$, followed by taking the one-loop corrected matrix element of O_9. It is obvious that this class contributes to the renormalization of diagram 3.1f), which we take into account when discussing the virtual corrections to O_9. We proceed in the same way with the counterterm just mentioned.

There is a second class of counterterm contributions due to $O_i^u \to O_9$ mixing. These contributions are generated by two-loop mixing of O_2^u into O_9 as well as by one-loop mixing and one-loop renormalization of the g_s factor in the definition of the operator O_9. We denote the corresponding contribution to the counterterm form factors by $F_{i,u\to 9}^{\mathrm{ct}(7)}$ and $F_{i,u\to 9}^{\mathrm{ct}(9)}$. We obtain

$$F_{i,u\to 9}^{\mathrm{ct}(9)} = -\left(\frac{a_{i9}^{22}}{\epsilon^2} + \frac{a_{i9}^{12}}{\epsilon}\right) - \frac{a_{i9}^{11}\,\beta_0}{\epsilon^2}\,, \quad F_{i,u\to 9}^{\mathrm{ct}(7)} = 0, \tag{42}$$

where we used the renormalization constant Z_{g_s} given by

$$Z_{g_s} = 1 - \frac{\alpha_s}{4\pi}\,\frac{\beta_0}{2}\,\frac{1}{\epsilon}\,, \quad \beta_0 = 11 - \frac{2}{3}N_f\,, \quad N_f = 5. \tag{43}$$

Besides the contribution from operator mixing, there are ordinary QCD counterterms.

The total counterterms $F_{i,u}^{\mathrm{ct(j)}}$ $(i = 1, 2;\ j = 7, 9)$, which renormalize diagrams 3.1a)–3.1e), are given by

$$F_{i,u}^{\mathrm{ct(j)}} = F_{i,u\to 4\mathrm{quark}}^{\mathrm{ct(j)}} + F_{i,u\to 9}^{\mathrm{ct(j)}}. \tag{44}$$

Explicitly they read

$$\begin{aligned} F_{2,u}^{\mathrm{ct}(9)} =& -F_{2,u,\,\mathrm{div}}^{(9)} - \frac{8}{25515}\left[2870 - 6300\,\pi^2 - 420\,i\pi + 126\,\hat{s} - \hat{s}^3\right] \\ &+ \frac{8}{25515}\left[-420 + 23940\,i\pi + 252\,\hat{s} + 27\,\hat{s}^2 + 4\,\hat{s}^3\right] L_\mu \\ &- \frac{136}{81}\,L_s^2 + \left[\frac{16}{243}(-2 - 57\,i\pi) + \frac{544}{81}\,L_\mu\right] L_s - \frac{512}{81}\,L_\mu^2, \end{aligned} \tag{45}$$

$$F_{2,u}^{\mathrm{ct}(7)} = -F_{2,u,\,\mathrm{div}}^{(7)} + \frac{2}{2835}\left(840\,L_\mu + 70\,\hat{s} + 7\,\hat{s}^2 + \hat{s}^3\right),$$

$$F_{1,u}^{\mathrm{ct}(9)} = -F_{1,u,\,\mathrm{div}}^{(9)} + \frac{4}{76545}\left[59570 - 6300\,\pi^2 - 34440\,i\pi + 126\,\hat{s} - \hat{s}^3\right]$$

$$+ \frac{68}{243}\,L_s^2 + \left[\frac{8}{729}(-160 + 57\,i\pi) - \frac{256}{243}\,L_\mu\right] L_s - \frac{256}{243}\,L_\mu^2, \tag{46}$$

$$F_{1,u}^{\mathrm{ct}(7)} = -F_{1,u,\,\mathrm{div}}^{(7)} - \frac{1}{8505}\left(840\,L_\mu + 70\,\hat{s} + 7\,\hat{s}^2 + \hat{s}^3\right).$$

The quantities $F_{i,u,\,\mathrm{div}}^{(j)}$ $(i = 1, 2;\ j = 7, 9)$ will compensate the divergent parts of the form factors associated with the virtual corrections to $O_{1,2}^u$ once this calculation is completed. They are given by

$$F_{2,u,\,\mathrm{div}}^{(9)} = \frac{128}{81\,\epsilon^2} + \frac{2}{2835\,\epsilon}\left[20790 - 23940\,i\pi - 252\,\hat{s} - 27\,\hat{s}^2 - 4\,\hat{s}^3\right] + \frac{16}{81\,\epsilon}(32\,L_\mu - 17\,L_s),$$

$$F_{2,u,\,\mathrm{div}}^{(7)} = \frac{92}{81\,\epsilon}, \tag{47}$$

$$F_{1,u,\,\mathrm{div}}^{(9)} = -\frac{64}{243\,\epsilon^2} - \frac{2}{76545\,\epsilon}\left[71820 - 23940\,i\pi - 252\,\hat{s} - 27\,\hat{s}^2 - \hat{s}^3\right] - \frac{8}{243}(32\,L_\mu - 17\,L_s),$$

$$F_{1,u,\,\mathrm{div}}^{(7)} = \frac{46}{243\,\epsilon}.$$

As mentioned before, we will take diagram 3.1f) into account only in Section 4. The same holds for the counterterms associated with the b and s quark wave function renormalization and, as stated earlier in this subsection, the $\mathcal{O}(\alpha_s)$ correction to the matrix element of $\delta Z_{i9} O_9$. The sum of these contributions is

$$\delta\bar{Z}_\psi \langle O_i\rangle_{\text{1-loop}} + \frac{\alpha_s}{4\pi}\,\frac{a_{i9}^{11}}{\epsilon}\,\left[\delta\bar{Z}_\psi \langle O_9\rangle_{\text{tree}} + \langle O_9\rangle_{\text{1-loop}}\right], \quad \delta\bar{Z}_\psi = \sqrt{Z_\psi(m_b) Z_\psi(m_s)} - 1,$$

and provides the counterterm that renormalizes diagram 3.1f). We use on-shell renormalization for the external b and s quark. In this scheme the field strength renormalization constants are given by

$$Z_\psi(m) = 1 - \frac{\alpha_s}{4\pi}\,\frac{4}{3}\left(\frac{\mu}{m}\right)^{2\epsilon}\left(\frac{1}{\epsilon} + \frac{2}{\epsilon_{\mathrm{IR}}} + 4\right). \tag{48}$$

So far, we have discussed the counterterms which renormalize the $\mathcal{O}(\alpha_s)$ corrected matrix elements $\langle d\,\ell^+\ell^-|O_i|b\rangle$ $(i = 1, 2)$. The corresponding one-loop matrix elements [of $\mathcal{O}(\alpha_s^0)$] are renormalized by adding the counterterms

$$\frac{\alpha_s}{4\,\pi}\,\frac{a_{i9}^{11}}{\epsilon}\,\langle O_9\rangle_{\text{tree}}.$$

4 Virtual Corrections to the Matrix Elements of the Operators O_7, O_8, O_9 and O_{10}

The virtual corrections to the matrix elements of O_7, O_8, O_9 and O_{10} and their renormalization is discussed in [1, 11]. For completeness we list the results of the renormalized matrix elements. They may all be decomposed according to

$$\langle d\,\ell^+\ell^-|C_iO_i|b\rangle = \widetilde{C}_i^{(0)}\left(-\frac{\alpha_s}{4\,\pi}\right)\left[F_i^{(9)}\langle\widetilde{O}_9\rangle_{\rm tree} + F_i^{(7)}\langle\widetilde{O}_7\rangle_{\rm tree}\right],$$

where

$$\begin{aligned}
\widetilde{O}_i &= \frac{\alpha_s}{4\,\pi}\,O_i \\
\widetilde{C}_7^{(0)} &= C_7^{(1)}, \quad \widetilde{C}_8^{(0)} = C_8^{(1)}, \\
\widetilde{C}_9^{(0)} &= \frac{4\,\pi}{\alpha_s}\left(C_9^{(0)} + \frac{\alpha_s}{4\,\pi}C_9^{(0)}\right) \quad \text{and} \quad \widetilde{C}_{10}^{(0)} = C_{10}^{(1)}.
\end{aligned}$$

Renormalized matrix element of O_7

The renormalized corrections to the form factors $F_7^{(9)}$ and $F_7^{(7)}$ are given by

$$F_7^{(9)} = -\frac{16}{3}\left(1 + \frac{1}{2}\,\hat{s} + \frac{1}{3}\,\hat{s}^2 + \frac{1}{4}\,\hat{s}^3\right), \tag{49}$$

$$F_7^{(7)} = \frac{32}{3}\,L_\mu + \frac{32}{3} + 8\,\hat{s} + 6\,\hat{s}^2 + \frac{128}{27}\,\hat{s}^3 + f_{\rm inf}\,. \tag{50}$$

The function $f_{\rm inf}$ collects the infrared- and collinear singular part:

$$f_{\rm inf} = \frac{\left[\frac{\mu}{m_b}\right]^{2\epsilon}}{\epsilon_{\rm IR}}\,\frac{8}{3}\left(1 + \hat{s} + \frac{1}{2}\,\hat{s}^2 + \frac{1}{3}\,\hat{s}^3\right) + \frac{\left[\frac{\mu}{m_b}\right]^{2\epsilon}}{\epsilon_{\rm IR}}\,\frac{4}{3}\,\ln(r) + \frac{2}{3}\ln(r) - \frac{2}{3}\ln^2(r), \tag{51}$$

where $\epsilon_{\rm IR}$ and $r = (m_d^2/m_b^2)$ regularize the infrared- and collinear singularities.

Renormalized matrix element of the operator O_8

The renormalized corrections to form factors of the matrix element of O_8 are

$$F_8^{(9)} = \frac{104}{9} - \frac{32}{27}\,\pi^2 + \left(\frac{1184}{27} - \frac{40}{9}\,\pi^2\right)\hat{s} + \left(\frac{14212}{135} - \frac{32}{3}\,\pi^2\right)\hat{s}^2 \tag{52}$$

$$+ \left(\frac{193444}{945} - \frac{560}{27}\,\pi^2\right)\hat{s}^3 + \frac{16}{9}\,L_s\left(1 + \hat{s} + \hat{s}^2 + \hat{s}^3\right),$$

$$F_8^{(7)} = -\frac{32}{9}\,L_\mu + \frac{8}{27}\,\pi^2 - \frac{44}{9} - \frac{8}{9}\,i\pi + \left(\frac{4}{3}\,\pi^2 - \frac{40}{3}\right)\hat{s} + \left(\frac{32}{9}\,\pi^2 - \frac{316}{9}\right)\hat{s}^2 \tag{53}$$

$$+ \left(\frac{200}{27}\,\pi^2 - \frac{658}{9}\right)\hat{s}^3 - \frac{8}{9}\,L_s\left(\hat{s} + \hat{s}^2 + \hat{s}^3\right).$$

Renormalized matrix element of O_9 and O_{10}

The renormalized matrix element of O_9 and O_{10}, finally, is described by the form factors

$$F_9^{(9)} = \frac{16}{3} + \frac{20}{3}\,\hat{s} + \frac{16}{3}\,\hat{s}^2 + \frac{116}{27}\,\hat{s}^3 + f_{\rm inf}\,, \tag{54}$$

$$F_9^{(7)} = -\frac{2}{3}\hat{s}\left(1 + \frac{1}{2}\,\hat{s} + \frac{1}{3}\,\hat{s}^2\right), \tag{55}$$

$$F_{10}^{(9)} = F_9^{(9)}, \tag{56}$$

$$F_{10}^{(7)} = F_9^{(7)}, \tag{57}$$

where $f_{\rm inf}$ is defined in Eq. (51).

The renormalized diagrams 3.1e) are properly included by modifying $\widetilde{C}_9^{(0)}$ as follows:

$$\widetilde{C}_9^{(0)} \to \widetilde{C}_9^{(0,\rm mod)} = \widetilde{C}_9^{(0)} - \frac{1}{\lambda_t}\left(C_2^{(0)} + \frac{4}{3}\,C_1^{(0)}\right)\left(\lambda_u H_0(0) + \lambda_c H_0(z)\right).$$

For $\hat{s} < 4\,z$ ($z = m_c^2/m_b^2$) the loop function $H_0(z)$ can be expanded in terms of $\hat{s}/(4\,z)$. We give the expansion of $H_0(z)$ for this case as well as the result for $H_0(0)$:

$$H_0(z) = \frac{1}{2835}\left[-1260 + 2520\ln\left(\frac{\mu}{m_c}\right) + 1008\left(\frac{\hat{s}}{4z}\right) + 432\left(\frac{\hat{s}}{4z}\right)^2 + 256\left(\frac{\hat{s}}{4z}\right)^3\right], \tag{58}$$

$$H_0(0) = \frac{8}{27} - \frac{4}{9}\,\ln(\hat{s}) + \frac{4}{9}\,i\,\pi.$$

5 Corrections to the Decay Width $B \to X_d\,\ell^+\ell^-$

In this section we first discuss the contribution of the virtual corrections to the decay width $d\Gamma(B \to X_d\,\ell^+\ell^-)/d\hat{s}$. Following [1, 11], we do also include those bremsstrahlung corrections needed to cancel the infrared- and collinear singularities. We then discuss in a second step the remaining bremsstrahlung contributions.

5.1 Virtual Corrections

In the literature (see eg [12]), the decay width is usually written as

$$\frac{d\Gamma(b\to X_d\ell^+\ell^-)}{d\hat{s}} = \left(\frac{\alpha_{em}}{4\,\pi}\right)^2 \frac{G_F^2\, m_{b,\text{pole}}^5\, |\lambda_t|^2}{48\,\pi^3}(1-\hat{s})^2 \times \left\{(1+2\,\hat{s})\left(\left|\widetilde{C}_9^{\text{eff}}\right|^2 + \left|\widetilde{C}_{10}^{\text{eff}}\right|^2\right) + 4(1+2/\hat{s})\left|\widetilde{C}_7^{\text{eff}}\right|^2 + 12\,\text{Re}\left(\widetilde{C}_7^{\text{eff}}\widetilde{C}_9^{\text{eff}*}\right)\right\}. \quad (59)$$

All corrections have been absorbed into the effective Wilson coefficients $\widetilde{C}_7^{\text{eff}}$, $\widetilde{C}_9^{\text{eff}}$ and $\widetilde{C}_{10}^{\text{eff}}$. We follow [1, 11, 12] and write the effective Wilson coefficients as

$$\begin{aligned}\widetilde{C}_9^{\text{eff}} &= \left(1+\frac{\alpha_s(\mu)}{\pi}\omega_9(\hat{s})\right)\left(A_9 - \frac{\lambda_c}{\lambda_t}\,T_9\,h(z,\hat{s}) - \frac{\lambda_u}{\lambda_t}\,T_9\,h(0,\hat{s}) + U_9\,h(1,\hat{s}) + W_9\,h(0,\hat{s})\right)\\ &\quad + \frac{\alpha_s(\mu)}{4\pi}\left(\frac{\lambda_u}{\lambda_t}\left(C_1^{(0)}F_{1,u}^{(9)} + C_2^{(0)}F_{2,u}^{(9)}\right) + \frac{\lambda_c}{\lambda_t}\left(C_1^{(0)}F_{1,c}^{(9)} + C_2^{(0)}F_{2,c}^{(9)}\right) + A_8^{(0)}F_8^{(9)}\right)\end{aligned}$$

$$\begin{aligned}\widetilde{C}_7^{\text{eff}} &= \left(1+\frac{\alpha_s(\mu)}{\pi}\omega_7(\hat{s})\right)A_7 \quad (60)\\ &\quad + \frac{\alpha_s(\mu)}{4\pi}\left(\frac{\lambda_u}{\lambda_t}\left(C_1^{(0)}F_{1,u}^{(7)} + C_2^{(0)}F_{2,u}^{(7)}\right) + \frac{\lambda_c}{\lambda_t}\left(C_1^{(0)}F_{1,c}^{(7)} + C_2^{(0)}F_{2,c}^{(7)}\right) + A_8^{(0)}F_8^{(7)}\right)\end{aligned}$$

$$\widetilde{C}_{10}^{\text{eff}} = \left(1+\frac{\alpha_s(\mu)}{\pi}\omega_9(\hat{s})\right)A_{10},$$

where we have provided the necessary modification to account for the CKM structure of $b \to d\,\ell^+\ell^-$. The form factors $F_{1,u}^{(7,9)}$ and $F_{1,u}^{(7,9)}$ are given by

$$F_{i,u}^{(j)} = F_{i,u}^{(j)}[a] + F_{i,u}^{(j)}[b] + F_{i,u}^{(j)}[c] + F_{i,u}^{(j)}[d] + F_{i,u}^{(j)}[e] + F_{i,u}^{\text{ct}(j)}, \quad \text{where} \quad i=1,2;\ j=7,9. \quad (61)$$

At the present time, the contributions $F_{i,u}^{(j)}[d]$ are not yet available.

The form factors $F_{1,c}^{(7,9)}$, $F_{2,c}^{(7,9)}$ and $F_8^{(7,9)}$ can be seen in [1, 11]. The functions $\omega_7(\hat{s})$ and $\omega_9(\hat{s})$ encapsulate the interference between the tree-level and the one-loop matrix elements of O_7 and $O_{9,10}$ and the corresponding bremsstrahlung corrections, which cancel the infrared- and collinear divergences appearing in the virtual corrections. When calculating the decay width (59), we retain only terms linear in α_s (and thus in ω_7, ω_9) in the expressions for $|\widetilde{C}_7^{\text{eff}}|^2$, $|\widetilde{C}_9^{\text{eff}}|^2$ and $|\widetilde{C}_{10}^{\text{eff}}|^2$. Accordingly, we drop terms of $\mathcal{O}(\alpha_s^2)$ in the interference term $\text{Re}\left(\widetilde{C}_7^{\text{eff}}\widetilde{C}_9^{\text{eff}*}\right)$ too, where by construction one has to make the replacements $\omega_9 \to \omega_{79}$ and $\omega_7 \to \omega_{79}$ in this term. The function ω_9 has already been calculated in [12], where

also the exact expression for $h(\hat{s}, z)$ can be found. For the functions ω_7 and ω_{79} and more information on the cancellation of infrared- and collinear divergences we refer to [1].

The auxiliary quantities A_7, A_9, A_{10}, T_9, U_9 and W_9 are the following linear combinations of the Wilson coefficients $C_i(\mu)$:

$$\begin{aligned}
A_7 &= \frac{4\,\pi}{\alpha_s(\mu)}\, C_7(\mu) - \frac{1}{3}\, C_3(\mu) - \frac{4}{9}\, C_4(\mu) - \frac{20}{3}\, C_5(\mu) - \frac{80}{9}\, C_6(\mu), \\
A_8 &= \frac{4\,\pi}{\alpha_s(\mu)}\, C_8(\mu) + C_3(\mu) - \frac{1}{6}\, C_4(\mu) + 20\, C_5(\mu) - \frac{10}{3}\, C_6(\mu), \\
A_9 &= \frac{4\pi}{\alpha_s(\mu)}\, C_9(\mu) + \frac{4}{3}\, C_3(\mu) + \frac{64}{9}\, C_5(\mu) + \frac{64}{27}\, C_6(\mu) \\
&\quad + \left[\frac{\lambda_u + \lambda_c}{-\lambda_t}\left(C_1(\mu)\,\gamma_{19}^{(0)} + C_2(\mu)\,\gamma_{29}^{(0)}\right) + \sum_{i=3}^{6} C_i(\mu)\,\gamma_{i9}^{(0)}\right] \ln\left(\frac{m_b}{\mu}\right), \\
A_{10} &= \frac{4\,\pi}{\alpha_s(\mu)}\, C_{10}(\mu), \\
T_9 &= \left(\frac{4}{3}\, C_1(\mu) + C_2(\mu)\right) + 6\, C_3(\mu) + 60\, C_5(\mu), \\
U_9 &= -\frac{7}{2}\, C_3(\mu) - \frac{2}{3}\, C_4(\mu) - 38\, C_5(\mu) - \frac{32}{3}\, C_6(\mu), \\
W_9 &= -\frac{1}{2}\, C_3(\mu) - \frac{2}{3}\, C_4(\mu) - 8\, C_5(\mu) - \frac{32}{3}\, C_6(\mu).
\end{aligned} \tag{62}$$

By this definition we do also include some diagrams induced by $O_{3,4,5,6}$ insertions, viz the $\mathcal{O}(\alpha_s^0)$ contributions, the diagrams of topology 3.1e) and those bremsstrahlung diagrams where the gluon is emitted from the b or d quark line (cf [13]).

We take the numerical values for A_7, A_9, A_{10}, T_9, U_9 and W_9 from [12], while $C_1^{(0)}$ and $C_2^{(0)}$ can be found in [9]. For completeness we list them in Table 5.1.

5.2 Bremsstrahlung Corrections

The bremsstrahlung contributions taken into account by introducing the functions $\omega_i(\hat{s})$ cancel the infrared divergences associated with the virtual corrections. All other bremsstrahlung terms are finite. This allows us to perform their calculation directly in $d = 4$ dimensions.

The sum of the bremsstrahlung contributions from $O_7 - O_8$ and $O_8 - O_9$ interference terms

	$\mu = 2.5$ GeV	$\mu = 5$ GeV	$\mu = 10$ GeV
α_s	0.267	0.215	0.180
$C_1^{(0)}$	-0.697	-0.487	-0.326
$C_2^{(0)}$	1.046	1.024	1.011
$\left(A_7^{(0)},\ A_7^{(1)}\right)$	$(-0.360,\ 0.031)$	$(-0.321,\ 0.019)$	$(-0.287,\ 0.008)$
$A_8^{(0)}$	-0.164	-0.148	-0.134
$\left(A_9^{(0)},\ A_9^{(1)}\right)$	$(4.241,\ -0.170)$	$(4.129,\ 0.013)$	$(4.131,\ 0.155)$
$\left(T_9^{(0)},\ T_9^{(1)}\right)$	$(0.115,\ 0.278)$	$(0.374,\ 0.251)$	$(0.576,\ 0.231)$
$\left(U_9^{(0)},\ U_9^{(1)}\right)$	$(0.045,\ 0.023)$	$(0.032,\ 0.016)$	$(0.022,\ 0.011)$
$\left(W_9^{(0)},\ W_9^{(1)}\right)$	$(0.044,\ 0.016)$	$(0.032,\ 0.012)$	$(0.022,\ 0.009)$
$\left(A_{10}^{(0)},\ A_{10}^{(1)}\right)$	$(-4.372,\ 0.135)$	$(-4.372,\ 0.135)$	$(-4.372,\ 0.135)$

Table 5.1: Coefficients appearing in Eq. (62) for $\mu = 2.5$ GeV, $\mu = 5$ GeV and $\mu = 10$ GeV. For $\alpha_s(\mu)$ (in the $\overline{\text{MS}}$ scheme) we used the two-loop expression with 5 flavors and $\alpha_s(m_Z) = 0.119$. The entries correspond to the pole top quark mass $m_t = 174$ GeV. The superscript (0) refers to lowest order quantities and while the superscript (1) denotes the correction terms of order α_s.

and the $O_8 - O_8$ term can be written as

$$\frac{d\Gamma^{\text{Brems,A}}}{d\hat{s}} = \frac{d\Gamma_{78}^{\text{brems}}}{d\hat{s}} + \frac{d\Gamma_{89}^{\text{brems}}}{d\hat{s}} + \frac{d\Gamma_{88}^{\text{brems}}}{d\hat{s}} = \left(\frac{\alpha_{em}}{4\,\pi}\right)^2 \left(\frac{\alpha_s}{4\,\pi}\right) \frac{m_{b,\text{pole}}^5\,|\lambda_t|^2\,G_F^2}{48\,\pi^3} \times \left(2\,\text{Re}\left[c_{78}\,\tau_{78} + c_{89}\,\tau_{89}\right] + c_{88}\,\tau_{88}\right), \quad (63)$$

where

$$c_{78} = C_F \cdot \widetilde{C}_7^{(0,\text{eff})}\widetilde{C}_8^{(0,\text{eff})*}, \quad c_{89} = C_F \cdot \widetilde{C}_8^{(0,\text{eff})}\widetilde{C}_9^{(0,\text{eff})*}, \quad c_{88} = C_F \cdot \left|\widetilde{C}_8^{(0,\text{eff})}\right|^2. \quad (64)$$

For the quantities τ_{78}, τ_{89} and τ_{88} we refer to [13].

The remaining bremsstrahlung contributions all involve the diagrams with an $O_{1,2}^u$ or $O_{1,2}^c$ insertion where the gluon is emitted from the u or c quark loop, respectively. The corresponding bremsstrahlung matrix elements depend on $\bar{\Delta}i_{23}^{(u,c)}$, $\bar{\Delta}i_{27}^{(u,c)}$, only. In $d = 4$

dimensions we find

$$\bar{\Delta} i_{23}^{(u)} = 8\,(q{\cdot}r)\int_0^1 dx\,dy\,\frac{x\,y\,(1-y)^2}{C^{(u)}}\,, \qquad \bar{\Delta} i_{23}^{(c)} = 8\,(q{\cdot}r)\int_0^1 dx\,dy\,\frac{x\,y\,(1-y)^2}{C^{(c)}}\,,$$
$$\bar{\Delta} i_{27}^{(u)} = 8\,(q{\cdot}r)\int_0^1 dx\,dy\,\frac{y\,(1-y)^2}{C^{(u)}}\,, \qquad \bar{\Delta} i_{27}^{(c)} = 8\,(q{\cdot}r)\int_0^1 dx\,dy\,\frac{y\,(1-y)^2}{C^{(c)}}\,,$$

where

$$C^{(u)} = \quad -2\,x\,y\,(1-y)(q{\cdot}r) - q^2\,y\,(1-y) - i\,\delta\,,$$
$$C^{(c)} = m_c^2 - 2\,x\,y\,(1-y)(q{\cdot}r) - q^2\,y\,(1-y) - i\,\delta\,.$$

The analytical expressions for $\bar{\Delta} i_{23}^{(c)}$ and $\bar{\Delta} i_{27}^{(c)}$ can be expressed in terms of functions $G_i(t)$:

$$\bar{\Delta} i_{23}^{(c)} = -2 + \frac{4}{w-\hat{s}}\left[z\,G_{-1}\Big(\frac{\hat{s}}{z}\Big) - z\,G_{-1}\Big(\frac{w}{z}\Big) - \frac{\hat{s}}{2}\,G_0\Big(\frac{\hat{s}}{z}\Big) + \frac{\hat{s}}{2}\,G_0\Big(\frac{w}{z}\Big)\right], \tag{65}$$

$$\bar{\Delta} i_{27}^{(c)} = 2\left[G_0\Big(\frac{\hat{s}}{z}\Big) - G_0\Big(\frac{w}{z}\Big)\right], \tag{66}$$

where $z = m_c^2/m_b^2$. $G_k(t)$ $(k \geq -1)$ is defined through the integral

$$G_k(t) := \int_0^1 dx\,x^k\,\ln\big[1 - t\,x(1-x) - i\,\delta\big], \quad G_1(t) = \frac{1}{2}G_0(t).$$

Explicitly, the functions $G_{-1}(t)$ and $G_0(t)$ read

$$G_{-1}(t) = \begin{cases} 2\,\pi\,\arctan\Big(\sqrt{\frac{4-t}{t}}\Big) - \frac{\pi^2}{2} - 2\,\arctan^2\Big(\sqrt{\frac{4-t}{t}}\Big), & t < 4 \\ -2\,i\pi\,\ln\Big(\frac{\sqrt{t}+\sqrt{t-4}}{2}\Big) - \frac{\pi^2}{2} + 2\,\ln^2\Big(\frac{\sqrt{t}+\sqrt{t-4}}{2}\Big), & t > 4 \end{cases}, \tag{67}$$

$$G_0(t) = \begin{cases} \pi\,\sqrt{\frac{4-t}{t}} - 2 - 2\,\sqrt{\frac{4-t}{t}}\,\arctan\Big(\sqrt{\frac{4-t}{t}}\Big), & t < 4 \\ -i\pi\sqrt{\frac{t-4}{t}} - 2 + 2\,\sqrt{\frac{t-4}{t}}\,\ln\Big(\frac{\sqrt{t}+\sqrt{t-4}}{2}\Big), & t > 4 \end{cases}. \tag{68}$$

The quantities $\bar{\Delta} i_j^{(u)}$ we obtain from $\bar{\Delta} i_j^{(c)}$ in the limit $z \to 0$:

$$\bar{\Delta} i_{23}^{(u)} = -2 + \frac{\hat{s}}{w-\hat{s}}\big[\ln(w) - \ln(\hat{s})\big]\,,$$
$$\bar{\Delta} i_{27}^{(u)} = -2\big[\ln(w) - \ln(\hat{s})\big].$$

Following [13] we write

$$\frac{d\Gamma^{\rm Brems,B}}{d\hat{s}} = \left(\frac{\alpha_{\rm em}}{4\,\pi}\right)^2 \left(\frac{\alpha_s}{4\,\pi}\right) \frac{G_F^2\, m_{b,\rm pole}^5\, |\lambda_t|^2}{48\,\pi^3} \times$$
$$\int_{\hat{s}}^{1} dw \left\{ (c_{11}+c_{12}+c_{22})\,\tau_{22} + 2\,{\rm Re}\Big[\,(c_{17}+c_{27})\,\tau_{27} + (c_{18}+c_{28})\,\tau_{28} + (c_{19}+c_{29})\,\tau_{29}\Big]\right\}, \quad (69)$$

In terms of the quantities $\bar{\Delta} i_{23}^{\rm eff}$ and $\bar{\Delta} i_{27}^{\rm eff}$, defined by

$$\bar{\Delta} i_{23}^{\rm eff} := -\frac{\lambda_u}{\lambda_t}\bar{\Delta} i_{23}^{(u)} - \frac{\lambda_c}{\lambda_t}\bar{\Delta} i_{23}^{(c)}, \quad (70)$$
$$\bar{\Delta} i_{27}^{\rm eff} := -\frac{\lambda_u}{\lambda_t}\bar{\Delta} i_{27}^{(u)} - \frac{\lambda_c}{\lambda_t}\bar{\Delta} i_{27}^{(c)}, \quad (71)$$

the quantities τ_{ij} introduced in Eq.(69) read

$$\tau_{22} = \frac{8}{27}\frac{(w-\hat{s})(1-w)^2}{\hat{s}\,w^3} \times \Big\{\Big[3\,w^2 + 2\,\hat{s}^2(2+w) - \hat{s}\,w\,(5-2\,w)\Big]\,\big|\bar{\Delta} i_{23}^{\rm eff}\big|^2 +$$
$$\Big[2\,\hat{s}^2\,(2+\,w) + \hat{s}\,w\,(1+2\,w)\Big]\,\big|\bar{\Delta} i_{27}^{\rm eff}\big|^2 + 4\,\hat{s}\Big[w\,(1-w) - \hat{s}\,(2+w)\Big]\cdot {\rm Re}\left[\bar{\Delta} i_{23}^{\rm eff}\bar{\Delta} i_{27}^{\rm eff*}\right]\Big\}, \quad (72)$$

$$\tau_{27} = \frac{8}{3}\frac{1}{\hat{s}\,w} \times \Big\{\Big[(1-w)\left(4\,\hat{s}^2 - \hat{s}\,w + w^2\right) + \hat{s}\,w\,(4+\hat{s}-w)\ln(w)\Big]\bar{\Delta} i_{23}^{\rm eff}$$
$$- \Big[4\,\hat{s}^2\,(1-w) + \hat{s}\,w\,(4+\hat{s}-w)\,\ln(w)\Big]\bar{\Delta} i_{27}^{\rm eff}\Big\}, \quad (73)$$

$$\tau_{28} = \frac{8}{9}\frac{1}{\hat{s}\,w\,(w-\hat{s})} \times \Big\{\Big[(w-s)^2(2\,\hat{s}-w)(1-w)\Big]\bar{\Delta} i_{23}^{\rm eff} - \Big[2\,\hat{s}\,(w-\hat{s})^2(1-w)\Big]\bar{\Delta} i_{27}^{\rm eff}$$
$$+ \hat{s}\,w\Big[(1+2\,\hat{s}-2\,w)\bar{\Delta} i_{23}^{\rm eff} - 2\,(1+\hat{s}-w)\bar{\Delta} i_{27}^{\rm eff}\Big]\cdot\ln\left[\frac{\hat{s}}{(1+\hat{s}-w)(w^2+\hat{s}\,(1-w))}\right]\Big\}, \quad (74)$$

$$\tau_{29} = \frac{4}{3}\frac{1}{w} \times \Big\{\Big[2\,\hat{s}(1-w)(\hat{s}+w) + 4\,\hat{s}\,w\ln(w)\Big]\bar{\Delta} i_{23}^{\rm eff} -$$
$$\Big[2\,\hat{s}(1-w)(\hat{s}+w) + w(3\,\hat{s}+w)\ln(w)\Big]\bar{\Delta} i_{27}^{\rm eff}\Big\}. \quad (75)$$

The coefficients c_{ij} include the dependence on the Wilson coefficients and the color factors.

$$\begin{aligned}
c_{11} &= C_{\tau_1} \cdot \left| C_1^{(0)} \right|^2, & c_{17} &= C_{\tau_2} \cdot C_1^{(0)} \widetilde{C}_7^{(0,\text{eff})*}, & c_{27} &= C_F \cdot C_2^{(0)} \widetilde{C}_7^{(0,\text{eff})*}, \\
c_{12} &= C_{\tau_2} \cdot 2\,\text{Re}\left[C_1^{(0)} C_2^{(0)*} \right], & c_{18} &= C_{\tau_2} \cdot C_1^{(0)} \widetilde{C}_8^{(0,\text{eff})*}, & c_{28} &= C_F \cdot C_2^{(0)} \widetilde{C}_8^{(0,\text{eff})*}, \\
c_{22} &= C_F \cdot \left| C_2^{(0)} \right|^2, & c_{19} &= C_{\tau_2} \cdot C_1^{(0)} \widetilde{C}_9^{(0,\text{eff})*}, & c_{29} &= C_F \cdot C_2^{(0)} \widetilde{C}_9^{(0,\text{eff})*}.
\end{aligned} \tag{76}$$

The color factors C_F, C_{τ_1} and C_{τ_2} arise from the following color structures:

$$\sum_a T^a T^a = C_F \mathbf{1}, \quad C_F = \frac{N_c^2 - 1}{2\,N_c},$$

$$\sum_{a,b,c} T^a T^c T^a T^b T^c T^b = C_{\tau_1} \mathbf{1}, \quad C_{\tau_1} = \frac{N_c^2 - 1}{8\,N_c^3},$$

and

$$\sum_{a,b} T^a T^b T^a T^b = C_{\tau_2} \mathbf{1}, \quad C_{\tau_2} = -\frac{N_c^2 - 1}{4\,N_c^2}.$$

6 Outlook

We will have to take care of the calculation of diagram 3.1d) first, of course. In addition, we will also be forced to think about how to account for the large resonant contributions due to $\bar{u}u$ intermediate states. As stated before, the process $b \to d\,\ell^+\ell^-$ is sensitive to CP violation. We are most eager to get predictions for the CP asymmetry

$$a = \frac{\Gamma\left(B \to X_d\,\ell^+\ell^-\right) - \Gamma\left(\bar{B} \to \bar{X}_d\,\ell^+\ell^-\right)}{\Gamma\left(B \to X_d\,\ell^+\ell^-\right) + \Gamma\left(\bar{B} \to \bar{X}_d\,\ell^+\ell^-\right)}.$$

There is also the hope that we might have learnt something which will turn out to be helpful in the analysis of $b \to s\,\ell^+\ell^-$ for high values of $\hat{s}$. To be precise, at least the diagram 3.1e) with a c quark running in the fermion loop can be calculated by means of dimension shifts and recurrence relations – also for values of $\hat{s} > 4\,z$.

A One-Loop Matrix Elements of the Four-Quark Operators

In order to fix the counterterms $F^{\mathrm{ct}(7,9)}_{i,u\to 4\mathrm{quark}}$ $(i = 1, 2)$ in Eq. (41), we need the one-loop matrix elements $\langle d\,\ell^+\ell^-|O_j|b\rangle_{\text{1-loop}}$ of the four-quark operators O_1^u, O_2^u, O_4, O_{11}^u and O_{12}^u. Due to the $1/\epsilon$ factor in Eq. (41) they are needed up to $\mathcal{O}(\epsilon^1)$. The explicit results (in expanded form) read

$$\begin{aligned}\langle d\,\ell^+\ell^-|O_2^u|b\rangle_{\text{1-loop}} = {} & \left(\frac{\mu}{m_c}\right)^{2\epsilon}\left\{\frac{4}{9\,\epsilon}+\frac{4}{27}\Big[\,2-3\,i\pi-3\,L_s\,\Big]+\right.\\ & \left.\frac{\epsilon}{81}\Big[\,52-24\,i\pi-21\,\pi^2-(24-36\,i\pi)L_s+18\,L_s^2\,\Big]\right\}\langle\widetilde{O}_9\rangle_{\text{tree}}\,,\end{aligned}$$

$$\langle d\,\ell^+\ell^-|O_1^u|b\rangle_{\text{1-loop}} = \frac{4}{3}\,\langle d\,\ell^+\ell^-|O_2^u|b\rangle_{\text{1-loop}}\,,$$

$$\begin{aligned}\langle d\,\ell^+\ell^-|O_4|b\rangle_{\text{1-loop}} = {} & -\left(\frac{\mu}{m_b}\right)^{2\epsilon}\left\{\left[\frac{4}{9}+\frac{\epsilon}{945}\left(70\,\hat{s}+7\,\hat{s}^2+\hat{s}^3\right)\right]\,\langle\widetilde{O}_7\rangle_{\text{tree}}\right.\\ & +\left[\frac{16}{27\,\epsilon}+\frac{2}{8505}\left(-420+1260\,i\pi-1260\,L_s+252\,\hat{s}+27\,\hat{s}^2+4\,\hat{s}^3\right)\right.\\ & +\frac{4\,\epsilon}{8505}\left(420\,i\pi+910-630\,L_s\,i\pi-420\,L_s-315\,\pi^2\right.\\ & \left.\left.\left.+\;315\,L_s^2-126\,\hat{s}+\hat{s}^3\right)\right]\right\}\langle\widetilde{O}_9\rangle_{\text{tree}},\end{aligned}$$

$$\langle d\,\ell^+\ell^-|O_{11}^u|b\rangle_{\text{1-loop}} = -\frac{64}{27}\left(\frac{\mu}{m_b}\right)^{2\epsilon}\left(1+\frac{5}{3}\,\epsilon+i\pi\,\epsilon+L_s\right)\,\langle\widetilde{O}_9\rangle_{\text{tree}}\,,$$

$$\langle d\,\ell^+\ell^-|O_{12}^u|b\rangle_{\text{1-loop}} = \frac{3}{4}\,\langle d\,\ell^+\ell^-|O_{11}^u|b\rangle_{\text{1-loop}}\,.$$

References

[1] H. H. Asatryan, H. M. Asatrian, C. Greub and M. Walker, *Phys. Rev.* **D 65** (2000) 074004, hep-ph/0109140.

[2] M. Misiak, *Nucl. Phys.* **B 393** (1993) 23; *Nucl. Phys.* **B 439** (1995) 461 (E).

[3] B. Grinstein, M. J. Savage and M. B. Wise, *Nucl. Phys.* **B 319** (1989) 271.

[4] O. V. Tarasov, *Phys. Rev.* **D 54** (1996) 6479, hep-th/9606018.

[5] P. A. Baikov, *Phys. Lett.* **B 474** (2000) 385, hep-ph/9912421.

[6] O. V. Tarasov, *Nucl. Phys.* **B 562** (1997) 455, hep-ph/9703319.

[7] V. A. Smirnov, *Renormalization and Asymptotic Expansions* (Birkhäuser, Basel, 1991).

[8] H. Simma and D. Wyler, *Nucl. Phys.* **B 344** (1990) 283.

[9] C. Greub, P. Liniger, *Phys. Lett.* **B 494** (2000) 237, *Phys. Rev.* **D 63** (2001) 054025, hep-ph/0009144.

[10] C. Bobeth, M. Misiak and J. Urban, *Nucl. Phys.* **B 574** (2000) 291, hep-ph/9910220.

[11] H. H. Asatryan, H. M. Asatrian, C. Greub and M. Walker, *Phys. Lett.* **B 507** (2001) 162, hep-ph/0103087.

[12] C. Bobeth, M. Misiak and J. Urban, *Nucl. Phys.* **B 574** (2000) 291, hep-ph/9910220.

[13] H. H. Asatryan, H. M. Asatrian, C. Greub and M. Walker, hep-ph/0204346, submitted to *Phys. Rev.* **D**.

[14] N. Cabibbo and L. Maiani, *Phys. Lett.* **B 79** (1978) 109.

[15] Y. Nir, *Phys. Lett.* **B 221** (1989) 184.

[16] C. Greub, T. Hurth and D. Wyler, *Phys. Rev.* **D 54** (1996) 3350.

Acknowledgements

In the first place my thanks go to Christoph Greub, who was not only an excellent supervisor of my thesis but also an equally gifted advisor. I did very much appreciate the collaboration, which always took place on a very friendly level. Further, I would like to thank D. Wyler for kindly agreeing to be second examiner of my work. I thank Patrick Liniger for liberally putting the Mathematica package `Dirac` at disposal and Kay Bieri for many helpful discussions and as many thrilling games of chess. I am very grateful to my parents, my sister and my friends for always reminding me not to forget that there is more in life than only physics. Last but not least my thanks go to Christoph Schmid for carefully proofreading the Introduction and Part I of this PhD thesis with regard to the style.

Curriculum Vitae

Personal Data

Name	Walker, Manuel Philipp
Date of birth	December 29, 1973
Place of birth	Bern, Switzerland
Nationality	Swiss
Marital status	unmarried
Present address	Institut für theoretische Physik Universität Bern Sidlerstrasse 5 CH-3012 Bern E-mail: `walker@itp.unibe.ch`

Schools

1980-1989	Schools in Thun
1989-1993	Gymnasium Thun
1993	Matura Typus C (University entrance exam)

University

1993-1999	University of Bern Studies in physics, mathematics and computer science
1999	University of Bern M.Sc in theoretical physics "$\eta \to 3\,\pi$" (supervised by Prof. Dr. H. Leutwyler)
1999-2002	University of Bern PhD in theoretical physics "QCD Corrections to the Rare Decays $B \to X_s\,\ell^+\ell^-$ and $B \to X_d\,\ell^+\ell^-$ in the Standard Model" (supervised by PD Dr. Ch. Greub)

Other Activities

1993, 1996	Obligatory military service
2001	55$^{\text{th}}$ Scottish Universities Summer School in Physics, A NATO Advanced Study Institute